DISSERTATION

ESTABLISHMENT OF GPS REFERENCE NETWORK IN GHANA

eingereicht von

Yaw Poku-Gyamfi, M.Phil.

Vollständiger Abdruck der an der Fakultät für Luft- und Raumfahrtechnik der Universität der Bundeswehr, München zur Erlangung des akademischen Grades eines Doktors der Ingenierwissenschaften (Dr.-Ing.) eingereichten Dissertation.

Vorsitzender: (Chairman)	Prof. Dr.-Ing. Bernhard Katzy

1. Berichterstatter: (1st Reviewer) — Prof. Dr.-Ing. Guenter Hein
2. Berichterstatter: (2nd Reviewer) — Prof. Dr.-Ing. Guenter Seeber
3. Berichterstatter: (3rd Reviewer) — PD Dr.-Ing. Torben Schueler

Der Dissertation wurde am 11.05.2009 bei der Universität der Bundeswehr München, Werner Heisenberg-Weg 39, 85577, Neubiberg eingereicht und durch die Fakultät für Luft- und Raumfahrttechnik am 16.11.2009 angenommen.

Tag der mündlich Prüfung: 16.11.2009

Table of Contents

Abstract

The quest for the use of GNSS in developing countries is on the rise following the realization of its numerous advantages over the conventional methods of positioning, navigation and timing. Africa's attempt to harness this technology has made it imperative to investigate the regional problems associated with its implementation by its member states, which constitute the AFREF. This study goes beyond the establishment of a GNSS reference network in Ghana by investigating and finding solutions to some of the regional problems associated with its implementation.

The problem of turbulent atmospheric conditions which includes the severe ionospheric fluctuations and the erratic tropospheric conditions coupled with the sparsely populated base stations has led to the development of a new concept of correction, the Corridor Correction, which is able to correct the atmospheric effect comparable with the established concepts like the Virtual Reference Station, VRS, Flaechen-Korrektur-Parameter, FKP and Master Auxiliary Concept, MAC.

In spite of the ionospheric problems in the equatorial region, the number of single frequency receivers in use for precise positioning is on the increase as compared with the relatively few multiple frequency receivers. This has necessitated the investigation of the code-plus-carrier processing approach which uses the idea of opposite signs of the propagation delay of the ionosphere in the code and carrier signals to eliminate the ionospheric delay, which normally requires dual frequency receivers to do same. This improved processing technique has led to the achievement of an accuracy of 5 cm with single frequency over a distance of 194 km. Sub-decimeter is generally achieved after 12 hours and 18 hours of observation for a distance of 200 km and 1200 km respectively with this technique as shown in this study.

In addition to the improved processing techniques, the ambiguity that characterizes the use of mean-sea-level for the definition of vertical references as a result of either the sea level change or movement of the earth crust can be resolved with the use of GNSS which is independent of these two phenomena. This is achieved by collocating a GPS base station at the reference tide gauge located at Takoradi. The orthometric height derived from the tide gauge and the corresponding ellipsoidal height at the collocated GNSS base station is used to determine the local quasi-geoid. This is compared with the global geoid derived from EGM96, the global model from NGA, to obtain a difference that can be applied as a correction factor to obtain orthometric heights. The release of EGM2008 which has undergone remarkable improvement over EGM96 in terms of resolution makes it important to investigate into how it can be used to improve the orthometric height determination using ellipsoidal heights from GNSS observation. This can be achieved by following up what has been derived with EGM96 at the Takoradi tide gauge with this newly released EGM2008.

To be able to move through a smooth transition from the existing geodetic reference system based on the War Office Ellipsoid to the newly established system based on the geocentric ITRF05, a set of seven parameter transformation has been derived for the project area, the Golden Triangle of Ghana.

Table of Contents

Zusammenfassung

Das Bestreben GNSS in Entwicklungsländern zu nutzen nimmt stetig zu, da man die zahlreichen Vorteile gegenüber herkömmlichen Verfahren der Positionierung, Navigation und Zeitübertragung erkannt hat. Afrikas Versuch, diese Technologie zu nutzen, gebietet es, die regionalen Probleme im Zusammenhang mit der Umsetzung durch die AFREF Mitgliedsstaaten zu untersuchen. Diese Abhandlung geht über die Errichtung eines GNSS Referenznetzwerks in Ghana hinaus, indem sie Lösungen zu einigen regionalen Problemen in der Umsetzung aufzeigt und untersucht.

Das Problem der turbulenten Atmosphäre, die schweren ionospärische Fluktuationen und sprunghafte troposphärische Bedingungen verbunden mit den sehr spärlich gestreuten Referenzstationen, hat zu der Entwicklung eines neuen Konzeptes von Korrekturverfahren, der Corridor Correction, geführt, die es ermöglicht, atmosphärische Einflüsse ähnlich wie etablierte Verfahren wie Virtual Reference Station, VRS, Flaechen-Korrektur-Paramter, FKP and Master Auxiliary Concept, MAC, zu korrigieren.

Trotz der Probleme mit der Ionosphäre in der Äquatorregion, übersteigt die Anzahl der Ein-Frequenz-Empfänger für die präzise Positionierung die der relativ wenigen Mehrfrequenzempfänger . Dies machte die Untersuchung des Code-plus-Carrier Prozessierungsansatzes notwendig. Dieser nutzt den Effekt von unterschiedlichen Vorzeichen bei der Änderung der Ausbreitungsgeschwindigkeit von Code- und Trägersignalen durch die Ionosphäre um den ionosphärischen Effekt zu eliminieren, was in der herkömmlichen Prozessierung Zweifrequenzempfänger benötigt. Diese verbesserte Prozessierungstechnik hat zur Erzielung von Genauigkeiten von 5 cm mit Einfrequenzempfängern über eine Basislinienlänge von 194 km geführt. Damit werden im Allgemeinen Sub-Dezimeter Genauigkeiten nach 12 Stunden Beobachtungsdauer für Basislinienlängen von 200 km bzw. 18 Stunden für Basislinien von 1200 km erreicht, wie diese Abhandlung zeigt.

Zusätzlich zu den oben genannten Verbesserungen in der Prozessierung, wird eine Methode aufgezeigt, die die Unsicherheit durch Meeresspiegeländerungen oder Bewegungen der Erdkruste, die der Gebrauch des mittleren Meeresspiegels als Definition des vertikalen Datums in sich birgt, durch den Gebrauch von GNSS, das von diesen beiden Phänomenen unberührt ist. Dies wird dadurch erreicht, dass GPS Basisstationen an Orten mit einer Pegelstation eingerichtet werden. Die orthometrische Höhe des Referenzpegels und die ellipsoidische Höhe der Basisstation werden dann zur Bestimmung eines lokalen Geoids verwendet. Das in dieser Abhandlung verwendete lokale Geoid ist an das globale Geoid angeschlossen worden, das aus dem EGM96, dem Modell der NGA, abgeleitet ist. Die Veröffentlichung des EGM2008, das gegenüber dem EGM96 im Hinblick auf die Auflösung erfahren hat bedeutende Verbesserungen, erfordert es, zu untersuchen, wie es Ghana zur Bestimmung von orthometrischen Höhen durch GNSS Beobachtungen nutzen kann. Das kann durch eine Weiterentwicklung des Ansatzes erreicht werden, der in dieser Studie schon mit dem EGM96 für Ghana bei Takoradi begonnen wurde. Das hierbei aufgebaute GNSS Referenznetzwerk wurde an den Pegel von Takoradi angeschlossen, einem der ältesten Level auf dem afrikanischen Kontinent.

Um einen glatten Übergang vom vorhandenen Referenzsystem, das auf dem War Office Ellipsoid basiert, zum neuen, auf dem ITRF05 basierendem System zu ermöglichen, wurde ein Satz von sieben Transformationsparametern abgeleitet, die auf den Messungen im Projektgebiet „Goldenes Dreieck“ in Ghana basieren.

Table of Contents

Table of Contents

Table of Contents

Table of Contents

Table of Contents

List of Figures

List of Figures

List of Figures

List of Tables

1 Introduction

1.1 Global Navigation Satellite System and Ghana

Global Navigation Satellite System (GNSS) is gradually becoming a household feature in most developed countries and its usage by default, is an indicator of the level of development in all the countries around the globe. For this reason and the continuous reduction in the cost of its equipment, there has been a recent scramble for its introduction into the developing world and Ghana is at the forefront of these GNSS seekers.

Countries may be categorized into three groups as far as GNSS is concerned. There are the countries that own this space technology, which includes the space vehicles with the generated signals and some augmentation systems. These countries are the United States of America with Global Positioning System (GPS), Russia with the improving GLONASS and the European Union with the fast approaching Galileo, and this category may be sooner or later, be joined by China with the Beidou (Compass). The second category includes those countries that do not have the space vehicles but are developing various complex augmentation systems to maximize the benefit of GNSS, like Japan with MSAS and QZSS, India with GAGAN, Canada, Australia and a few others. The third category is the set of countries that do not have any of these and at best use simple single-base station differential correction systems and it is in this third category that Ghana can be placed. The countries in the third category are generally characterized with lack of GNSS infrastructure, expertise and with little or no motivation to adopt and develop GNSS and its applications which could enhance their general development. These countries need good government policies, strong political will, human resource development, public and private participation for effective utilization of this technology. This may be the only way to reverse the ever widening gap between the third group and the rest in terms of development especially in GNSS.

The initial introduction of the use GNSS in Ghana in the middle of nineteen-nineties did not get the reception it deserved since it was perceived not to be accurate enough for almost all applications that the surveying and mapping experts required. As years went by, the drastic change in GNSS technology has made it very attractive to the survey and mapping experts in Ghana as well as the prospective user community in Ghana. The improvement in GNSS has not yet been enjoyed in Ghana significantly due to lack of basic GNSS infrastructure, lack of adequate knowledge as well as lack of standard GNSS equipment. One of the main drawbacks is the skepticism of the decision-makers about the reliability of GNSS as compared with the conventional methods which they are used to.

Despite these setbacks, there have been popular requests for example as in (Kuntu-Mensah P. , 2006) to utilize this signal in space by the would-be user in the land delivery processes to ensure faster economic growth as promised by the Land

Administration Project (LAP) (Odame-Larbi, 2008); (Karikari, 2006), which aims at supporting the establishment of a multi-purpose geodetic reference network in Ghana for both local and international applications.
The decision makers, opinion leaders, public and private organizations still have not been sensitized enough by GNSS experts to make them understand and accept this technology and invest in it. This therefore calls for a systematic and pragmatic way of introducing this well tested and approved technology into a country like Ghana which needs it most, and this thesis aims to provide such service.

1.1.1 Global Navigation Satellite System in Ghana

Despite the numerous shortcomings in the exploitation of GNSS in Ghana, its use is gradually gaining popularity amongst some private and public organizations and the growth looks quite promising as users find it very convenient despite the problems they encounter due to lack of some basic GNSS infrastructure for differential corrections. One of the healthy developments is the acceptance and use of GPS by the National Mapping Organization, the Survey Department of Ghana, which has started using this technology for cadastral surveys, and is encouraging the private sector to do likewise, though on a small scale for now. With the establishment of the GNSS Reference Network (GRN) in the Golden Triangle of Ghana, and the plans for the coverage for the entire country, under the Land Administration Project, the country is now preparing to reap a reasonable benefit from this technology. The Building and Road Research Institute (BRRI), has started using this technology for research and development in the field of traffic and transportation and has now established a permanently running GNSS base station for its activities. Some mining companies have been running base stations for their survey and mapping needs, a few research institutions in the universities have been applying differential corrections for research and development components of their activities. Some private companies have also joined in the establishment of the reference stations in the country and have started trying to explore its potential. Most of the applications as at now however do not require very high accuracy and integrity but with the increasing interest in this technology, much needs to be done in terms of the accuracy and integrity to exploit the full potential for the benefit of not only the country but the sub-region. The establishment of a single reference network is an advantage over the emerging trend of various institutions trying to set up individual reference stations for different applications

1.1.2 The Challenges

The modest success made in the field of GNSS, especially with the establishment of the reference network in the Golden Triangle of Ghana and the formation of a team in charge of GNSS application by the Survey Department of Ghana, comes with a lot of challenges. These include lack of knowledge and solutions of the basic problems that

militate against the accuracy of the GNSS observations in Ghana which is located in the tropics between latitude 4°43’30" and 11°10’10" N. Prominent among these are the atmospheric delays, displacement of the ground station due to natural forces on the planet like attractions due to celestial bodies, plate tectonic activities, local effects and others. In addition, lack of basic infrastructure like easy access to communication facilities which may include internet, GSM, UMTS and other telemetric facilities limits the use of GNSS to only post-processing applications. Unreliable power supply poses a big problem and calls for the exploitation of alternative sources like solar power. While the use of single frequency receivers for precise surveying is generally decreasing in the category-1 countries, they are increasing in the developing countries like Ghana and this must be addressed as it poses problems especially in the equatorial regions. Lack of human resources leads not only to the problem of poor observation methods, but also poor data processing methods as well as inability to explore new areas where the system can be used. Lack of guidelines and standards for the user to make the best of the available resources is one of the shortcomings of GNSS as far as Ghana is concerned. The change from the Ghana’s old classical reference system based on the War Office 1926 Ellipsoid, to the GNSS-based geocentric ITRF has been a great challenge to the survey community due to the inherent inaccuracies in the original system that has affected the transformation parameters between the two systems. The vertical reference datum of Ghana, which has been referenced to the mean-sea-level observed at the discontinued Accra tide gauge has been a problem to surveyors and other map users not only due to the local infrastructural problems at the tide gauges, but also the ambiguity associated with the use of the mean-sea-level for vertical referencing in general. This thesis has tried to address most of the problems outlined above, most of which will be applicable to other developing countries especially those in the AFREF region.

1.1.3 The Socio-Economic Perspective

The utilization of the GNSS technology in Ghana has a huge impact on the socio-economic development of the country and this has been the main driving force for the implementation of the Geodetic Reference Network (GRN) under the Land Administration Project (LAP) by the Survey Department of Ghana which is to serve as the backbone to the all spatially referenced activities in the country. Ghana aims at implementing good land policies through appropriate land management and related activities to help in the economic growth and this space technology is to play a leading role in achieving this goal. GNSS is thus to ensure efficient and cost-effective land delivery system for the country, replacing the conventional survey methods which have stifled vital land delivery components like the compulsory Land Title Registration (LTR) (Kuntu-Mensah P. , 2006). The problem of poor land delivery has caused a lot of land disputes which does not only scare away investors and but also cause unrests in the society and hinders development. GNSS is therefore to be used as tool for conflict prevention and resolution, poverty reduction, food security, and

other socio-economic benefits. The recent Systematic Land Titling Project under LAP is a typical example of the use of GNSS in the land delivery in Ghana. Emergency response and disaster management, traffic and congestion management have been causing problems in the cities in Ghana. With GNSS as a tool, travel times can be reduced and this will lead to saving of fuel and in turn lead to the reduction of air pollution. Reducing air pollution will improve health of the community, increase wealth and productivity. The use of GNSS in meteorology will be improved and in the field of geo-informatics, the quality and cost of data capture for Geographic Information System GIS will be also improved. With these among others GNSS is expected to take the centre stage of the socio-economic development of Ghana and other countries in the third category, if well implemented.

1.1.4 The National Preparedness

The nation in general has started preparing for the take off of a functional GNSS infrastructure development, following the initiation of the LAP project, and the establishment of plant pool system to ensure that GNSS equipment can be rented out to users. The establishment of a GRN Office to maintain the geodetic reference network also indicates the national acceptance of GNSS and its usage. The interest shown by the private practitioners and government institutions is a positive indicator. The policy direction as to the changing over from the War Office to the ITRF, and the provision of GNSS reference points in the ITRF for users within the Golden triangle attests to the fact that the nation is prepared and is waiting for a project like this.

1.2 Aims and Objectives

The project aims at establishing a network of functional Geocentric Reference Network based on ITRF05/WGS84, to replace the existing classical Geodetic Reference Frame based on the War Office Ellipsoid in the Golden Triangle region of Ghana. This is to be achieved through the following objectives:

- Establishing first order control points in Ghana located in Accra, Kumasi and Takoradi based on the International Terrestrial Reference Framework (ITRF) coordinate system using the appropriate IGS stations on the African continent
- Provision of second and third order geocentric control points for the Golden Triangle of Ghana to serve as reference points for the GNSS user community
- Define the vertical reference datum of Ghana by linking the existing traditional mean-sea-level reference approach with this internationally accepted satellite geodesy technique in line with the AFREF proposals, for all countries in Africa.
- Provision of Transformation Parameters to link the old War Office coordinate system and the new ITRF established in this project to ensure conversion in both directions.

- Investigate into the drawbacks in the processing of GNSS data and the introduction of appropriate processing techniques including the code-plus-carrier approach for the optimum use of GNSS in Ghana.
- Investigate the ambiguity fixing under the Ghanaian environment in preparation towards the standard and recommended practice for the optimum use of GNSS
- Investigate into the appropriate atmospheric correction models suitable for the country with emphasis on the Corridor Correction concept developed in this project.
- Maintain the established reference network in Ghana.

1.3 Outline of Thesis

The **chapter two** deals with the existing old geodetic based on War Office 1926 ellipsoid, its shortcomings and the need to change to the geocentric ITRF, and describes mapping in Ghana based on the old system and ends with the potential applications expected with the introduction of GNSS. Augmentation systems have been explained in the **third chapter**, emphasizing on differential GNSS and introduces the new Corridor Correction concept, which has been developed in this study, especially for countries with fewer reference stations having problems with the atmospheric disturbances on the GNSS signals like Ghana. The **fourth chapter** is on the geocentric coordinate systems which Ghana wants to adopt and goes on to explain the design and the spatial distribution of a nationwide geodetic reference network, adding some considerations in telemetry. **Chapter five** deals with the design of the horizontal network within the Golden Triangle of Ghana as well as GNSS field data collection. The **sixth chapter** covers the pre-processing corrections at the station, during signal propagation and at the satellite position and the selection of appropriate mapping function for the processing. The **chapter seven** treats the data processing using the scientific software developed by the Federal Armed Forces University in Munich, PrePos GNSS Suite, for very long baselines between the primary stations and some appropriately selected IGS stations, and also for short base lines between the primary and secondary stations and uses adjustment module NEADS for the network adjustment. Off-the-shelve commercial software, Trimble Total Control, has been used for coordinating the reference markers. Transformation parameters for the project area between War Office ellipsoid and the WGS84 (ITRF05) have been determined using both the Helmert's Seven Parameter Similarity Transformation approach and the Polynomial Function approach in the **Eighth Chapter**. In the **Chapter Nine**, the establishment of infrastructure for the future definition of Ghana Vertical Datum is treated by the integration of GNSS to the traditional method of referencing to the mean-sea-level. Preliminary results of the geoidal separation investigation have been presented. The **Tenth Chapter** provides improved data processing and analysis by analyzing the code-plus-carrier concept which is used in processing long baselines with single frequency data and also

investigates the optimum use of GNSS in the Ghanaian environment by analyzing various techniques for ambiguity fixing. The **Eleventh Chapter** is devoted to the new innovation of this study, the Corridor Correction Concept, going through the development of the concept and analyzing its effectiveness using data from Germany in the middle latitude and Ghana in the lower latitude. This concept is compared with the Area Correction Parameter approach as well as other methods for precise positioning. The final chapter which is the **Twelfth Chapter** gives summary of the major conclusions and recommendations for future development of GNSS in Ghana.

2 Surveying and Mapping in Ghana

2.1 Mapping in Ghana

Ghana is a West African country located between latitudes 4° 30´ N and 11° N and longitudes 3° W and 1° E, Ghana's Geodetic Survey started as far back as June 1904 by the Governor of the then Gold Coast, Gordon Guggisberg, who made observation for latitude from a pillar in Accra with a zenith telescope, to 15 stars giving the final probable error of 0,360″. According to (pp. Gold Coast Survey, 1936)(Mugnier, 2000), the longitude was also observed in November and December of the same year by exchanging telegraphic signals with Cape Town in South Africa. These have been adopted as the basic longitude and latitude for the country although it was found not to be very accurate as later works proved that the Accra measurement was influenced by local attraction. The coordinates from both triangulation and traversing were computed using the transverse mercator projection system and heights were measured with aneroid barometer. Further astronomical observations were taken at four different stations, West End Base of Akuse, North End Base of Obuasi, Apam and Nsuta by the Astronomical Wireless Party in 1925. More accurate time and the rate of the chronometer were obtained by means of time signal from Bordeaux and Lyon. The astronomical coordinates compared well with the trigonometric coordinates as stated in (pp. Gold Coast Survey, 1936). These formed the basis for the computation of the geographical coordinates of Ghana, adopting War Office ellipsoid as the figure of earth for the then Gold Coast.

The War Office ellipsoid has the following parameters:

Semi-major axis (a) = 20926201.2257 feet

Semi-minor axis (b) = 20855504.6001 feet

Flattening (f) = (a-b)/a = 1/296

Conversion factor (feet/meter): 1ft = 0.3047997062 m

a = 6 378 300 m

This system was used alone until 1977 when the control network was improved and readjusted with more observations and the use of improved computation techniques resulting in the proposed change from the War Office ellipsoid to the modified Clarke 1880 ellipsoid (Legon datum) with the following parameters:

a = 6 378 249 m

1/f = 1/293·465

Since there was no official endorsement of the Clarke 1880 (Ghana modified), the use of the War Office ellipsoid persisted till now. There are however some data

running on this and has been creating confusion for users who sometimes mix them up. (Graham et al, 2000) highlights on this concurrent running of reference systems in Ghana.

2.1.1 Geodetic Network Frame of Ghana

The Ghana framework diagram of Geodetic Network which is a blend of triangulation, traverses and precise levels, is covered with triangulation points with baselines of up to a maximum of about 55 miles and is controlled by three measured bases; one base near Krobo Odumase in the Eastern Region, the second one is at Obuasi in Ashanti Region and a third at Laura in the Brong Ahafo Region. The triangulation was mainly in the mountainous south, up to latitude 8º 20' N and parts of the Volta Basin; the northern regions and the coastal lowlands were covered with traverses. These were supplemented with secondary traverses and primary levels. Primary traverses are found along the coastal belt with the exception of less than 100 km stretch between Accra and Apam in the Central Region of Ghana which has triangulation points. This network was published by the Survey Department in 1970, and is what has been used to provide controls for mapping in the country.

In the existing framework, controls are very sparse in most areas of the country especially in the Northern Regions of Ghana making it difficult to reference landed properties to the National grid. Another common problem with this network is the obliteration of the reference point monuments, which has rendered most of the points unusable as they are sometimes difficult and expensive, under the conventional survey methods, to re-establish them after they have been tempered with or destroyed, usually out of ignorance.

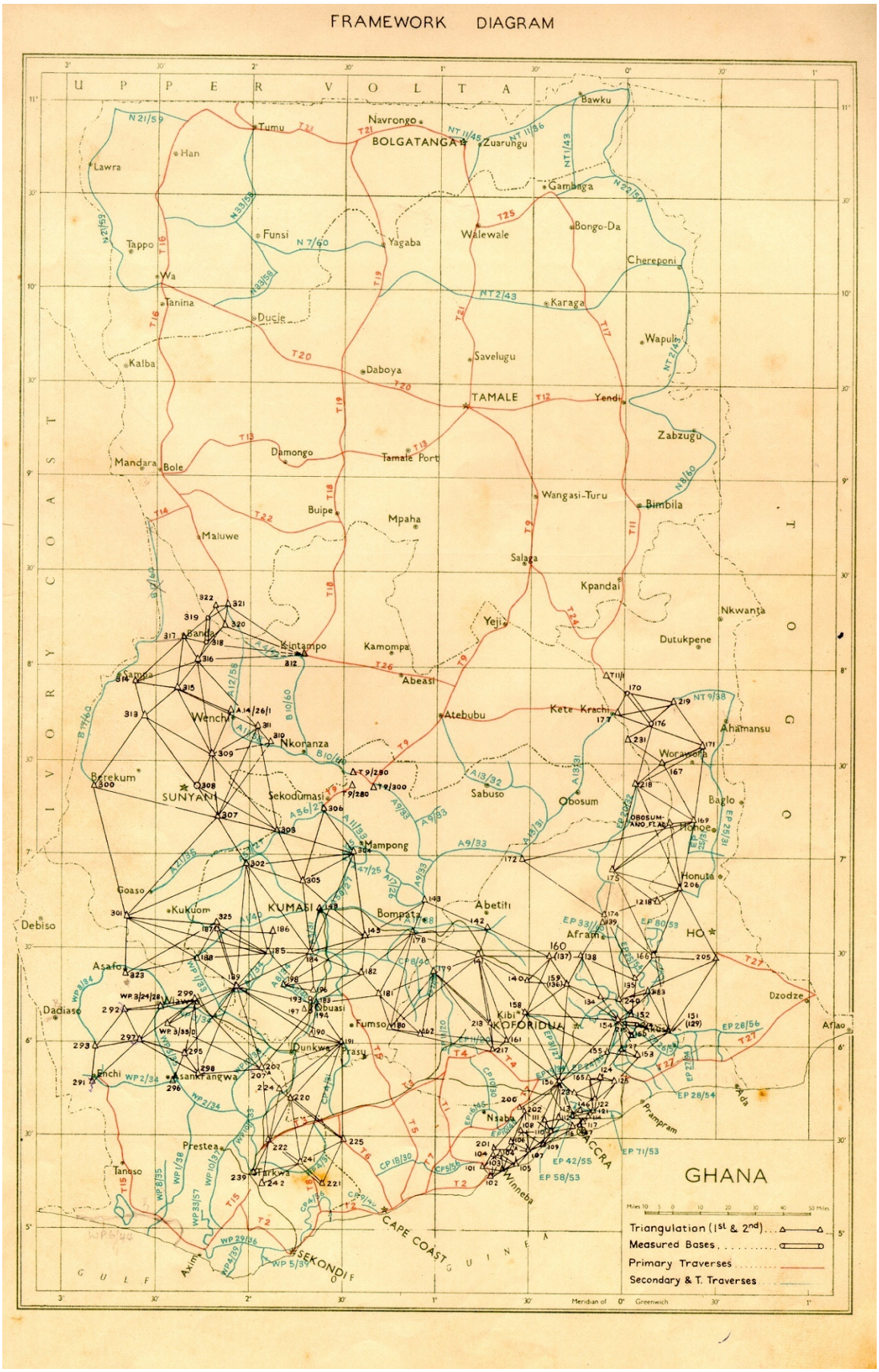

Figure 2-1: Map of Ghana showing the triangulation network and the primary and secondary traverses. (Source: Survey Department of Ghana Report of 1966)

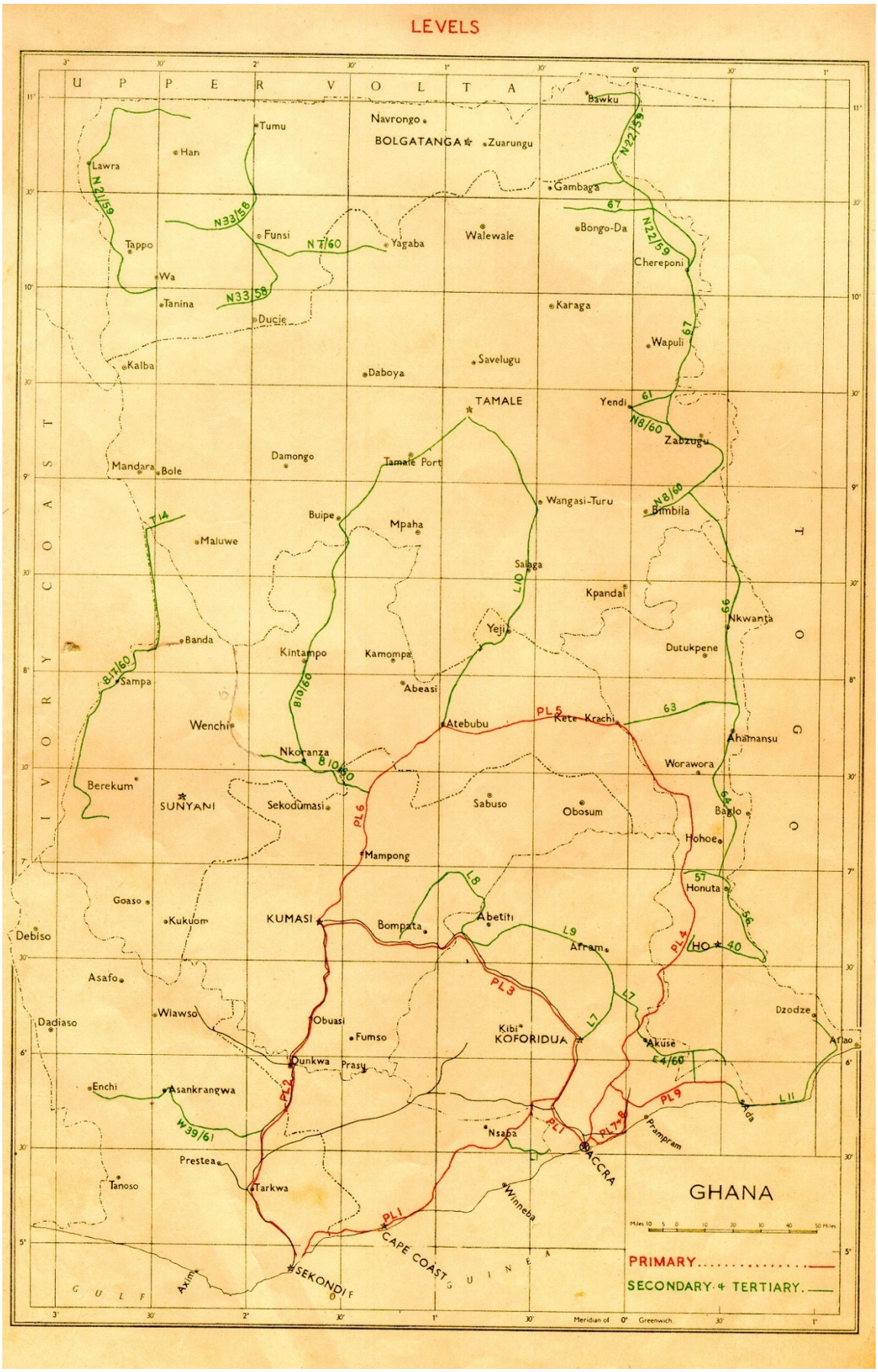

Figure 2-2:Map of Ghana showing the Primary, Secondary and Tertiary Levels.(Source: Survey Department of Ghana, Report of 1966)

Primary leveling in Ghana started in 1933 referencing to the MSL in Accra along the main road to Takoradi. The second primary level PL2 was undertaken from Takoradi to Kumasi, followed by from Kumasi to Accra PL3. The loop comprising of PL1-6 run from Accra to Kete Krachi through the Volta Region, through Atebubu in the Brong-Ahafo region, through Mampong in the Ashanti Region and ended in Kumasi. The level lines PL7-8 were made along the coast of Accra, and PL9 takes off from PL4 and ends at Ada. Secondary and tertiary levels have been run at various parts of the country.

2.1.2 The Ghana National (Colony) Grid

For cadastral applications, geographical coordinate system had to be converted to a more convenient system, so Gold Coast (Ghana) had to adopt a plane rectangular coordinate system on the Transverse Mercator Projection. The country was placed on the same origin of 4° 40' N for X coordinates and 900000 ft added to the Y coordinates to avoid negative coordinates. A central meridian of 1° W was adopted for the country and a scale factor of 0.99975, making the scale error exceeding the projection values only at the extreme ends of the country.

2.1.3 Geographic Transformation System

The mapping systems used in Ghana generally do not have any officially confirmed parameters to transform it into an international geocentric system like the WGS84 or the ITRF. There is the Three-Parameter Transformation from the National Imagery and Mapping Agency (NIMA) of the USA (Mugnier, 2000), the UK Military (Graham et al, 2000) and other local and foreign organizations but these are not approved officially by the Director of Surveys hence they cannot be used to work officially. The urgent need to derive the National Transformation Parameters became apparent after it was realized that land delivery system in the country could be greatly improved with the use of GNSS. Under the Land Administration Project, (LAP) in collaboration with the Institute of Geodesy and Navigation of the University FAF Munich, an acceptable Helmert's Seven Parameter Transformation for the Golden Triangle of Ghana has been derived and is undergoing field test. A nationwide set of transformation parameters is yet to be derived in the second phase of the GRN under the LAP.

2.1.4 ITRF as a National Reference System

The International Terrestrial Reference Frame (ITRF) was formed from the contributions of space geodetic solutions for global set of coordinates and velocities combined. This frame specifies how its origin, orientation, scale and their time evolutions are materialized. It has the center of mass of the earth as its geo-center.

Its defining parameters are implicitly defined by the combination of worldwide tracking sites of VLBI, SLR, DORIS and GPS (GNSS) involved in the IERS global solutions.

Although the coordinate frame of the WGS84 is accessible through broadcast and precise ephemeris there is an advantage of using the ITRF due to the associated velocity at each station which indicates its time-dependent absolute displacement associated with movements in the earth's crust. The ITRF has undergone improvements, with only 13 fiducial GPS stations collocated with SLR or VLBI used for the coordinates taken from ITRF92, ITRF93, and ITRF94 successively, the limited distribution and availability, and performance of the fiducial network was improved by 1997. With the introduction of ITRF96 on March 1998, the set of fixed fiducials was greatly expanded and improved to 47 sites, and later to 51 with ITRF97 on 1 August 1999. The ITRF2000 orientation time evolution was believed to satisfy the no-net-rotation (NNR) conditions at about 2 mm/yr level or better. (Ray et al, 2005). The current realization ITRF2005, like the preceding ones, included the four techniques IGS, ILRS, IDS and IVS, but with increased number of stations, about 800 stations at about 500 locations. However unlike the previous ones, the ITRF05 included the daily Earth Orientation Parameters (EOPs) and time series of station positions which according to (Altamimi, et al, 2007) is consistent with the combined or C04 and pole motion and length of day LOD is as good as the official IGS combined series 30 μs for pole motion and 15 μs for length of day.

As explained by (Arias E. F.; W. Lewandowaki, 2008) the ITRF, whose orientation is maintained in continuity with the past international agreements endorsed by IUGG, is aligned with WGS84 at a few cm-level similar to that of the future Galileo Terrestrial Reference Frame (GTRF) which is also aligned at a few cm. Other systems that is linked to this primary system ITRF, is the PZ-90 used by GLONASS, which is fast approaching its full operational capability. Though the PZ-90.02 (2007) agrees better than 40 cm, with the use of transformation parameters as derived for example by (Rossbach, 2001) it can be as an additional option for positioning like other GNSS systems. With these systems basically aligning to the ITRF it is advantageous to adopt it as a national reference system in order to make the use of GNSS easier in Ghana especially as Galileo is fast approaching its operational capability. The adoption of the ITRF as a country, on the African continent is also in line with a requirement of AFREF (Neilan, R., Wonnacott, R, 2002).

2.1.5 Map Production in Ghana

The Survey Department of Ghana which produces the core dataset for the country is the main institution in charge of mapping in Ghana. With offices in all the ten regions of Ghana, the organization has representation in all the one hundred and twenty districts in the country and has basic data covering the whole country. There are other organizations that produce maps but they usually use the core data sets of the Survey department to produce thematic maps.

The Department has produced various map series including the 1:1250, 1:2500, 1:50000, 1:2500000 and others. The department is also responsible for Geodetic Framework Diagram, Photomaps (1:2500), other aerial photographs, digital maps and others. Their large scale maps cover only the major cities and towns and some of these are produced by private survey companies and it is checked and approved by the Director of Surveys or his representative. These are usually contracted by the Stools or the Skins, the Ghanaian traditional designation of the monarchical authorities, to which land is vested. The Photomaps, like the large scale base maps also cover only some of the major cities, they were flown under the Urban II Project of the World Bank, aimed at developing the infrastructure of the selected cities (Poku-Gyamfi, 2000). The digital maps include 1:2500 cadastral maps and 1:50000 topographical databases.

Organizations like the Centre for Remote Sensing and Geographic Information Services (CERSGIS) of the University of Ghana, Council for Scientific and Industrial Research (CSIR), Meteorological Services Department, Ghana Minerals Commission, Lands Commission, Wildlife Division, Volta River Authority (VRA), Ghana Statistical Service, Ghana Highway Authority (GHA) and many others are in charge of various thematic maps of the country but these institutions mainly use the base maps of the Survey Department.

The mapping needs of the country are diverse and need a lot of coordinated efforts to meet the ever growing demands of the nation. With many organizations preparing various maps for different applications, a lot of precious funds are wasted due to duplication as well as incompatibility of their spatial data resulting from different standards for the preparation of the maps. This led to the formation of the National Framework for Geospatial Information Management (NAFGIM), an offspring of the Ghana Environmental Resources Management Project (GERMP) which was organized between 1993 and 1998. This was to facilitate data development and management and the building of metadata. A Spatial Data Infrastructure (SDI) was thus created to facilitate mapping in Ghana.

Private mapping organizations are also playing a very important role in the mapping industry in Ghana. Although the Survey Department of Ghana is the national mapping authority, private mapping agencies also contribute a lot, from flying aerial photographs, production of digital maps and cadastral maps. Some of these private companies have started the use of GPS and are yet to reap the full potential of it due to some bottlenecks that include lack of basic GNSS infrastructure, standards and specifications. Due to the high demand of mapping experts in the country, there is another category of engineers who though are not licensed get into cadastral surveying but who have to be checked by a licensed Surveyor before their products can be accepted officially.

2.1.5.1 Cadastral Mapping in Ghana

Cadastral mapping which is an integral part of cadastral system plays an important role in land use, planning and administration. This is yet to be well developed in Ghana to let it play its expected role in the general land management. In Ghana the impact of cadastral survey is felt only in the cities and towns whilst the rural areas are in most cases neglected. Apart from a few plans executed by surveyors and referenced usually to the base maps for land ownership documentation, ownership and records are mainly by oral tradition and at best demarcation with special trees as monuments. These usually lead to a lot of land disputes which sometimes end up in very unfortunate incidences. Recently there were about sixty thousand cases involving land disputes in the law courts of Ghana and it is believed that similar number was before the various houses of chiefs (Prah, 2004). This is a big drain on the national economy and a hindrance to sustainable development.

Contrary to the problem of the absence of cadastral maps in the rural areas, a number of towns and cities in all the ten regions in Ghana have cadastral maps at the scale of 1:2500 with a few of them benefiting of photomaps at the same scale and these are used for physical planning schemes. With the decentralization of the Survey Department to all the 115 districts in Ghana, it is expected that all these district capitals and some major towns will have their base maps prepared for cadastral activities for development. The biggest challenge in cadastral mapping is the rate at which the cities are spreading, which is faster than the production of cadastral maps. This leads to uncontrolled and haphazard development and reduces the value of the land which causes drain to the economy.

A lot of measures have been taken by the Government, mapping agencies, and the donor agencies like the introduction of the Land Title Registration in 1986 PNDC Law 152, the Land Administration Project (LAP) which is financed jointly by six international institutions, the Urban Land information System which is jointly organized by the Ministry of Local Government and Rural Development of Ghana and the Swedesurvey of Sweden (SWEDESURVEY, 2004). These entire efforts hinge round a good mapping system and for Ghana to be successful, cost-effective survey methods must be used, and it is not surprising that GPS has been proposed for cadastral mapping in Ghana. According to (Kuntu-Mensah P. , 1997) the field survey methods as currently used, are not the cheapest, fastest, or most cost-effective and the accuracies being imposed are overly burdensome for initial parcel delineations. Means of upgrading accuracies of parcel delineations over time should be considered. The Survey Department and the Survey profession should be less expensive, fast and proven technologies like GPS for Cadastral surveying is most appropriate

Cadastral Surveying is mainly executed by private companies and has to be checked and approved by the Survey Department. Production of base maps is sometimes executed by the surveyors usually financed by the custodian of the land, and on

completion submitted to the Regional Surveyor who checks and approves it before it is sent for physical planning at the Town and Country Planning Department (TCPD). On acceptance and approval by the political head of the District and the Director of the TCPD it is sent to the surveyor for demarcation for individual land users. In some cases production of cadastral maps are financed by the District Administration but in consultation with the skin or stool that owns the land.

A few areas in the major cities have been declared Land Title Registration Districts which is a result of the enactment the Land Title Registration Law of 1986 (PNDCL152, 1986) which aims at bringing sanity in land transactions. Experts are still advocating for the use of GNSS for cadastral survey component to enhance the rate of land registration as the use of the conventional survey methods is not only time consuming but expensive. This will go a long way to alleviate the land problems due to population growth, land ownership insecurities, costly adjudication of land disputes and litigations and hindrance to infrastructure developments.

2.1.5.2 Thematic Mapping in Ghana

The Survey Department after producing the base maps, which comprises mainly 1:2,500, 1:25,000, 1:50,000 1:250,000 map series, Geodetic Framework, Aerial Photographs, Photomaps, National, Regional and District boundary maps and other, in both analogue and digital formats make them available to various organizations to add on their themes. Some institutions like CERSGIS, Soil Research Institute (SRI), Environmental Protection Agency (EPA), Forestry Commission, Institute of Renewable Natural Resources (IRNR) and a few others that have their own GIS laboratories digitize the Survey Department's analogue maps and add on their appropriate themes, for example satellite imagery by CERSGIS, soil and ecological maps by SRI, forest reserve maps by the Forestry Commission and others. Other organizations use the digital maps produced by the Survey Department as the base maps for developing their thematic maps.

In all cases data needs to be collected from the real world and these spatial data, in order to optimize cost data has to be collected with the best and appropriate methods and most organization prefer the GNSS approach. Some of these organizations have started using GPS although the infrastructure has not been well developed. The enthusiasm in the potential GNSS user agencies and individuals is commendable.

2.1.5.3 Topographic Mapping in Ghana

The Ghana Government through the assistance of other international bodies including the Canadian Government has been able to cover the whole country with the topographic maps in the 1:50000 series and an earlier version 1:65000 series. These are the main base maps for most thematic maps of the country. Notable

among them is the Geological maps of Ghana which covers the whole country at the scale of 1:50000. Though, the topographic maps have not been revised for decades, most of the core data sets like the drainage, contours and political boundaries have undergone very little changes. Road networks, human settlements and other important features must be used with caution as there have been significant changes in them over the years. GNSS can play an important role in the map revision of the topographic maps.

2.1.5.4 Digital Mapping in Ghana

The demand for Digital maps is on the increase in Ghana due to the awareness created by the Spatially Aware Professionals on the versatility of Geographic Information System, GIS. The training institutions, especially the universities are shifting emphasis on GIS hence digital map production. The Department of Geomatics of the Kwame Nkrumah University of Science and Technology, KNUST, the Geography Departments of the University of Cape Coast and the University of Ghana have set up GIS laboratories and are training graduates for the industry. Institutions within the universities like the Centre for Remote Sensing and Geographic Information Service, CERSGIS of the University of Ghana and the Institute of Renewable Natural Resource IRNR of the KNUST have GIS laboratories and produce digital maps. Other institutions like the Soil Research Institute of the CSIR, the Environmental Protection Agency, the Forestry Commission and others produce digital maps as well.

The Survey Department of Ghana is the main producer of digital maps for the country. The above mentioned institutions mostly use the core data sets produced by the Survey Department or digitize the analogue maps produced by the department.

Some private organizations also produce digital maps on subscription. These companies are linked to some international agencies like Digital Globe System that delivers high-resolution imagery and geospatial data that seamlessly integrate with any existing information management systems. This is yet to be tried and tested in the Ghanaian system.

2.2 Vertical Datum of Ghana

The mean sea level is commonly used to define the vertical datum since it provides the materialization of an equipotential surface. Tide-gauges are normally used to estimate the mean sea level by averaging (preferably) continuous observations of the vertical variations of sea level with respect to physical markers located on a stable solid ground. The time-series should be long enough, over 18.6 years, (Baki Iz, 2006), in order to remove variations associated with tides and other short-period effects. The definition of the vertical datum for the country which is part of this study has been treated in Chapter 9

The vertical datum for Ghana at the moment is defined by the reference to the mean sea level obtained from the tidal observation from a point in Accra from 9th April 1922 to 30th April 1923. This was linked to an established monument GCS 121 which was consequently linked to the trigonometric network to obtain the orthometric heights for the points in the network (Gold-Coast-Survey, 1936). This reference point in Accra was used for the first primary levelling from Accra along the main road to Takoradi which started in 1933, by which time the tide gauge at Takoradi (1927) had been established. Due to the significant changes in the mean sea level at Takoradi annually, another tide-gauge was established at Tema, in 1963 for the sake of comparison and control for the levelling in the country. The Tema gauge is no longer working but plans are far advanced to restore it.

The vertical variations at the tide-gauges could be due the rise in sea level resulting from the global warming phenomenon or the solid earth motion like the tectonic plate movement. In the case of Southern Ghana, where these tide-gauges have been installed, seismic activity can be an important cause for sudden variations. Two major earthquakes occurred on the mainland in Accra in 1862 and 1906 and a third, an offshore one, was experienced in 1939. The later occurred after the establishment of the vertical datum with the Accra tide-gauge. The use of an integrated system (collocating GPS station near the tide-gauge) can contribute to the monitoring and quantifying of such movements with direct consequences in the Vertical Datum of Ghana.

2.3 Role of GNSS in Surveying and Mapping in Ghana

Surveying and Mapping are some of the main applications for which GNSS is expected to be used in Ghana. For example the Land Title Registration which started in 1986 has been crippled due to the backlog of works that has been left undone as a result of the use of the conventional survey methods. The Ghanaian economy depends mainly on the land, farming, lumber production and mining which are the main foreign-exchange earners are all land dependent. Land has got a remarkable socio-political value to the Ghanaian, thus there are always problems especially boundary disputes between stools, skins, families and individuals due to poor land management. Fast and cost effective survey and mapping coupled with good tenancy agreements, is the solution in the Ghanaian land management system. The numerous cases at the government courts and the traditional courts, which has been a drain on the economy as well as a hindrance to development, will be minimized. The use of GNSS for surveying which is not only fast and efficient but also cost-effective, is a better option as compared with the conventional surveying methods which currently dominating surveying and mapping in Ghana

2.3.1 Potential GNSS Applications in Ghana

The Global Navigation Satellite System technology is yet to be tapped by most developing countries, and Ghana is not an exception. Due to its numerous advantages, many experts have proposed this technology as a means of accelerating development in a sustainable manner (Henaku, 1999);(Silayo, 2005). In Ghana, the potential of GNSS is enormous and the following are just a few of them.

2.3.1.1 Traffic and Transportation Applications

GNSS has a great potential in the Traffic and Transportation sector in Ghana. This can be in the field of route and engineering surveying, navigation, fleet and congestion management, route inventory taking, research and development and many others. Air and water transports will benefit from this technology. The approval of NEPAD to utilize EGNOS is in the right direction (NEPAD, 2004). The Ghanaian harbours can utilize broadcast corrections from GNSS base stations to guide vessels to dock. The rail and road sector of the Ghanaian transportation will benefit most as they constitute over 95% of the vehicular transportation in Ghana. With the formation of the Ghana Ambulance Service for emergency response, the need to incorporate real-time ambulance monitoring in Ghana cannot be overemphasized. Expert advice is required in the field of GNSS for this purpose. The Building and Road Research Institute (BRRI), which is in charge of traffic and transportation research in Ghana has planned to integrate GNSS as one of the tools of their research in this field. With the problem of traffic flow, road administration, precise vehicle location, congestion management, pollution assessment in our cities, GNSS technology will be very appropriate.

2.3.1.2 Geographic Information System

Geographic Information System has become an important tool in the daily activities of most research and development activities in Ghana. Private and public organizations are now using it to their advantage as it gains popularity in their activities. This has led a lot of institutions to invest in this technology. Training institutions are emerging and a lot of people are now seeing it as an inevitable tool in the development of a nation in a sustainable manner.

With the Survey Department producing the core data sets which is used by most institutions, the rest of the data must be collected by these institutions to generate their required outputs. It is generally known that data acquisition takes about three quarters of the cost of producing GIS solutions. An efficient and less expensive method of data collection must be sought for, and since most of the data is spatial, GNSS has proved to be the best choice all over the world. GPS is used not only for core data set preparation but also the thematic data collection as well.

2.3.1.3 Geodynamics Studies

Ghana is located on the south-eastern margins of the West African craton, although it is far away from the major earthquake zones that mark the present day lithospheric plate boundaries, it has however suffered from damaging earthquakes dating as far back as 1636. Three major ones occurred on 1862, 1906 and 1939 and it has suffered many minor tremors. Most of these earthquakes are located in south-eastern Ghana in the vicinity of the capital city Accra (Amponsah P. , 2002);(Andam, 2004). The heavily faulted area on the eastern coast around Accra is very active and continuously registers below 4 on the Richter scale. Experts are predicting high fatalities should there be any earthquake and are estimating that should the 6.5 Richter which occurred on June 22 1939, had occurred in 2000 the fatalities of 17 out of the population of 77,000 would be 600 out of the population of 1,719,100, using a linear regression estimates (Andam, 2004). This will be far worse today with the population over 2.5 million.

In view of the economic, social and political role Accra plays in the life of the Ghanaian, and some of the cities and towns along the coastal region of Ghana, it is very important to scientifically study the crustal activities in these areas so as to be able to know more, predict and mitigate the events of earthquake. Opinion leaders are showing concern and it is now time for GNSS experts to team up with the Geological Survey Department, which is working hard with other methods to investigate the seismic activities in this region as, pertains in many parts of the world with the GNSS technology.

2.3.1.4 Engineering Survey and Deformation Studies

With the recent increase in physical infrastructural development, time has come for engineers to come out with better ways of executing their construction and other engineering application. The tremendous improvement of GNSS in accuracy, availability and continuity of service makes it the best candidate for most of the applications and can execute high quality jobs at very competitive costs and benefits. Gradually Ghanaian cities especially Accra are attracting high-rise buildings and as has already been explained, some of the cities are heavily faulted and therefore these buildings need to be monitored for subsidence and other deformation studies and with GNSS this can be achieved at a reasonable cost. Other structures that require monitoring using the GNSS technology include the Akosombo Dam which holds the Volta Lake, one of the biggest artificial lakes in the world which generates almost all the electrical energy in the country. Due to the important role it plays in the life and economy of the country it must be monitored to realize any deformation. Other structures like the Adomi Bridge and all the major bridges require the same treatment and the preferred method is the GNSS approach.

2.3.1.5 Applications in Agriculture Sector

Ghana being an agrarian country stands to benefit if GNSS is applied in the agricultural activities, especially in precision farming, product delivery etc. Recent studies by CERSGIS (pp. Faalong et. al., 2006) showed how GPS-GIS integration has helped in the mapping, harvesting and delivery of pineapples for the farms for on-time delivery to European importers. Mechanized farming which is gradually being developed in the country will be enhanced with the application of GNSS for the purposes of land acquisition, preparation, cropping, and addition of fertilizer, harvesting and transport of products. The installation of a reference station at Winneba basically for the benefit of agro-industries in the neighboring area in September 2008, testifies to this assertion.

2.3.1.6 Mining

Mining which follows Agriculture in contribution to economy of Ghana, stands to benefit with the development of GNSS in the country. Due to the advantage in its usage, some mining companies have started using this technology for most of their mapping needs, (Pudder, 2006) gives several applications of GNSS in Ghana which include the mining.

3 Differential GNSS (Augmentation) Techniques

3.1 Positioning with GPS

There are two fundamental observables for positioning with GNSS: pseudorange (code) and carrier-phase, which are both subject to errors, systematic and random. The geometric range between the satellite and the receiver which is usually distorted by lack of synchronization, the media of propagation, usually the ionosphere and the troposphere and others. The carrier-phase technique is based on interferometric measurements of the carrier frequencies.

3.1.1 Pseudorange (Code) Measurement

Pseudorange is a measure of the distance between the satellite and the antenna of the receiver, given by the time difference between the epoch of signal transmission at the satellite and the epoch of its reception by the receiver. The transmission time is which is measured by correlating identical pseudorandom noise (PRN) codes generated by the satellite with those generated internally by the receiver, is plagued with unavoidable errors including the timing, atmospheric errors, orbit errors. The general expression for the pseudorange is given as in Equation 3-1. Literature on this has been widely written and can be obtained from (Seeber, 1993); (Leick, 1995). The measured range is always longer than the geometric distance as the signals encounter the dense atmosphere.

Pseudorange:

$$\mathrm{PR} = \rho + c(dt_r - dt^s) + \delta I + \delta T + \varepsilon_{Code} \qquad 3\text{-}1$$

Where,

PR	Pseudorange between receiver R and satellite S
dt_r	Receiver clock correction
dt^s	Satellite transmit correction
c	Speed of light in vacuum
ρ	true range
δI	ionospheric delay
δT	tropospheric delay
ε_{Code}	Pseudorange noise

Two different codes are used, the coarse acquisition (C/A) code and the precise (P) code. The C/A pseudorange, which has a wavelength (24 MHz bandwidth) of 300 m is ten times as long as the P code which is 30 m and respectively have frequencies or chipping rates of 1.023 MHz and 10.23 MHz. Rough rule is that peak correlation

function can be determined to 1% of width (with care) (Herring, 2003), therefore 3 m for C/A code and 0.3 m for P code.

3.1.2 Carrier Phase Measurement

As far as a receiver is locked on a particular satellite, there is an additional measurement aside the codes based on Doppler frequency shift on the carrier frequencies. There is a wavelength count as well as the advance in carrier phase determined by integrating the carrier Doppler frequency offset over the interval of an epoch. At the end of each epoch a fractional phase measurement is made by the receiver. This represents the difference between the phases of the receiver generated carrier signal and the carrier signal received from a satellite at the instant of measurement. The phase of the received signal at any instance can be related the phase at the satellite at the time of transmission in terms of the transit time of the signal and this carrier phase measurement can be written as,

$$\varphi = \rho + c(dt_r - dt^s) - \delta I + \delta T + \lambda N + \varepsilon_{Phase} \qquad 3\text{-}2$$

Where,

ρ	geometrical range between satellite and receiver
N	carrier phase integer ambiguity
λ	carrier wavelength
δI	ionospheric delay
δT	tropospheric delay
ε_{Phase}	carrier phase noise
dt_r	receiver clock correction
dt^s	satellite transmit correction
c	speed of light in vacuum

The relative motions between satellites and receivers accounts for the changing Doppler frequency shift on the frequency bands. Integrating this Doppler frequency offsets results in an extremely accurate measurement of the advance in signal carrier phase between time epochs (Cosentino, R. J., D. W Diggles, 1996). This however has problem with integer ambiguity which remains constant as long as the carrier tracking loop maintains lock and must be resolved to benefit from the extreme accuracy of the carrier phase measurement.

Both the code and carrier measurements are corrupted by a variety of biases and errors which have to be kept at appreciable levels to be able to attain the resolution level of 1% or better of the wavelength of the carrier signal that is 3 m for code measurement and 2 mm for carrier phase measurements.

These biases are the satellite dependent ones like the ephemeris and satellite clock errors, receiver dependent biases like the receiver clock and noise, station coordinate errors and observation dependent ones like the ionospheric and tropospheric delays and carrier phase ambiguities. The errors may include carrier phase cycle slips, multipath disturbances antenna phase offsets and others.

All GPS-based positioning techniques operate under a set of constraints. A very important technique to eliminate or drastically minimize these systematic errors is the by building differences, which is an old surveying technique. This principle of differential corrections has led to the development various augmentation techniques round the GNSS world based on the user requirements.

3.2 Augmentation Techniques

Augmentations of the signal-in-space are required to enhance the accuracy of geographic positions of the user, which is improved by removing the correlated errors between the user and a reference station. The reference station which usually has precisely surveyed geographical coordinate is used as the base is electronically measured for its coordinates. The common error which is derived from the difference between the precisely measured coordinate and the one observed electronically at a discrete point in time is assumed to represent the differential corrections. This is used to correct coordinates of the rover at the same epoch as the base, broadcast in real time or stored and processed along the user position data at a later time as post-process.

Local area correction is generally employed over relatively short baselines, and as the area increases for example countrywide, there is the need to overcome the decorrelation errors which are distance dependent, by establishing a network of stations for area correction. These corrections are broadcast via geostationary satellites. Such space-based technique employed in the correction transmission is referred to as the wide area differential technique (Kaplan, 1996)

3.2.1 Space Base Augmentation Techniques

Satellite-based Augmentation System (SBAS) consist of GNSS compatible geostationary navigation payloads over a region that have been designed to receive satellite navigation signals, supported by ground stations which generally consists of reference stations and mission control centers and uplink earth stations. User differential range errors (UDREs), improved ionosphere and troposphere grid models, and improved navigation satellite ephemeris are transmitted to the navigation payloads which then re-transmit them in addition as a GPS-like signal to the user receivers. SBAS improves the performance of the signal-in-space in terms of accuracy, time to alert, continuity and availability

SBASs though primarily defined as regional systems, they are expandable depending on the needed coverage. The existing systems include Wide Area Augmentation System WAAS of North America; European Geostationary Navigation Overlay System (EGNOS) of Europe, the Multi-functional Transport satellite (MTSAT) Satellite-based Augmentation System (MSAS) of Japan and recently GPS and Geo Augmentation Navigation GAGAN of India and Satellite Navigation Augmentation System (SNAS) of China.

Other forms of Space-Based Augmentation DGPS System have been developed by multinational companies, including SkyFix XP of Thales GeoSolutions Group, Starfix HP of Fugro Chance Inc. and Starfire of the NavCom Technology Inc. They provide Wide Area DGPS (WADGPS) services worldwide on commercial basis (Bisnath et al 2003). These rely on several ground stations around the world that collect data for different regions, generate corrections, and upload them to a geostationary satellite which then re-transmit to the signals users.

3.2.1.1 Wide Area Augmentation System

WAAS currently consists of two geostationary satellites PanAmASat and Telesat located at 133°W and 107°W respectively. These have replaced AOR-W and POW which were located at 142°W and 178°E. The ground component consist of ground reference stations that are spread over the whole of the USA at precisely surveyed locations known as the Wide-Area Reference Stations (WRS), Wide-Area Master Stations (WMS) and Ground Uplink Station (GUS), refer to Figure 3-1.

GPS signals are received by the WRSs which are precisely surveyed and therefore detect any accompanying errors and relay the data to the WMSs where the correction information is computed and correction algorithms computed integrity of the system assessed. A correction message is prepared and relayed to the GUS for onward uplink to the GEOs. These correction messages are then broadcast on the same frequency as GPS L1 (1575. 42 MHz). The GPS-like signal from the navigation transponder can be used by the WAAS enabled receiver as additional navigation signal for position determination, thereby improving the signal availability to users.

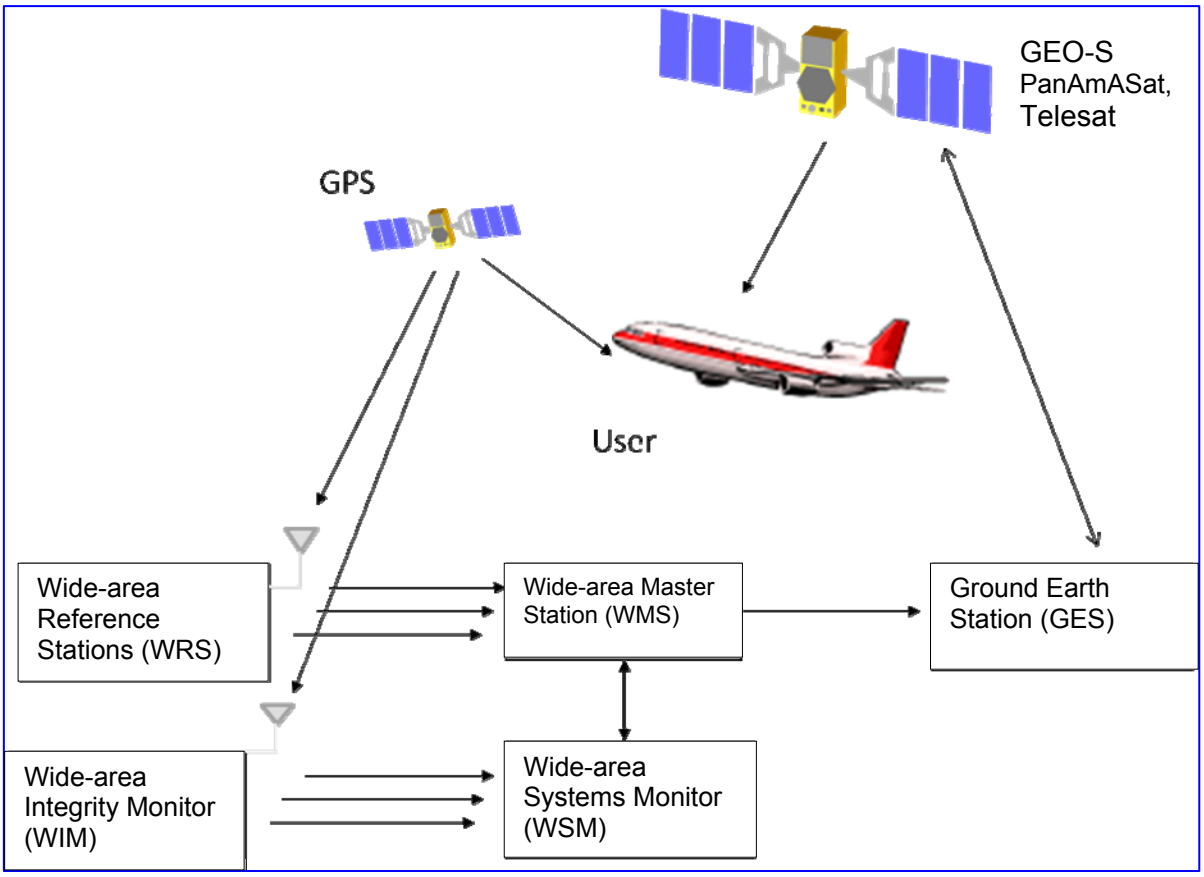

Figure 3-1: Schematic diagram showing the WAAS Architecture

The recent modernization did not affect only the replacement of the geostationary satellites but also expanding the coverage of the system on the continental USA by establishing new GUS in Mexico, Canada and Alaska and also establishing new WMS in Hampton. Georgia USA

With the current modernization, accuracies of 2-4 m laterally and 4-6 m vertically are attainable. For integrity, the time to alert is within 6 seconds as compared with 30 seconds for GPS only (Snow, 2007).

3.2.1.2 European Global Navigation Overlay System

European Geostationary Navigation Overlay Service (EGNOS) is the European GNSS Satellite Based Augmentation System (SBAS) developed by the European Tripartite Group (ETG) made up of the European Commission (EC), European Space Agency (ESA) and the European Organization for the safety of Air Navigation (Eurocontrol). EGNOS aims at improving GNSS services in terms of accuracy, service guarantee and signal availability, so that all modes of transport, air, sea and land as well as other user needs will be met. The serviced requirements are to be fulfilled by means of overlay augmentation of GPS, GLONASS and in the near future

Galileo and other emerging satellite systems, based on broadcasting through geostationary satellites, GPS-like navigation signals containing integrity and differential-correction information applicable to the navigation signals of the satellite systems. (Gauthier et al, 2001). Of these modes of applications, civil aviation requirements are the most stringent; in terms of integrity and continuity hence EGNOS performance objectives are mostly driven by the needs of civil aviation, covering then the needs of land and marine user communities (Ventura-Traverset J. , 2003).

3.2.1.2.1 EGNOS Services

The main services offered by EGNOS are, according to (Hein, 2000); (Gauthier et al, 2001,)

1. Wide Area Differential (WAD), which is the broadcasting of differential corrections to improve the accuracy of the GNSS signals
2. GNSS Integrity Channel (GIC), which is the broadcasting of integrity information to enhance the safety requirements of the GNSS signal
3. GEO Ranging (R-GEO), which is the transmission of GPS-like signals from the GEO satellites thereby augmenting the number of available satellites to users. (This is not enabled)

3.2.1.2.2 EGNOS Architecture

Like all SBAS, EGNOS is composed of four segments, space segment, ground segment, and user segment and support facilities. The space segment consists of geostationary satellites, Inmarsat III AOR-E (15.5°W), Inmarsat III IOR (65.5°E) and Artemis (21.5°E). The ground segment consists of the Ranging and Integrity Monitoring System (RIMS), the Master Controls Centre (MCC) and the Navigation Land Earth Station (NLES). The support facilities include the Development Verification Platforms (DVP), Application Specific Qualification Facilities (ASQF) and Performance Assessment System Checkout Facility (PACF), see Figure 3-2.

The user segment consists of an EGNOS standard receiver that utilizes this signal-in-space for aviation, marine, land and other applications.

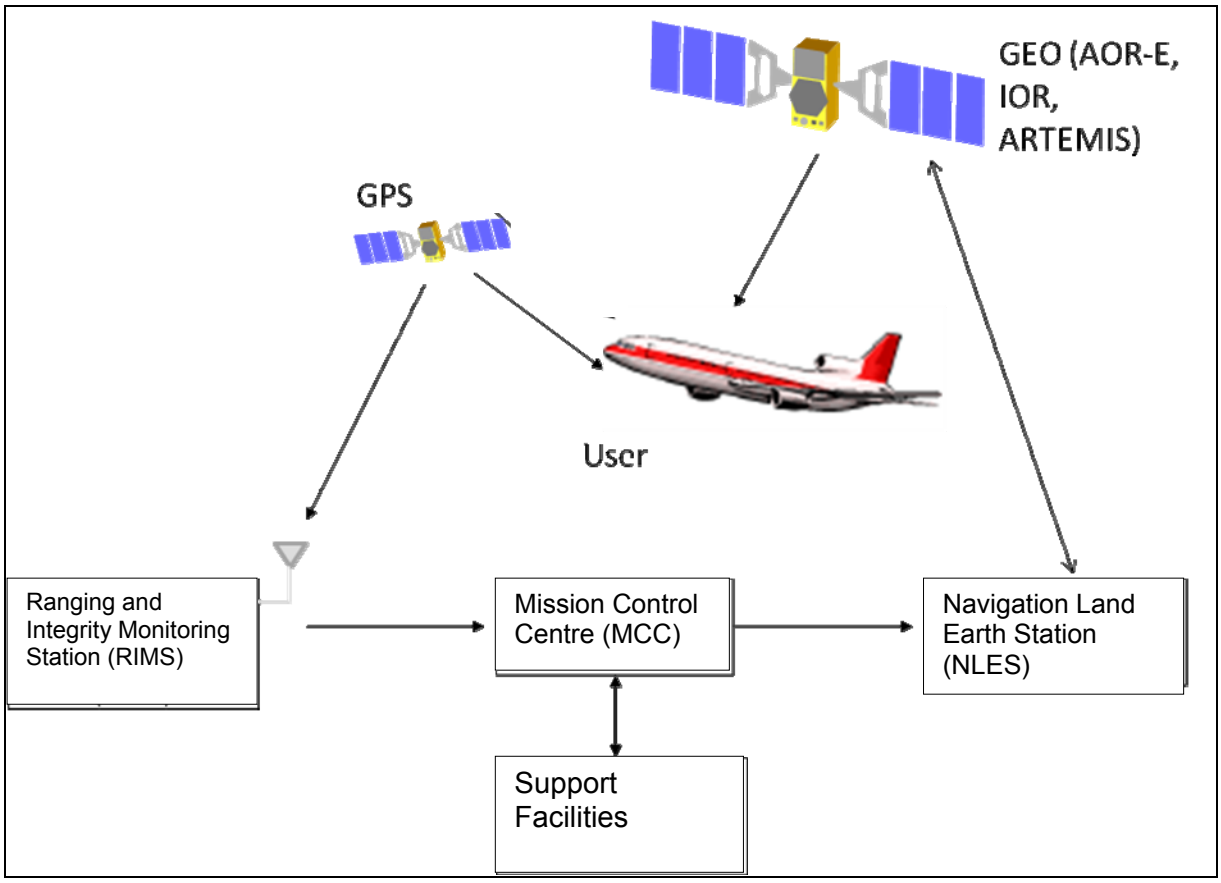

Figure 3-2: Schematic diagram showing the EGNOS Architecture

The RIMS basically perform the following functions among others (Brocard et al, 2000)

- Signal quality monitoring: local interference and local multipath mitigation detection of excessive interference and multipath levels
- Satellite pseudo-ranges measurements (code plus carrier) on GPS and the SBAS geostationary satellite signals
- Messages formatting and transmission towards EGNOS MCCs
- Measurement of the time offset between a reference UTC clock and the EGNOS network time (ENT)

The MCC is the 'brain' of EGNOS, where signal processing techniques are more intensively used. It includes a processing-set and two check-set units. The processing-set is a data processing facility where data coming from the different receivers located at the RIMS are processed to generate the EGNOS navigation message. The check-set implements specific signal processing algorithms to perform various checks to the EGNOS products.

The NLES synchronizes the uplink signal to the EGNOS Network Time (ENT) at the output of the GEO-L1 band antenna. It generates a GPS-like signal and transmits to a GEO transponder. A specific processing function is built to control the code/carrier

coherency of the transmitted signal and to check in the downlink format/content of the message sent. The support facilities are needed to support the system operation and future qualification (Ventura-Traveset et al, 2001).

3.2.1.3 MTSAT Satellite-based Augmentation System (MSAS)

MTSAT Satellite-based Augmentation System (MSAS) is the Japanese version of SBAS based on the Multi-Function Transport System, MTSAT, funded by the Japanese Civil Aviation Bureau (JCAB-Japan, 2003). This was conceived as a result of the need to improve the air navigation system with the introduction of Communication, Navigation, Surveillance and Air Transport Management (CNS/ATM) in global Air Navigation System. Like the WAAS, this system relies completely on GPS as the Japanese and the US Governments issued a joint statement in September 1998 in the use of GPS (Abousalem et al, 2001)

The space segment is made up of geostationary satellites, MTSAT-1R and MTSAT-2. The ground segment is made up of two Ground Earth Stations (GES) and two Tracking Telemetry and Command (TT&C) Stations located at the Kobe Aeronautical Satellite Centre and Hitachi-Ota Aeronautical Satellite Centre. There are Monitoring and Ranging Stations in Australia and Hawaii and Monitoring stations at Naha, Sapporo, Tokyo and Fukuoka, see Figure 3-3. Redundancy built into the systems ensures high reliability, integrity and availability even in case of satellite and/or ground system malfunction or outages due to natural disasters, (JCAB-Japan, 2003)

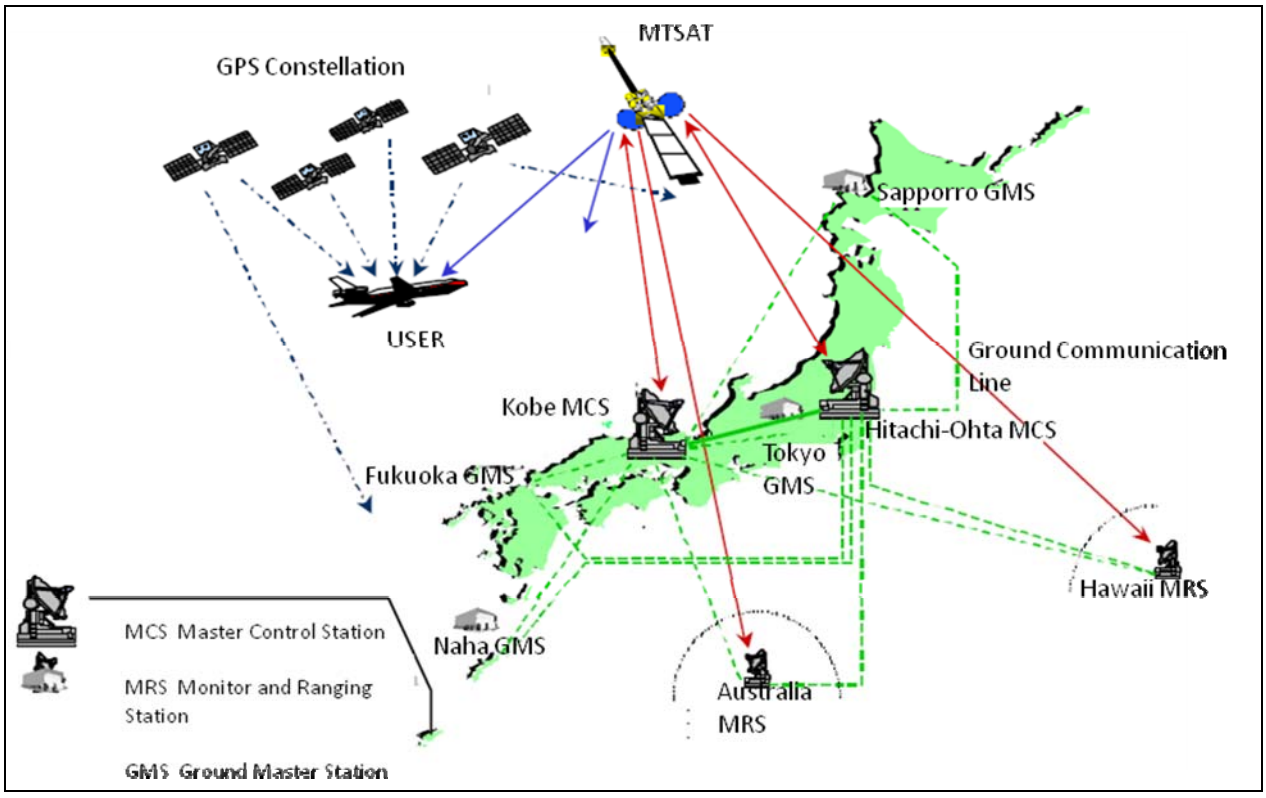

Figure 3-3: MSAS Configuration; courtesy JCAB (Japan), 2003

Global beam of MTSAT covers most of Asia /Pacific airspace, with spot beams covering heavy traffic areas to meet the demands of increasing air traffic. The GPS augmented information generated by MSAS is broadcast according to the formats defined in the ICAO standards, (KASC, 2007)

3.2.1.4 GPS and Geo Augmentation System (GAGAN)

GPS/GLONASS and Geo Augmentation System (GAGAN) is India's contribution to the SBAS. This is intended to bridge the gap between the European EGNOS and the Japanese MSAS to provide a seamless navigation system across the globe, (Kibe, 2003), a target that ICAO is trying to meet when all the SBASs are in full operation. GAGAN is aimed at becoming operational by 2011. This is jointly being undertaken by Airport Authority of India (AAI) and India Space Research Authority (ISRO).

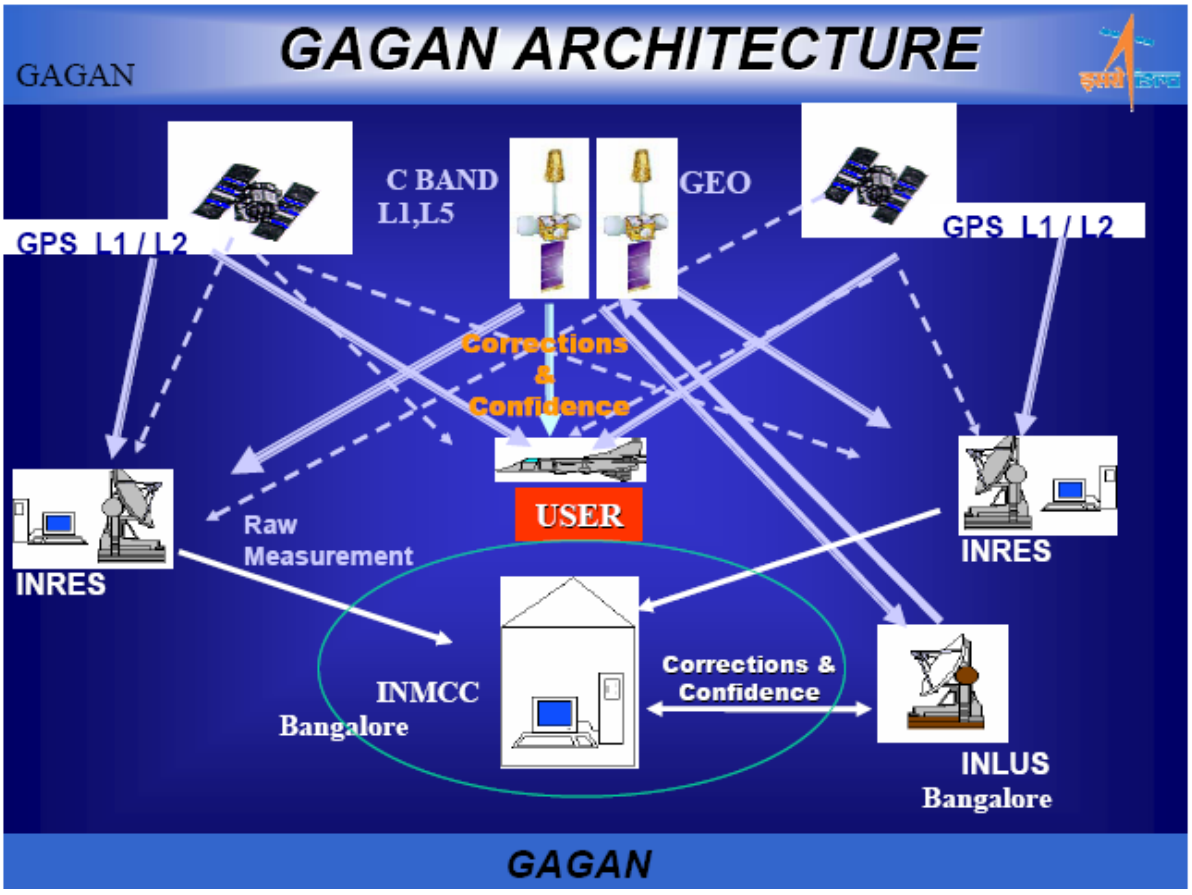

Figure 3-4: GAGAN Architecture (source: Jain, 2008)

The space segment of GAGAN is made up of two operational navigation payloads on Indian GEOs and one in orbit as spare. (Jain, 2008). The payload is compatible with the GPS L1 and other modifications to enhance services. The ground segment consists of Indian Reference Stations (INRES), Indian Master Control Centre (INMCC) and an Indian Navigation Land Uplink Station (INLUS). There is a

communication link that interconnects the ground elements refer to Figure 3-4. Like EGNOS this system will use both the GPS and GLONASS (Singh, 2004).

3.2.1.5 Beidou

Beidou-1 and Beidou-2 Compass Satellite Navigation System (CSNS) is the Chinese contribution to GNSS which are supposed to be regional and global systems respectively. The Beidou-1 which is a form of Space-based augmentation system consists of five geostationary satellites, the first four being experimental and the fifth as the first operational spacecraft. These satellites provide location without the use of other navigation satellites. The ground systems include the central control station, three ground tracking stations for orbit determination located at Jamushi, Kashi and Zhanjiang, ground correction stations and user terminals (SinoDefence, 2008).

The Beidou-2 (COMPASS) will consist of 30 medium earth orbiting satellites (MEO) which unlike the Beidou-1 which requires dual-way transmission between the user and the central control station via the satellite will allow ground receiver to calculate its position by measuring the distance between itself and three or more satellites similar to the operation of the currently operating global satellite systems (Lemmens, 2007). This was designed for military use and started in 2001 and was later joined by civilian users in 2004. The first Beidou-2 (CSNS) satellite was launched in April 2007 into orbit at an altitude of 21,500 km

3.2.1.6 NIGCOMSAT

This is the first attempt of Africa towards SBAS, launched by Nigeria in corporation with China, under the National Space Research and Development Agency (NASRDA) of Nigeria, NigComSat aimed at providing Navigation Overlay Service (NOS) based on the EGNOS technology (Suleiman, 2006). Among the variety of transponders it carried was a set of two L-band, transmitting L1 and L5 signals. This was to be used for augmentation in aviation, maritime, survey and mapping, defense and security, traffic and transportation, telecommunication agriculture among others. The 5,150 kg NigComSat-1 satellite was launched on the 13th of May 2007 is located at 42ºE and has a lifespan of 15 years (Anza, 2008). This has however been lost in space.

3.3 Ground-Based Augmentation Systems (GBAS)

GBAS is the system of augmentation of GNSS signals by employing terrestrial means for data transmission especially for real time positioning. The corrections of such augmentation systems is achieved using a network of multiple stations, a single station or, two stations, as introduced in this study, for the correction within a corridor

linking two reference stations. This study considers both real time and post-processing modes.

3.3.1 Real Time Kinematics Mode

Centimetre-level accuracy positioning in real-time based on GNSS measurements referred to as RTK ("real-time kinematics") positioning involves a reference receiver transmitting its raw measurements or observation corrections to a rover receiver via some sort of data communication link (e.g., VHF or UHF radio, cellular telephone). The data processing at the rover site includes ambiguity resolution of the differenced carrier phase data and coordinate estimation of the rover position. This system could be based on a single reference station. However a drawback of this single base RTK approach is that the maximum distance between reference and rover receiver must in most cases, not exceed approximately 10 km in order to be able to rapidly and reliably resolve the carrier phase ambiguities, as over a distance of greater than 10 km, errors could be comparable to the GPS signal wavelength and would interfere with the ambiguity resolution algorithm (Petrovski et al, 2001). This limitation is caused by distance-dependent biases such as, ionospheric and tropospheric signal refractions and orbit error. These errors, however, can be accurately modeled using the measurements of a network of GNSS reference stations surrounding the rover site. This then brings in the need for the establishment of RTK positioning using a multi-base technique that is the network RTK.

In order to provide such a service to a larger geographical region or a whole country many reference stations have to be set up and maintained. Here, the development of a multi-base has a tremendous advantage over establishing various single base station RTK, since the number of reference stations can be reduced drastically thus saving operational cost per unit area.

The data processing for Network RTK positioning consists of three distinct steps. In the first processing step ambiguity fixing is performed in the reference station network. Only observations with fixed ambiguities can be used for the precise modelling of the distance-dependent biases. The usually long distances between the reference stations, sometimes over 100 km, requires the fixing of the ambiguities in real-time, making this processing step the main challenge of Network RTK. This is followed by modelling the distant–dependent biases which are mainly ionospheric and tropospheric effects, at the network processing centre. The resulting modelled data is then broadcast to the rover which uses it to process its corrected position with those from the network. The operational mode at this juncture distinguishes between the concept of Virtual Reference Station (VRS) and the Area Correction Parameters, the Flaechen Korrektur Parameter (FKP) and the Master-Auxiliary Concept (MAC) which are currently the three systems in use. Other systems are being developed like the In-receiver or Tightly Coupled Approach (Minmin, 2005); (Alves et al, 2004), which requires no control centre as all the needed information is collected and

processed at the rover receiver. The single RTK positioning and network adjustment are integrated into a tightly coupled filtering.

3.3.2 Single Reference Base Station Concept

This is one of the primary positioning modes designed to improve the accuracy of GNSS known as relative positioning, DGNSS or DGPS. It employs two or more receivers, a reference or base receiver, which is placed on known 3D coordinates and a set of receivers termed the rovers whose coordinates can be determined relative to the reference receiver. Observations are made at the reference and rover stations to the satellites in view as can be seen in Figure 3-5 at the same epoch of time to the same set of satellites. The measured bias errors at the reference point is computed and corrected and these corrections, which is the difference between the observed position and the known position. This is then used to correct the positions observed at the unknown rover site either in real time or in post-processed mode. It is assumed that the errors observed at the reference station and the rover stations are similar and identical within a limited base length, and can therefore be eliminated by building these differences.

This system has a limitation when it comes to the real time applications. One main significant drawback of use of differential correction from single base is that the maximum distance between reference and rover receiver must not exceed 10 to 20 kilometers in order to be able to rapidly and reliably resolve the carrier phase ambiguities. This limitation, caused by distance-dependent biases such as orbit error, and ionospheric and tropospheric signal refraction, is severe in Ghana which is closer to the geomagnetic equator where ionosphere is quite severe and also located in the low latitude region the troposphere is very unstable (Prasad, N., A. D. Sarma., 2007); (Musa, Samsung, & Rizos, 2005). These errors, however, can be accurately modeled using the measurements of an array of GNSS reference stations surrounding the rover site. Thus, RTK positioning is improved with the change from a single base to a multi-base technique. This also applies to post-process application and also where single frequency users are involved.

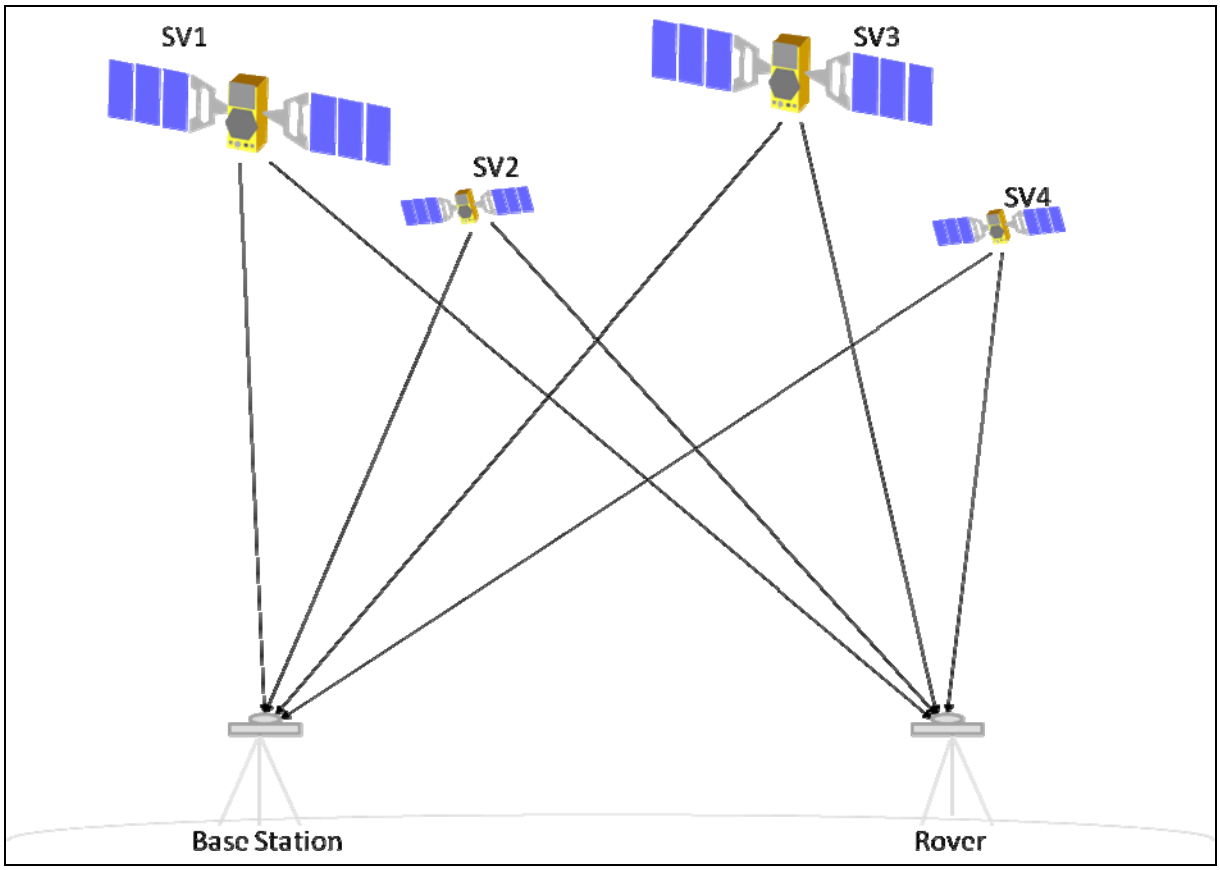

Figure 3-5: Diagram showing single reference differential correction concept

3.3.3 Multi-Referenced Base Station Concept

Application of GNSS survey over larger areas may require the establishment of several reference stations. These stations could be linked together through simple network solutions like one-dimension or two-dimension modeling for post processing differential corrections or complex real-time network systems. These network systems could be classified depending on mode of correction and transmission of the corrected data. The basic factor that cuts across all these systems is the fact that the systematic errors are modeled for the area in question and the rover uses this correction between the observed and known coordinates of the reference station to correct what is observed from the same satellites by the rover, to obtain better results by removing the modeled error. These could be classified into static or kinematic, real time or post-process and others depending on the system operated by the rover.

Network of stations offering differential corrections are being developed nowadays by national mapping organizations, public and private institutions and educational and scientific organizations for various applications. By using this system users are in principle able to use only one receiver to perform high precision positioning by utilizing the error modeling capabilities of multiple reference station.

Both pseudo-range based DGPS and carrier phase-base positioning are possible depending on the required accuracy as well as the capability to fix ambiguities which

depends largely on the atmospheric conditions. Multipath can be a nuisance and is dominant in this operation.

Depending on the inter-station spacing, very accurate results can be realized for various applications. Most countries are now relying on GNSS reference station networks to develop their geodetic reference network for various applications as expressed by(Higgins, 2002) in Australia, SAPOS in Germany and so many other countries. Applications such as high precision scientific and geodetic observation have been undertaken using this system like the GEONET in Japan which comprises of a network of over 1000 receivers across a country of an area of 378,000 square kilometers (Takeshi, 2004); (Imakire, T., Y. Nakahori, 2001) and a network of over 100 receivers for the South California Integrated GPS Network (SCIGN) for the monitoring of crustal activities in these areas (Hudnut et al, 2001). A great number of applications are not satisfied only by the accuracy but also time to solution, hence the real time solution which requires an appropriate telemetric solution. Various telemetric considerations have been taken, for example network service, SAPOS (SAPOS, 2004) considers Mobile Radio (GSM), NTRIP, VHF, Internet, Long Wave, and other Data Carriers, depending on the application, more details can be found in (Wegener, V; Wanninger, L., 2005).

The concept of multiple reference networks has a basic scheme of processing and this runs through all the various concepts that are now in operation. This include

- Collection of observations from all the reference stations to a central location
- Resolve the ambiguities between the reference stations
- Fit model parameters to deviation
- Derive correction model for rover position using modeled parameters
- Correct observation for rover
- Calculate rover position

These approaches include the Virtual Reference Station, Area Correction Parameters and the Master Auxiliary Concept.

As a contribution to differential positioning, this study introduces yet another concept which is different from the three named above, and this is the Corridor Correction Concept which corrects along a line instead of within an area and uses two instead of three reference stations. This concept has been introduced in section 3.3.4 of this chapter.

3.3.3.1 Virtual Reference Station (VRS) Concept

Virtual Reference Station (VRS) is a form of network real time kinematics (RTK) that uses data from a fixed reference station network to model GNSS errors in a region. This model generates a ‘virtual’ reference station near a surveying location, which then provides a localized set of standard format virtual measurements to a roving

receiver. All users in the region are provided with centimetre accuracy and improved performance reliability.

This basically consists of a rover, a minimum of three reference stations and a processing centre as shown in Figure 3-6. Data from the reference station network is transferred to the processing centre to be used to compute models of ionospheric and tropospheric errors. Carrier phase ambiguities are then fixed for the network baselines to derive centimetre accuracy using the fixed carrier phase observations. The error models are generated for the network and the error at the user location can be predicted thus creating the VRS data which is then transmitted to the user in standard formats (RTCM).

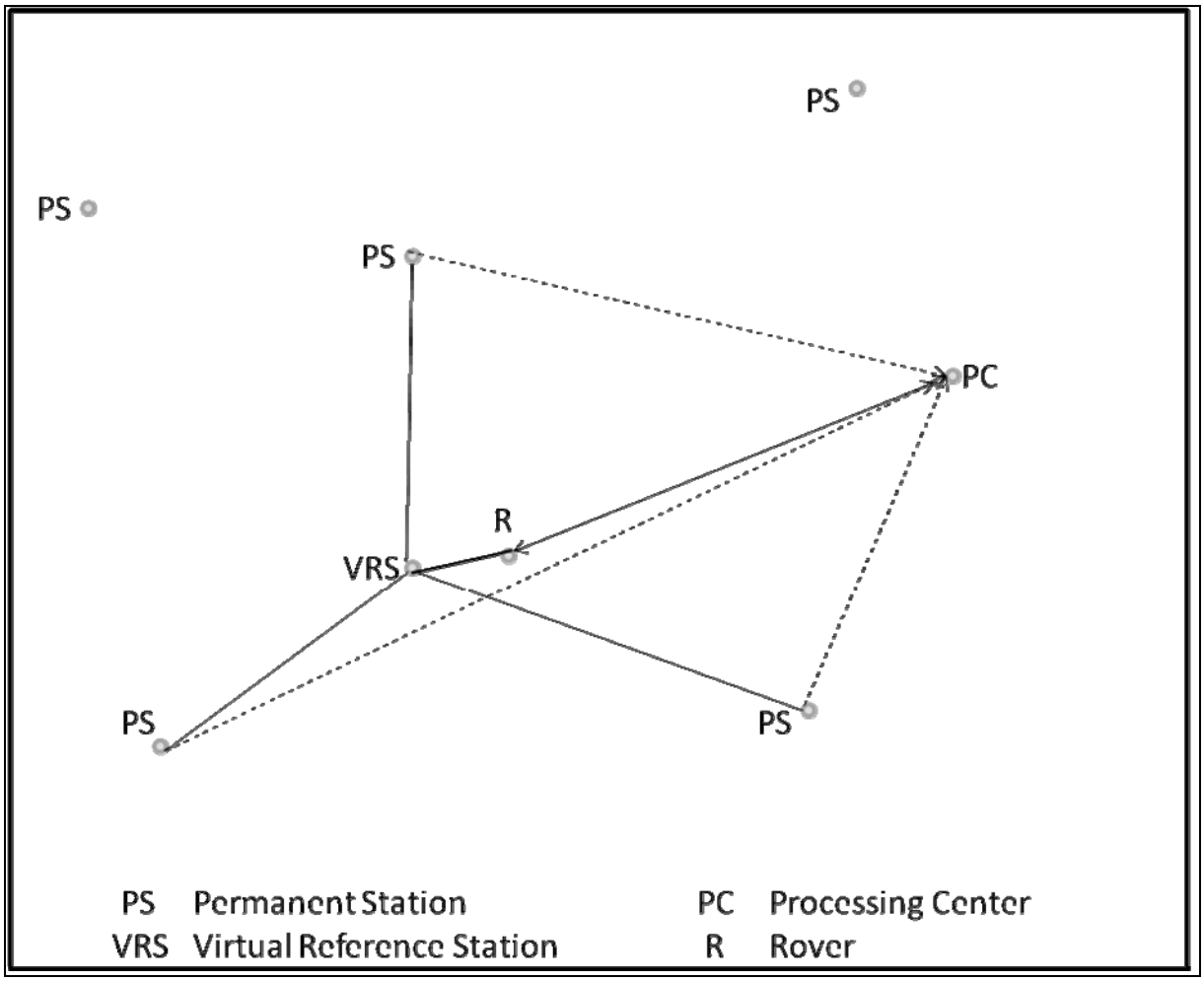

Figure 3-6: Schematic diagram explaining the VRS concept

The rover receiver determines the location with a navigation solution without any correction and transmits it to the processing centre for authentication. The processing centre immediately sends the VRS data to the rover on the field (Vollath et al, 2000).

At the level of the reference station, quality control and assurance procedures are analyzed to check cycle slips, wrong code ambiguity, coarse carrier phase

fluctuations and others, to ensure that the integrity of the station is acceptable. There is further integrity check on the differential observables using baselines. This is supported by basic GNSS software modules, for instance the DGPSNet. All the reference stations transmit this data to the processing centre for the modelling of the long term, large area error by the troposphere, ionosphere and satellite orbits with DGNSS software. For instance using this error model, the carrier phase ambiguities within the network are resolved. Local errors by ionosphere, troposphere and orbits at the rover are then derived to centimetre level accuracy using RTK software like the RTKNet (Landau et al, 2002).

3.3.3.2 Area Correction Parameters (FKP) Concept

Like the VRS, FKP estimates the double difference ambiguity after the preliminary solution at each reference station. This is then followed by the building of a set of coefficients modeling ionosphere, troposphere and orbit effects from each satellite to cover a specific network area (correction plane). These are then updated at specific intervals, at least at every 10 seconds. These coefficients are then transmitted to the rovers which then use them to interpolate their own corrections from the correction plane (Minmin, 2005)

The FKP concept uses broadcasting method which is unidirectional unlike the VRS that uses bi-directional mode of message transfer restricted to cellular phone. This makes it possible to cover remote areas where cellular phones are not available, although the use of cellular phones is convenient. Another difference between the two systems is that the rover is tasked to do more computation as far as FKP is concerned unlike the VRS which finds the less work for the rover as the processing centre does most of the computation, though with the advent of good processing capabilities, this advantage is becoming less significant.

FKP automatically recomposes the correction plane in case of any trouble at the reference station such as multipath reflection or occultation of GPS signal by tall buildings (Hiroshi et al, 2004). The basis of this FKP is the state space model, which is composed from analyzed GPS data observed at the reference station in the network. Pseudorange correction derived from the state space model is converted to correction plane as shown in Figure 3-7. This is further explained in(Sumio U., Hiroshi H., Junshiro K., Koji W., Satoshi T, 2004)

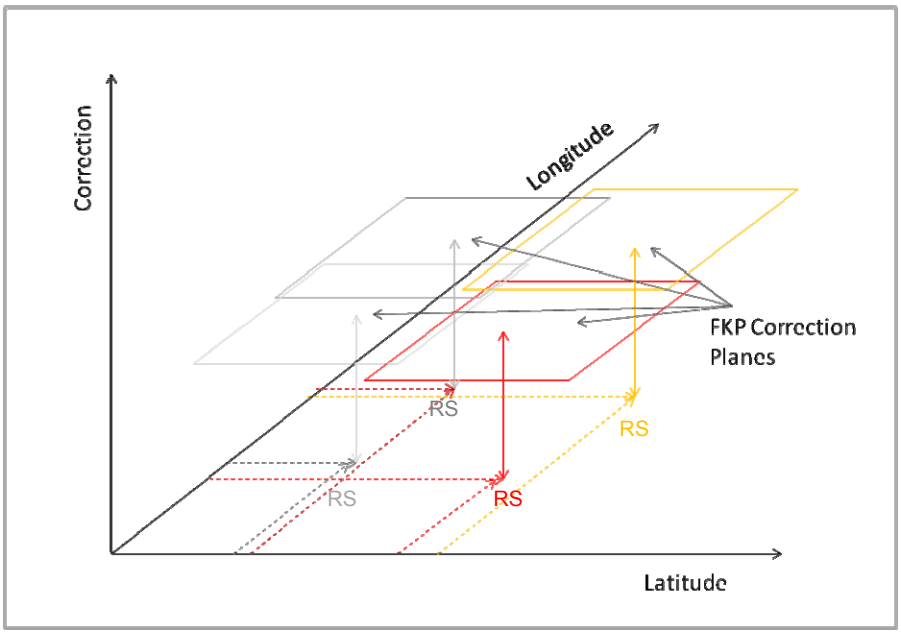

Figure 3-7: A schematic view of FKP correction plane (Hiroshi et al 2004)

Each FKP plane, in Figure 3-7, shows a position dependent error derived from a linear area polynomial, which is referenced to a surface defined parallel to the WGS84 ellipsoid in the height of the reference station.

Geographical coordinates (φ, λ) for a rover are referenced to this surface to derive the distance dependent error using the following expression as stated by (Wuebbena & Bagge, 2002).

$$\delta_{r_0} = 6.37(N_0(\varphi - \varphi_R) + E_0(\lambda - \lambda_R)\cos\varphi_R) \quad 3\text{-}3$$

$$\delta_{r_I} = 6.37H(N_I(\varphi - \varphi_R) + E_I(\lambda - \lambda_R)\cos\varphi_R) \quad 3\text{-}4$$

$$H = 1 + 16\left(0.53 - \frac{E}{R}\right)^3 \quad 3\text{-}5$$

δ_{r_0}	distance dependent error for the geometric (ionosphere free) signal [m]
δ_{r_I}	distance dependent error for the geometric (narrow lane) signal [m]
N_0	the FKP in north south direction for the geometric (ionosphere free) signal in ppm
N_1	the FKP in north south direction for the ionospheric signal (influence on the 'narrow lane') in ppm
E_0	the FKP in east west direction for the geometric (ionosphere free) signal in ppm
E_I	the FKP in east west direction for the ionospheric signal (influence on the 'narrow lane') in ppm
φ_R, λ_R	the geographic coordinates of the reference coordinates in WGS84 datum in radians

E angle of elevation of the satellite in radians

The distance dependent error for L1 and L2 signals is computed using the following equations

$$\delta_{r_1} = \delta_{r_0} + (120/154)\,\delta_{r_I} \quad 3\text{-}6$$

$$\delta_{r_2} = \delta_{r_0} + (154/120)\,\delta_{r_I} \quad 3\text{-}7$$

δ_{r_1} the distance dependent error for L2

δ_{r_2} the distance dependent error for L1

3.3.3.3 Master Auxiliary Concept (MAC)

The system consists of a network of stations which form subnets called clusters and data information that stream from the reference stations of this subnet are interchangeable (Euler, 2005). The cell is a sub-net which includes a Master Reference Station (MRS) and some Auxiliary Reference Stations (ARS), as shown in Figure 3-8. Data from all the stations are streamed to a Network Processing Facility (NPF), usually situated at a central location where integer ambiguities between all the auxiliary stations and the master are resolved and correction differences determined. The master station transmits the original raw data while the auxiliary stations transmit differences with respect to the master, thereby reducing the amount of data hence the transmitting time. This also means there is no need to use wide bandwidth for the transmission.

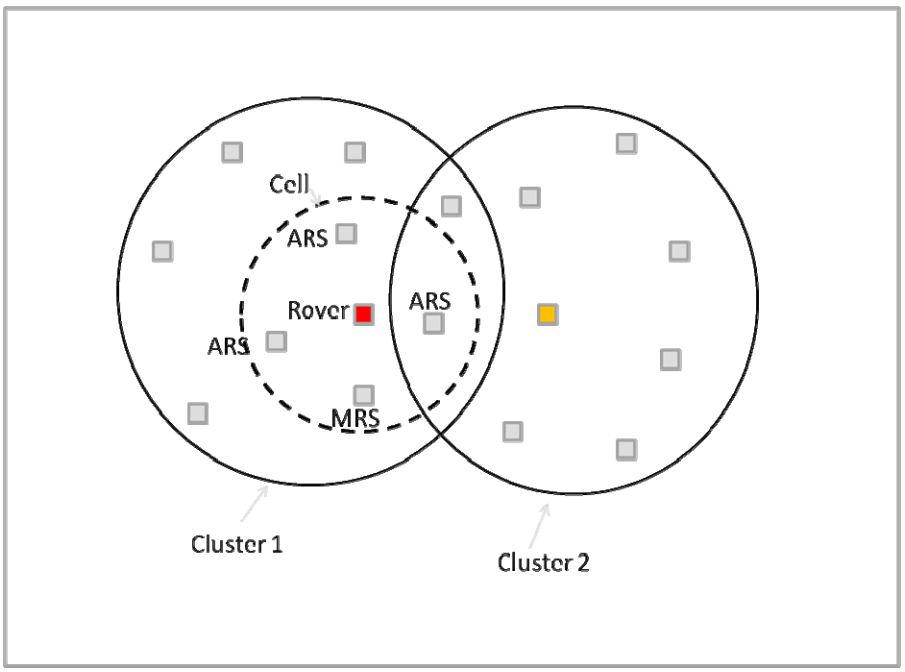

Figure 3-8: The Schematic diagram of MAC arrangement

The MAC uses both uni-directional and bi-directional mode for the respective transmission of Single Cell Correction (SCC) and the Automatic Cell Correction (ACC). In the SCC mode the user chooses from among known predefined cells in accordance to its position, on the other hand for the ACC, the rover transmits its navigation coordinate to the processing center, the NPF, for a cell to be defined with a master station and the auxiliary stations. The MAC uses dispersive and non-dispersive phase corrections to compress network RTK information without the need to standardize correction models.

4 Framework for a Nationwide GNSS Reference Network Design

The establishment of a Nationwide GNSS Reference Station Network has been proposed as Ghana's attempt to effectively use the potential in GNSS. This has been generally accepted and steps have been made to join the international GNSS user community for development using this technology. This is in fulfillment of calls that have been made by organizations like AFREF, UNECA, NEPAD, (Wonnacott, 2007); (Wonnacott, 2006); (NEPAD, 2004) other African countries, some local institutions including the research institutions and the universities.

In designing a nationwide GNSS Reference Network for a country like Ghana, consideration was given to the national requirements, spatial distribution of potential users, the available human and material resources for the establishment and the maintenance of the network and linkages with the appropriate institutions that can impart the relevant technology for such an endeavor.

4.1 Available facilities

One of the basic but costly requirements for the establishment of a Network of Reference Stations is accommodation for the GNSS equipment and its accessories. Provision was made by the Survey Department (SD) of Ghana which is technically responsible for mapping in the country. SD, the National Mapping Organization has offices in all the ten regional capitals in the country which can accommodate the proposed Regional Base Stations. These can be supplemented by the District Assemblies when it becomes necessary to expand the network or achieve the required coverage.

Data broadcasting is also one of the most expensive components of D-GNSS, so the proliferation of radio stations and other communication systems can be used to the advantage of the country as theoretically they can be used to broadcast data to real time user community. The use of GSM service, though expensive in Ghana, is an option that cannot be ruled out. Other facilities that can be utilized include the 600 km Fiber Optic network in the country which runs along the Golden Triangle of Ghana. The use of the internet facilities which is gradually becoming a key player in telemetry in GNSS, is fast improving across the country, and it is worth investigating into how this can be used in the development of GNSS in Ghana.

Power supply, which is one of the main considerations in the establishment of permanently operating GNSS reference station, is very unstable in Ghana especially in the rural communities. The use of solar energy at the permanent stations is a good option for Ghana where there is enough solar energy due to its geographical location.

4.1.1 National Geodetic Network Design

The National GNSS Reference Network consists of four components, a Fundamental Station, the Regional Reference Stations, the Hub Stations and the Passive Reference Station network. These will be located at various locations of the country based on the available infrastructure at the location, the potential application in the locality, the physical stability of the geology of the area and other considerations.

4.1.1.1 Ghana's Fundamental Point

The Ghana Fundamental Point which is supposed to be an accurately positioned station is to be geodetically tied to the ITRF. This is supposed to be used to control the network in Ghana and more importantly shall be linked to the proposed AFREF. The location of this point should therefore be well investigated. It should be away from seismically active zone, it should be centrally placed as it will be used to coordinate the rest of the stations, and it should have enough infrastructures to support its maintenance. Including Accra, most of the cities along the coast are heavily faulted with frequent occurrence of tremors (Andam, 2004); (Amponsah P. , 2002) and are therefore not stable for a fundamental station to be located. Despite the almost 70 years' silence of the western fault which is also along the coast, closer to Takoradi, where the severest earthquake in the history of Ghana occurred, has made Takoradi lose its credibility as a candidate for the location of a fundamental station. Kumasi which is further away from the seismically active areas of the Ghana and meets most of the requirements for a fundamental station is an obvious choice; moreover, it is more centrally placed than the other candidates. Kumasi has the Geomatics Engineering Department of the KNUST, a Regional Survey Department and research institutions like the Building and Road Research Institute which makes it resourceful in terms of human resources to maintain this facility. There is the proposal to develop the Kumasi site into an IGS station to serve not only Ghana but the international GNSS community.

4.1.1.2 Network of Reference Stations

The Survey Department of Ghana which controls the survey and mapping activities has branches in all the ten regional capitals of Ghana. With the human resources and physical infrastructure, an active base station can be set in all these regions at a reasonable cost. Assuming that every point in the country is to be less than or equal to 100 km from an active reference station then more than 70% of the country will be satisfied when reference stations are established in these Regional Offices. Five regions including the Greater Accra, Eastern, Central, Upper East and Upper East Regions will fully covered while the rest will be partly covered.

To obtain 100% coverage nationwide such that any user will be within 100 km from a permanent reference station, there must be additional five Hub Reference Stations

established. These may be located in Wiawso in the Western Region, Kete Krachi in the Volta Region, Yendi and Bamboi in the Northern Region and Atebubu in the Brong Ahafo Region (Poku-Gyamfi, Y; Hein, G.W, 2006). Though these are not Regional capitals, they have some basic infrastructure to support the running of a reference station, being district capitals. The demand for the service which is a requirement for the setting up of a network may however be lower than that in the regional capital, and will therefore be made to operate as and when there is demand of service. It is suggested however that the monuments with a fixed antenna will be installed to ensure permanency of the station coordinates.

The network should include another category of reference stations that will be used as a link to the conventional method of survey, which needs inter-visibility between points with known coordinates. This set of stations is termed the 'Passive Reference Stations'. The location must be selected at secured places like the other stations; there should be power supply, stable foundation, open sky and preferably internet connection. These are to be located on top of Government and Public buildings. In addition to these monuments, there must be three witness markers, reasonably located with at least one inter-visible baseline between two of the markers. The azimuths and distances between these points must be provided. In addition description of the access from major landmarks should be provided, including digital photographs. These will act as points of departures for survey activities in the country. The Passive Reference Stations should be at most 50 km from each other and must be well distributed in the whole country, and could be made denser where there is the need.

4.1.1.3 Phasing out the Network Establishment

Due to budgetary constraints for such projects, there is the need to phase out the implementation, and this study proposes three main phases which could be changed in the advent of an unforeseen demand. The proposed phases are

- The Golden Triangle (three permanent stations as shown in Figure 4-1) which has basically been established under this project.
- The Northern Triangle with a link station (additional three permanent stations and a hub station as in Figure 4-2) which is on-going.
- The rest of the country (a total of 10 permanent stations and five hub stations as shown in Figure 4-3) which has not yet received any budgetary support.

This study included the implementation of the first phase of the entire network, which consists of the derivation of the geocentric coordinates, the determination of transformation parameters to change the coordinates from the old classical ellipsoid to the new geocentric reference system. This is to be replicated with the implementation of the other phases. An advantage of phasing out this project is the re-engagement of the human resources who would have already had enough

experience needed for the subsequent phases. Logistical support will not be over stretched. On the other hand there is going to be repetition of derivation of a new set of parameters of transformation which may be different from what is supposed from what is derived from the first phase.

4.1.1.3.1 **Phase One- The Golden Triangle**

This consists basically of three permanent stations at the vertices of the Golden Triangle of Ghana on which this project is focused as seen in Figure 4-1. This has the three largest cities and most important in terms of the economy of Ghana at the corners of this triangle which include Accra the national capital, Kumasi, the second largest city, and the capital of the Ashanti Region of Ghana, and Takoradi, the capital of the Western Region and the third largest city in Ghana.

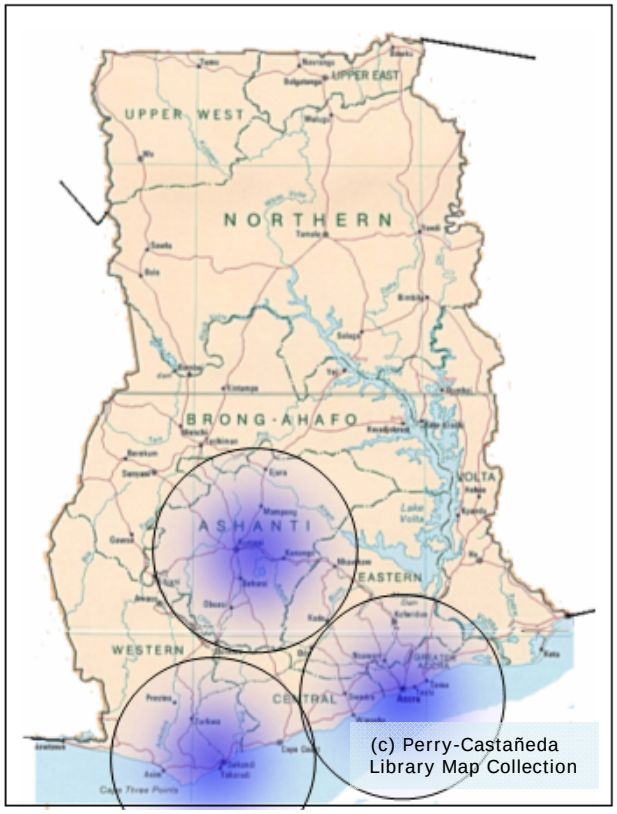

Figure 4-1: Map showing the location and 100 km radius coverage of the reference stations for the Phase 1 of the GRN Project

4.1.1.3.2 **Phase Two: The Northern Triangle and the Kintampo Link.**

The phase two includes the establishment of permanent stations in the regional capital of the three Northern Regions that is Tamale, Wa and Bolgatanga. With the exception of the Bolgotanga station which should be collocated with the Absolute Gravity Station for seismographic research, the rest must be located at the Regional Survey Department offices. These cover the most economically viable areas in the

Northern Ghana. This is to be linked to the Golden Triangle with a Hub Station at Kintampo, located between the North and the South, see Figure 4-2.

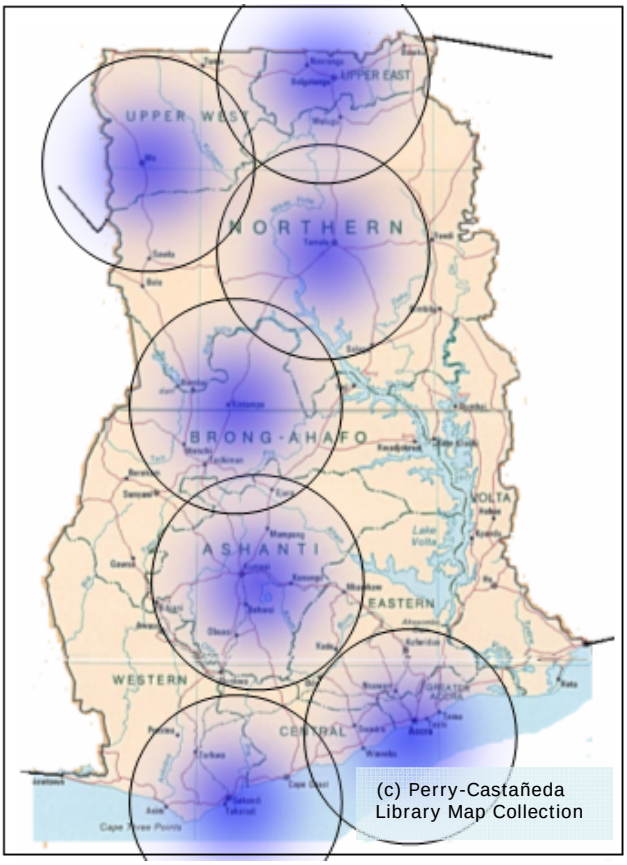

Figure 4-2: Map showing 100 km radius coverage for the Phase II of the GRN project

4.1.1.3.3 **Phase Three: The Rest of the Country**

To cover approximately the rest of the country with a network of 100 km baselines or better, eight more stations have to be established, four permanent stations in all the regional capitals which include Cape Coast, Koforidua, Ho, and Sunyani, regional capitals of Central, Eastern, Volta and Brong Ahafo Regions and four Hub stations at Wiawso in the Western Region, Bole and Yendi in the Northern Region and Kete Krachi in the Volta Region as shown in Figure 4-3

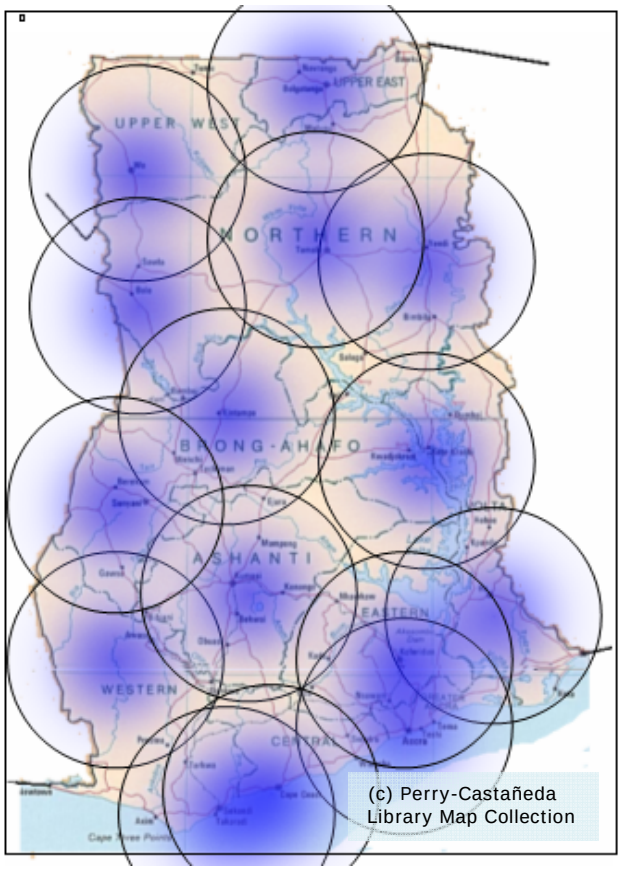

Figure 4-3: Map showing the full 100 km radius coverage of Ghana for the GRN

Though the above selection was done based on the present and future requirements, it did not take into consideration proposals of other private and government institutions that may like to establish reference stations for other purposes and may like to be linked to this proposed network. For example the proposed establishment of a Reference station at Winneba by the Millennium Challenge Authority (MCA) may warrant the relocation of the proposed station at Cape Coast. The same applies to the proposed collocation of a station at the Seismic Research Observatory at Kukurantumi less than twenty kilometers from Koforidua. There should therefore the need to maintain a degree of flexibility so as to maximize the benefit of the available resources, by cooperating and sharing resources.

4.2 Telemetry Considerations

With the growing interest that has been generated in the public and private sectors on the use of GNSS, measures should be taken to sustain this momentum. This calls for the development of cost effective telemetry products to enable moving beyond the current post-process products to the real time products. The use of the existing facilities will go a long way to help Ghana achieve these goals. The use of FM radio sub-carrier system which is prominent among the telemetry systems cannot be overemphasized; for example the use of 57 kHz sub-carrier from a network of FM stations to broadcast Differential GPS corrections to the user community in the USA by Differential Corrections Inc. of the USA (Bradley, 2004) could serve as a guide to

Ghana. According to (Weber, 2002), the streaming of DGPS corrections over internet and cellular network is feasible and has promising advantages for service providers and again this promises to be one of the ways forward for Ghana. Germany uses ALF (Low Frequency Radio) operating on 123.7 kHz DGPS service to cover radius of over 600km with accuracy of up to 5m which is mainly used for navigation, centimetre accuracy on the other hand has been achieved by SAPOS through GSM or telephone for geodetic positioning (SAPOS, 2004). There are many more examples round the world to be studied and see the possibility of technology transfer into the Ghanaian environment. There is no doubt that there is a wide range of choice in telemetry to consider in the design of a network of reference station for Ghana depending on the potential applications.

4.2.1 Telemetry in Ghana

The available telemetry systems that can be considered include radio sub-carrier systems, fibre optic network, mobile cellular network, internet facilities and wireless modems. The present use of the available resources and how this technology can share the use in a constructive manner should be the prime aim of a GNSS research team in Ghana.

4.2.1.1 FM/AM/SW/MW Sub-Carrier Systems

Several radio sub-carrier systems are the most established systems in Ghana and the cover all the country as compared with the other systems. Technically these can be used as data transmitters to their coverage areas and a careful study has to be made to know the potential applications. The FM systems are usually limited to a maximum of 60 km, but have very high update rate, typically of 2 seconds, while the medium frequency radio links can reach a maximum of 700 km, but have slower update rates, typically between 10 and 15 seconds, and the frequencies are subject to atmospheric conditions. SAPOS (SAPOS, 2004) gives the application of such broadcasting media.

For a nationwide broadcast therefore, the use of the MW sub-carrier systems will be the most appropriate, whilst the FM systems could be used on projects designated for a locality.

4.2.1.2 The Ghana Fibre Optic Network

Transfer of voice, data and video between major cities like Accra, Kumasi, Takoradi and many others is available under the project ‘GhanaNet’. There are plans to extend it to Lome Togo and Abobo Ivory Coast. There is already in place a 600 km network covering the Golden Triangle of Ghana (ABB-Group, 1999).

This project offers state-of-the-art Synchronous Digital Hierarchy (SDH) technology

- 2 Mbit/s access links
- 11 based on optical fibre
- 19 based on radio links
- modern de-central IT infrastructure
- point-to-multipoint radio-link technology
- backbone net connection with 155 Mbit/s

The Fibre Optic Network is one of the potential options in the telemetry solutions in the establishment if a nationwide network of GNSS Reference Network as there is planning to link all districts of the country. This will then cover all the proposed base stations in the country. As at now the Golden Triangle of Ghana has already been linked by this technology.

4.2.1.3 Mobile Cellular Network

Mobile telephony has now had a remarkable penetration in the recent past, this covers all the major cities and towns in all the 10 regions of the country and has a potential of being used in the field of GNSS, but the main disadvantage is the high cost. With improvement in technology and the increase in customers, which can result in the decrease in tariffs, it can become competitive in the GNSS market in future. The four major service providers are constantly exploring ways of improving and increasing their products and services and this again is a good indication that data transmission in the field of GNSS will be embraced by these service providers.

4.2.1.4 Internet

The use of internet for data transmission in the field of GNSS is becoming more important due to its relatively low cost and Ghana stands to benefit with the recent emphasis on information and communication technology (ICT). Although this is yet to be very reliable especially in the rural areas of the country, it is very relevant to the successful implementation of GNSS network in Ghana. The use of Network Transport of RTCM via Internet Protocol (NTRIP) is gaining popularity worldwide hence emphasis should be made on the use of this technology for successful implementation and maximum benefit from the GNSS technology. Internet has become mandatory for the running of modern base stations as most of the systems have integrated internet accessibility.

4.2.1.5 Wireless Modem

Depending on the coverage, application, topography, radio performance parameters and frequency band availability, wireless modem can be designed to provide the telemetry component for the needed GNSS services. This will require the installation of a network of antennas all over the country and many other components. A cost-benefit analysis of such venture may not be favorable. A demand-driven approach is advisable for such installation and this will surely come out with the phasing out of such venture. For localized applications over small coverage areas, this is more effective and is advisable to use.

4.3 Management and Financial Considerations

The success rate of projects of this nature is not encouraging in developing countries due to inadequate technical and financial management. Proposal has been made to help sustain and improve GNSS in Ghana.

4.3.1 Management

The concept of Establishment of a Nationwide GNSS Reference Network is usually the responsibility of the National Mapping Organization (NMO) which in Ghana is the Survey Department of Ghana, headed by the Director of Surveys. Due to its multi-disciplinary nature and lack of local experts, its management needs the assistance of both local and international organizations. This calls for the proposed National GNSS Group which will be made up of GNSS experts in the country, who are to support the Director of Surveys on GNSS implementation. The support of international partners on GNSS and donor agencies is vital to the management of GNSS and its sustenance in Ghana. The implementation of GNSS and its management require the support of the research institutions and the universities in the country, professional bodies and the Survey Department and most importantly the stake holders.

4.3.2 Research, Development and Maintenance

A successful implementation of GNSS Reference Station Network in Ghana will require the involvement of various public and private institutions especially those that form the part of the user community. Institution like the Ghana Institution of Surveyors and the Licensed Surveyors Association of Ghana with their human resource capacity and the Geomatics Department of the KNUST, where the country's geodetic engineering experts are trained, research institutions like BRRI which runs a base station for GNSS in Traffic and Transportation and Land Surveying, and CERSGIS which has been using GNSS in GIS application. Private companies which are trying to popularize the use of GNSS, can share their experience in the running of their base station and a few mining companies that operate base stations. People from

these institutions will collaborate with the Survey Department for effective running of the Geodetic Reference Network (GRN).

For GNSS to be sustained in Ghana there is the need to form a National GNSS Research Group that will research into problems pertaining especially to Ghana and the sub-region like the problem of the high ionosphere scintillation, solar effects, electromagnetic storm, and troposphere effects in low latitude regions etc. This group could be responsible for the general development of GNSS infrastructure and applications in Ghana.

Figure 4-4 shows a proposed management structure for the maintenance of GNSS in the country. Headed by the Director of Surveys, who has now created the Geodetic Reference Network Team in Ghana, there is the need to get a National GNSS Advisory Group made up of Ghanaians with technical know-how in the field of GNSS to advice the Director of Surveys. There must be the link to the international bodies like the AFREF, IGS, IAG, UNECA, UNOOSA, RECTAS and others to obtain the necessary technical assistance. The role of the universities and research institutions is needed to support in the development of this technology and to train human resources, the assistance of the Professional Bodies that trains the professionals especially in private sector must be linked up with the GRN Team and the Survey Department that regulates the use of Survey and Mapping in the country. The GNSS stake holders that will consist of public and private institutions and individuals must finally play a useful role for GNSS to be sustained in the country.

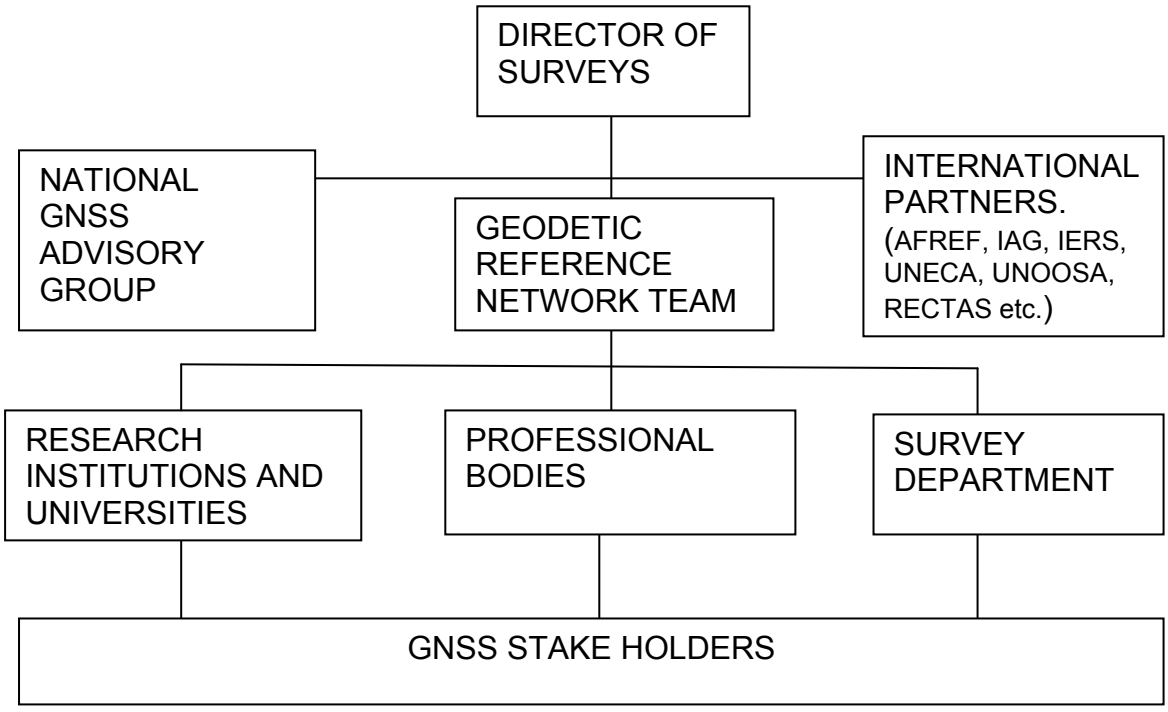

Figure 4-4: Proposed Management Structure for the Ghana National Geodetic Network

With the proposed management structure in place GNSS can be sustained in the country, especially if there is support from the Policy Makers to ensure that this cost effective technology is supported financially despite its initial cost in the building and expanding the basic infrastructure

4.3.3 Data Centres

There is the need to set up data centres at the Regional Centres for the collection, quality checking and processing, archiving and transmitting data to the appropriate destinations. These should be the point of contact to the local user community where differential corrections and other services can be obtained and will be the source of income generation from the user community, where products may be sold. There should be a Data Coordination Centre (DCC), where all the data in the network should be sent to periodically for analysis and with time, experience and improved infrastructure, real time analysis can be made to maintain the integrity and accuracy of the system. It is from the DCC that the National Geodetic Framework will be analyzed; stabilities of the various regional permanently reference stations will be checked. This DCC which will be the central computing facility and will be in charge of scientific research all GNSS related activities throughout the country and beyond.

The idea of getting the network integrated to that of the international community then calls for data standardization to be able to be accessed by the IGS participants and all external users more importantly AFREF community. The data should include

- daily files of GNSS data at a 30-second sampling rate
- hourly files of GNSS data at a 30-second sampling rate
- high-rate, low-latency GNSS data as available could be obtained on request.

The data should be available in RINEX format and should include broadcast ephemeris and meteorological data files.

4.3.4 Regional and Continental Integration

Ghana like most African countries has maintained our own reference frame which is different from her neighbors, and this usually results in improper edge-matching at the borders. This, in most cases, increases the potential in border conflicts and misunderstanding, and also makes it difficult to undertake transnational and continental projects. As we approach regional integration through peace and security, environmental management, communication, trade and industry, maps that are continuous across national boundaries is needed. (Ezigbalike, D., D Berhanu, 2006) The African Reference Frame (AFREF), the continental reference system, and the West African Reference Frame (WAFREF), the regional frame, aim at meeting these

goals. The establishment of a fundamental station, as described above, consistent with IGS standard therefore meets the requirements for the integration into these frames.

4.3.5 African Reference Frame (AFREF)

This is the realization of a modern continental Geodetic Reference System for Africa which aims at answering to the some of the problems on the continent through science, technology and multi-disciplinary approach using GNSS. (Wonnacott, 2005); (Neilan, 2008)

This African initiative aims at

- determining a continental reference frame consistent and homogeneous with ITRF as a basis for 3D reference network for all member states
- establishing permanently operating GNSS base stations such that all users will be within 1000 km their radius
- realizing a unified vertical datum through the establishment of African Precise Geoid
- determining the relationship between existing national reference frames and the ITRF
- provision of sustainable development for technology transfer to enhance national reference networks and other GNSS applications
- assisting in establishing in-country expertise for the development of modern geodetic techniques

5 Network Design for the Golden Triangle of Ghana

The network for this study was designed to cover the Golden Triangle of Ghana which is located in the southern part of the country with the three largest cities in the country at the vertices. The selection of these cities was based on economic and social factors, infrastructural support, potential application and population distribution, among others. With a 100 km radial coverage from the stations in these cities, the following are covered, 100% of the existing railway network, the two sea ports at Takoradi and Tema and the major airports. This covers about 57% of the total population, about 36% of the landmass, almost all the major mines, about 50% of the road network of the country, 86% of the coastline etc (Poku-Gyamfi, Y; Hein, G.W, 2006)

The network of this phase constitutes the five primary points, three permanent stations and two hub station, eighteen second order reference points and sixty third order reference points. The selection of these points were guided by the following factors

- spatial distribution
- accessibility
- stability of the foundation
- visibility to the sky
- security of the station
- available utilities services (power supply, communication, etc)
- clearance from reflecting surfaces and sources of radio interferences

5.1 Types of monuments

Four different types of monuments were designed for the realization of the objectives of this project depending on their function. These were for permanent stations, hub stations, second order stations and reference markers.

5.1.1 Permanent Stations

The three permanent stations located in Kumasi, Accra and Takoradi were chosen for the project with the Kumasi station as a fundamental station for the country. Kumasi was selected as the fundamental station mainly due to the relative seismic stability, facilities available and its central position in the country. These Permanent stations form a well conditioned triangle with sides approximately 200 km as can be seen in Figure 10-36.

5.1.2 Hub Stations

The hub stations which were located at Kade and Assin Fosu were selected to strengthen the permanent network such that all points of interest in the project area which included the selected trigonometric points to serve as common points for the determination of transformation parameters and the new Second Order stations, will be at most 80 km away from a primary point. They were made to operate throughout the duration of the campaign and therefore acted as continuously operating reference station.

5.1.3 Second Order Reference Network

The fundamental function of these points is to replace the old Control Points which were mostly located on top of mountains and at places that are not easily accessible to the user community. The project aimed at locating these reference points at approximately 50 km intervals which will make it easy for users to have relatively short baselines for their operations. These could act as permanent stations to provide corrections whenever necessary, therefore the selection of Government buildings which could offer office accommodation, power and communication, was given a high priority.

5.1.4 Reference Markers

In the vicinity all of the newly established Reference Station, three pillars were fixed as witness marks. These were to be used as points of departure for users of conventional survey methods, as access to the main points which were mostly on rooftops would not be convenient. At least two of these points were to be inter-visible to help the use of optical instruments which requires the line of sight. Coordinates as well as azimuth were determined to provide orientation of the points and also grid coordinates were provided for the users. Due to the easy accessibility, protective stakes were planted near them to alert of their presence.

5.2 Monumentation

The main task in the monumentation was the fabrication of antenna mount and the masonry work of the monument. This followed the careful selection of appropriate sites for the various types of monuments.

5.2.1 Antenna Mount Construction

The antenna mount attaches the receiver antenna to the monument, holding it in position to receive signals from the satellite. A good mount should be able to rotate in

the horizontal plane and should be able to ensure horizontal level using a mode of adjustment. One should be able to dismantle the mount leaving the marker intact and assemble it when necessary without significantly changing the eccentricity.

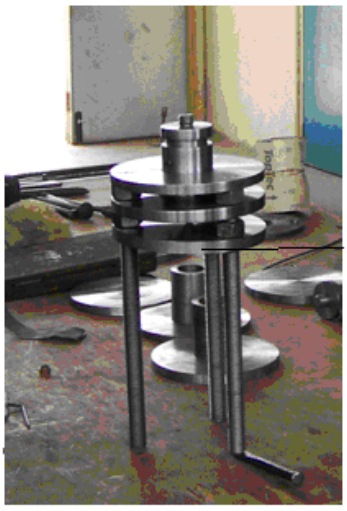

Figure 5-1: Photograph of a completely assembled antenna mount

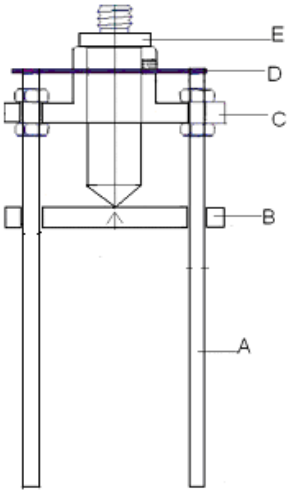

Figure 5-2: A schematic diagram of a completely assembled antenna mount

The Antenna Mount constructed for this project consists of five major components that have been assembled together to attach the antenna to the monument. The component ‘A’ is made of three metal bars that have been threaded to ensure firm grip in the concrete used for the monument. A hole is drilled on top of each bar to fit a screw used to fix the component D.

The second component ‘B’ is a circular plate of thickness 12 mm and diameter of 150 mm. It has three holes bored in them, forming equilateral triangle, which allows the threaded rods ‘A’ to pass through them. After setting the mount these rods are welded to the plate to fix them together. At the center of this circular plate is engraved the physical marker to be used for the station.

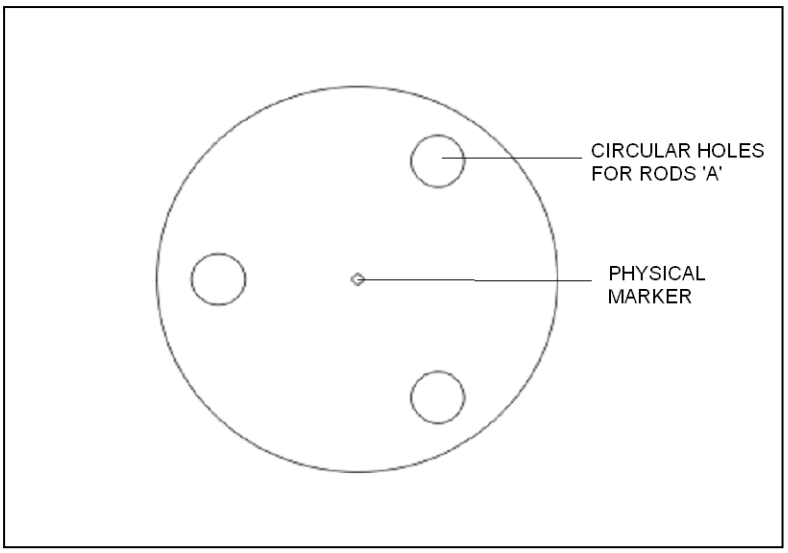

Figure 5-3: The cylindrical plate B with the engraved reference marker

The third component ‘C’ is a composite of two cylindrical pieces; one is a 150 mm diameter circular plate with three holes that can be aligned to the set of holes in plate B, thus making it possible for A to pass through. At the center is fixed the second cylinder with an internal diameter of 40mm and a height of 50mm. This allows the passage of D. This second cylinder has a hole for fixing a screw that keeps the component D tightly fixed.

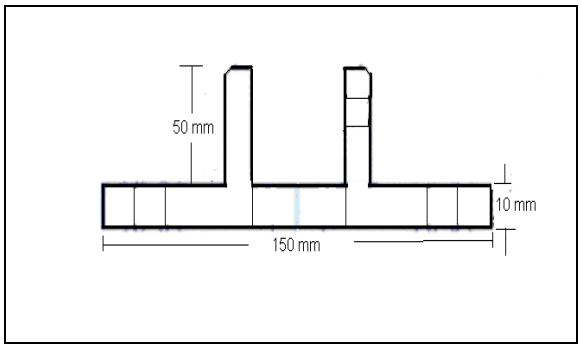

Figure 5-4: Showing the drawing of component C which supports the antenna holder

Figure 5-5: Photograph of component C

The component D is a cylindrical piece with diameter 40mm, but has a larger edge on top. There is a 5/8" screw on top that fits standard GPS antenna. This is the most critical component as the height which represents the eccentricity in the height, has its tip touching the physical marker and the screw on to fitting the antenna such that the bottom of the antenna rests on top of the cylinder.

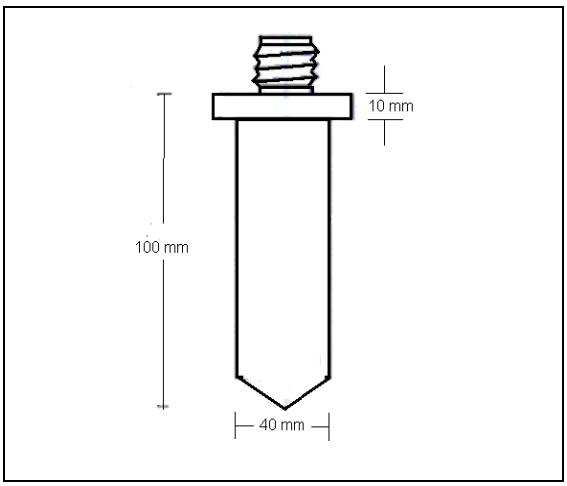

Figure 5-6: Shows the diagram of the cylinder E which links the antenna to the reference marker

Figure 5-7: Shows the photograph of four of the cylinder E

The last major component which is a cylindrical plate with a diameter 150mm and height of 10mm, has got holes bored such that they are aligned to those in B and C but these are made for screws that are made to fix the top of the rods A to ensure stability.

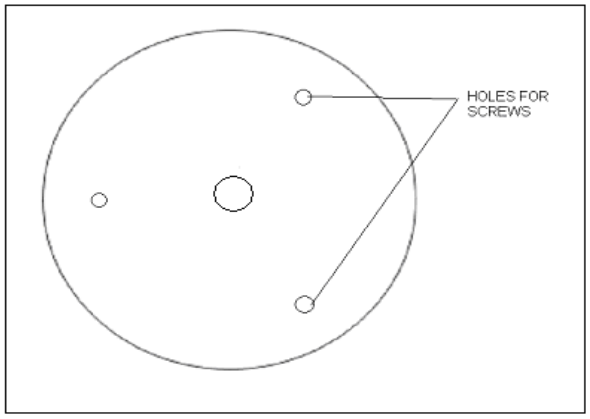

Figure 5-8: Shows the cylinder D which holds the rods A and the composite cylinder C to ensure stability

Figure 5-9: Show the photograph of the fixed component D

Bolts are put on top and below the on top of C for each of the rods A. This used to slightly level the antenna when the need arises.

5.2.2 Monument Construction

In all four types of monuments were constructed for this project. These included the ground-based monument for permanent stations, rooftop monument for permanent stations, ground-based monuments for reference markers and rooftop monuments for reference stations.

5.2.2.1 The Kumasi Fundamental Station Monument

The Ground-based monument was located in Kumasi at the premises of the Building and Road Research Institute, of the Council for Scientific and Industrial Research of Ghana. This is sited about 20 meters from the office room that has been dedicated to the receiver and its accessories. Factors that were considered for the selection of this location included security from vandalism and theft, power supply availability, internet connection, clear view to the sky, clearance from reflecting surfaces and also not close to any high power microwave transmitters that may cause interferences.

This is one of the two permanent station monuments that were constructed on the ground see Figure 5-11. A one meter diameter hole of three meter depth was excavated, filled with concrete and reinforced with a 5 meter bound iron rod. Half the length was put into the substructure and the other half above the ground.

A formwork of height 2.6 m and diameter 30 cm was installed and supported by timber props and filled with concrete. One meter asbestos cylinder with a diameter of 20 cm was fixed into the pillar leaving about 50 cm of it above the formwork and was left for a day. This was then filled with concrete followed by the antenna mount. To

ensure verticality and horizontality spirit level was used to check before and after curing of the concrete structure.

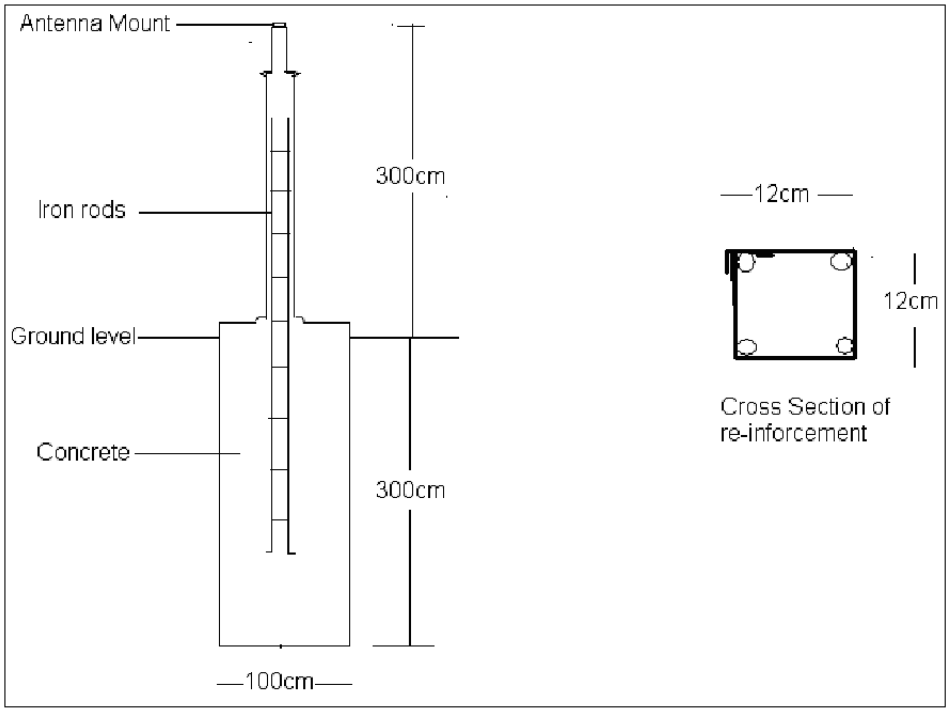

Figure 5-10: Schematic Diagram of the Kumasi Ground-based Monument

Figure 5-11: Shows the photograph of the Kumasi Ground-based monument

5.2.2.2 The Accra Permanent Station Monument

The Accra monument located on top of the Survey School Building, Figure 5-12, is less than 10m away from the location of the receiver. This building which was constructed about 80 years ago shows no visible signs of cracks and any other form of deformation or subsidence. The monument is made up of base of crossed metal which was welded perpendicularly to a metal bar that was used for reinforcement for the monument. This formed metal was bolted to the concrete rooftop. A cubic base was then cast with the reinforcement projecting vertically from it. Cylindrical hollow pre-cast concrete units were laid vertically on top of each other around the vertical reinforcement. These were filled later with concrete. A final cylindrical hollow pre-cast concrete smaller in diameter was laid on top as the final unit to hold the antenna mount. A spirit level was used to ensure the horizontality of the mount.

Figure 5-12: Shows the Roof-Top monument in Accra

5.2.2.3 Takoradi Monuments

Two monuments were constructed at Takoradi, about two kilometres from each other; one was located at the Takoradi Harbour (TKTG), Figure 5-13 about 40 m away from one of the oldest Tide Gauges in Africa and the other, (TADI), Figure 5-14, one of the permanent stations located at the vertices of the Golden Triangle of Ghana. The TKTG was ground based the TADI was located on a rooftop less than 10 m from the office of the Regional Surveyor.

The TADI and TKTG monuments were constructed with pre-cast cylindrical hollow concrete tubes, arranged vertically around a footing and reinforcement of iron rods and filled with concrete made of Portland cement and quarry dust. Antenna mounts were fixed on top of the pillars and the horizontality was ensured using a spirit level.

Figure 5-13: Shows the monument collocated at the Takoradi Tide Gauge

Figure 5-14: Show the monument located at the Takoradi Regional Survey Office as part of the GRN

5.2.3 Consideration of the Thermal Expansion of Monuments

All the monuments were made from sand-stone-Portland cement concrete which has coefficient of thermal expansion of between 0.74 and 1.3 x 10^{-6}/°C. With temperature range in the project area averaging 10°C and the total length of the monument including the substructure being 6m, the expected expansion will be less than 1mm

Coefficient of expansion of Sand-Stone-Portland Cement

$$\Delta L = \alpha_e L_o \Delta t \qquad 5\text{-}1$$

Where

ΔL	Linear expansion
α_e	Coefficient of linear expansion
L_o	length of monument
Δt	Change in temperature

ΔL = 1.3 x 10^{-5}/°C x 6 m x 10.7°C

= 8.346 x 10^{-4} m
= 0.83 mm

This is significant for scientific applications and has to be taken care of for very high precision applications. For most applications however, this sub-millimetre level expansion has little significance. These include the immediate accuracy need for the GRN.

5.2.4 Reference Station and Markers Monument

Seventeen second order Reference Stations were established throughout the Project Area with monuments, located on mainly on rooftops; at each of these stations, three reference markers were established, and also at the three permanent stations amounting to sixty reference markers. These markers were located on the ground around these main stations such that at least two of them would be inter-visible. One of them was located at least 100 meters away from the main station. These points as usual had to fulfill the requirements of standard GNSS reference station which included security and stability of the foundation, open sky, clearance from reflecting surfaces and possible microwave signals that could interfere with the GPS signals. The Reference markers were protected using special protective stakes which made the conspicuous for the public to prevent from intentional disturbances. These reference markers were established as points of departures for users especially those who use optical instruments

5.3 Systems Installation

The receivers that were used at the Permanent Stations were Sokkia GSR 2600 brand, shown in Figure 5-15, a dual frequency with the capability to perform both RTK and post-processing application. It has 12 L1 and 12 L2 channels with a removable internal Compact Flash memory card. This receiver has a power port that allows the use of current from the mains and in addition 12 V battery was connected to automatically replace the mains when there is power outage. It was quite robust and could withstand the harsh environmental conditions. Though there were a few problems especially with the data management, the performance was generally good. SOK 702 antenna, which was used with the receiver, pictured in Figure 5-16 utilizes the Pinwheel Technology. This is listed in both the NGS and JPL phase centre calibration table.

Installation of the GPS receivers and their accessories were made at the three Permanent Stations and the two Hub Stations located at Kade (KADE) and Assin Fosu (ASFO). With the exception of the Takoradi TADI system which used 10 m antenna cable all the rest had a 30 m long cable. Each station had a standby power supply which automatically powered the system when there is failure of the mains. In this project no dedicated computers were installed at the permanent stations to directly download the data but rather data was manually downloaded periodically. The system design which included the use of solar energy as a power back up is under consideration. There are plans to use base station receivers that are capable of streaming data online and in real time to the user, but for this study which is restricted to post-process data, the GSR 2600 was good enough.

Figure 5-15: Picture of a GSR2600 receiver used for the GRN Field campaign

Figure 5-16: Picture of an antenna SOK702 used for the data collection mounted on a tripod

5.4 Rover Deployment Pattern, Leap-Frog versus Radiation Method

Strategies of deployment pattern usually employed in such GPS data collection are the Leap-Frog Method and the Base Station Radiation Method, as illustrated in Figure 5-17. With the leap-frog method, assuming six receivers are deployed for observation; all the receivers are made to observe in one session, after the session four will be deployed to new stations in the adjacent area for the next session as two will be made to continue in observing in this session. At the end of the session, another four which may include the two that served in the two sessions will be deployed to a new set of four adjoining stations. This will continue until all the stations are occupied. This has an advantage of easy communication especially where the observation team may require supervision or external support as the group will be operation within a relatively small coverage area. The baselines are quite short and most processing software is able to resolve the ambiguities. Another advantage is that processing software that is not able to process over long baselines can be used unlike the radial method. The main disadvantage is that the propagation of error accumulates as the campaign progresses. It is also difficult to correct mistakes made during the campaign that require re-observation as the whole observation may have to be repeated. There is the need for better time synchronization of observation for this method and a breakdown of one observation team affects the whole programme. This process takes a longer observation period. On the travel distance which the main non-productive component of the observation, it can be observed by selecting a station say S1 on Session 1, the observer has to move to S5 on Session 2, and remains there on Session 3 and moves to S14 on Session 4, travelling round the coverage area.

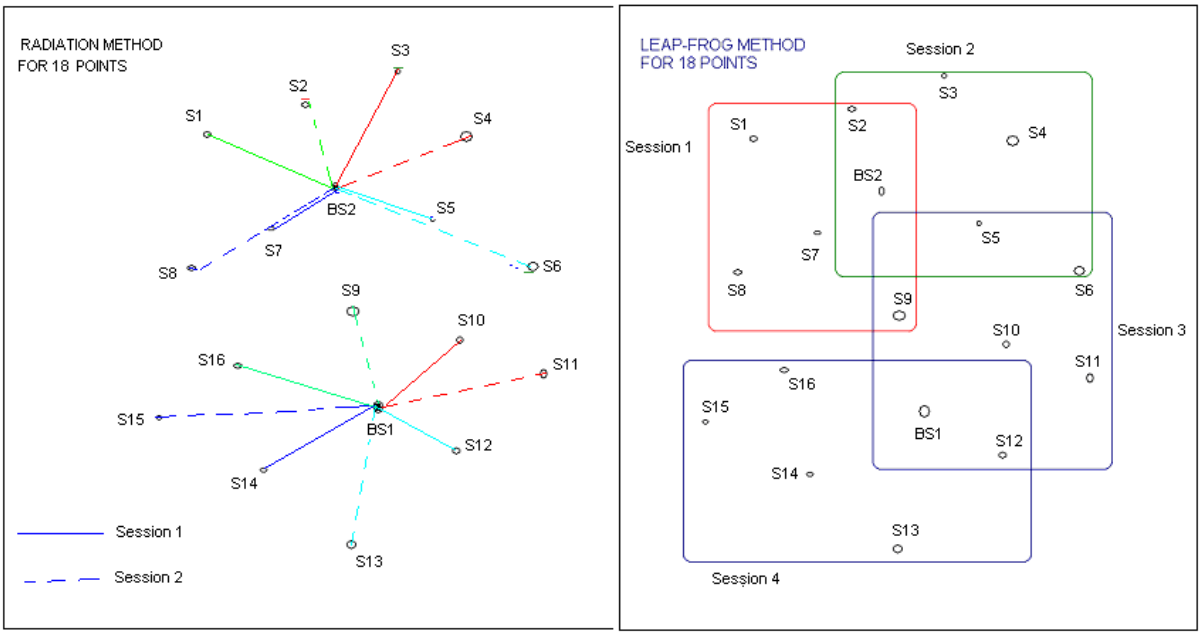

Figure 5-17: A diagram explaining two options of data observation methods, the Radiation and the Leap-Frog methods

The second method which was the preferred choice, the Base Station Radiation Method, has base stations fixed throughout the observation period as baselines are formed to all the stations to be observed. In the above scenario, two base stations are fixed, with four as rovers. At any session for a rover, there are at least baselines to the base stations; added to this will be the other three rovers which may have common observation period. There is enough redundancy that most of the baselines between the rovers may not be required. This is more flexible in terms of time synchronization. Any problematic observation can be repeated so far as the base station is made to operate and does not involve the other observers as pertains in the leap frog method. Another advantage is the relatively short travel distances by the observers. This however sometimes calls for temporally base station (Hub Stations) where the coverage area is large and long baselines are involved in a permanent network, in order to reduce the distance dependent errors. With improved processing software, longer baselines can be processed with high accuracies so one can sometimes do away with the hub stations especially where the processing software is reliable.

This project employed the Base Station Radiation Method; creating two hub stations at Assin Fosu and Kade. The introduction of these two hub stations reduced the longest base-length between a rover and the corresponding base to 81 km as against 110 km if it had not been introduced. Over 90% of the baselines for all observed rover stations were less than 70 km with the introduction of the hub stations, as against 90km if they had not been introduced. These base stations were made to run for a long time to ensure accuracy.

5.5 Scheduling

With the logistical support including six vehicles, twenty dual frequency receivers with enough back-up power supply, and twenty-five trained operators and their assistants, a comprehensive plan was drawn to minimise the non-productive time for the observation by employing a well planned schedule. The stations were selected such that two teams could be served by one vehicle. Each team had a receiver set and shared a third to be shared between the two teams. This shared receiver which was an integrated system RadianIS was to be used for observation of only the reference markers for easy data management. This implied that at least a team was constrained to work on a trigonometric point at a time. Despite this constraint, the teams were able to cover within seven days all the thirty trigonometric points, seventeen new points and the sixty reference markers. Five extra days were added to the schedule to correct the observations that could not meet the required standard.

5.6 Field Data Collection

The data collection for the Permanent Stations started after the installation starting from 16th May 2007 and recorded continuously throughout and after the observation period. The Hub Stations were made to run throughout the roving period and lasted for fourteen days and were discontinued after the roving campaign. The observation of the Trigonometric Stations were made for twelve hours each while New reference Stations were also observed for twelve hours but was repeated in a second round of observation to make it twenty-four hours. Each of the three Reference Markers at each station was observed for four hours one after the other, and were made to observe along their respective Reference Stations. The observation involved documentation of receiver and antenna using a specially designed field sheet. See Appendix D2. This involved height measurement of the antenna height, logging interval and elevation angle, checks on storage and power supply etc. Information of the site including description of station, sky obstruction sketch, weather condition, date of observation, start and end time and the identification of the observer.

In all 30 sessions were observed for the Trigonometric Points observation and 140 sessions for the permanent stations, hub stations, second order stations and the reference markers. The deployment pattern was aimed at reducing the non productive time of the campaign period with the available logistics, equipment and manpower. Ten groups were formed and were assigned to various stations. With effective scheduling, all the observations were made within 7 days, there was a quick quality checks for all the data with a few stations that had to be re-observed before finally discontinuing with the observations at the hub stations.

5.7 Data Storage

Copies of the data from all the receivers that were stored on Compact Flash Cards installed in the receivers in the raw proprietary format of Sokkia were downloaded onto a computer and were grouped under the designed data management scheme into various team files, in their respective Julian Dates. A copy of the same file converted into the RINEX format is also stored. All the data was stored on an external hard disk as well as compact disks for further quality checks and processing.

6 Data Pre-Processing

This chapter discusses the input data and the required corrections that are needed before the processing begins. Due to the peculiar problems in the low latitude tropics that the project area is located, emphasis is laid in corrections due to the troposphere and ionosphere, more especially as most users operate with single frequency receivers.

6.1 Data Input

The observed data from the field campaign in addition to Standard Product 3 (SP3) orbit data for the observed satellites and observation data for the selected IGS stations at Maspalomas MAS1 and Libreville NKLG were downloaded as input data for processing in addition to the observation files for the local stations and the respective antenna calibration data. These were the main required input data for GTCE.

Figure 6-1: Map showing the IGS stations considered for the establishment of ITRF for the study

6.1.1 Data Preparation and Management

Appropriate data structure was developed for this study based on the order of observed stations, day of year of observation, field crew grouping, receiver type etc. All the permanent and hub stations data were grouped together as base stations with the rest as rover stations. The data was grouped into base stations, new stations, trigonometric stations and reference marker stations. Daily stations were created by slitting and splicing of observation data that were made overnight. The management structure was developed for the various applications.

After the data conversion from the Sokkia proprietary format to RINEX using Spectrum Survey software from Sokkia, the data was organized into an appropriate format that was acceptable by the processing software PrePos GNSS Suite (PGS). This was mainly on the header of the RINEX observation file where the marker name (unique four character name) was provided, the antenna type was added as shown on the list of the NGS or IGS set of antennas with standard PCV corrections. The antenna phase center corrections have to be confirmed at this stage before the processing. Translation, editing and quality check (TEQC), the toolkit developed by UNAVCO for solving many pre-processing problems with GNSS data was used to check the quality of the data after the preparation.

After putting in the appropriate prepared RINEX data into the processing software, as in the case the PrePos GNSS Suite (PGS) and other scientific software, a couple of corrections have to be made to minimize the systematic errors. These are associated with the stability of occupied stations that is the coordinates of the marker point on the monument, the errors encountered as the signal travel from the satellite to the antenna of receiver, that is the signal propagation error, and the error due to maneuvers and the construction of the satellite vehicles.

6.1.2 Station Corrections

The station coordinates are affected by several natural phenomena that cause varying displacements that need to be corrected before the processing of station coordinates. These occurrences are mainly due to the non-rigidity of the earth and its influence by the gravitational attraction of the extra-terrestrial bodies including the moon and the sun, as well as the temporal deformation caused by loading due to the ocean tide and the atmosphere. This station specific displacement also include plate tectonics, pole tides, sub-daily earth rotation can cause displacement from a few millimeters to several decimeters. Other corrections at the stations to be considered are the antenna geometric and phase centre eccentricities which depends on the antenna. Table 6-1 shows the magnitudes of some of these natural phenomena on the station coordinates.

Displacement Phenomenon	Approximate Magnitude
Solid Earth Tides	A few decimeters
Earth Orientation Parameters	A few centimeters
Ocean Loading	A few centimeters
Station Velocity	A few centimeter per year
Receiver Antenna Phase Center Eccentricity	A few centimeters

Table 6-1: Showing the approximate magnitudes of various phenomena that causes displacement at the stations

The various phenomena are relevant for special applications which need high precision, although most applications in this Golden Triangle network may not. For example, the station velocity becomes relevant when a user is interested in seismic activities which threaten the Accra region of Ghana. Ocean loading becomes relevant as Ghana is bordered in the south by the Atlantic Ocean. Ghana's location near the equator makes the correction for solid earth tides relevant, though it may not be very significant as far as the lengths of the baselines within the Golden triangle is concerned

6.1.2.1 Station Velocity

The station velocity, which is explained by the plate tectonic theory, causes time dependent three dimension linear movement of a station on one plate relative to another and with respect to the satellite systems. To correct this, the initial measurement is tagged with a fixed time usually expressed in decimal year. The solution is usually expressed in the ITRS in the form ITRFYY where 'YY' indicates the year up to which the data was used for the realization. To correct the station displacement a reference epoch is established and added as an input. This input which is the linear velocity for the station with respect to the Earth-Centered-Earth-Fixed coordinate frame, resulting from the global plate motion is applied. A typical example of this plate movement the relative motion of Ghana (Nubia Plate), with respect to the Somali Plate at the velocity of 5.5-6.5 mm/year (Gordon, 1998)

$$\bar{X}(t) = \bar{X}(t_{ref}) + (t - t_{ref})\bar{V}(t_{ref}) \qquad 6\text{-}1$$

Where,

t	observation epoch in decimal years
t_{ref}	reference epoch in years as given in the network solution file
$\bar{X}(t)$	ECEF position vector at observation epoch t in meters
$\bar{X}(t_{ref})$	ECEF position vector at reference epoch t_{ref} in meter
$\bar{V}(t_{ref})$	velocity vector of station at reference epoch in meter per year

6.1.2.2 SOLID EARTH TIDES

These are periodic movements of the earth related in amplitude and phase of to some natural geophysical force, mainly due to the variation of the gravitational field exerted on the surface of the earth as a result of the regular movement of the sun-earth and moon-earth systems. This deformation which is the result of the pliable nature of the earth has an amplitude range of about 40 cm, typically with maximum at low latitude regions of the globe. This displacement is at predominantly semi-diurnal and diurnal frequencies (Watson et al, 2006): (Lambeck, 1988). According to (Kouba J. P., 2000), this site displacement vector due to solid earth tide resulting from a disturbing body, which is $\Delta \mathrm{r}^{\mathrm{T}}$ equal to $|\Delta x, \Delta y, \Delta z|$ is given by

$$\Delta \bar{\mathrm{r}} = \sum_{\mathrm{j}=2}^{3} \frac{\mathrm{GM_j}}{\mathrm{GM}} \frac{\mathrm{r}^4}{\mathrm{R_j^3}} \left(\left(3\mathrm{l}_2 (\widetilde{\mathrm{R}_\mathrm{j}} \tilde{\mathrm{r}}) \widetilde{\mathrm{R}_\mathrm{j}}\right) + \left(3\left(\frac{\mathrm{h}_2}{2} - \mathrm{l}_2\right)(\widetilde{\mathrm{R}_\mathrm{j}} \tilde{\mathrm{r}})^2 - \frac{\mathrm{h}_2}{2}\right)\right) + \left(0.025\mathrm{m} \sin \emptyset \cos \emptyset \sin(\theta_\mathrm{g} + \lambda)\right)\tilde{\mathrm{r}} \qquad 6\text{-}2$$

Where GM and GM_j are the product of the gravitational constant mass of the Earth and the celestial bodies e.g. Moon (j=2) and the Sun (j=3); $\mathrm{r}, \mathrm{R_j}$ are the geocentric state vectors of the station, the Moon and the Sun with the corresponding unit vectors of $\widetilde{\mathrm{R_j}}, \tilde{\mathrm{r}}$ respectively; h_2 and l_2 are the nominal second degree Love and Shida dimensionless numbers (about 0.609 and 0.085 respectively); $\emptyset$ and λ are the site longitude and latitude (positive east) and θ_g is Greenwich Mean Siderial Time.
The tidal correction from Eqn. 6.2 can reach about 30 cm in the radial and 5 cm in the horizontal. For differential positioning of short baselines (<100 km) both positions have almost identical displacements and are therefore unaffected by the solid earth tides. (Phillips et al, 1999)

6.1.2.3 Ocean Tide Loading

Ocean Tide Loading displacement is caused by the pressure exerted by the periodic change mass distribution of the waters in the ocean, mainly due to the gravitation attraction of the sun and moon. The impact is felt most at the coastal regions and decreases inland. This periodic displacement affects mainly the radial component and to a lesser extent on the horizontal plane. Ocean Tide Loading in Southern Ghana, using the most dominant wave, diurnal lunar (M2), as displayed in Figure 6-2 and Figure 6-3, shows a displacement of almost 20 mm but reduces to about 10 mm about 240 km away from the ocean. For most applications this is not very significant, but its relevance is felt where millimeter accuracy is required. This is modeled using the amplitudes and phase angles of the project area in a specified format obtained from the Onsala Space Observatory, (ONSALA, 2007 (Last Update)), as an input data for the correction in the PrePos GNSS Suite. According to (McCarthy, 1992) the site three dimensional displacements due to ocean loading Δc for each of the 11 significant waves is given by

$$\Delta c = \sum_j f_j A_j \cos\left(\omega_j t + \chi_j + \mu_j - \Phi_j\right) \quad 6\text{-}3$$

Where f_j and μ_j are depend on the longitude of the lunar node, A_j and Φ_j are the amplitude and phase for each displacement, ω_j is the frequency of the tide j and χ_j is the astronomical argument at t=0. The three components of displacement, radial, northing and easting can be computed as described by (McCarthy, 1992). The tidal loading at a point is computed by interpolating from pre-calculated gridded points 1° x 1° globally. Four nearest neighbors are computed in the grid, and bilinear spatial interpolation is then used to compute the appropriate amplitude and phase at the point of interest.

A plot of the radial displacement of the most significant wave M2 (diurnal Lunar) is as shown below for the project area. In reality the correction takes into account the combined effect of all the 11 significant amplitudes computed with their respective phases.

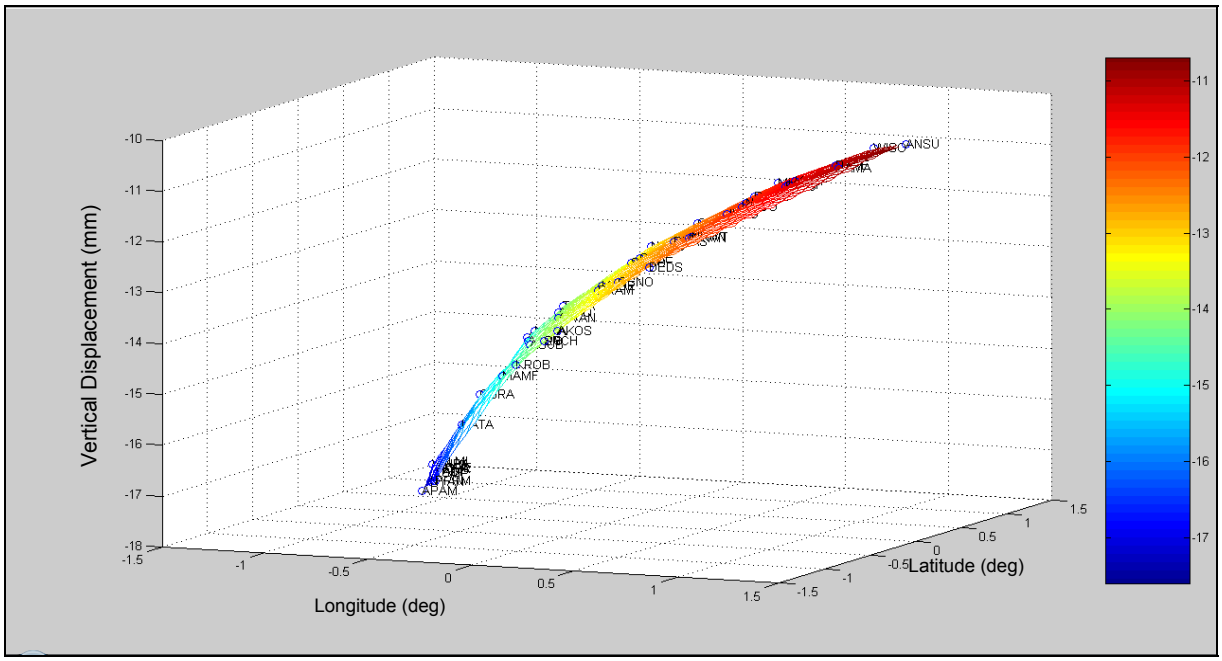

Figure 6-2: A plot showing the trend of vertical displacement in the Golden Triangle of Ghana

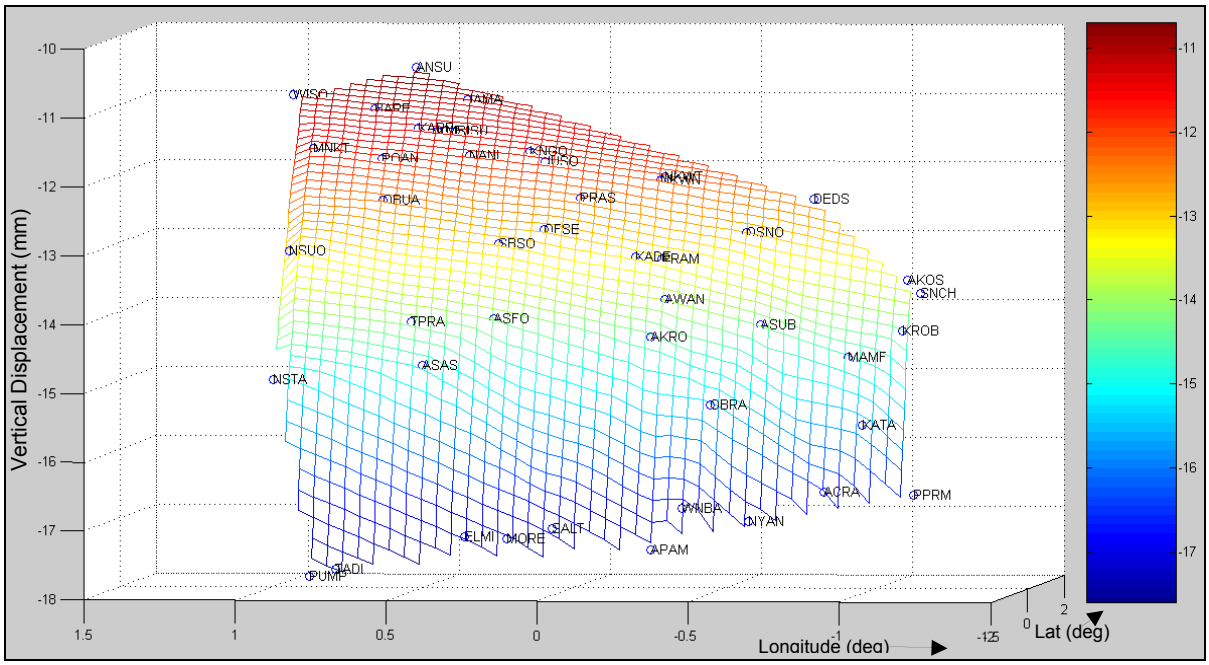

Figure 6-3: A plot showing the impact of Ocean Tide Loading at the various stations observed for the GRN

6.1.2.4 Earth Orientation Parameters

The EOP describes the irregularities of the earth's rotation with respect to a non-rotation reference frame. This orientation of the earth with respect to the celestial reference frame affects positioning with GNSS. The effect of the variation of the position of the poles causes periodical deformations of the earth as a result of small changes in the earth's centrifugal potential. According to (IERS, 1996), using second degree Shida and Love numbers, the correction to latitude (ø), longitude (λ) and height is approximately

$$\Delta\emptyset = -9\cos 2\emptyset\left(X_p \cos\lambda - Y_p \sin\lambda\right) \quad 6\text{-}4$$

$$\Delta\lambda = 9\cos\emptyset\left(X_p \sin\lambda + Y_p \cos\lambda\right) \quad 6\text{-}5$$

$$\Delta h = -32\sin 2\emptyset\left(X_p \cos\lambda - Y_p \sin\lambda\right) \quad 6\text{-}6$$

X_p and X_p are the pole position coordinates in seconds of arc.

To be consistent with ITRF the above corrections must be subtracted from the position solutions. This according to (Kouba J. , 2002) has a period of 430 days and can reach a maximum of 25 mm in height and 7 mm in the horizontal directions as the polar motion can reach a maximum of 0.8 arcsecond. A concise explanation has been treated by the (IERS), (IERS, 1996)

6.1.2.5 Receiver Antenna Eccentricity Corrections

This is the correction that has to be made in the computation of coordinates as a result of geometrical displacement of the antenna reference point from the physical station marker, usually significant only in the radial direction after centering the receiver on top of the mark. This correction is usually required in the RINEX header of the observation file, for the computation of the coordinates.

$$\Delta X_{AE} = \begin{bmatrix} \Delta N_{AE} \\ \Delta E_{AE} \\ \Delta R_{AE} \end{bmatrix} \quad 6\text{-}7$$

ΔN_{AE} correction in the northing direction
ΔE_{AE} correction in the easting direction
ΔR_{AE} correction in the vertical direction

6.1.2.6 Receiver Antenna Phase Centre Eccentricity Correction

The nominal antenna reference point (ARP) does not really coincide with the actual antenna phase center (APC) and the vector between these two is the antenna phase center eccentricity. The APC is neither physical nor stable and changes with the change in direction of the signal that is the angle of elevation of the signal and the azimuth, as well as the frequency of the signal (Schmid et al, 2005), for example the difference between L1 and L2 for Dorne Margolin antenna is about 2 cm (Schueler T. , 2001). There is need to employ the calibrated values from NGS or IGS, failure can lead to an error of about 10 cm in the vertical according to (Mader, 1999). The azimuth effect is caused by the local environmental reflections. The need to use the standard calibration of GNSS antenna is to ensure interoperability within the growing community of GNSS antenna types for high precision application is very important.
Until baseline length approaches several thousands of kilometers, there is practically no difference in using absolute or relative calibrations. As the baseline length increases the curvature of the earth causes same satellites to appear at increasingly different elevations at the ends of the baselines.

6.1.3 Signal Propagation Corrections

The propagation of the GPS signals from satellite to receiver encounter a delay due to the constituents of medium through which it passes. These signals encounter a number of propagation effects, with the magnitude depending on the angle of elevation of the satellite. The constituents are the dispersive ionosphere which causes group delay and scintillation, the neutral and non-dispersive wet and dry troposphere which causes group delay as well as attenuation.

6.1.3.1 The Atmospheric Effects

The physical reason of the delay of the signals through the atmosphere is variation of the refractive index in the atmosphere, which increase with decrease in altitude, as the speed of propagation is less than that in a vacuum and decreases with the increase in the refractive index.

For the combined atmospheric effect the equation as explained in (Hein G.W., B. Eissfeller, 1986) is given as in 6-8.

$$\Delta t_{Atm} = \frac{1}{C_0}\int_0^{\rho_{trop}} N_{Trop}\, d\rho + \frac{1}{C_0}\int_0^{\rho_{Iono}} N_{iono}\, d\rho \qquad 6\text{-}8$$

Where

N_{trop}	refractive index in the troposphere
N_{iono}	refractive index in the ionosphere
ρ_{trop}	upper limit of the troposphere
ρ_{iono}	upper limit of the ionosphere
C_0	speed of propagating signals in vacuum

6.1.3.1.1 The Tropospheric Delay

Troposphere is one of the main components that cause delay of propagating signals in the atmosphere as shown in Eqn. 6-9. Its effect requires mitigation for almost all applications in positioning with GNSS. An in-depth study of the profile of the atmosphere as shown in Figure 6-4 is necessary for the understanding of the troposphere.

The homosphere generally refers to the neutral component of the atmosphere from the surface of the earth to about 80 km. The uppermost part, the mesosphere which is separated from the ionosphere by the mesopause, is characterized by a general decrease in temperature with the increase in height. This is separated from the stratosphere, which stretches from a little below 20 km to about 50 km, by the stratopause. This is characterized by a general increase of temperature with the height.

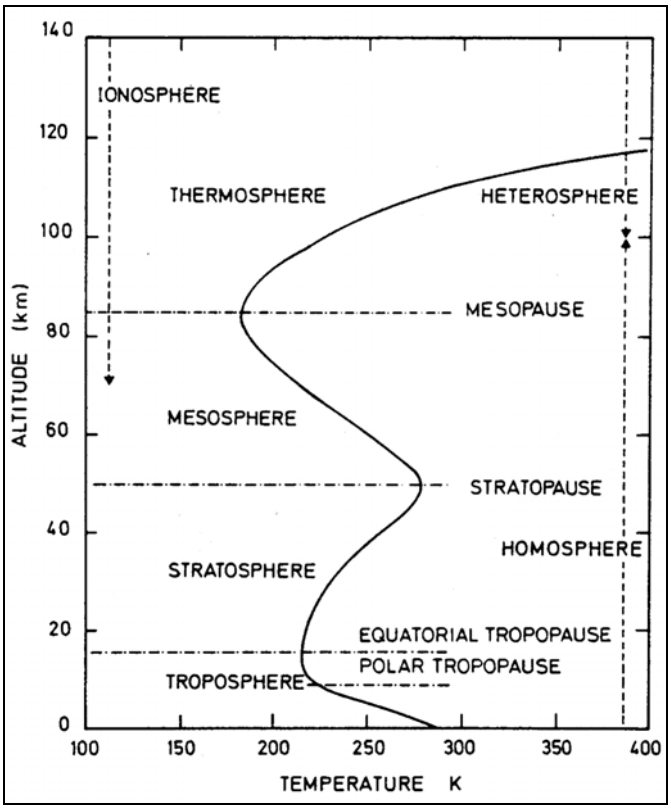

Figure 6-4: Profile of the atmosphere (Marsh, 2004)

Below this is the troposphere which is the lower homosphere, located between the surface of the earth and the tropopause. The tropopause which is the boundary between the stratosphere and the troposphere exhibits temporal and spatial variation in altitude, about 8-12 km in winter and 10-12 km in summer the higher at the equator and lower at the poles. There is a general decrease in temperature with height in the troposphere as shown in Figure 6-3 with a lapse rate of -5 to -7°C per km of altitude increase from sea level. At higher altitudes in winter and night time, temperature inversion can occur in 0.5 to 2 km region before the beginning of the temperature lapse rate (Spilker, 1996).

The troposphere which is non-dispersive contains about 75% of the mass of the atmosphere, has the same refractive index for both the carrier phases and the code modulation of the GPS signals. There is propagation delay caused by the combined effect of hydrostatic and wet delays which does not only slows down the propagation but also reduces the amplitude causing attenuation. This action cause delay in the signal propagation by about 2.5 m in the zenith direction, with zenith hydrostatic delay accounting for about 2.3 m while the zenith wet delay contributes to about 0.15 m (Schueler T. , 2001). According to (Spilker, 1996); (Grove-Rasmissen, 2002) the wet component which is rather small is more difficult to model as it is unevenly distributed while on the other hand, modeling the dry component is not complicated. The delay is about 10 times higher near the horizon due to the longer travel time through the troposphere from satellite to receiver as compared to that through a vacuum. This delay varies with temperature, pressure and humidity is also dependent

on the height of the tropopause which predicts higher values in the lower latitude Equatorial region as stated earlier. The spatio-temporal variations of the tropospheric conditions calls for an in-depth study of the troposphere if one wants to conduct a very precise GNSS survey in the Equatorial area like Ghana.

6.1.3.2 Modeling the Troposphere Delay

In modeling the troposphere various approaches are employed including the use of radiosondes, remote sensors, balloons, satellite observation aircrafts and ground based sensors are being employed to measure these parameters. The delay of the GPS signal as it passes through the troposphere is given by the difference between the ray passing through the atmosphere and the geometrical distance which is represented by a virtual path through a vacuum. This is given mathematically by

$$\partial S_A^i = \int_{atm} n(s)\, ds - \int_{vac} ds \qquad 6\text{-}9$$

∂S_A^i the total neutral slant delay from receiver antenna A to satellite i

$\int_{atm} n(s)ds$ path of ray through the atmosphere from receiver antenna to satellite

$\int_{vac} ds$ geometrical distance from receiver antenna to satellite

$$\partial S_A^i = \partial S_{A(hyd)}^i + \partial S_{A(wet)}^i \qquad 6\text{-}10$$

$\partial S_{A(wet)}^i$ the wet slant path delay

$\partial S_{A(wet)}^i$ the hydrostatic slant path delay

The effect of the delay in the signal propagation depends on the refractivity of the troposphere N which is due to the combination of hydrostatic and wet components.

$$N = N_{hyd} + N_{wet}\, Z_w^{-1} \qquad 6\text{-}11$$

$$N_{hyd} = K_1 \frac{R_0}{M_d} \rho = K_1 R_d \rho \qquad 6\text{-}12$$

$$N_{wet} = K_2 \frac{e}{T} + + K_3 \frac{e}{T^2} \qquad 6\text{-}13$$

N_{hyd} hydrostatic refractive index

N_{wet} surface wet refractive index

R_0 universal gas constant

T temperature

Z_w^{-1}	inverse compressibility of water
M_d	molar weight of dry air
R_d	specific gas constant
e	partial water vapor
K_1, K_2 and K_3	are the refraction constants
ρ	Total density

The equations 6-12 and 6-13 show the relationship of the measured meteorological quantities with the refractive indices which when integrated give the zenith tropospheric delays. Further details have been treated in (Schueler T. , 2001).

6.1.3.3 Meteorological Quantities

The meteorological quantities to be considered are temperature, pressure and water vapor. Referring to figure 6-3 provided by (Marsh, 2004), temperature shows a linear decrease with height up to the tropopause, that is the temperature lapse rate, and stays constant for a period around the tropopause, and starts to increase to the stratopaεuse where it turns to decrease again with height in the mesopause. In the thermosphere there is again an increase with respect to height. To model the troposphere, the lapse rate of temperature is needed. The first few 100 m there are however disturbances in the temperature.

Pressure which is also used to model the atmosphere varies exponentially with height. The standard temperature at the mean-sea-level is about 1013 hPa and between 300 hPa and 70 hPa at the equatorial tropopause. Pressure can be modeled using height and temperature and temperature lapse rate.

Water vapor is not homogenously distributed either horizontally or vertically due to variation in temperature with respect to location as well as the influence of wind etc. This is concentrated in the lower troposphere and decreases with height which according to (Askne J., H Nordius, 1987), reduces in the same manner as pressure.

6.1.3.4 Modeling the Troposphere

The required parameters for modeling the troposphere are water vapor, mean temperature and pressure. Knowing that the total tropospheric delay in the direction of a particular satellite, slant path delay (SPD) is the sum of the slant hydrostatic delay and the slant wet delays. These can be projected into the zenith using mapping function thus

$$SPD = m_H(\varepsilon)ZHD + m_W(\varepsilon)ZWD \qquad 6\text{-}14$$

$m_H(\varepsilon)$	mapping function for the hydrostatic delay

$m_W(\varepsilon)$ mapping function for the wet delay
ZHD Zenith Hydrostatic delay
ZWD Zenith Wet Delay

As already stated the modeling of the ZHD, which is incidentally larger, can easily be achieved using the total pressure at the antenna site. Saastamoinen model which is one of the most accurate models can be used for most applications, (Mendes, V.B., R.B. Langley, 1995). With accurate surface weather measurement, the dry zenith model is accurate to the mm level using the eqn. 6-15

$$\mathrm{ZHD} = \frac{0{\cdot}0022767\left[\frac{\mathrm{m}}{\mathrm{hPa}}\right]\cdot \mathrm{P}}{1-0{\cdot}00266\cos 2\varphi - 0{\cdot}00028\left[\frac{1}{\mathrm{km}}\right]\mathrm{h}} \qquad 6\text{-}15$$

φ Ellipsoidal latitude
h Surface height above the ellipsoid in [km]
pp Surface pressure in [hPa]

The zenith-wet-delay, ZWD, can be modeled using ground-based gridded blind model which employs meteorological parameters. The formula 6-16 uses the physical constants to estimate the ZWD.

$$ZWD = 10^{-6}\frac{\mathrm{k_3}}{\mathrm{T_m}}\frac{\mathrm{R_d}}{\mathrm{g_m}}\frac{\mathrm{e_0}}{\lambda+1} \qquad 6\text{-}16$$

$\mathrm{k_3}$ Refraction Coefficient 370100±1200[K^2hPa^{-1}]
$\mathrm{R_d}$ Gas constant of dry air: 287·054[$Jkg^{-1}K^{-1}$]
$\mathrm{T_m}$ Mean Temperature [K]
$\mathrm{g_m}$ Weighted mean gravity acceleration [m sec^{-2}]
λ Water vapour lapse rate

6.1.3.5 Tropgrid

Tropgrid, a new approach in the provision of a blind model which featured prominently in this study is derived using the combination of the ZWD and ZHD of Saastamoinen. This is estimated at the user position using in addition the estimates of the meteorological parameters from a 1° x 1° grid. The horizontal interpolation of the position using nine surrounding grid points is computed using the inverse of the square of the distance as weight, (Krueger, E., T. Schueler, G. W. Hein, A. Martellucci, G. Blarzino, 2004) gives further details.

6.1.3.6 Numerical Weather Model

Numerical Weather Model (NWM) which is a 3D weather field is applied in the determination of tropospheric delays in the atmosphere. Data in the output fields are organized in vertical layers of geo-potential heights for a corresponding pressure as well as temperature levels and relative humidity as well. In the horizontal direction, data is stored in matrix layout with 181 rows and 360 columns corresponding to 1° X 1° around the globe. Data for tropospheric delay modeling can be extracted and stored in separate files and are referenced to the model surface or the total atmospheric column and can be vertically reduced with the help of reduction coefficient. (Schueler et al, 2000) gives more insight into the GDAS numerical weather fields. According to (Krueger, E., T. Schueler, G. W. Hein, A. Martellucci, G. Blarzino, 2004), the use of the ZPD data from the NWM shows a better accuracy than the blind models TropSite and TropGrid, which in turn were better than that of the MOPS-Model used by WAAS. For very precise measurement, the ZPD data must be split into the ZHD and ZWD and the corresponding mapping functions used. This strategy is applied in GTCE and SEMIKA.

6.1.4 The Ionospheric Delay

In addition to the delay due to the passage through the troposphere, the ionospheric delay which is also a matter of concern to GNSS users, must be also considered as shown in equation 6-15. This should be a matter of interest to Ghana as most GNSS users are using single frequency receivers for cadastral applications

6.1.4.1 The Ionosphere

The ionosphere is that part of the upper atmosphere, located at about 85 km, away from the surface of the earth, just above the mesosphere to about a 1000 km. This layer is characterized by the occurrence of free electrons in sufficient density to have an appreciable dispersive influence on the propagation of radio frequency electromagnetic waves. The ionization of this layer depends primarily on the sun and its activities.

Ionospheric effects vary greatly with time of the day, seasonally and the solar cycle (every 11 years). It also varies with geographical location for instance polar, auroral zones, mid-latitudes, and equatorial regions. Ionospheric effect is also constrained to follow the earth's magnetic flux.

The major part of the ionization is produced by activities of the sun, for example, solar X-ray, ultraviolet radiations. The most noticeable effect is seen in the diurnal rotation of the Earth with respect to the Sun. Ionospheric effects increases in the daytime when the suns radiation is high and reduces during the night in the shadow of the sun. Ionosphere is also controlled by the variations of the geomagnetic field.

6.1.4.1.1 **Deriving the Ionospheric Delay**

The dispersive nature of the ionosphere causes the radial propagation of the electromagnetic signals from the satellite to the receiver to delay. This delay is equivalent to the difference between the distance travelled by signal and the geometric distance through a vacuum, (Schueler T. , 2001) expresses

$$\partial S_{ion}^{z=0} = \int_{ion} n_{ion}(h)dh - \int_{vac} dh \qquad 6\text{-}17$$

n_{ion}	refraction index of the ionosphere
dh	differential increment in height
z	zenith angle
ion	path of a ray passing in radial direction through the ionosphere
vac	virtual path of a ray passing in radial direction through the vacuum

$$n_{ion} = 1 + \frac{C_2}{f^2} + \frac{C_3}{f^3} + \frac{C_4}{f^4} + \cdots \qquad 6\text{-}18$$

C_{2-4}	coefficients of series expansion
f	frequency of carrier

$$n_{ion} \approx 1 + \frac{C_2}{f^2} = 1 + \frac{CN_e}{f^2}. \qquad 6\text{-}19$$

$$c = 40.28 m^3/s^2$$

N_e	electron density in electron/m^2

The ionospheric delay can be practically divided into first order, second order and third order, the first being the effect of the second term of eqn. 6-19, the second and third are contributed by the third and the fourth terms respectively. GPS signals are delayed by the ionosphere by a magnitude proportional to the Total Electron Content (TEC). Rapid phase and amplitude variations (Scintillations) in the GPS signal can resulting from the effect of the ionosphere can cause receiver to lose lock. Unmodeled delay in the ionosphere therefore affects the range measurements to the GPS satellites. The effect of ionosphere is most severe in the Equatorial Region and affects baselines of a few 100km for a large part of the day almost daily.

6.1.4.1.2 The Ionospheric Corrections

Ionospheric group delays can cause significant errors in pseudorange measurements by up to about 300 ns especially at low elevation angles during the daytime but can reduce to as low as 5 to 15 ns at night at a good elevation angle. Most of this delay can be corrected using dual frequency measurements, but must be modeled for correction if a single frequency receiver is used if one requires precise positioning.
The correction of the ionosphere is classified into the first-order and the higher order corrections, with the first order being the dominant contributor. According to (Seeber, 1993), the maximum vertical ionospheric range error due to L1 frequency is 32.5 m and that for the L2 is 53.5 m. These can however be almost completely eliminated using the ionosphere-free linear combination. The second order has a maximum of 3.6 cm for the L1 and 7.6 cm for L2 and the third 2 mm for L1 and 7 mm for L2. These higher order effects can however not be completely eliminated by linear combination. This is usually ignored for most applications, but for precise positioning this is quite significant and has to be eliminated through modeling.

In order to estimate the higher order errors using dual frequency GNSS observables, the magnetic field within the ionosphere is needed. The use of the field value at the ionosphere piercing point (IPP) at 350 km altitude has to be modified and the International Geomagnetic Reference Field (IGRF-10) is assumed (Seebany et al, 2006). The IPP is affected by currents induced in the magnetosphere during ionospherically stormy times. The use of IPP at 350 km also assumes the bulk of electrons being at that altitude when in reality according to (Mannucci et al, 2005), it has been observed to occur at higher altitudes where magnetic field is weaker.

6.1.4.1.3 Klobuchar Model of the Ionosphere

The Klobuchar model is a functional-based model which is broadcast to predict the global TEC distribution at a given period for real time correction of the ionospheric effect on a single frequency GPS measurement. This simple algorithm has been developed to use eight coefficients to describe a worldwide behavior of the Earth's ionosphere.
The model represents the zenith delay as a constant value at night time and half cosine value during the day (Misra, P., P. Enge, 2001). The zenith ionospheric delay estimate at a local time is given by

$$\frac{\mathrm{I_t}}{\mathrm{C}} = \left(\mathrm{A_1} + \mathrm{A_2}\cos\left(\frac{2\pi(\mathrm{t}-\mathrm{A_3})}{\mathrm{A_4}}\right)\right) \qquad 6\text{-}20$$

If

$$\lfloor t - A_1 \rfloor < \frac{A_4}{4}$$

Otherwise t equals A_1

I_t the zenith ionospheric delay at the local time
A_1 the night time value of the zenith delay (fixed at $5x10^{-2}$ s)
A_2 the Amplitude of the cosine function for day time values
A_3 the phase correspondence to the peak of the cosine function fixed at 50400 s local time
A_4 Period of the cosine function (≥72000 s)
c the obliquity factor

The value A_2 and A_4 are specified in the navigation message broadcast by each satellite in terms of four coefficients each of a polynomial function. A pool of 370 sets associated with different seasons and levels of solar activities is available from which eight coefficients are selected to derive the ionospheric correction.
This model corrects about 50% of the expected ionospheric error, there can however be more improvement in the correction using the functional approach, but this will be at the expense of complexity of the model as demonstrated graphically in Figure 6-5.

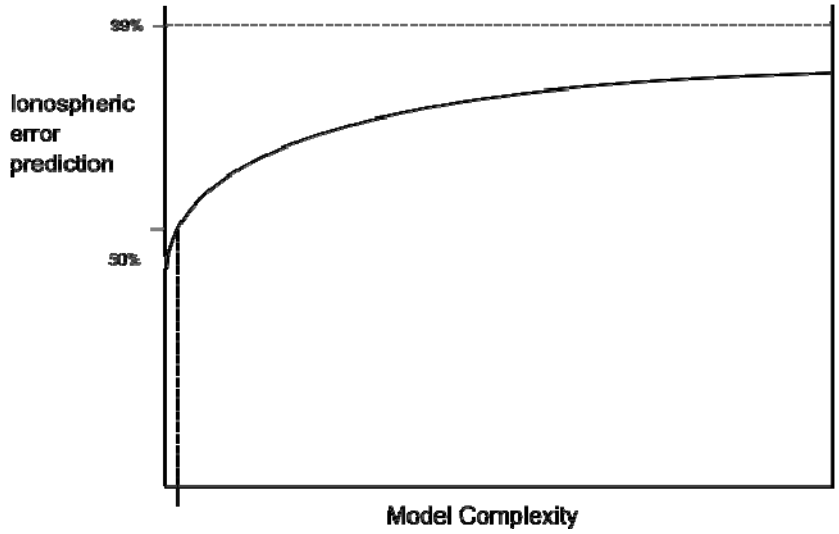

Figure 6-5: Relative model complexity versus ionospheric error correction, (Klobuchar, 1996)

6.1.4.1.4 NeQuick Approach for Ionospheric Delay

NeQuick is a future Galileo climate ionospheric model proposed to calculate corrections for single frequency Galileo users (Aragon-Angel et al 2003). It reproduces TEC along a given ray path for a given period, geographic longitude, latitude and height. The main input parameter for NeQuick is the effective ionization level Az which is approximated with a second degree polynomial of the modified dip latitude. The three coefficients of this polynomial are supposed to be determined on a daily basis utilizing a future global network of Galileo tracking stations. NeQuick

according to (Somieski et al, 2007), corrects for approximately 70% of the ionospheric delay as compared with the 50% by the Klobuchar model.

6.1.4.2 IONEX Maps

IONEX maps are grid-based, epoch specific, multi-layered three dimensional TEC maps which supports earth-fixed reference frames. An example is as given in (Schaer S., W. Gurtner, J Feltens, 1998), where data is gathered from several analysis centers around the globe are put together for the IONEX maps, with horizontal resolution of 5°° longitude and 2.5° latitude and temporal resolution of 2 hours. Twelve VTEC maps and twelve RMS maps describing the accuracy are produced daily. The accuracy of this is better than the Klubochar approach.
To use the IONEX files, the VTEC data for the area of interest need to be interpolated both in the horizontal and temporal data. As already stated in section 6.1.4.1.2, the ionospheric pierce point (IPP), is about 350 km above the surface of the earth and all satellites in view will have different IPP and these must be derived. The VTEC grid is represented by geocentric longitudes and latitudes; therefore there must be a conversion factor that has been appropriately derived. According to (Schueler T. , 2001), the horizontal interpolation is obtained by selecting the 4 nearest stations contained in the VTEC map, compute the weighted mean using their reciprocal spherical distances raised to the power of 1.5 as the weighting coefficient. For the temporal interpolation, IONEX files for the previous and next day are required as the system normally processes diurnal data batches. A ten-point-polynomial, which allows the modeling of periodic behavior of the VTEC series, is employed.

6.1.4.3 Ionosphere-Free Linear Combination

Modeling the ionosphere becomes difficult due to the various irregular time dependent influences, it therefore more efficient to eliminate it using dual frequency signals. This is explained for both code ranges and carrier phase.

For the code pseudo-range R

$$R = c\,\Delta t = \rho + c\Delta\delta \qquad 6\text{-}21$$

With the dependency of the pseudo-range dependent on the frequency of the ionosphere, a delay due to the ionosphere is introduced obtaining

$$R = c\,\Delta t = \rho + c\Delta\delta + \Delta^{iono}(f_L) \qquad 6\text{-}22$$

Thus

$$R_{L1} = c\,\Delta t = \rho + c\Delta\delta + \Delta^{iono}(f_{L1}) \qquad 6\text{-}23$$

$R_{L2} = c\,\Delta t = \rho + c\Delta\delta + \Delta^{iono}(f_{L2})$ 6-24

Where f_{L1} and f_{L2} are then frequencies of the two carriers

A linear combination of the two equations are formed with the introduction of arbitrary factors n_1 and n_2 with the aim of canceling out the ionospheric delay, therefore

$R_{L1L2} = n_1 R_{L1} + n_2 R_{L2}$ 6-25

To cancel out the ionosphere therefore

$n_1 \Delta^{iono}(f_{L1}) + n_2 \Delta^{iono}(f_{L2}) \cong 0$ 6-26

Assuming that $n_1=1$

Then

$n_2 = \frac{\Delta^{iono}(f_{L1})}{\Delta^{iono}(f_{L2})}$ 6-27

$\Delta^{\mathrm{iono}}(f_L) = \frac{C}{f^2}.VTEC$ 6-28

Substituting 6-28 into 6-27

$n_2 = -\frac{f_{L_2}^2}{f_{L_1}^2}$ 6-29

Substituting 6-29 into 6-24 an ionosphere-free linear combination is obtained for code ranges

$R_{L1L2} = R_{L1} - \frac{f_{L_2}^2}{f_{L_1}^2} R_{L2}$

Similarly for carrier phase measurements

$\Phi_{L1}\lambda_{L1} = \rho + c\Delta\delta + N_{L1}\lambda_{L1} + \Delta^{\mathrm{iono}}(f_{L1})$ 6-30

$\Phi_{L2}\lambda_{L2} = \rho + c\Delta\delta + N_{L2}\lambda_{L2} + \Delta^{\mathrm{iono}}(f_{L2})$ 6-31

Dividing through by the wavelength

$\Phi_{L1} = \frac{1}{\lambda_{L_1}}\rho + f_{L1}\,\Delta\delta + N_{L1} + \frac{1}{\lambda_{L1}}\Delta^{\mathrm{iono}}(f_{L1})$ 6-32

$$\Phi_{L2} = \frac{1}{\lambda_{L_2}}\rho + f_{L2}\Delta\delta + + \frac{1}{\lambda_{L2}}\Delta^{iono}(f_{L2}) \quad 6\text{-}33$$

Where

$c = f\lambda$

Combining 6-32 and 6-33 linearly

$$\Phi_{L1,L2} = n_1\Phi_{L1} + n_2\Phi_{L2} \quad 6\text{-}34$$

$$= \frac{n_1}{\lambda_{L1}}\rho + \Delta\delta + + \frac{n_1}{\lambda_{L1}}\Delta^{iono}(f_{L1}) + \frac{n_2}{\lambda_{L2}}\rho + f_{L1}\Delta\delta + + \Delta^{iono}(f_{L2}) \quad 6\text{-}35$$

$$= \rho\left(\frac{n_1}{\lambda_{L1}} + \frac{n_2}{\lambda_{L2}}\right) + \Delta\delta(n_1 f_{L1} + n_2 f_{L2}) + n_1 N_{L1} + n_2 N_{L2} - \frac{n_1}{\lambda_{L1}}\Delta^{iono}(f_{L1}) - \frac{n_2}{\lambda_{L2}}\Delta^{iono}(f_{L1}) \quad 6\text{-}36$$

For the elimination of the ionosphere

$$\frac{n_1}{\lambda_{L1}}\Delta^{iono}(f_{L1}) + \frac{n_2}{\lambda_2}\Delta^{iono}(f_{L2}) \cong 0 \quad 6\text{-}37$$

Again assuming n_1= 1 and substituting into equation 6-37

$$n_2 = \frac{f_{L2}}{f_{L1}}\Phi_{L2}. \quad 6\text{-}38$$

Substituting 6-38 into 6-34

$$\Phi_{L1,L2} = \Phi_{L1} - \frac{f_{L2}}{f_{L1}}\Phi_{L2} \quad 6\text{-}39$$

Linear combination however increases the noise in the measurement despite its effectiveness in mitigating ionospheric effects (Schueler 2001; Landau 1988).

6.1.5 Mapping Function

Tropospheric delay is shortest in the zenith direction and increases with the zenith angle. For practical applications the zenith path is projected into the slant direction by using the Mapping Function, m(ε), which is defined as the ratio of the path length through the atmosphere at a geometric elevation to the path length in the zenith direction

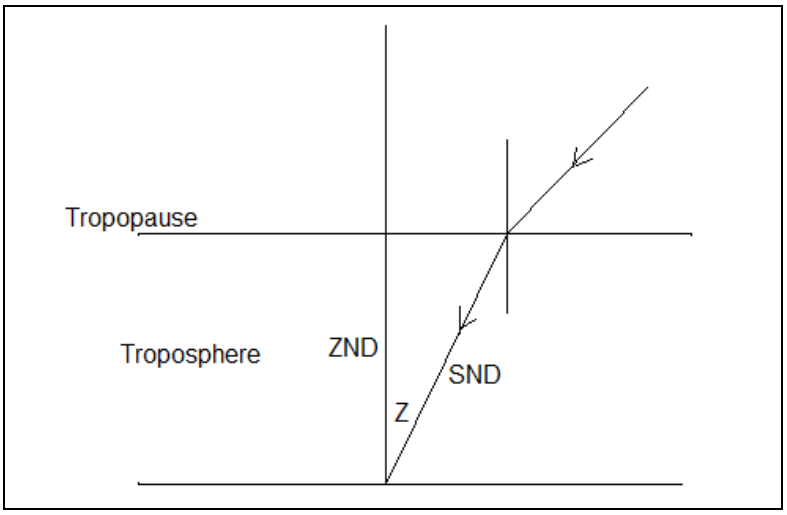

Figure 6-6: A simplified diagram explaining the determination of mapping function in the atmosphere

Assuming the earth without its curved surface with a uniform tropospheric refractive index 'n', and a vacuum beyond the tropopause, then a ray ZND in the zenith direction will satisfy the Snell's Law such that the ratio of the slant path to the zenith path will be equal to the sine of the refracted angle

$$\sin Z = SND/ZND = n \quad \text{or} \qquad (6\text{-}40)$$

$$ZND/SND = \cos Z$$

This is the simplest mapping function that is used for high elevation angle observations. This however produces very inaccurate results as the elevation angle decreases as explained by (Mendes, V.B., R.B. Langley, 1995), (Schueler T. , 2001) The figure below shows the comparison of various Mapping Functions as investigated by (O'Keefe, 2001) in an experiment organized in a tropical region showing the performances of 10 different Mapping Functions, Figure 6-7. It showed that for observations above 10° elevation angle the use of the weakest model will be suitable for most applications. This however looks very optimistic especially as one considers equation 6-40.

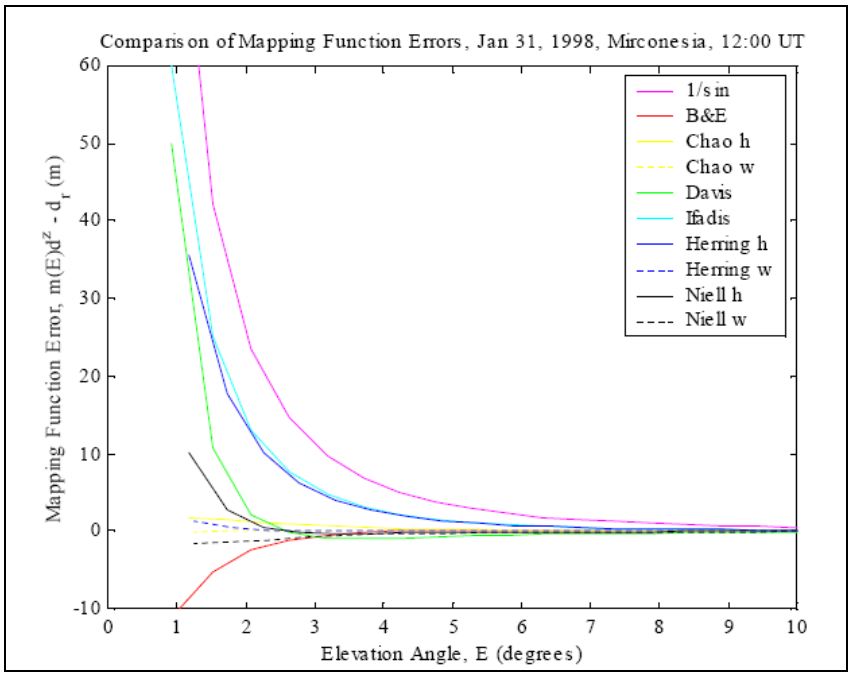

Figure 6-7: Comparison of Mapping Function Errors, Jan 31, 1998 12:00 UT (O'Keefe, 2001)

Other improved functions have been developed and among them is the Marini's continued fraction which introduces constants to cater for the earth's curvature and the varying density of the atmosphere. This is expressed in the equation 6-41

$$m(\varepsilon) = \frac{1+\frac{a}{1+\frac{b}{1+c}}}{sin\varepsilon+\frac{a}{sin\varepsilon+\frac{b}{sin\varepsilon+c}}}. \qquad 6\text{-}41$$

Where ε is the elevation angle of the in-coming ray, a, b and c are constants that depend on several properties that may include some atmospheric properties like surface pressure, partial water vapor pressure, surface temperature, as used by Ifadis, Davis and others. Developers like Neill, Chao and others, considered seasonal changes for the derivation and Herring introduced site latitude and height above sea level to obtain the value of these coefficients.

All the above parameters for the determination of the Mapping Function are a matter of concern for Ghana and for that matter the low latitude Equatorial Region. In selecting a Mapping Function, one has to consider the precision required for the intended application. For most applications at present in the project area almost all the Mapping Functions are acceptable, but considering future applications where precision for low elevation satellites may be required there is the need to search for the best for the region. As already stated, even the simple m(ε) = 1/sin (ε) mapping function can be used depending on the accuracy requirement especially if the elevation angle is more than 60°. However those functions that use meteorological data are generally not very reliable for low elevation angles for high precision applications as the data estimated at the receiver is not representative of the conditions along the actual path of the signal; there is poor correlation at higher altitude especially for temperature. While (Mendes, V.B., R.B. Langley, 1995)

recommended Herring, Ifadis or Neill models for high precise, Chao and Neill models are recommended by (O'Keefe, 2001), see figure 1. Neill is used as an option in PrePos GNSS Suite and is a good candidate for low latitude regions like Ghana and was used for the processing of the data.

6.2 Satellite Corrections

6.2.1 Eclipsing Season

This is the period when the satellite vehicle enters the shadow of the earth and is unable to align its solar panel to the sun despite the constant attempts to trace it. This results in movements around the yaw-axis. There is however no yaw-rate information provided in the orbit file hence the difficulty in accounting for this movement and this result in the loss of accuracy which according to (Schueler T. , 2001), is in the range of up to 300 m. For very precise positioning especially over very long baselines, in excess of 1000 km, the satellites in eclipsing season must be excluded completely or weighted down. For this reason, such satellites must be identified and the identification process can be read in (Fliegel et al, 1992).

6.2.2 Satellite Orbit Correction

The satellite orbit corrections are determined from satellite orbit predictions based on several days of global solutions by IGS Orbit Service using the combination of data from several analysis centers. The statistics from the IGS are used to exclude problematic orbit data from the prediction process. The orbit predictions are updated as soon as a new set of global solutions are available and the resulting average ephemeris are output to daily files in Standard Product 3 (SP3) format. The satellite accuracy codes displayed are based on the weighted RMS of the satellite (Lahaye, F., J. Kouba, 1994)

6.2.3 Satellite Antenna Phase Centre Correction

The position obtained from SP3(c)-files from GPS satellites is referenced to the mass center of the satellite, not the phase center. The resulting eccentricity depends on the type of satellite, for example the Block II satellites have about 1m eccentricity and therefore a correction has to be applied for precise applications over longer baselines. The new generation satellites however may have negligible eccentricity and may need no correction

PrePos GNSS suite and most scientific GNSS processing software take into consideration most of the above corrections for the processing of long base line especially where precision is needed. These were considered in this project

7 Data Processing

7.1 Overview of PrePos GNSS Suite

PrePos GNSS Suite (PGS), the main software for this study is GNSS scientific software developed for the processing of GPS and the future Galileo data in the Institute of Geodesy and Navigation of the Federal Armed Forces University-Munich. PGS which has been developed to perform precise GNSS positioning by post-mission analysis was found suitable for this study due to its ability to process over short and long baselines. The long baselines required in this Ghana's geodetic network renewal stems out from the fact that IGS stations which are to serve as reference points are very sparse on the African continent unlike in most other parts of the world.

The software which has been organized in three major modules include GTCE (GNSS Troposphere and Coordinate Estimation) for static GNSS data analysis in large networks, SEMIKA (Semi-Kinematic and Kinematic GNSS Positioning) and the third module consists of shared programs and auxiliary tools. See Figure 7-1.

The modules and add-ons relevant for this study been marked in red boxes consists of GTCE, DITON (Datum Transition Tool) a datum transformation utility, an add-on to GTCE, SEMIKA, which is dedicated to precise semi-kinematic and kinematic surveys, NEADS (3D Network Adjustment Utility) a combined 3D network adjustment using SEMIKA baseline results and GTCE network solutions and NEREUS (GNSS Network Analyzer for SEMIKA Users) for active GNSS network corrections using for example area corrections. For more details see the PrePos GNSS Suite (PGS) Documentation[1].

After going through several methods to minimize errors of the station coordinates, due to the propagation of signals through the atmosphere and as a result of the movement of the satellites and the station markers, the task now is to process the data collected from the field campaign. This has been done mainly with the PrePos GNSS Suite (PGS) by establishing geocentric coordinates using selected IGS stations, and following this with the determination of coordinates for lower order of coordinates. The processing included getting the WGS84 coordinates of the source data for the determination of transformation parameters for the Golden Triangle of Ghana.

[1] The PrePos GNSS Suite Documentation, which comes along with the software can be obtained at the Institute of Geodesy and Navigation, Universität der Bundeswehr, München D-85577 Neubiberg, Germany

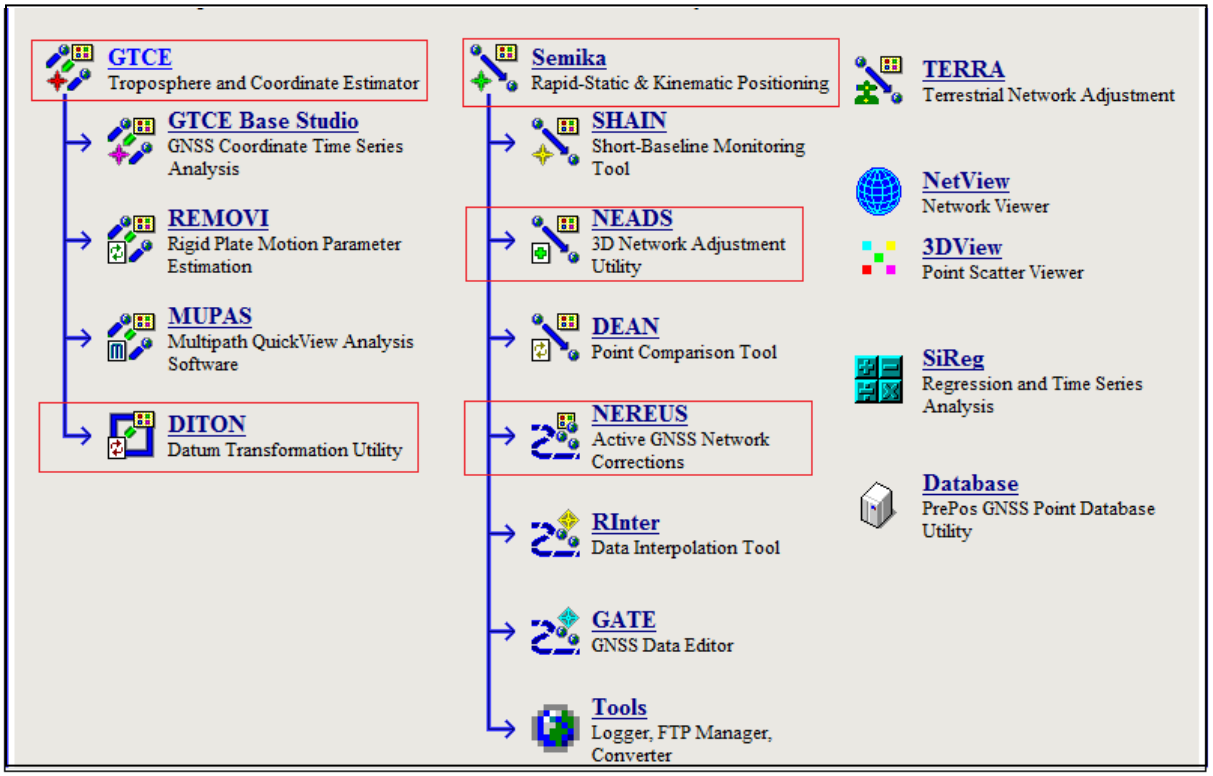

Figure 7-1: Modules of the PrePos GNSS Suite with the components used for this study in red boxes

7.2 Deriving Geocentric Coordinates for Ghana using GTCE

GNSS **T**roposphere and **C**oordinate **E**stimator, GTCE, is one of the three main modules of the PrePos GNSS Suite (PGS) which deals with the estimation of coordinates for reference networks especially over long baselines. It was developed for developed for concise data analysis of static GPS observations. The analysis software uses Kalman filter based on double differences for the estimation process Details can be found in the PrePos GNSS Suite (PGS) Documentation[2]. This in addition is used to estimate tropospheric Zenith Path Delay used as input to model the atmospheric delay in subsequent processing using SEMIKA.

7.2.1 Selection of IGS Stations

To be able to link to the geocentric ITRF, one has to process the stations with respect to IGS stations which for this study were selected based on criteria including proximity of station, (refer to Figure 7-2), and data of high quality. Selection of NKLG and MAS1 over other candidates like DAKA, MBAR and YKRO were based on individual assessment of the stations. YKRO in Ivory Coast which is the closest was not running at the time of this observation and therefore could not be used; DAKA in

[2] The PrePos GNSS Suite Documentation, which comes along with the software can be obtained at the Institute of Geodesy and Navigation, Universität der Bundeswehr, München D-85577 Neubiberg, Germany

Senegal is also quite close but had poor data quality with a lot of outages. MBAR in Uganda produced relatively good quality data but NKLG in Libreville Gabon, which is closer (1239 km), and has equally good quality data was preferred due to proximity. MAS1 which is in Maspalomas (Spain), 2949 km away, though relatively far, was a better candidate as the sampling interval of 10 seconds was identical to that of the observation interval specified for the project. Data downloaded from these stations were included in the input data for GTCE.

Figure 7-2: Map showing the locations of the IGS stations considered for use in this study

7.2.2 Input Data Preparation

The input data are basically, the prepared observation RINEX data for the stations involved, downloaded RINEX file of the IGS stations (NKLG and MAS1) and the SP3 satellite orbit files of the selected days and their previous and next day's files.

7.2.2.1 Preparation the RINEX files

The RINEX data, which is stored in the observation file, must follow a special naming order (ssssdddf.yyt), four character station name designation, (ssss) which must be

unique, day of year (ddd), file sequence within a day (f), year (yy), type of file (‘o’ or ‘d’). The type of observation recorded for this project included phase measurements on L1 and L2, pseudorange using C/A-code on L1 (C1), pseudorange using P-code on L1 and L2 (P1 and P2) and Doppler frequency on L1 and L2 (D1 and D2).

GTCE required a special format for the RINEX header and may reject any file that does not conform to this format. This include the input of four character unique identifier, the marker number or name, antenna number, antenna type, antenna eccentricity and also time of first observation. The four character identity may be the station designated name. This should be unique thus should not be already in use in the IGS network. The antenna number is usually the serial number of the antenna which is relevant for identification especially where it is being used at a permanent station, which could be replaced by a different one of the same brand. This reason also goes for the receiver type and number. The next important consideration is the antenna type, which must be stated exactly as in the calibration table. This is needed to search for the antenna phase-centre correction which is needed as a component for the derivation of the coordinate. In this study, relative antenna phase center variation from the National Geodetic Survey (NGS) of the USA was used. The geometric eccentricity between the marker of the monument and the antenna reference marker, usually measured in meters, has coordinates in the east, north and radial. This is a component that links the marker of the monument representing the station to the antenna marker, see Figure 5-6. For this project only the radial component was provided as the observers had to center the antenna on the markers making the horizontal eccentricity negligible. The first time of observation in all the cases for this project 0:00:00 hours to 23:59:50 for all the permanent stations involved in the GTCE processing except NKLG which ended at 23:59:30 due to the 30 seconds recording intervals, while the rest including MAS1 was 10 seconds.

One major task that was conducted in the data preparation was the splicing of the data into daily files. Since the data observed at the stations were not stored into daily files as needed by GTCE, there was the need to manually splice them into daily files and the header modified to that effect.

7.2.2.2 Handling of the SP3 files

In the handling of precise SP3 files, one had to take into consideration that PGS does not accept SP3 files with velocities and therefore only position data is used. The bad satellite identification and exclusion option was activated. To avoid boundary swing-out effect, SP3 files of both the previous and next day are included in the processing. For long baselines as involved in this project, the satellite antenna phase center corrections were enabled.

7.2.2.3 Coordinates and Troposphere Estimation

This involves the pre-processing and the processing of the input data. This was achieved by tightly constraining the IGS stations and computing differences with the five first order stations of the GRN project. The pre-processing of the input data follows these steps

- Identification of station to process as datum point
- Selection of day to process
- Reading of Klobuchar model parameters
- Reading of RINEX files of the observed stations and downloaded IGS stations
- Reading of the SP3 files of the previous, current and the next days
- Pre-processing observation and satellite data, making all relevant corrections like EOP, Ocean Loading etc as explained in Chapter 6, and confirming useable data.
- Building of baselines between stations (this is hard disk challenging for large networks especially for computers with small memories due to the numerous double differences formed alongside the networking)
- Storing the final network configuration

After this stage the actual processing goes through the following steps

- Combined Kalman Filtering
- Analysis of the log file
- Finalizing network solution
- Analyzing the final coordinates
- Iteration on solution, in case one or more sites have too many outliers
- And finally analyzing the wet delay values.

7.2.2.4 The Combined Network Solution

The network solution is in form of daily SINEX for the individual days processed. This included the file reference, input acknowledgement, sites information, receiver, antenna and antenna phase center descriptions, sites eccentricities, mean solution epochs for the sites, the a priori and estimated solutions for the Cartesian X, Y and Z coordinates of all the stations with their standard deviations. Since GTCE combines two sets of solutions at a time for averaging, it was structured to combine the first and the last and find the mean; the second is combined with the last-but-one and the mean is computed. This process continues until the final combined network solution was obtained. See Appendix B

7.2.3 Quality Assurance of GTCE

The estimation of coordinates for the fundamental stations required comprehensive quality assurances and GTCE has both statistical and graphical tools for these. The data quality is checked from the pre-processing stage as shown in the error-log file where information is given in the metadata and the observation data in the RINEX file, display of data gaps at a station, number of epochs at the end of a given baseline. Error-log file of the filter engine displays all the deleted measurements of the epochs that could not meet the set criteria. Cycle Slip Statistics displays the deleted epochs as a result of cycle slips which might be caused by tracking losses, multipath and ionosphere fluctuation on L1, L2, or both frequencies. These are rejected to ensure quality. Plots showing the graphical representation of combination of forward and backward residuals coordinate time series, standard deviation and troposphere time series are available aid to data quality checks. The use of the coordinate comparison function of the PGS is another means of getting the quality checked as it shows the difference between the initial and final coordinates of the coordinates after processing.

7.3 Results

After tightly constraining the IGS stations MAS1 and NKLG, with initial standard deviation of 0.1 mm, the results obtained for seven full days from 19th to 25th of May 2007, to for the primary points for the five local stations were as follow. For the full SINEX file see Appendix 2

Station	Component	Coordinate (m)	St Dev.(mm)
NKLG	Sta. X	6287385.761	0.1
	Sta. Y	1071574.577	0.1
	Sta. Z	39132.947	0.1
MAS1	Sta. X	5439192.219	0.1
	Sta. Y	-1522055.445	0.1
	Sta. Z	2953454.891	0.1
KMSI	Sta. X	6332788.128	6.5
	Sta. Y	-168938.560	5.5
	Sta. Z	740370.540	2.8
ACRA	Sta. X	6348052.681	5.0
	Sta. Y	-20212.882	4.1
	Sta. Z	617243.597	2.1
TADI	Sta. X	6352080.522	6.5
	Sta. Y	-194364.546	5.4
	Sta. Z	541029.361	2.8
KADE	Sta. X	6341683.082	6.5
	Sta. Y	-92631.920	5.4
	Sta. Z	674048.0334	2.8
ASFO	Sta. X	6345407.175	7.2
	Sta. Y	-141728.751	6.1
	Sta. Z	629324.067	3.2

Table 7-1: Showing the GTCE derived Geocentric Coordinates for the first order Permanent Stations in Ghana and the tightly constrained IGS stations MAS1 and NKLG.

7.4 Estimation of Zenith Path Delay

One of the main and useful products of GTCE is the generated self-estimated Zenith Path Delay. GTCE, using the filter, estimates the zenith residual delays for each epoch as plotted in Figure 7-3, and models it into the zenith path delay files. This is smoothed on hourly intervals generating linear functions for each block, thus generation 24 blocks daily. This smoothing out reduces the impact of multipath effects. The modeled ZPD is used to model the troposphere while using SEMIKA and is very effective as proved in Chapter 10. This GTCE estimated ZPD worked better than the other modeling approaches used in this data processing like the Numerical Weather Model, NWM, the Area Correction Parameter, ACP, and the Corridor Correction, CC etc. This is demonstrated in chapter 10

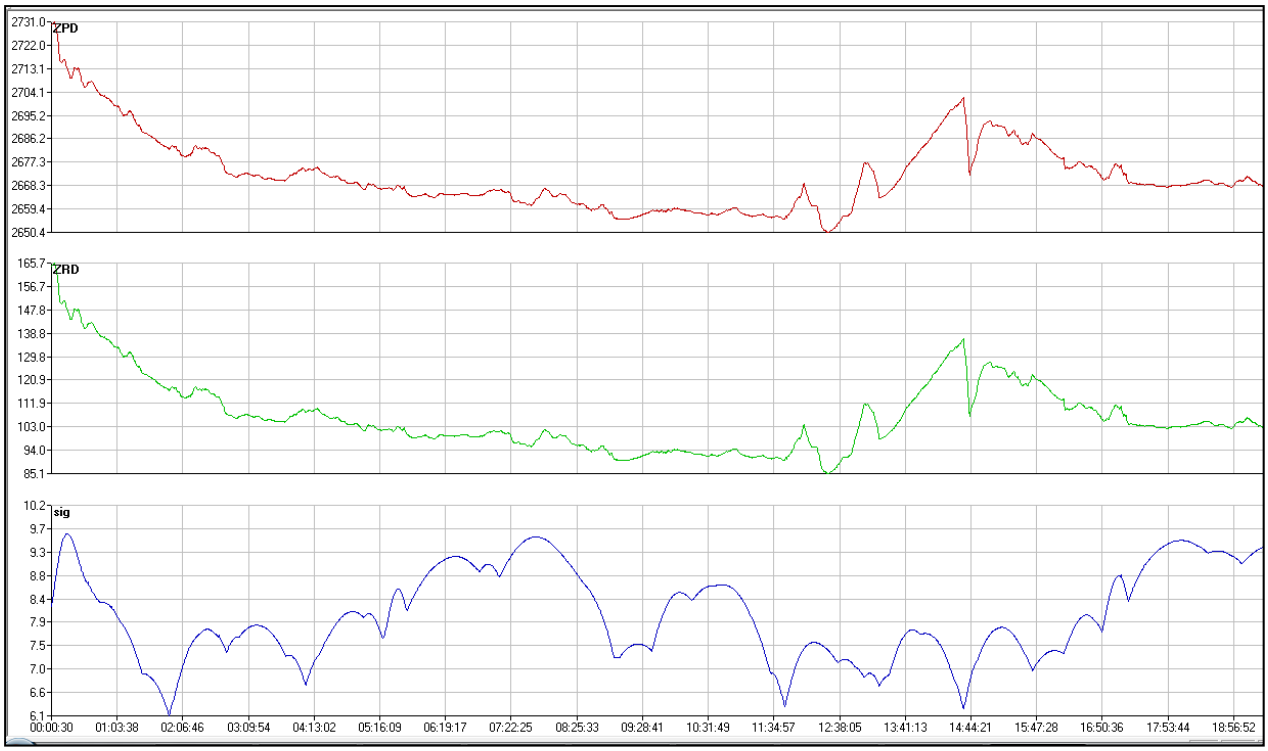

Figure 7-3: A screenshot of a plot of the zenith path delay ZPD, Zenith Residual Delay, ZRD and the standard deviation against the GPS time at a station

7.5 Deriving the Coordinates of the New Second Order Points Using SEMIKA

SEMIKA which is a Rapid-Static and Semi-Kinematic Positioning tool is one of the major modules of PGS, see (PrePos GNSS Suite Documentation, 2007[3]). It is capable of processing data of less than 1 minute to several hours. This module was used to provide coordinates of the remaining 15 newly established stations of the project. To achieve this, the GTCE computed geocentric primary coordinates were used as known coordinates and were tightly constrained for the provision of differential corrections for these new stations as well as the thirty old trigonometric points used in the determination of transformation parameters for the project area as shown in Chapter 9. The GTCE derived ZPD files for the coordinates was used to model the tropospheric delay for the area and used as an input for the coordinate determination.

7.5.1 Data Preparation

Similar to GTCE, the header and observation components of the RINEX input data were checked and the necessary modifications like four character ID, the antenna eccentricity and number etc. The data that spanned over one or more days were spliced and finally checked using TEQC. The epoch for the establishment of the coordinate was fixed at 2007.279, to cater for the crustal movement in the region.

[3] The PrePos GNSS Suite Documentation, which comes along with the software can be obtained at the Institute of Geodesy and Navigation, Universität der Bundeswehr, München D-85577 Neubiberg, Germany

Elevation mask of 15 degrees and elongation angle of 10 degrees was set for this computation.

7.5.2 Coordinate Estimation Procedure using SEMIKA

The procedure for attainment of the required solution is in threefold, the Pseudo-range Solution, the Relative Carrier-Phase solution and the Block Adjustment.

The pseudo-range solution (DGPS) performs data pre-processing resulting in DGPS solution using pseudo-ranges for the period starting from the time given in the configuration. The original input data is read, cycle slips checked, ambiguities analyzed, and a binary data file generated for further processing. Below are the steps

- Identify stations and processing day
- Read satellite eccentricity
- Read atmospheric model
- Read SP3 files
- Make station correction e.g. EOP, TDT etc
- Access RINEX measurement files
- Analyze the pseudo-range solution
- Read observation files for ambiguity analysis
- Restore observation file
- Delete observations that do not meet the required threshold

This is continued by the time velocity solution which determines the coordinate increment by triple difference carrier phase measurement, generating a special data file which contains input data for the carrier phase block adjustment. The following are the relevant steps in this process.

- Extract pseudo-range solution from its directory
- Computes and analyzes the relative-carrier phase solution
- Analyzes the observations for adjustment
- Analyzes the number of epochs for block adjustment
- Performs the final quality checks including final cycle slips detection

The Carrier-Phase Block Adjustment follows the two previous processes is the least square adjustment of the input data from the Relative Carrier-Phase solution obtained from the immediately preceding process. The relevant steps are as follows

- Perform least square adjustment after reading the input data
- Fix ambiguities if necessary and repeat adjustment
- Perform the relevant statistical analysis and archives the essential files.

7.5.3 Processing the Coordinates of the New Points

For the best results to be obtained the baselines between the individual stations and the closest primary stations were used. In most cases referencing a new station with

one or two permanent station was sufficient. As already stated the introduction of the Hub Stations played a good role in reducing the lengths of these baselines. The quality of each baseline was checked.

7.5.4 Data Quality Management of SEMIKA

A very useful component of SEMIKA is the use of both statistical data and graphical displays to manage the quality of the data. Like the GTCE the information in the result browser displays the number of disqualified measurements like cycle slips, wrong ambiguity fixes, etc. With the graphical displays like the 2D and 3D visualization, as shown in the Figure 7-4 and Figure 7-5 respectively, one can visualize the extent of the scatter, which indicates the distribution of observations at each epoch which assists in the deletion of outliers.

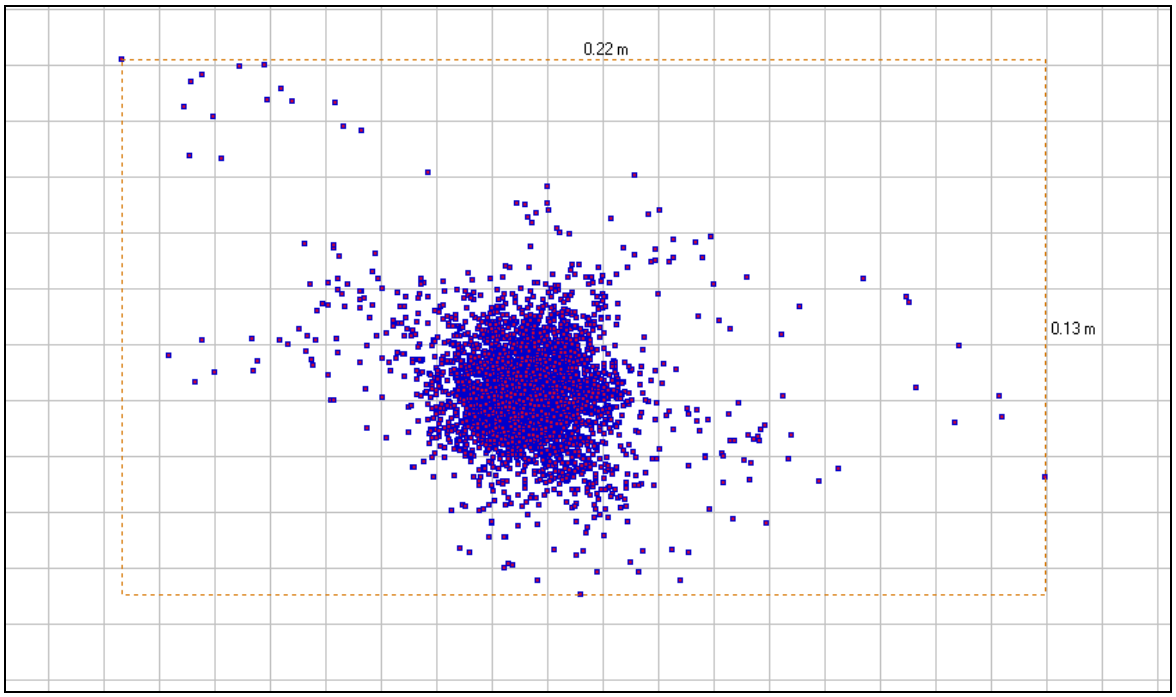

Figure 7-4: A screenshot of a two-dimensional scatter plot of an observed station

The 2D scatter plot utilizes the spatial distribution to determine the quality of the data while the Figure 7-5 utilizes in 3D not only the spatial dispersion but also the color effect to display the data quality, with deep blue color with the least displacement and the red, the maximum. This also utilizes the rotational mode to view the distribution of the plot, show the maximum and minimum displacements in all directions and also provides a count of the number of epochs. All these and other properties help in visualizing the data and can work towards its improvement if not satisfied with the some points.

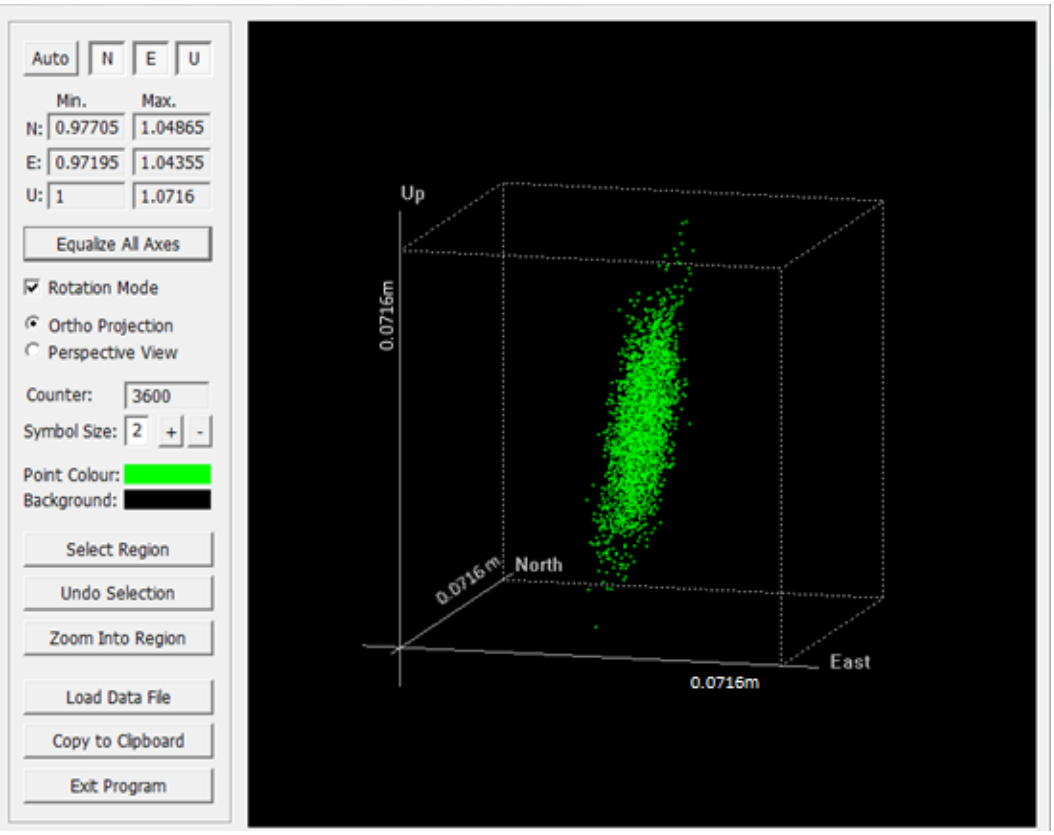

Figure 7-5: A screenshot of three-dimensional scatter plot with equalized axes

Another tool that was used in the data quality management is the time dependent properties like displacement, number of double differences, number of satellites,
This enables one to crop out some undesired time window, interactively and with each modification one can check the impact of that action on the overall quality of the results

The information on the number of visible satellite used, the total number of double differences which also plays a role in the quality of the data is displayed in the Figure 7-6.

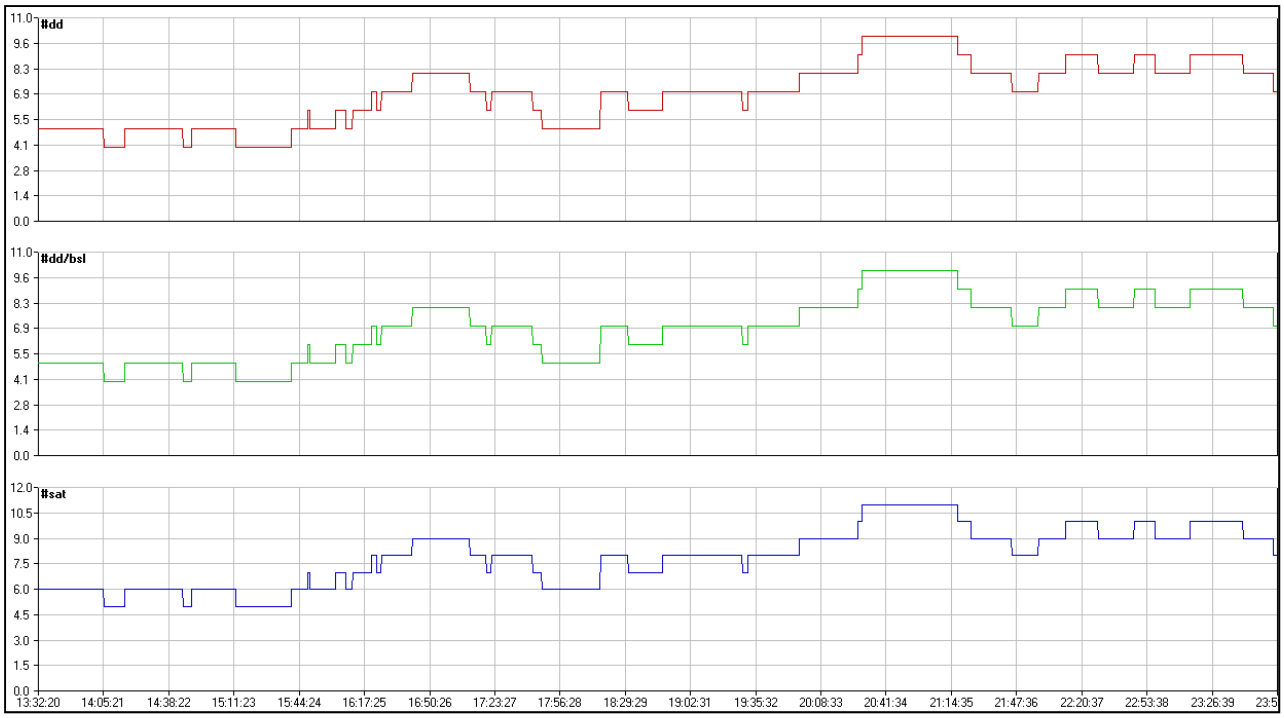

Figure 7-6: A screenshot showing a plot of total number of double differences (dd) used in the DGPS epoch-to-epoch solution, the total number of double difference observation per baseline (dd/bsl) and the total number of satellite before double differencing (#sat)

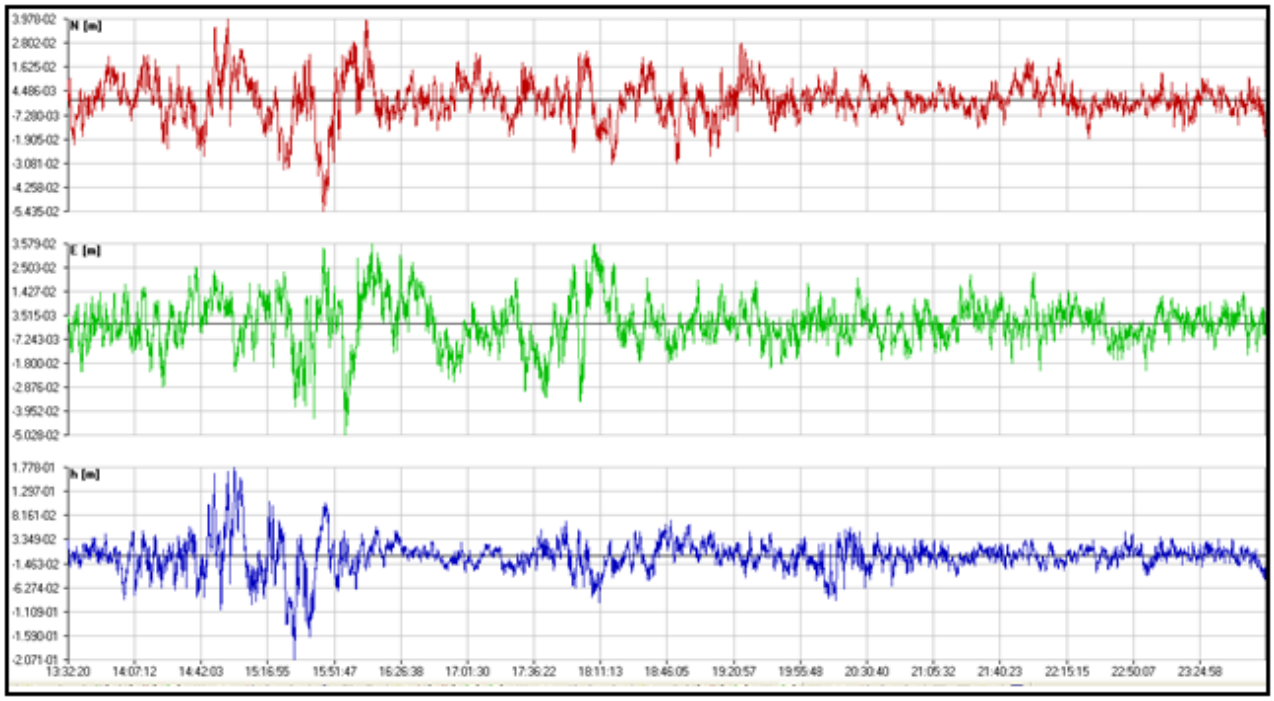

Figure 7-7: A screenschot of Coordinate Component Plot

The plot of the coordinates N, E and H as shown in Figure 7-7, is an important visual too to crop out poor observation sections along the time axis, and re-processing to see the impact of the exclusion of such sections. With such interactive actions the data can be optimized.

After the quality checks and optimization the final product of SEMIKA is then adjusted using NEADS, the network adjustment add-on to SEMIKA.

7.6 Three dimensional network adjustment using NEADS.

NEADS is the Network Adjustment tool of the PGS which can combine data from both SEMIKA and GTCE for network adjustment. This study employed SINEX file of the already adjusted fiducial five points as has been explained in GTCE and the SEMIKA derived coordinate points which are to be adjusted. The Point Mode adjustment option was selected over the baseline mode constraining the fiducial points which were located such that the baselines for the base station were very short hence was quite accurate. The adjustment affected stations which had more than one dataset. Such stations had their adjusted values averaged. The adjustment was referenced to the epoch 2007.39.

NEADS displays visually the confidence ellipses, vectors of residuals which are useful tools for users, see Figure 7-8 for some confidence ellipses and the magnitudes of the horizontal and vertical of the errors at some observed points. The large error at OBRA for instance is resulted from obstruction by the tree canopy encountered at this site, resulting in high dilution of precision at the site as well as relatively short time of effective observation.

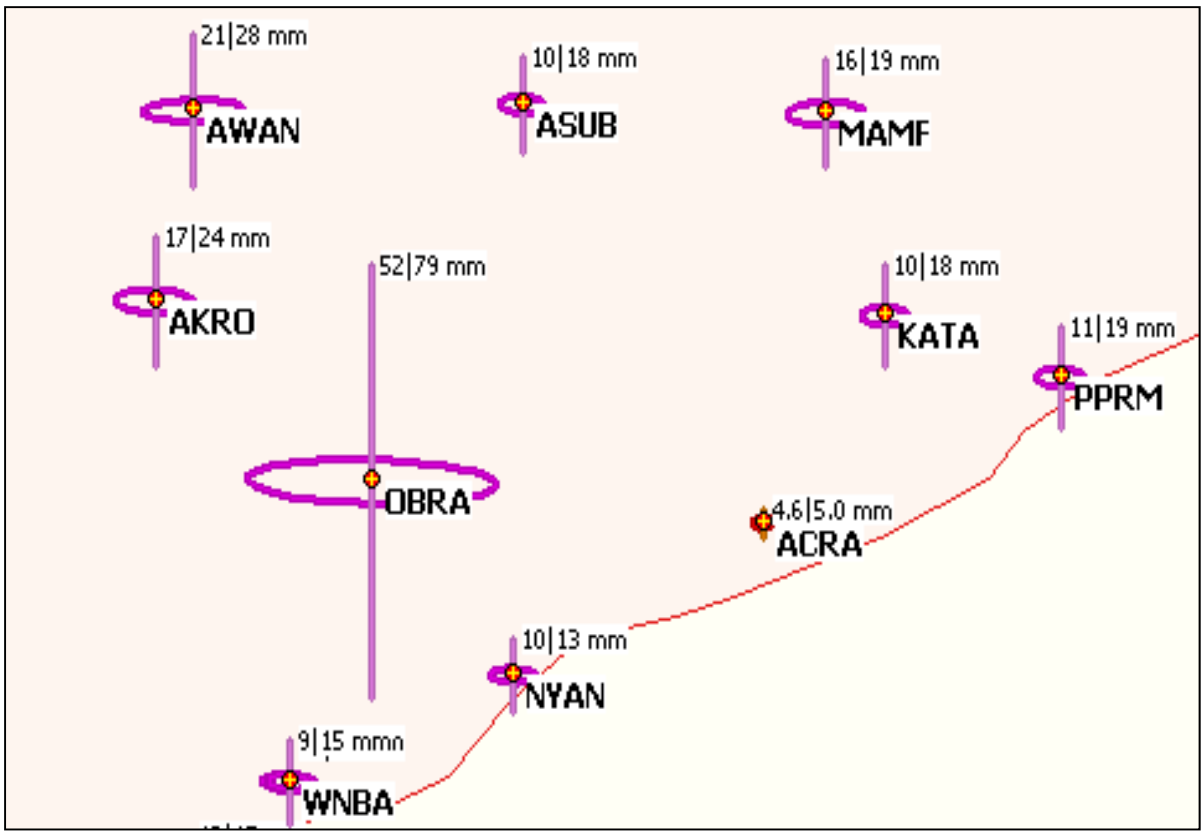

Figure 7-8: A Screenshot showing the confidence ellipses with the left-hand-side figure representing the standard deviation of the horizontal and the left-hand-side representing that of the height components

7.7 Final Coordinate Results in ITRF05

Results after the 3D adjustment using NEADS is given in the Table 7.1 see Appendix D4 for the full SINEX file.

Station ID	X (m)	Y (m)	Z (m)
ACRA	6348052.681±0.007	-20212.882 ± 0.005	617243.597 ± 0.003
KMSI	6332788.128±0.009	-168938.560 ± 0.007	740370.540 ± 0.004
TADI	6352080.522±0.009	-194364.546 ± 0.007	541029.361 ± 0.004
KADE	6341683.082±0.008	-92631.920 ± 0.007	674048.034 ± 0.004
ASFO	6345407.175±0.009	-141728.751 ± 0.008	629324.067 ± 0.004
AKOS	6340187.138±0.013	5916.015 ± 0.012	693630.689 ± 0.003
AKRO	6345564.337±0.031	-84885.370 ± 0.022	638056.369 ± 0.007
ASUB	6343991.999±0.023	-45870.599 ± 0.012	656450.268 ± 0.005
DEDS	6336420.263±0.018	-30479.966 ± 0.013	726610.838 ± 0.004
EJSU	6332800.818±0.014	-162440.859 ± 0.010	741693.374 ± 0.003
ELMI	6351356.921±0.019	-148750.377 ± 0.015	563220.582 ± 0.004
KNGO	6334684.452±0.015	-134496.181 ± 0.012	730769.046 ± 0.004
NKWN	6336366.794±0.018	-86269.289 ± 0.018	723494.733 ± 0.004
OBUA	6338570.535±0.017	-185719.357 ± 0.012	684512.241 ± 0.004
OFSE	6340469.394±0.018	-126360.212 ± 0.012	679783.246 ± 0.005
OSNO	6339340.602±0.038	-53389.526 ± 0.018	700079.988 ± 0.007
PPRM	6346696.648±0.025	11749.825 ± 0.013	630892.299 ± 0.005
SALT	6350984.849±0.014	-117105.975 ± 0.016	574738.720 ± 0.004
TPRA	6345578.401±0.028	-171389.924 ± 0.016	619288.503 ± 0.006
WNBA	6349968.225±0.011	70722.530 ± 0.007	593005.924 ± 0.002

Table 7-2: The Final Adjusted Coordinates of the Control Points in the Golden Triangle

The over all standard deviations in the X-, Y- and Z-coordinates for the twenty newly established points comprising the observed primary and secondary points were 1.72 cm, 1.09 cm and 0.45 cm respectively in the Cartesian coordinate system. These translate to an average of 1.71 cm and 1.20 cm in the vertical and horizontal components respectively.

7.7.1 Results Interpretation and Discussion of Results

There are two distinct observations in the results in Table 7-2. These are the higher standard deviation in the X-coordinates as compared with Y- and Z-coordinates, and the relatively small standard deviation for the three permanent stations and the two hub stations as compared with the 15 second-order control points.
The X-coordinates which has average standard deviation of 1.72 cm bears practically all the error in the vertical component due to the fact that the tangent plane of the area covering Ghana especially the project area, which is in the south and closer to the Equator, is perpendicular to the to the X coordinate. With the Prime Meridian passing through Ghana with the farthest station only about 2° to the west, as well as

the closeness to Equator, the tangent plane is parallel to the Y and Z axes hence the relatively high standard deviation experienced in the vertical component of GPS measurement does not reflect so much in these two axes.
Due to data smoothing, there is improvement in positional accuracy as the observation period increase. This explains the lower standard deviation for the 7 days of continuous data for the permanent and stations as compared with the two 12-hour data of the second order reference points.

7.8 Determining Coordinates of the Reference Markers

The study was aimed at bringing GNSS to level of all users and for this aim to be achieved three reference marker located at the new stations had to be coordinated and transformed from the geocentric Cartesian coordinates to both geographic and plane coordinates. To do this, the conversion tool of Trimble Total Control (TTC) which is commercial software was used for the benefit of the general public.
At this stage the data was processed with the TTC for all the new stations fixing the new second order stations and processing to obtain coordinates for the reference markers. A typical example of the final product for a station, e.g. AKRO is as shown in Figure 7-9. This gives a plot of the station with the reference markers, followed by tables of

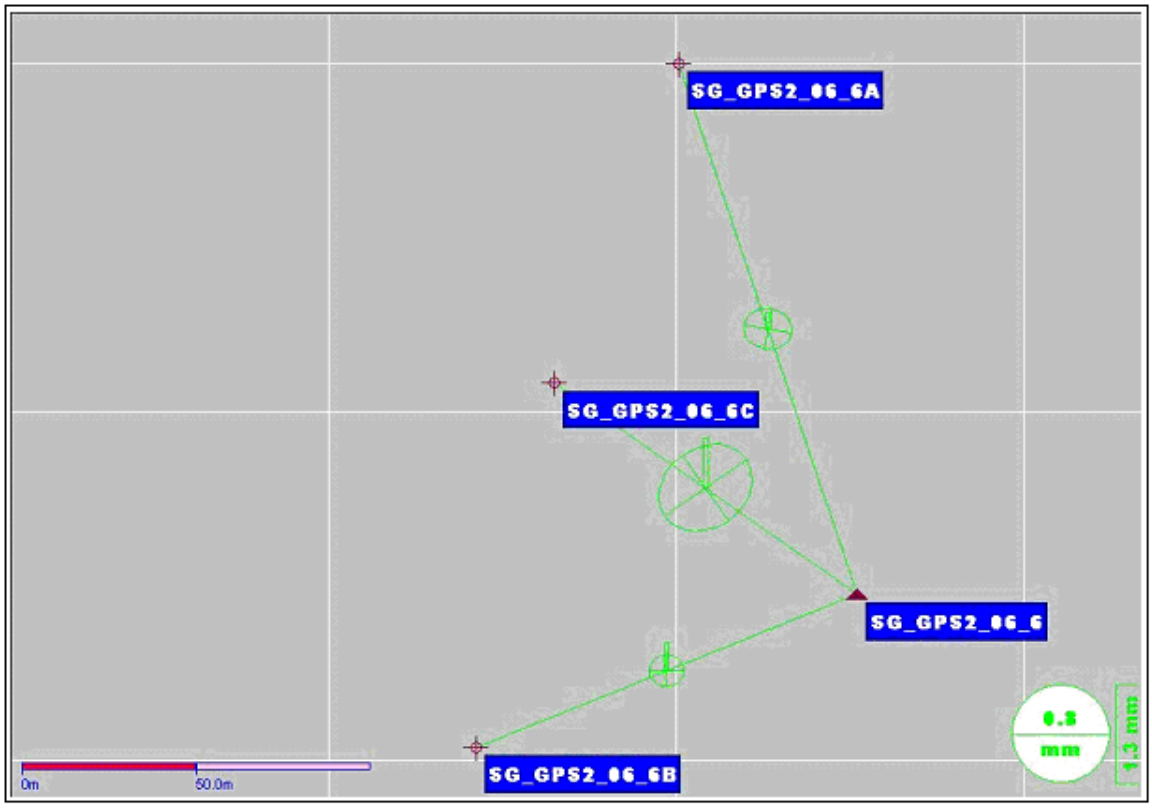

Figure 7-9: A screenshot of the plot of the AKRO station and the three satellite stations

WGS84 - Cartesian Geocentric Coordinates

Point Name	X	Y	Z
SG_GPS2_06_6A	6345530.293 m	-84936.344.m	638206.391 m
SG_GPS2_06_6B	6345540.087 m	-84994.703 m	638009.940 m
SG_GPS2_06_6C	6345534.657 m	-84972.184 m	638114.604 m
SG_GPS2_06_6	6345564.337 m	-84885.370 m	638056.369 m

Table 7-3: The Cartesian coordinate in WGS84 for the AKRO and the satellite stations

A table showing the extracted geocentric coordinates from the adjusted coordinates is provided to the user. These are usually not useful for most users as they cannot be directly used. This called for the conversion to a user friendly form as shown in the subsequent tables.

Azimuths, Distances and Elevations

From	To	NS-Fwd Azimuth	Ground Distance	ΔElevation
SG_GPS2_06_6	SG_GPS2_06_6A	341° 22' 44.1''	161.0496 m	-18.080 m
SG_GPS2_06_6	SG_GPS2_06_6B	248° 10' 50.9''	118.1087 m	-27.344 m
SG_GPS2_06_6	SG_GPS2_06_6C	304° 53' 22.9''	106.3131 m	-22.506 m
SG_GPS2_06_6A	SG_GPS2_06_6C	201° 17' 30.6''	98.5332 m	-4.426 m
SG_GPS2_06_6A	SG_GPS2_06_6B	196° 30' 11.5''	204.9603 m	-9.264 m
SG_GPS2_06_6C	SG_GPS2_06_6B	192° 05' 52.1''	107.0874 m	-4.838 m

Table 7-4: Computed Azimuths, Distances and Elevations for the AKRO station

Providing azimuths, ground distances and elevation differences between the established points at each new point males it an easy point of departure for conventional survey application especially as at least there is a set of points which are inter-visible for each site

WGS84 - Geographical Coordinates

Point Name	Latitude	Longitude	Height
SG_GPS2_06_6A	N 5° 46' 52.25442''	W 0° 46' 00.73574''	187.328 m
SG_GPS2_06_6A	N 5° 46' 45.85720''	W 0° 46' 02.62813''	178.064 m
SG_GPS2_06_6A	N 5° 46' 49.26580''	W 0° 46' 01.89866''	182.9024m
SG_GPS2_06_6A	N 5° 46' 47.28623''	W 0° 45' 59.06431''	205.408 m

Table 7-5: Geographical Coordinates in WGS84 for AKRO and the satellite stations

Some mapping applications require the conversion to the geographic coordinates therefore the longitude-latitude and ellipsoidal height in WGS 84 has been provided in this study as shown in Table 7-5 for all the newly established stations.

WGS84 – UTM

Point Name	Easting (X)	Northing (Y)
SG_GPS2_06_6A	747297.635 m	639501.650 m
SG_GPS2_06_6B	747240.166 m	639304.842 m
SG_GPS2_06_6C	747262.206 m	639409.672 m
SG_GPS2_06_6	747349.676 m	639349.185 m

Table 7-6: UTM coordinates for AKRO and the satellite stations

For the purposes of engineering, cadastral and other survey application, there is the need to use plane coordinates. The Universal Transverse Mercator projection was used to project the geographical coordinates to the northings and eastings to cater for such applicants.

Though this could satisfy most of the present requirements of surveying and mapping in the country, the need to convert the large amount of data based on the old classical War Office ellipsoid into this new system and vice versa could not be overlooked. The parameters for such changes had to be determined.

8 Transformation Parameter

8.1 The need for Transformation Parameter

Following the large amount of data in the old coordinate system and the cost of replacing them by establishing a new data set based on the newly established Geocentric Coordinate System, there was the need to provide a mathematical means of transforming the old classical datasets into this new system. This called for the establishment of a set of transformation parameters in this study covering the Golden Triangle of Ghana. After getting the adjusted precise coordinates of the selected common points using SEMIKA, the points were ready for conversion from this new coordinate system to the War Office Ellipsoid of 1926 and vice versa.

8.2 Transformation Parameter Determination

To determine the transformation parameters, a set of points established in the War Office Ellipsoid were selected as common points in such a way that had a good spread within the GT area as shown in Figure 8-1. The War Office geographic coordinates 1936 of these selected points were extracted from (Gold-Coast-Survey, 1936) compiled by the then Surveyor General J Clendinning.

Figure 8-1: Showing the locations of the Trig Points for the determination of Transformation Parameters

These coordinates had an assumed epoch of 1930 to account for any movement over time due to plate motion. The GPS observation included 30 points out of which the under-listed 22 in Table 8-1 were used in this project; the others were removed

after the quality checks. The orthometric heights that is radial component of the extracted coordinate were converted to ellipsoidal height using the equation 9-1

Stn Id. No	Location	Latitude (° ′ ′′)N	Longitude (° ′ ′′)W	Orthom Hght (m)
306	Anyinasu	7 13 59.262	1 37 50.580	513.283
102	Apam	5 16 47.850	0 44 04.840	60.320
225	Asaasetre	5 27 08.187	1 30 04.875	249.784
305	Barekese	6 50 36.940	1 44 37.235	388.711
302	Wiawso	6 54 35.054	2 01 01.221	535.229
179	Prasokuma	6 22 09.631	1 02 00.869	465.978
125	Katamanso	5 45 48.930	0 03 55.626	73.152
150R	Krobo Hills	6 04 39.815	-0 02 59.783	321.552
155	Mamfe	5 56 10.455	0 07 20.246	499.028
304	Jamasi	6 59 22.062	1 26 44.176	590.581
185	Manso Nkwta	6 28 55.215	1 55 31.467	615.666
142	Nkawkaw	6 34 22.932	0 45 57.034	755.294
109	Nyanyano	5 27 26.297	0 25 25.844	55.474
207	Nsuopun	5 50 48.567	1 57 59.053	374.210
242	Nsuta	5 16 18.937	1 58 23.562	186.660
145	Nyameani	6 33 14.933	1 24 43.778	476.616
200	Obrakyere	5 37 22.854	0 33 34.551	279.715
217	Osenase	5 56 25.190	0 43 47.920	285.720
213	Pramkese	6 07 31.505	0 44 57.032	297.715
152	Senchi	6 10 55.143	0 02 39.070	438.699
180	Subriso	6 03 03.624	1 17 11.272	411.023
184R	Poano	6 28 07.645	1 41 42.307	446.288
178	Juaso	6 34 06.931	1 09 53.754	590.398

Table 8-1: Geographic Coordinates of the Common Points for the derivation of the Transformation Parameters in the Golden Triangle of Ghana

There was a further conversion from the Geographic Coordinate System to Cartesian Coordinates in War Office 1926 Coordinate System (X,Y,Z) using the following equations.

$$X = (n + h)cos\varphi cos\lambda \quad 8\text{-}1$$

$$Y = (n + h)cos\varphi sin\lambda \quad 8\text{-}2$$

$$Z = \left((1 - e^2)n + h\right)sin\varphi \quad 8\text{-}3$$

$$n = \frac{a}{\sqrt{1 - e^2 sin^2\varphi}} \quad 8\text{-}4$$

$$e = \frac{a^2 - b^2}{a^2} = 2f - f^2 \quad 8\text{-}5$$

$$b = (1 - f)a \quad 8\text{-}6$$

where

n	Prime vertical radius
h	height above the ellipsoid
λ	longitude
φ	latitude
e	eccentricity
f	flattening
a	semi-major axis
b	semi-minor axis

For the reverse that is converting from Cartesian coordinate system to the Geographic Coordinate System, the following equations are used

$$\varphi = arctan\left[\frac{Z + e^2 v sin\varphi}{\sqrt{X^2 + Y^2}}\right] \quad 8\text{-}7$$

$$\lambda = arctan\left({}^{Y}/_{X}\right) \quad 8\text{-}8$$

$$h = Xsec\lambda sec\varphi - n \quad 8\text{-}9$$

The reverse is required to calculate back to the original coordinate system after a transformation process. The Cartesian coordinates in the War Office ellipsoid were as shown in Table 8.2 were obtained. For more details refer to (Vermille, 2002).

8.2.1 The WGS84 Geocentric Coordinates of the Common Points

These Trigonometric Old Stations selected were observed each for 12 hours and the data processed while fixing the three Permanent Stations and the two Hub Stations as explained in Chapter Seven. The coordinates for these selected Common Points were therefore in the WGS84/ITRF05 system and were computed at the epoch 2007.39. These were in the Cartesian coordinate system and War Office coordinates of these points had to be converted to the Cartesian System before they were transformed.

Location	WGS84 (ITRF05) Coordinates			
	ID	X (m)	Y (m)	Z(m)
Anyinasu	ANSU	6325647.708	-180057.465	798084.883
Apam	APAM	6350787.213	-81407.555	583332.576
Asaasetre	ASAS	6347537.393	-166338.255	602325.783
Awaham Nkwanta	AWAN	6343878.253	-80798.416	656032.723
Barekese	BARE	6330440.752	-192684.758	755315.113
Mampong Jamasi	JAMA	6329617.012	-159704.179	771354.582
Juaso	JUSO	6335813.855	-128807.116	725133.427
Katamanso	KATA	6346169.830	-7215.792	636569.206
Krobo Hills	KROB	6342843.266	5560.000	671151.114
Mamfe	MAMF	6344637.416	-13509.064	655606.800
Manso Nkwanta	MNKT	6334661.223	212926.774	715622.573
Nyameani	NANI	6335269.925	-156146.906	723533.841
Nkawkaw	NKWT	6336666.372	-84673.839	725640.186
Nsuta	NSTA	6347589.300	-219868.306	582844.556
Nsuopun	NSUO	6341808.320	-217709.798	645757.441
Nyanyano	NYAN	6349294.509	-46938.168	602857.884
Obrakyere	OBRA	6347620.924	-61967.047	621119.348
Poano	POAN	6335460.896	-187460.010	714150.813
Pramkese	PRAM	6341714.762	-82896.345	676390.452
Prasokuma	PRAS	6338453.732	-114324.021	703224.437
Subriso	SBSO	6341641.164	-142384.569	668219.748
Wiawso	WISO	6328716.633	-222856.919	762594.119

Table 8-2: The Geocentric Coordinates obtained from the processed data from the GPS observation of the Common (Trigonometric) Points

War Office Coordinates				
Location	ID	X (m)	Y (m)	Z (m)
Anyinasu	ANSU	6325843.057	-180090.822	797764.061
Apam	APAM	6350979.362	-81440.190	583010.958
Asaasetre	ASAS	6347730.534	-166371.304	602000.813
Awaham Nkwanta	AWAN	6344074.306	-80831.152	655710.690
Barekese	BARE	6330639.557	-192719.183	754993.798
Mampong Jamasi	JAMA	6329814.453	-159737.108	771033.098
Juaso	JUSO	6336014.914	-128840.914	724811.321
Katamanso	KATA	6346365.706	-7249.756	636245.849
Krobo Hills	KROB	6343043.446	5528.678	670826.717
Mamfe	MAMF	6344835.095	-13542.265	655282.671
Manso Nkwanta	MNKT	6334858.050	-212961.176	715299.828
Nyameani	NANI	6335468.752	-156180.983	723211.373
Nkawkaw	NKWT	6336864.879	-84706.610	725318.495
Nsuta	NSTA	6347776.745	-219902.790	582517.844
Nsuopun	NSUO	6342002.182	-217744.393	645433.617
Nyanyano	NYAN	6349488.533	-46972.201	602535.949
Obrakyere	OBRA	6347814.416	-61999.925	620797.184
Poano	POAN	6335660.336	-187494.071	713828.753
Pramkese	PRAM	6341908.433	-82928.859	676067.360
Prasokuma	PRAS	6338651.322	-114357.123	702901.488
Subriso	SBSO	6341837.545	-142417.467	667896.629
Wiawso	WISO	6328918.856	-222891.499	762272.252

Table 8-3: The Cartesian Coordinates of the Common Points transformed from the War Office Geographic Coordinates

8.2.2 Deriving Transformation Parameter

Two approaches were used for the determination of the transformation parameters in this study. These were the Helmert's Transformation Method and the Polynomial Transformation approach. Although DITON uses both methods for the determination of transformation parameters, a script was written in MATLAB to derive seven transformation parameter was generated using the Helmert's shown in equation 8-18

8.2.2.1 The Polynomial Transformation

The second approach, the Polynomial Method, fits the coordinate differences between two systems with a polynomial function. This polynomial is then used to predict the coordinate differences of other points of interest. Since one dimensional fitting method is used, the coordinate differences of the components (longitude, latitude and height) are fitted with separate polynomials. The general expression for the model as found in (Chen, W., C. Hill., 2005) is as shown

$$dS_l = \sum_{i=1}^{n} \sum_{j=1}^{n} C_{ij} \left[k_{0,l}(\Phi_1 - \Phi_m)\right]^i \left[k_{0,l}(\lambda_1 - \lambda_m)\right]^j \quad 8\text{-}10$$

where

dS_l	coordinate component (lon, lat or height) differences
$k_{0,1}$	constant
n	order of the polynomial
$C_{i,j}$	coefficient of the polynomial
Φ_1, λ_1	longitude and latitude of station in system one
Φ_m, λ_m	coordinates of an appropriate geographic coordinate of the region

According to (Chen, W., C. Hill., 2005), the Polynomial Method has a few problems associated with it, the best fit is obtained when the order of the model is high, but rather creates higher distortions when using the derived transformation parameters. There is therefore the need to keep the order as low as possible; six was used for this derivation. The second problem is the difficulty in extrapolating the use beyond the boundaries of the area in question which makes it difficult to rely on it for areas outside the network and this problem becomes more severe with the increase in the order of the polynomial. The points should also be well distributed within the area as the error increases significantly in blank spaces especially for higher order polynomial transformations.

In computing the transformation between the War Office Ellipsoid and the WGS84 data for the Golden Triangle of Ghana using DITON, twenty common points were involved and omitting the height component the values below were obtained.

Minimum Value of Latitude (φ_{min}) in deg	5.27995833
Minimum Value of Longitude (λ_{min}) in deg	-2.01700583
Change in Latitude ($\Delta\varphi$) in deg	1.95590263
Change in Longitude ($\Delta\lambda$) in deg	1.95185878

The following constants were derived for the transformation from the target System (WGS84) back to War Office 1926 (old) system. These are used to determine the transformed coordinates using

a_0	1.435979109976948e-003
a_1	9.999661609469996e-001
a_2	-4.004662202738984e-006
b_0	1.252501867936573e-004
b_1	4.131438426924206e-007
b_2	1.000024893752392e+000

Transformation Parameter

The reverse, which is from War Office 1926 (old) System back to target (WGS84) System, yielded the constants below.

a_0	-1.436027988928279e-003
a_1	1.000033839906488e+000
a_2	4.004526866108193e-006
b_0	-1.252463798646630e-004
b_1	-4.132416902002944e-007
b_2	9.999751067527396e-001

8.2.2.1.1 **Coordinate Conversion of Polynomial Transformation**

After obtaining the results of the computation one needs to convert form one coordinate system to another using the steps that follows:

Convert the source coordinates into degree decimals, and then normalize the coordinates for numerical stabilization by substituting the values of the minimum latitude/longitude and the change in longitude/latitude obtained from the processing in the following equation

$$\varphi^*_{wo}=(\varphi_{wo}-\varphi_{min})/\Delta\varphi \quad 8\text{-}11$$

$$\lambda^*_{wo}=(\lambda_{wo}-\lambda_{min})/\Delta\lambda \quad 8\text{-}12$$

The above computed values for the latitude and longitude are substituted in the equations along with the constants a_0…..a_n and b_0…..b_n for a six (eight) parameter polynomial

$$\varphi^{\#}_{wgs} = a_0\varphi^*_{wo} + a_1\lambda^*_{wo} + a_2{\lambda^*_{wo}}^2(+a_3\varphi^*_{wo}\lambda^*_{wo}) \quad 8\text{-}13$$

$$\lambda^{\#}_{wgs} = b_0\varphi^*_{wo} + b_1\varphi^*_{wo} + b_2{\varphi^*_{wo}}^2(+b_3\,\varphi^*_{wo}\lambda^*_{wo}) \quad 8\text{-}14$$

To obtain the transformed values in the WGS84 coordinate system (φ_{wgs},λ_{wgs}) the following equations are the used

$$\varphi_{wgs} = \varphi^{\#}_{wgs}\Delta\varphi + \varphi_{min} \quad 8\text{-}15$$

$$\lambda_{wgs} = \lambda^{\#}_{wgs}\Delta\varphi + \lambda_{min} \quad 8\text{-}16$$

A test of the Polynomial Function for the transformation from WGS84 to the War is shown in the Table 8-4.

Point ID	Residual (Northing)(m)	Residual (Easting)(m)
ANSU	1.210	0.262
APAM	2.002	0.448
BARE	0.511	-0.544
JAMA	0.441	0.618
JUSO	-0.219	-0.388
KATA	-0.432	-1.483
MAMF	-0.472	-0.690
NANI	-0.432	-0.462
NKWT	0.400	0.237
NSUO	-0.775	-0.532
NYAN	1.383	-0.212
OBRA	1.095	0.029
POAN	-0.046	-0.151
PRAM	-0.191	0.481
PRAS	-0.635	0.165
SBSO	-0.460	0.617
ASAS	-1.557	0.656
AWAN	0.738	0.300
MNKT	-0.437	-0.363
KROB	-2.125	1.010
Statistics		
Maximum	2.002	1.010
Minimum	-2.125	-1.482
Standard Deviation	0.994	0.594

Table 8-4: Results and analysis of residuals after transformation with the Polynomial Function approach

Transformation Parameter

8.2.3 Helmert's Transformation Method

Helmert's Transformation is about modeling between two systems using seven average systematic biases which include three rotations, three translations and a scale. This linear transformation between the source and the target data is ideal for networks that do not have significant regional distortions.

To transform from a global coordinate to local coordinate systems using the Helmert's approach the equation below, 8-17 is used

$$\begin{bmatrix} X_{trans} \\ Y_{trans} \\ Z_{trans} \end{bmatrix} = \begin{bmatrix} \Delta X \\ \Delta Y \\ \Delta Z \end{bmatrix} + m \begin{bmatrix} \cos(\varepsilon_y)\cos(\varepsilon_z) & \cos(\varepsilon_x)\sin(\varepsilon_z) + \sin(\varepsilon_x)\sin(\varepsilon_y)\cos(\varepsilon_z) & \sin(\varepsilon_x)\sin(\varepsilon_z) - \cos(\varepsilon_x)\sin(\varepsilon_y)\cos(\varepsilon_z) \\ -\cos(\varepsilon_y)\sin(\varepsilon_z) & \cos(\varepsilon_x)\cos(\varepsilon_z) - \sin(\varepsilon_x)\sin(\varepsilon_y)\sin(\varepsilon_z) & \sin(\varepsilon_x)\cos(\varepsilon_z) + \cos(\varepsilon_x)\sin(\varepsilon_y)\cos(\varepsilon_z) \\ \sin(\varepsilon_y) & -\sin(\varepsilon_x)\cos(\varepsilon_y) & \cos(\varepsilon_x)\cos(\varepsilon_y) \end{bmatrix} \begin{bmatrix} X_{input} \\ Y_{input} \\ Z_{input} \end{bmatrix} \quad 8\text{-}17$$

Assuming that the rotation angles are small, the above formula can be simplified to equation 8-18

$$\begin{bmatrix} X_{trans} \\ Y_{trans} \\ Z_{trans} \end{bmatrix} = \begin{bmatrix} \Delta X \\ \Delta Y \\ \Delta Z \end{bmatrix} + m \begin{bmatrix} 1 & \varepsilon_z & -\varepsilon_y \\ -\varepsilon_z & 1 & \varepsilon_x \\ \varepsilon_y & -\varepsilon_x & 1 \end{bmatrix} \begin{bmatrix} X_{input} \\ Y_{input} \\ Z_{input} \end{bmatrix} \quad 8\text{-}18$$

$[X_{trans}, Y_{trans}, Z_{trans}]$	the target coordinate
$[X_{input}, Y_{input}, Z_{input}]$	the source Coordinate
$[\Delta X, \Delta Y, \Delta Z]$	the translation parameters
$\varepsilon_x, \varepsilon_y, \varepsilon_z.$	the three rotational parameters
m	the scale parameter.

Mathematically three common points measurements are more than enough, however to have a good quality set of parameters, one has to use as many as possible common points for the reason of redundancy in the equation.

The above expression has been used in PrePos GNSS Suite as well as a Matlab script to produce the results in Table 8-7.

Transformation Parameter

8.2.3.1 Results of the Helmert's Transformation Approach

Based on the equation 8-18, a script in MATLAB was written for the derivation of a set of transformation parameters. Eight well distributed stations, ASAS, AWAN, BARE, SBSO, PRAS, NKWT, MNKT and NSUO were selected from the GT for this derivation. Several combination and permutations were made to check the problematic stations. Analyzing the results led to the rejection of one station SBSO and finally seven were used to generate the final set of transformation parameters shown in Table 8- which transformed the coordinates from the Geocentric WGS84 (ITRF05) to the War Office Coordinate system.

Translation in X	78.1260 m
Translation in Y	52.0420 m
Translation in Z	-74.0535 m
Rotation in X	-1.4797 arcsec
Rotation in X	-8.3842 arcsec
Rotation in X	2.5527 arcsec
Scale	1.00001458

Table 8-5: Results of the Transformation Parameters from WGS84 (ITRF05) to War Office 1926

Since it was necessary to transform in the reverse direction that is from the War Office Coordinate System to the WGS84 for the purposes of transforming the old data into the proposed ITRS the reverse direction of the parameters were provided as shown in the Table 8-6

Translation in X	-78.1260 m
Translation in Y	-52.0420 m
Translation in Z	74.0535 m
Rotation in X	1.4797 arcsec
Rotation in Y	8.3842 arcsec
Rotation in Z	2.5527 arcsec
Scale	.99998542

Table 8-6: Transformation Parameters from War Office to WGS84 (ITRF05)

8.2.4 Testing the Helmert's Transformation Parameters

To test the derived Transformation Parameters, they were used to transform the data obtained from the GPS field observation data which had been obtained by processing with SEMIKA. The results obtained are as shown in Table 8-7. This is then compared with the Target Data, which is the War Office coordinates. The residual which is the difference between the expected values and the obtained value

determines the nearness to the truth. The residuals in X, Y and Z (cartesian) coordinates are shown in Table 8-8 with the target coordinates, the War Office.

Results of Transformed Coordinates			
ID	*X*	Y	Z
ANSU	6325848.266	-180092.060	797764.070
APAM	6350980.630	-81439.483	583008.318
ASAS	6347730.483	-166371.517	602001.325
AWAN	6344074.531	-80830.771	655709.810
BARE	6330639.485	-192719.290	754993.391
JAMA	6329816.793	-159738.335	771033.364
JUSO	6336012.260	-128841.227	724811.505
KATA	6346366.261	-7246.963	636246.444
KROB	6343041.212	5528.809	670829.083
MAMF	6344834.521	-13540.444	655284.333
MNKT	6334858.154	-212961.369	715299.956
NANI	6335467.889	-156180.737	723211.722
NKWT	6336865.326	-84706.660	725318.553
NSTA	6347780.936	-219902.209	582519.428
NSUO	6342002.456	-217744.050	645433.480
NYAN	6349489.124	-46969.715	602534.219
OBRA	6347816.070	-61998.923	620795.909
POAN	6335658.094	-187494.233	713828.325
PRAM	6341911.810	-82928.850	676067.909
PRAS	6338651.434	-114357.136	702902.192
SBSO	6341837.143	-142417.881	667896.662
WISO	6328915.263	-222891.922	762272.357

Table 8-7: Transformed points in the Cartesian coordinate system

Stn Id	War Office Coordinates			Residuals		
	X (m)	Y (m)	Z (m)	dH (m)	dE (m)	dN (m)
ANSU	6325843.057	-180090.822	797764.061	5.209	-1.238	0.009
APAM	6350979.362	-81440.190	583010.958	1.268	0.706	-2.640
ASAS	6347730.534	-166371.304	602000.813	-0.051	-0.213	0.512
AWAN	6344074.306	-80831.152	655710.690	0.225	0.381	-0.880
BARE	6330639.557	-192719.183	754993.798	-0.072	-0.107	-0.407
JAMA	6329814.453	-159737.108	771033.098	2.340	-1.227	0.266
JUSO	6336014.914	-128840.914	724811.321	-2.654	-0.313	0.184
KATA	6346365.706	-7249.756	636245.849	0.555	2.794	0.595
KROB	6343043.446	5528.678	670826.717	-2.234	0.131	2.366
MAMF	6344835.095	-13542.265	655282.671	-0.574	1.821	1.662
MNKT	6334858.050	-212961.176	715299.828	0.104	-0.193	0.128
NANI	6335468.752	-156180.983	723211.373	-0.863	0.246	0.349
NKWT	6336864.879	-84706.610	725318.495	0.447	-0.050	0.058
NSTA	6347776.745	-219902.790	582517.844	4.191	0.581	1.584
NSUO	6342002.182	-217744.393	645433.617	0.274	0.344	-0.137
NYAN	6349488.533	-46972.201	602535.949	0.591	2.486	-1.730
OBRA	6347814.416	-61999.9250	620797.184	1.655	1.002	-1.275
POAN	6335660.336	-187494.071	713828.753	-2.243	-0.162	-0.429
PRAM	6341908.433	-82928.859	676067.360	3.377	0.009	0.549
PRAS	6338651.322	-114357.123	702901.488	0.112	-0.013	0.704
SBSO	6341837.545	-142417.467	667896.629	-0.402	-0.414	0.033
WISO	6328918.856	-222891.499	762272.252	-3.593	-0.423	0.105

Table 8-8: The Residuals and the Target coordinates for the Common Points

Statistics			
	Radial (dH)	Easting (dE)	Northing (dN)
Maximum	5.208 m	2.793 m	2.366 m
Minimum	-3.593 m	-1.238 m	-2.640 m
Standard Deviation	2.133 m	1.009 m	1.094 m

Table 8-9: Statistical Analysis of the Residuals after Helmert's Transformation

Analyzing the results of residuals showed no systematic distortion, however further investigation in the vertical components revealed that the errors in the vertical component were further investigated and it was realized that NSTA had a cluster of three stations and the one that was observed was different from the one used for the computation. This had to be corrected and the data reprocessed. Another outlying station was ANSU which is suspected to have had a human error as a result of the over 5 m residual, which is most likely to be the error from the existing old War Office data rather than the observed GPS data.

Further analysis revealed that the stations located south eastern part of the Golden Triangle had the highest residual, a test of stations around that locality. The results below were the worst results from the test that was carried for the set of parameters.

Transformation Parameter

With the above revelation it became necessary to derive a localized set of parameters for the area. A new set of Transformation Parameters was derived using the local common points APAM, AWAN, KATA and NYAN as shown in Table 8-10. There was a remarkable improvement for the test coordinates.

Test Site ID	Cartesian Coordinates			GT Parameters		S-E Parameters	
	X (m)	Y (m)	Z (m)	dE (m)	dN (m)	dE (m)	dN(m)
SS66	6348050.514	-20201.084	617174.799	2.620	0.802	0.031	0.058
SGE3	6346681.406	-19125.799	631318.184	3.163	0.220	0.061	0.689
GCSE	6346510.177	16018.141	632480.346	3.164	0.601	0.445	0.257

Table 8-10: Results of the transformation using the locally derived set of Seven Parameter from the Helmert's Method

The improved accuracy resulting from the use of the localized transformation parameter calls for the future consideration of the Grid-Look-Up approach, where regular grids could be made to cover the entire country and parameters for each grid determined.

8.2.5 Comparison between Helmert's Transformation Parameter and the Polynomial Function Transformation

Although the Polynomial Function Approach in this study did not consider the radial component, comparison can be made in the horizontal components of both methods. The two show comparable result in terms of average of the residuals, but the Polynomial Function Approach shows a lower standard deviation of the residuals which shows its stability within the study area. The situation is expected to change when used for areas out of the study region, where the Helmert's Parameters could perform better. The Helmert's approach should however be used with caution in these areas as it also tilts away into error as long as the three rotation angles are considered.

The Figure 8-2 shows generally the poor residuals in the south eastern part of the country for both approaches. The figure does not reveal any clear-cut systematic errors. For both approaches, the residuals are generally better at the central part of the study area and deteriorate as one moves outwards.

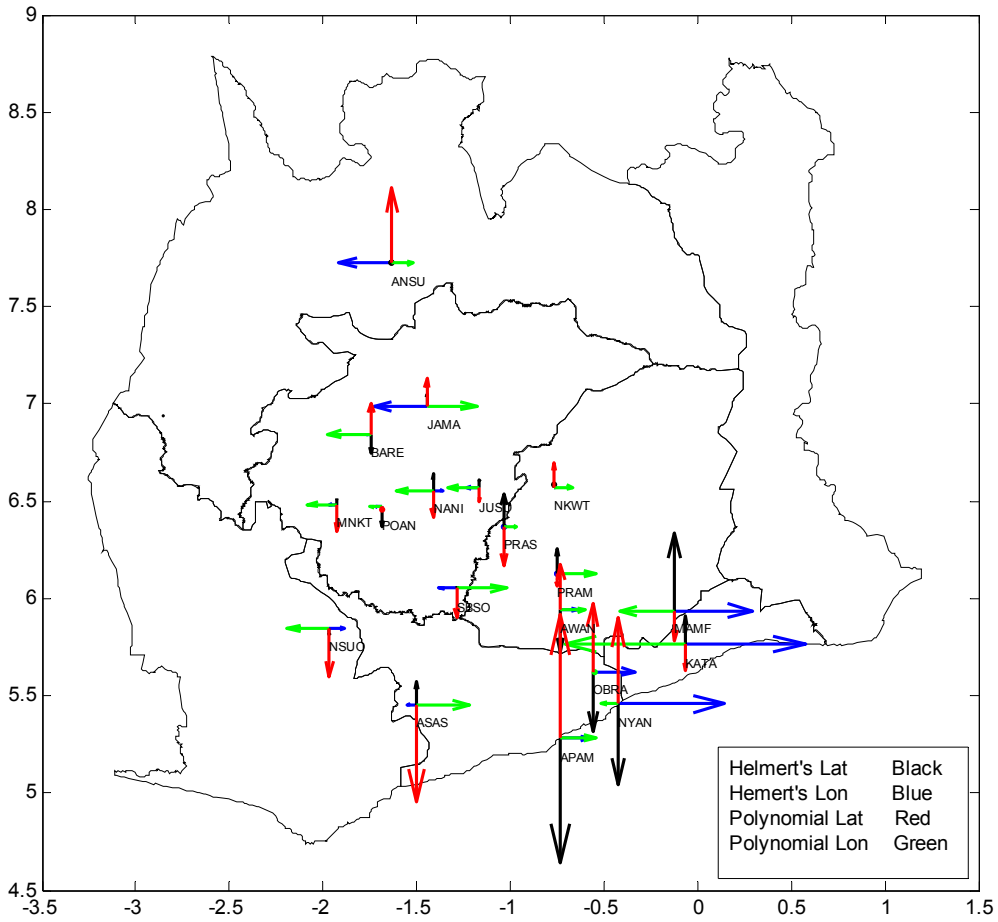

Figure 8-2: Graphical representation of the residuals of both Helmert's and Polynomial approaches

9 Ghana's Vertical Datum Definition

The decision to use high precision GNSS technique to establish, monitor and maintain a national horizontal datum for Ghana is a step to enable the use this cost effective technology for several applications in the country. This is however not adequate for other range of applications that require precise height differences. The need to establish the vertical datum for the country therefore cannot be overemphasized. To do this there must be the inclusion of GNSS and other techniques, to the mean sea level which is currently being used as the only means to reference the national vertical datum. The reasons for the need of improvement of the national vertical reference by including other methods is due to, among others, the impact of seismic activities along the Ghanaian coastal region and disturbances by physical infrastructural development activities at the harbours where the tide gauges are located. The Tema Tide Gauge for instance has already been affected by the renovations at the harbour resulting in the discontinuation of measurements and that of Takoradi faces a similar fate due to the impending renovation at the harbour. The Accra Tide Gauge which was used as the original tide gauge has not only discontinued for several decades, but was not physically protected and has consequently been lost. These factors call for the inclusion of the use of GNSS as well as gravity methods to complement the use of the mean-sea-level from these Tide Gauges.

One of the major reasons for the necessity to include GNSS into vertical reference definition is that there is generally an ambiguity in the referencing with only the MSL as a change in the sea level could be due to the sea-level rise or subsidence of the land. This ambiguity cannot be removed unless the agent of removal is not linked to either the movement of the solid earth or the changing sea level. This calls for the linking of the mean-sea-level measuring tide gauges to the space-based GNSS reference network.

9.1 The Need for Gravity Survey

While the ellipsoidal heights obtained from GNSS has a clear geometric meaning and is easy to derive, it unfortunately has limited practical use. It has no direct relationship to the earth's gravity potential required for physical application of height and therefore has to be transformed to orthometric height. This transformation will enable GNSS to be utilized in most topographic and engineering applications. When combined with a known geoid height, the ellipsoidal height can be transformed into the widely acceptable orthometric height using the equation 9-1 that can be derived from Figure 9-1.

$$h = H + N \qquad 9\text{-}1$$

H	orthometric height
N	geoidal undulation
h	ellipsoidal height

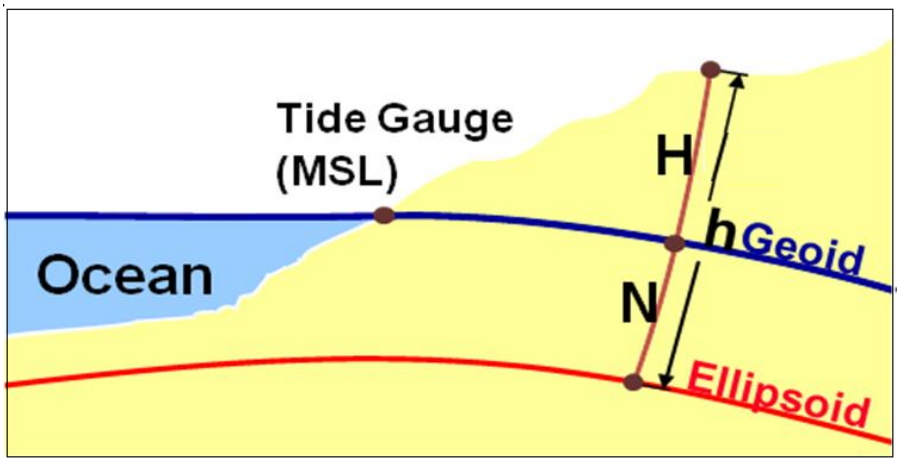

Figure 9-1: A schematic diagram showing the relationship between geoid, ellipsoid and orthometric heights

Obtaining the ellipsoidal height from the GNSS measurement, and the geoidal undulation from a geoid map or a derivation from gravity potential of the area, one can derive the orthometric height. This therefore calls for the determination of the national geoid hence the need to obtain gravity data.

9.2 National Geoid

Determination of the geoid is a very important component as far as this and future land development projects are concerned and the establishment of a Geodetic Reference Network in Ghana becomes more meaningful with the determination of the National Geoid. As stated already, most land use activities require the knowledge of more precise vertical components and as heights in the country have been always referred to the mean sea level which approximates to the geoid. Knowing the precise geoid, which has got a mathematical relationship with the ellipsoidal height obtained from GPS measurement (see Equation 9-1), vertical heights, can be deduced from the GPS observation. Since the geoid is a physical quantity, physical measurements are always required for its determination, and the most appropriate method for this project is the use of the terrestrial gravity measurement method, although airborne gravimetry is another option that can be considered.

The determination of transformation parameter for instance, involves the computation of the geoidal separation to convert the ellipsoidal heights to orthometric heights, and in the determination of Ghana's Transformation Parameters, the global EGM96 which was used was not adequately precise and this affected the accuracy of transformed coordinates. The determination of precise geoid will therefore enable one to deduce orthometric heights with the GNSS measurement and this can replace the time consuming traditional spirit levelling to save time and cost. Until the National Geoid is determined, use can be made of the global geoid data for example, the NGA's EGM96, which is freely available and can be used as a National Geoid Model. This global model is however more generalized and should not to be used for applications that require high precision.

The already established Absolute Gravity Network in Ghana by the Geological Survey Department (GSD) of Ghana and the Finnish Geodetic Institute (FGI) is a very important step towards the determination of a precise Geoid Map of Ghana.

9.3 The Earth Gravitational Model

The worldwide Earth Gravitational Models considered in this study are the EGM96 and EGM2008 which are developed by the National Geospatial-Intelligence Agency (NGA) of the USA. This according to (Pavlis et al, 2008) requires compilation of very high resolution global topographic database, to be used consistently in the computation of all terrain-related quantites necessary for the pre-processing of gravity data. The recently released EGM2008 is an improvement over the earlier version, the EGM96. The Table 9-1 shows the characteristics of the two versions as described by (Kenyon, S., Factor, 2007)

EGM96	EGM2008
1. Degree and order 360 spherical harmonic expansion model 2. Worldwide data at 30' X 30' resolution 3. Long-wavelength gravity information from about 40 satellites 4. Elevation data from about 29 different sources for topographic database 5. Satellite altimetry from TOPEX, ERS1 and GEOSAT for the main areas 6. Accuracy goal was 0.5 – 1 m RMS worldwide	1. Degree and order 2160 spherical harmonic expansion model 2. Worldwide data at 5' X 5' resolution 3. Improved long-wavelength gravity model from GRACE (significantly accurate than the satellite modelling) 4. The use of the Shuttle Radar Topographic Mission (SRTM) data and other sources including GTOPO 30, ICESAT etc to develop worldwide 30' X 30' topographic database for terrain correction and residual terrain modelling (RTM) 5. Utilizes the mean sea surface (MSS) over the ocean and associated dynamic ocean topography (DOT) 6. Accuracy goal 15 cm RMS worldwide

Table 9-1: Comparison between EGM96 and EGM2008

9.4 Validating the Global EGM96 in Ghana

In this study the global EGM96 was used hence the vertical components of derived orthometric heights contain the inherent inaccuracies of the global model. This has however an accuracy of about 50 cm for a country like Ghana with low density of gravity measurements as can be deduced from (Merry, 2003); (Kenyon, 2006). This is however good for some applications. A plot of the geoidal undulation of EGM96 through TADI and ACRA the longitude using the NGA website, Figure 9-2, shows a

relatively steep gradient at the coast especially in Takoradi. The series 1 and series 2 show the undulation through Takoradi and Accra respectively from the equator to the northern part of Ghana. The rapid change in the coastal region affects the predictions and estimations of the geoid separation and therefore there is the need to really determine the geoid instead of using the global EGM96 for national vertical reference datum.

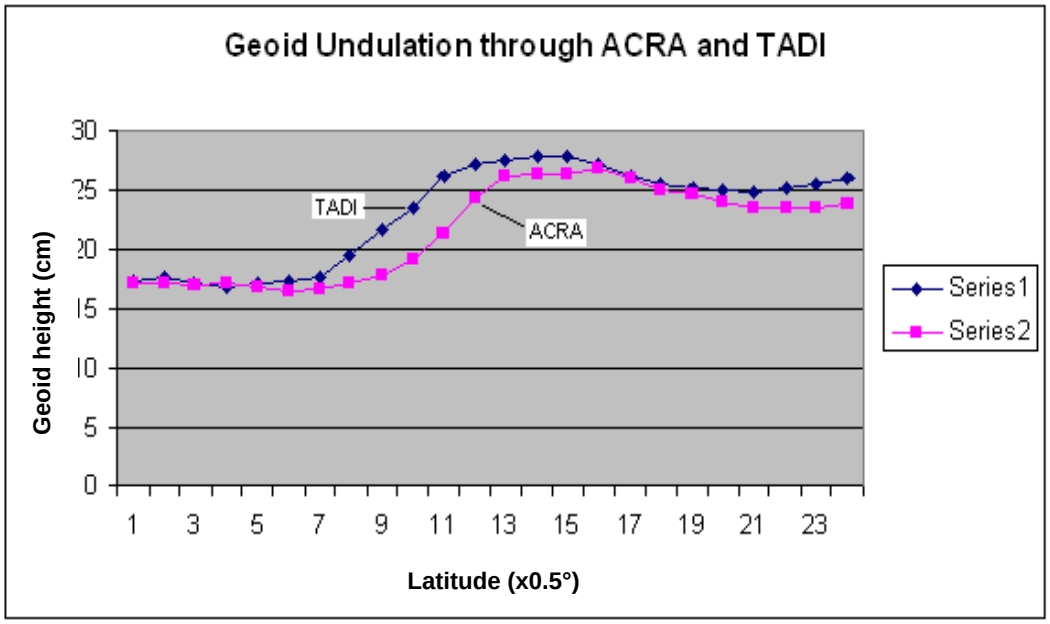

Figure 9-2: A plot of the EGM96 Geoid Undulation along the meridians through TADI and ACRA

9.4.1 The Expected Impact of the EGM08 in Ghana

The root-mean-square accuracy of 15 cm is the global goal of the EGM2008 which is a significant step over the previous 50 cm to 100 cm of the EGM96 for the geodetic community. In view of the improvements made in the worldwide topographic database and improved gravity information, Ghana with its contribution in form of gravity data to the NGA's database is expected to have an accuracy of about the global average.

9.5 Collocating a GNSS Permanent Station at the Tide Gauge

The TADI Permanent Station which is approximately 2 km away from the Takoradi Tide Gauge is a good candidate for the definition of Ghana's vertical datum, which has been established using the MSL. However in such distances, vertical variations due to local heterogeneities may be present and can cause a difference in absolute vertical motions on the GNSS site and on the tide-gauge.

One way to verify possible relative variations between the tide gauge and TADI is to perform repeated leveling surveys through the years. However, this has some disadvantages, namely the extensive resources required to accomplish this survey of

the two km. Furthermore, in case of TADI, the marker is located on the roof of a building; see Figure 9-3, which necessitates the combination of geometric and trigonometric leveling. This could cause degradation in the quality of the solution for the vertical difference between the GNSS site and the tide-gauge. Therefore, it was necessary to install a second GNSS station, coded TKTG, in the proximity of the tide gauge, about 40 m. This station is to be used to measure the absolute variations of the local area where the tide-gauge is located. It should be noted that since the tide-gauge is located in an old pier, it does not ensure stability, and consequently, the existence of local variations is probable. TKTG is located on a slightly stable area formed by compacted sediments. However, the relative motion between TKTG and the tide-gauge can be easily observed periodically due to the short distance between both markers through precise leveling, consequently, the absolute vertical variation of the tide-gauge itself can be estimated.

Since TKTG is also not installed in a very stable area, the observed vertical variations might be not representative of the true vertical variations for whole area. However, the direct measurement of the baseline between these two stations, TKTG and TADI, will permit the computation of the true vertical motion of the tide-gauge. In addition, the benchmarks installed near the system, as shown in Figure 9-4 and Figure 9-5, will ensure a more efficient and precise tie between these systems. The installation of these benchmarks permits more efficient precise leveling between the GNSS systems and the tide-gauge. Furthermore, in case of any disturbance of any of the systems or some the benchmarks, the network can still are reconstructed.

The goal is to determine an accurate geoid undulation at the GNSS stations, convert them into orthometric heights and use the GNSS station reference points to get insight into the stability of the ellipsoidal heights.

Figure 9-3 Pictures of the installed GNSS stations in Takoradi: TADI station (right); TKTG station (left)

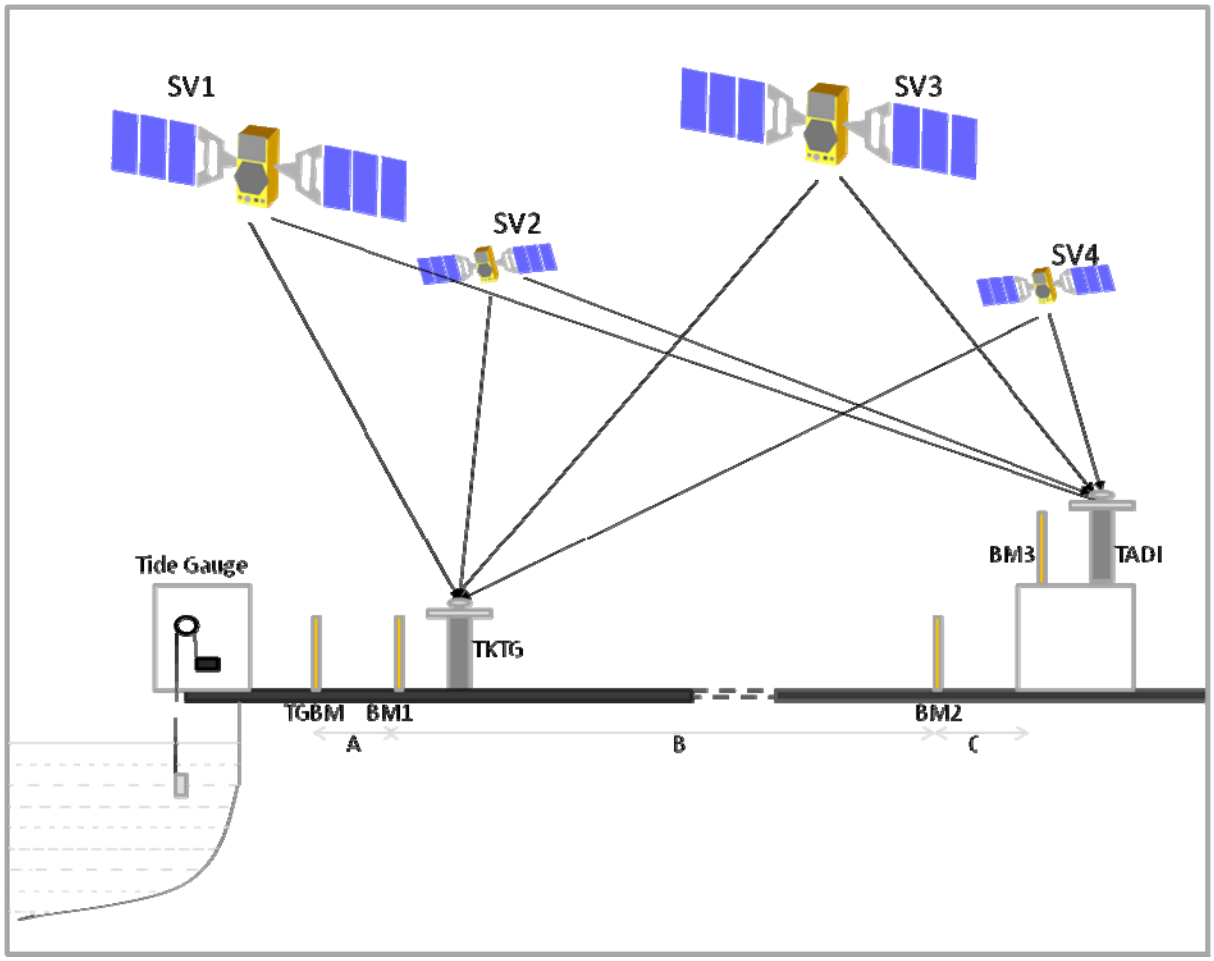

Figure 9-4: Sketch of the location of all benchmarks that were observed and the location of the two different systems (GNSS and tide-gauge).

9.5.1 Linking TKTG to the Geodetic Reference Network

A high-precision leveling was conducted between the two GNSS stations, the benchmarks and the tide-gauge using an automatic precise level. In the high-precision leveling, seven closed circuits between the GNSS stations and the tide-gauge were surveyed. All of these circuits were observed two times and the closing error varied between 1 mm and 2 mm, which is under the tolerance for high-precision leveling. With the location of TADI on the rooftop, trigonometric leveling, between BM2 and BM3 (shown in Figure 9-4) had to be used to connect the precise levels of the surrounding benchmarks to the TADI marker.

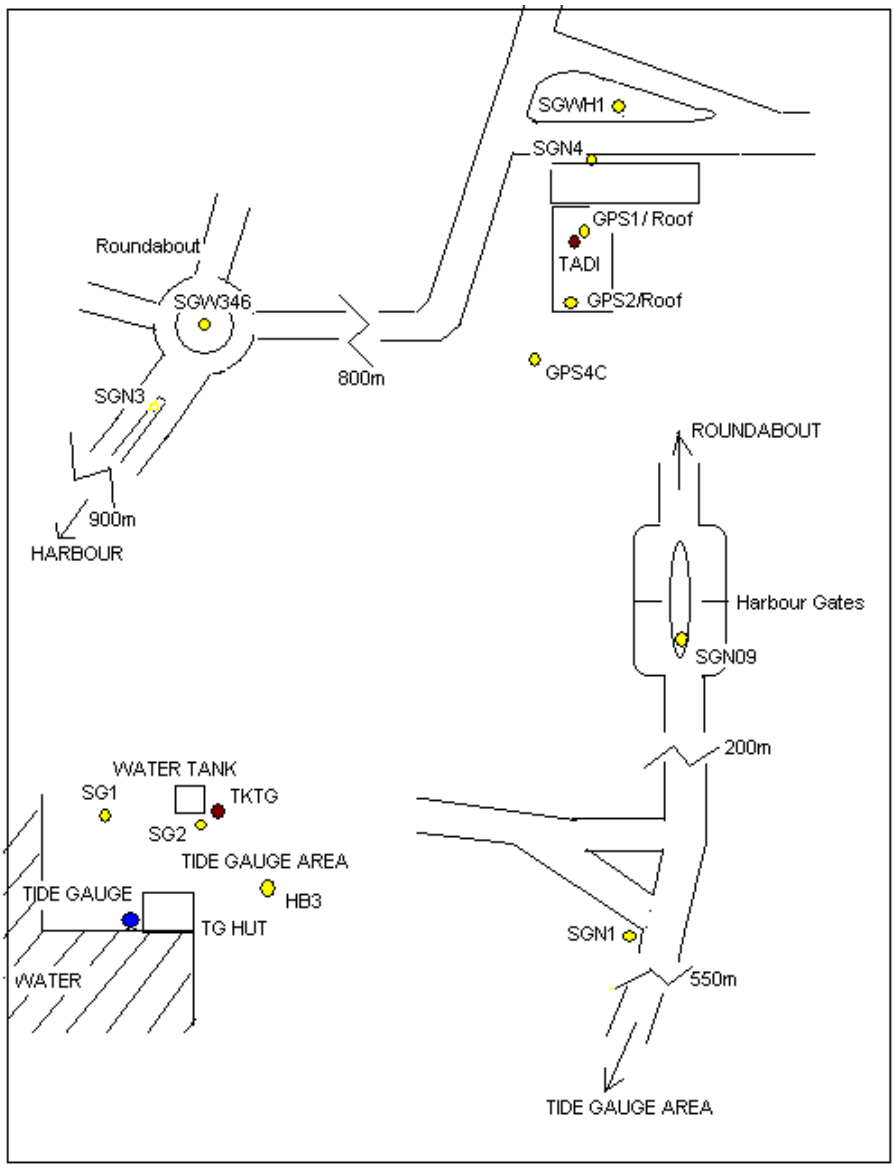

Figure 9-5: A Sketch of the location where TADI and TADI are installed and the components of the geodetic network which include: TADI and TKTG GNSS Stations and tide-gauge (red) together with existing (blue) and installed (yellow) benchmarks

9.6 Comparison between Ellipsoidal Heights at different times at TADI

Table 9-1 shows the values obtained for the ellipsoidal height of TADI computed by combining the solutions for several days at two different times, June 2007 and January 2008 using GIPSY, (Fernandes et al, 2008).

	Ellipsoidal Height (m)	Standard deviation (m)	Daily files
June 2007	59.3544	0.0012	7
January 2008	59.3549	0.0013	5

Table 9-2: Comparison between Ellipsoidal Heights

These results show that there is no significant variation between the vertical position of the TADI station for the period considered. Although this time-span is too short to derive any definitive conclusions about the stability of the TADI station on the vertical component, these results point into that direction. Since TADI is one of the permanently operating reference stations in this project, time series analysis should be conducted to ensure a permanent monitoring of the stabilities of this station

9.7 Comparison between Ellipsoidal and Pseudo-Orthometric Height

The aim of this aspect of the project is estimate the geoidal undulation at the station and compares it with the global estimate that is in use now. This requires the orthometric height at both stations. The precise leveling provides the height difference between the two stations TKTG and TADI and the Tide Gauge Bench Mark which is referenced as the 'zero' height. Although close to the orthometric national system of Ghana, this height is not identical, therefore the prefix "pseudo" was introduced to make such distinction, hence the term pseudo-orthometric height as used in Table 9-2. These heights are compared to the values computed for the ellipsoidal heights for TADI and TKTG for January 2008.

Site	Ellipsoidal Height (m)	Pseudo-Orthometric Height (m)	Geoid Undulation (m)
TKTG	28.545	2.981	25.564
TADI	59.255	33.669	25.586

Table 9-3: Comparison between Ellipsoidal and Pseudo-Orthometric Heights

There is a difference of 2.2 cm between the geoid heights of the two stations which are only 2 km apart, which according to Land Information, New Zealand (LINZ) 1-2 km at its maximum resolution of 56 km, which translates to approximately 3.6-7.2 cm for the two km separation. This compares well with the results obtained from this

study despite the steep gradient around Takoradi in particular and along the coastal region of Ghana as shown in Figure 9-2. The Pseudo-Geoid Undulation of 25.586 m at TADI cannot be however compared with the estimation from the EGM96 which is 23.13 m for the same station. This can be due to the generalization of the global geoid and therefore calls for the determination of a national geoid map for the country. Until the precise geoid separation is determined to obtain the orthometric heights for the stations EGM96 which according to (Merry, 2003) forms the basis of the African Geoid Project, AGP2003 could be used. On the assumption that the global geoid forms the basis for local geoid, then a constant value representing the difference between the pseudo-geoid and the EGM96 which is 2.456 m can be used as a correction factor. This can until a precise geoid is determined, can be used as the geoid for the determination of orthometric height from the ellipsoidal height obtained from GNSS observation.

10 Improved GNSS Data Analysis Methods

This chapter deals with various approaches to ambiguity fixing which is

Ambiguity Fixing

In addition to developing an appropriate method for the provision of differential corrections, there was the need to determine the carrier cycle integer ambiguity (N) in Equation. 3-2 for carrier phase measurement.

10.1.1 Methods of Ambiguity Resolution

To achieve a reliable ambiguity resolution, a reasonably high probability of correct ambiguity estimates is required. This ambiguity success rate depends on the following

- The functional model which describes the relationship between observation and parameters to be estimated
- The observation variance-covariance matrix (stochastic model) which captures the correlation and measurement uncertainty.
- The method used to estimate the integer ambiguities.

SEMIKA employs both types of functional models, geometry-free and geometry-dependent approaches in ambiguity fixing. The geometry-free analysis determines ambiguity by code-carrier-combination after the initial range run. These code range and carrier phase measurements are employed to resolve ambiguities without any knowledge of the antenna position. The main steps of the geometry-dependent ambiguity resolution are the estimation of the float solution, normally using combined code and carrier phases, searching for the candidate solutions where several methods are employed in a more sophisticated manner, using sets of integer ambiguities around an initial estimate to be tested with several fixed carrier phase solutions and comparing the variance for each solution. If a given estimated variance is found to be smaller than all others, the ambiguity is said to be resolved (Cosentino, R. J., D. W Diggles, 1996). The best solution is validated by verifying that with a high probability this best solution is really the correct solution using statistical tools like Ratio-Test, and others (Teunissen, P. J. G; Odjik, D, 2003), (Vollath, 2004). Further explanation to this has been given in (Seeber, 1993).

The geometry-dependent approach can be selected from the following methods

- Floating Ambiguity Solution
- Nearest Integer Round-off Method
- The Observation Space Ambiguity Search Method (LAMBDA)
- Geometry-Reduced Resolution Approach
- The Quick Ambiguity Resolution Procedure

10.1.2 Floating Ambiguity Solution

This is the estimation of ambiguities not accounting for their integer nature, typically using least squares adjustment. It can be either geometry-free or geometry dependent. There is difficulty in solving the ambiguities due to the de-correlation biases in GPS observations as a result of atmospheric effects and satellite orbit biases for longer baselines. Multipath can be a dominant error source when pseudo-range and carrier phase observations are incorporated and make it difficult to solve ambiguities because of the quasi-random behaviour over short time span. The difficulty posed by pseudorange is however relatively higher than carrier-phase (Donghyun, K., Langley, R.B., 2000).

Optimal estimates of the ambiguities is derived from the float solution process and in addition a realistic estimates of the variance-covariance matrix of the ambiguity estimates, which serves as an input for the search of and validation process for fixed solution, is obtained.

10.1.3 Nearest Integer Round-off

This is the simplest integer estimator with the lowest success rate as compared with the other methods. It rounds off the float ambiguity solutions to their nearest integer values. A float vector thus maps onto a certain integer vector when the absolute difference between this integer vector and the corresponding float vector is considerably less than half cycle. Though this is an acceptable integer estimator, it does not take ambiguity into account hence does not usually satisfy the minimization criteria (Odjik, 2002).

$$\text{Min} = \left| N_{float} - N_{fixed} \right|^2 \qquad 10\text{-}1$$

This minimization criterion will be satisfied when there is no correlation between the ambiguities that is when the ambiguity variance-covariance matrix is a diagonal matrix. The convergence of the float ambiguity estimates tend to be slow because measurements taken within a couple of seconds of each other tend to be highly correlated and the rounding off float estimates to integer values can be an error-prone process (Misra, P., P. Enge, 2001)

10.1.4 Observation Space Ambiguity Search Method

The Observation Space Ambiguity Search Method uses mainly the Least squares AMBibuity Decorrelation Adjustment (LAMBDA) method for the integer ambiguity determination which is based on the least square principles. The integer estimation is

preceded by a de-correlation step to increase its efficiency by aiding the search space which is an ellipsoidal space induced by the covariance matrix of the float ambiguity. The de-correlation enables the search space to be spaced such that it contains only the best vectors of integer ambiguity, to a large accuracy.
In effect this method uses the estimated float solution and the variance-covariance matrix as inputs for the computation of the estimated integer ambiguity which is finally used to compute the fixed solution. (Teunissen, 1995)

10.1.5 Geometry Reduced Resolution Approach

The Geometry-Reduced Resolution Approach is a special method implemented in Semika, originally developed for fixing ambiguities via short baselines. This approach makes use of selected linear combinations featuring a low geometric error impact, i.e. an initial position error will not have full influence on the ambiguities, but only a reduced one. The initial position can be derived from a differential pseudo-range position, but it will still be in error in the range of at least a couple of decimeters. Hence it is important to reduce this geometrical error down to a limit which is no longer harmful for ambiguity resolution. Typical geometry-reduced linear combinations for a dual-frequency GPS receiver are L34, L45 and L79. The advantage of these linear combinations is a higher noise level compared to original L1 and L2 carrier phases and an increase of the ionospheric error impact, because these linear combinations are similar to the so-called "ionospheric residuum" which is commonly used by scientists for observation of the ionosphere. This automatically implies that the geometry-reduced ambiguity resolution method is normally limited to smaller baselines.

In contrast to geometry-free methods, this approach is still completely based on carrier phase measurements and does not require the combination with noisy range observations (apart from the use of a smoothed range-derived initial position). The linearly combined ambiguities of at least two such combinations need to be resolved until the original ambiguities for the L1 and L2 carries can be figured out. In practice, a third linear combination can optionally be taken into consideration in order to increase the reliability of this method by cross-checks due to the increased redundancy.

10.1.6 The Quick Ambiguity Resolution Procedure

This method is provided to resolve ambiguities very quickly, even with data of less than a minute. It combines the Observation Space Search Method and the Geometry-Reduced Approach. This method uses the coordinate constraint from the DGPS solution in SEMIKA and also special linear combination approaches are used. After the resolution of the integer ambiguities the final position adjustment is

performed with the ionosphere-free linear combination, therefore it is only the troposphere and multipath error that can remain.

10.1.7 Comparing the Various Ambiguity Search Methods with data from Ghana

The objective of this analysis is to find the performance of the different methods and which to employ for various tasks under the same conditions including the time to fix and both positional and horizontal accuracies. These methods which have been implemented in SEMIKA and were analyzed included

- Floating Ambiguity Solution (FAS)
- Nearest Integer Round-off Method (NIROM)
- The Observation Space Ambiguity Search Method (OSASM)
- Geometry-Reduced Resolution Approach (GRRA)
- The Quick Ambiguity Resolution Procedure (QARP)

10.1.8 Analysis of he Ambiguity Search Methods Implemented in SEMIKA

Time windows increasing in the steps of 5 minutes were processed, using the various discussed ambiguity fixing methods, for one hour, showing the results graphically in Figure 10-3 to Figure 10-7. A new set of 10-second time-window was selected for the Quick Ambiguity Resolution Procedure (QARP) which unlike the other methods, had already fixed the ambiguities after less than five minutes. Figure 10-1 and Figure 10-2 show that all the methods got fixes in twenty minutes, for the 58 km baseline between ASFO and AKRO. The importance of this analysis was to have an idea of how long one has to observe at a station to get reasonable results. A more detail results for the various methods is discussed in the proceeding section.

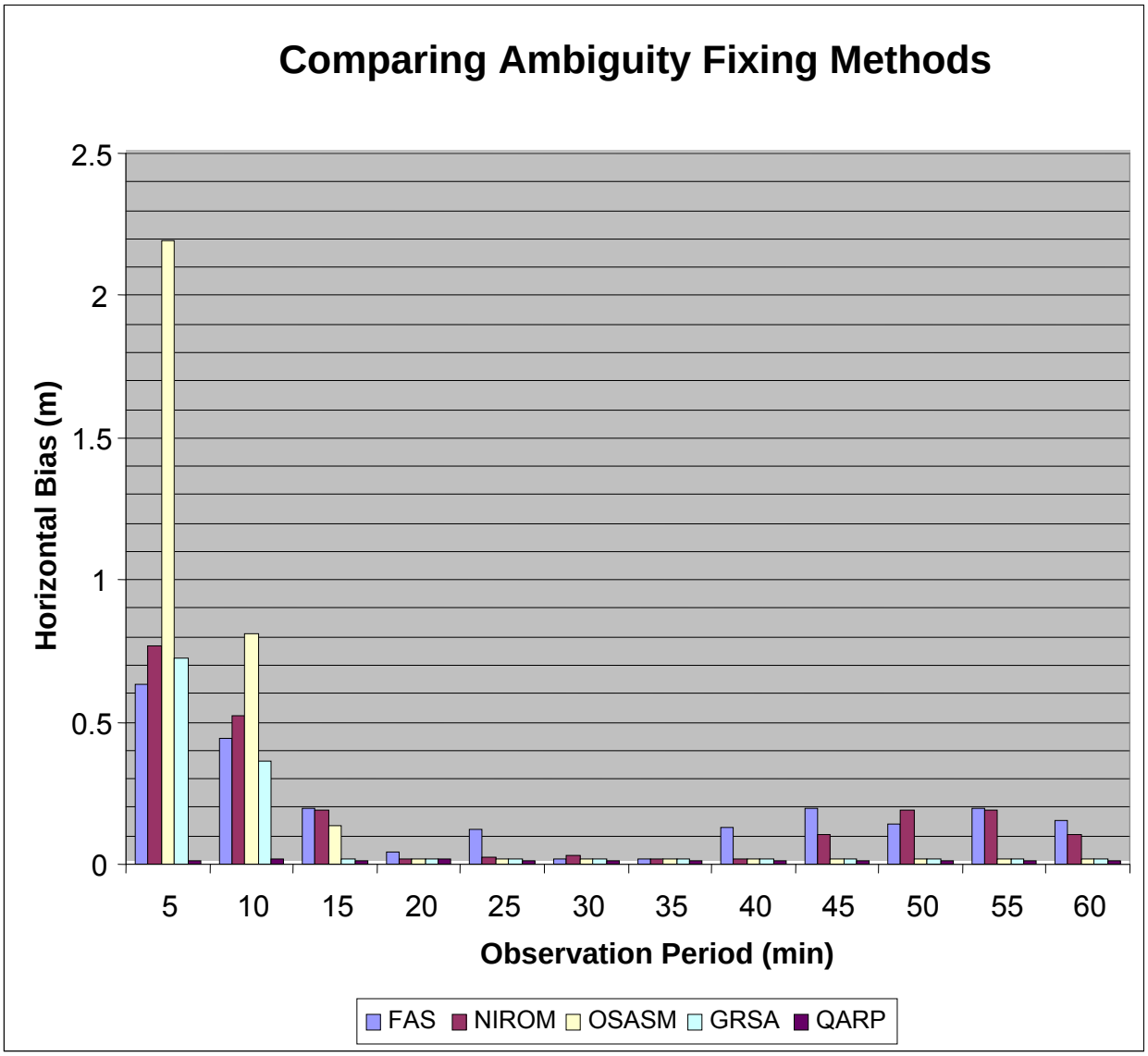

Figure 10-1: Comparing the performances of the various ambiguity fixing methods using the horizontal bias

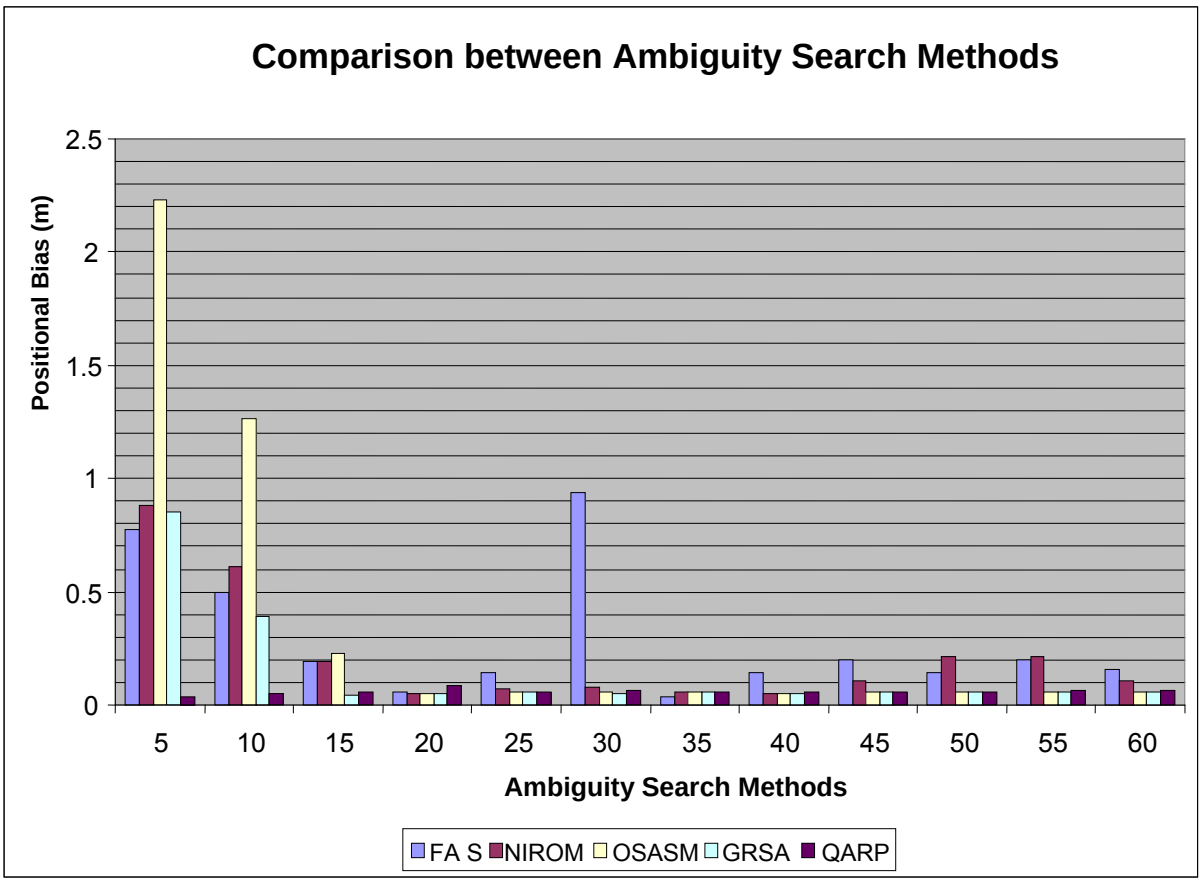

Figure 10-2: Comparing the performances of the various ambiguity fixing methods using the Positional bias

10.1.9 The Analysis of Ambiguity Resolution using the various Methods

The float ambiguity showed a general improvement of the bias with time. There is an unexpected low biases at 20th 30th and 35th minute,

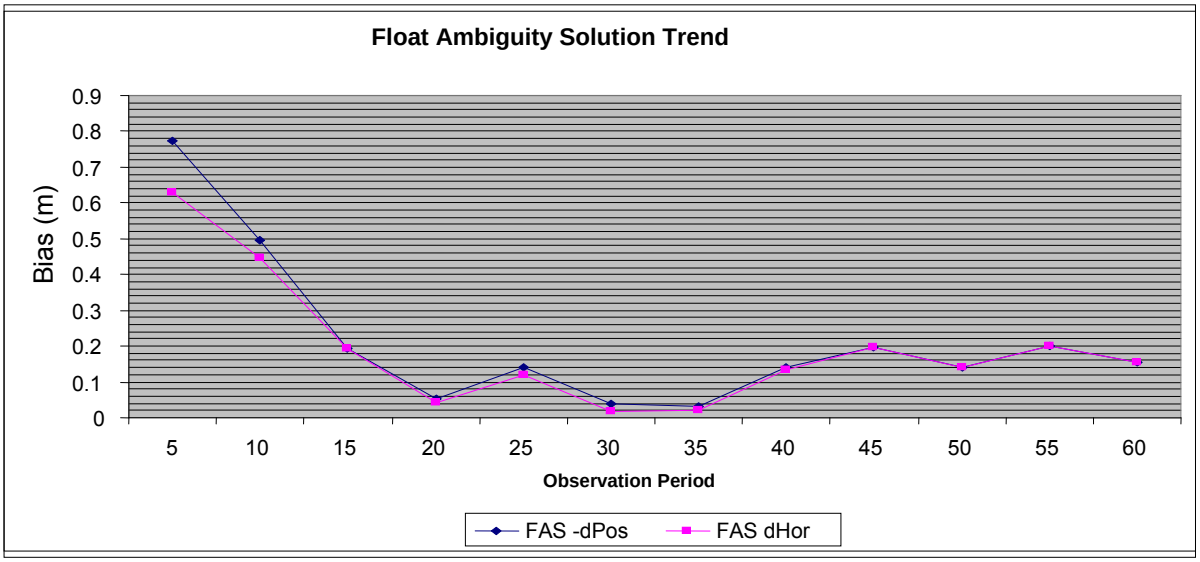

Figure 10-3: Convergence of the Float Ambiguity Solution Method

The Nearest Integer Round-Off approach followed the expected trend of improvement with time of the biases, there was however deterioration at the 50th and 55th minutes

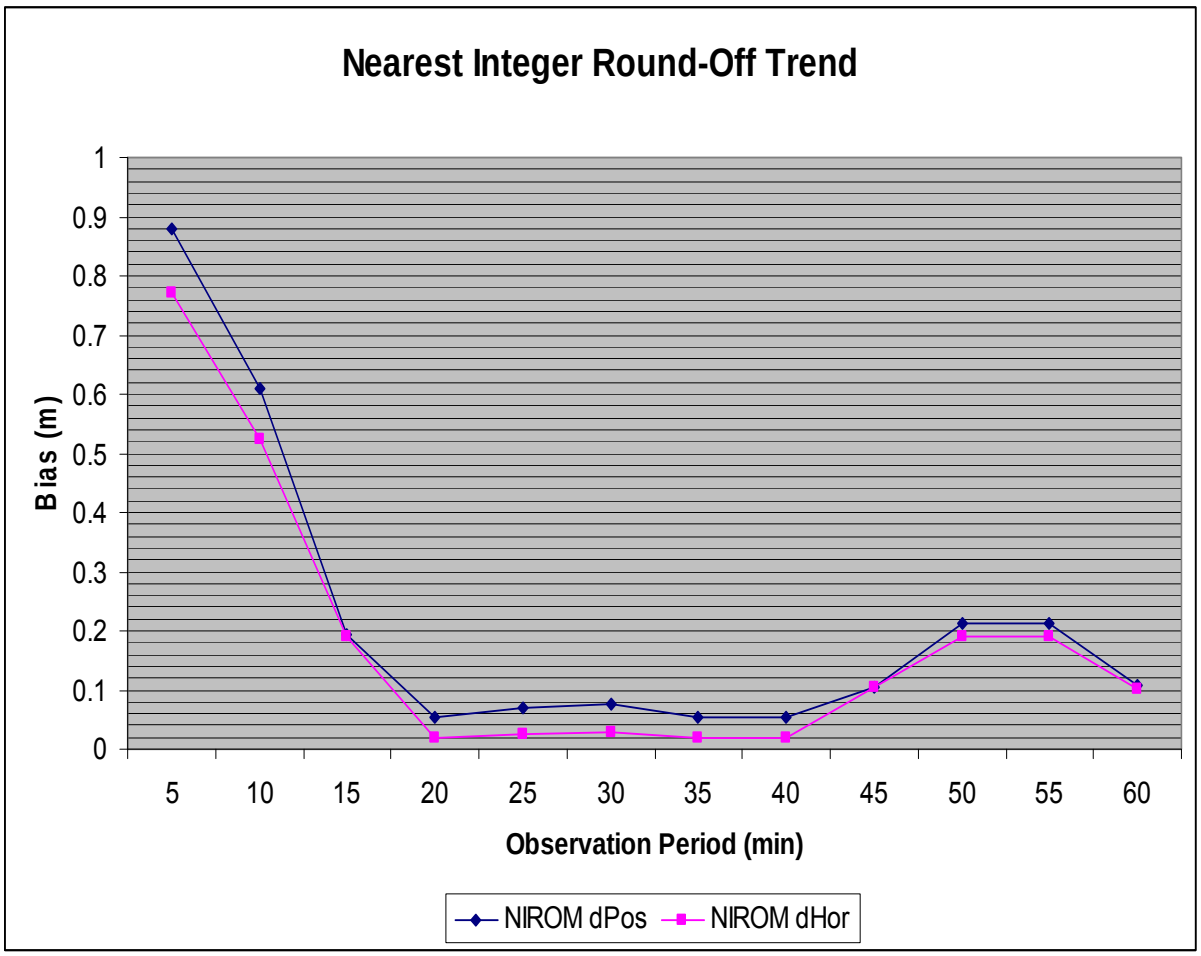

Figure 10-4: Convergence of the Nearest Integer Round-Off Method

The Geometry Reduced Resolution Approach got its fix relatively earlier than the rest and was maintained afterwards showing a greater stability as compared with the two previous approaches discussed.

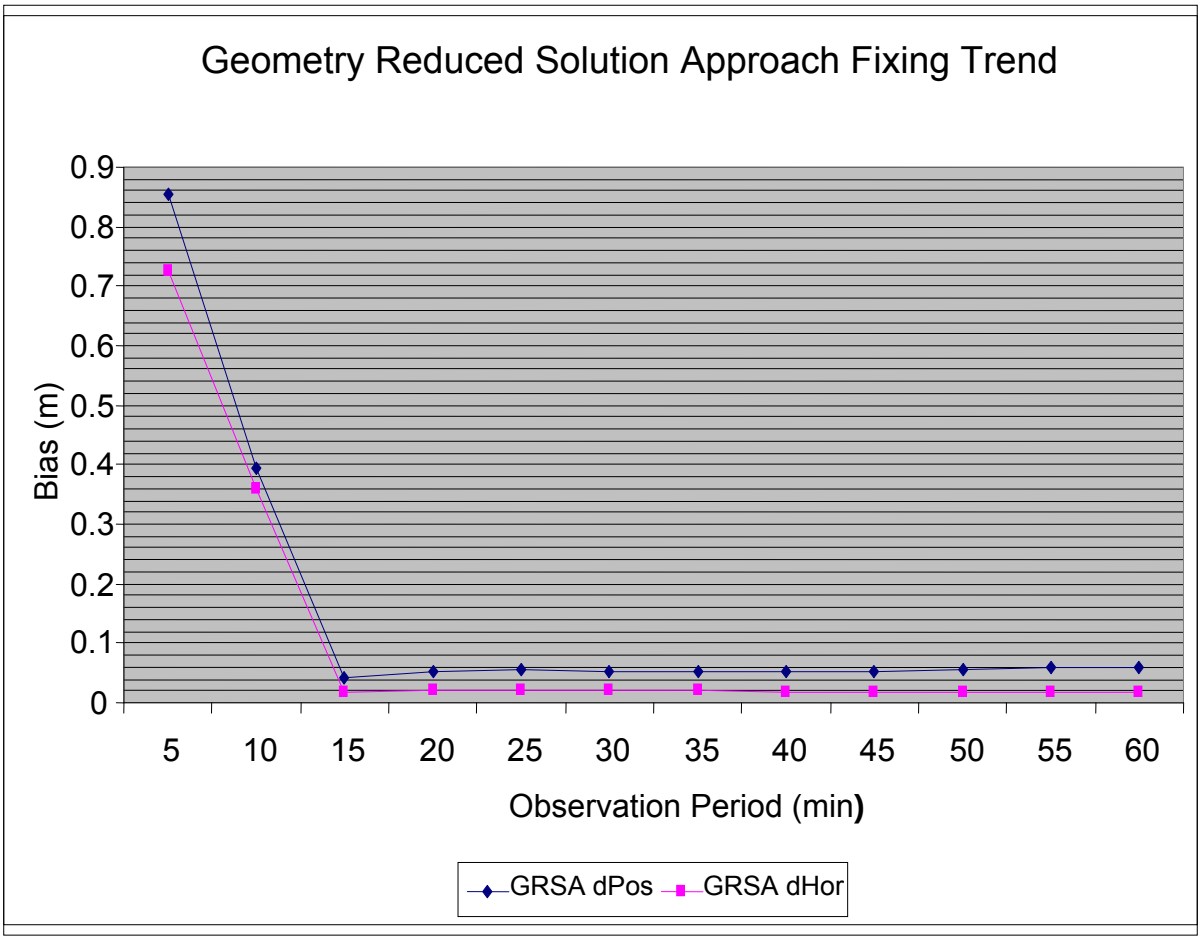

Figure 10-5: Convergence of the Geometry Reduced Solution Approach Method

The Observation Space Ambiguity Search Method started from a very poor solution at the beginning before fixing after 20 minutes and maintained a stable accuracy to the end of the measurement. This poor solution may be due to the poor float estimation, an initial requirement of the space search approach

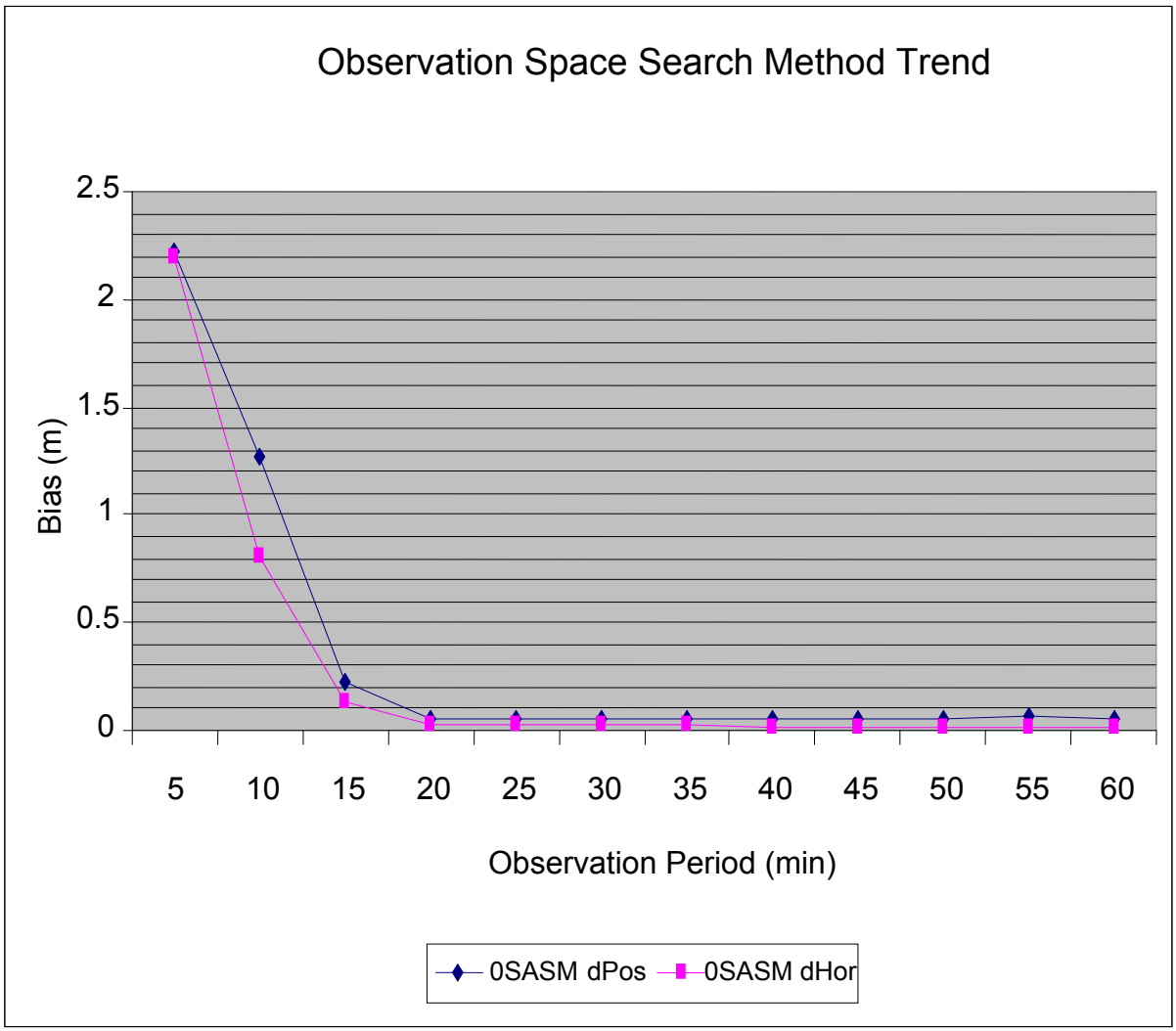

Figure 10-6: Convergence of the Observation Space Search Method

This had the quickest fix which occurred within the first five minutes and despite the surge at the 20th minute it remained stable till the end of the observation, this was then followed up with further investigation to find the time-to-fix of this option by starting from 20 seconds in steps of 10 seconds. As shown in Figure 10-8, ambiguity was resolved after 30 seconds

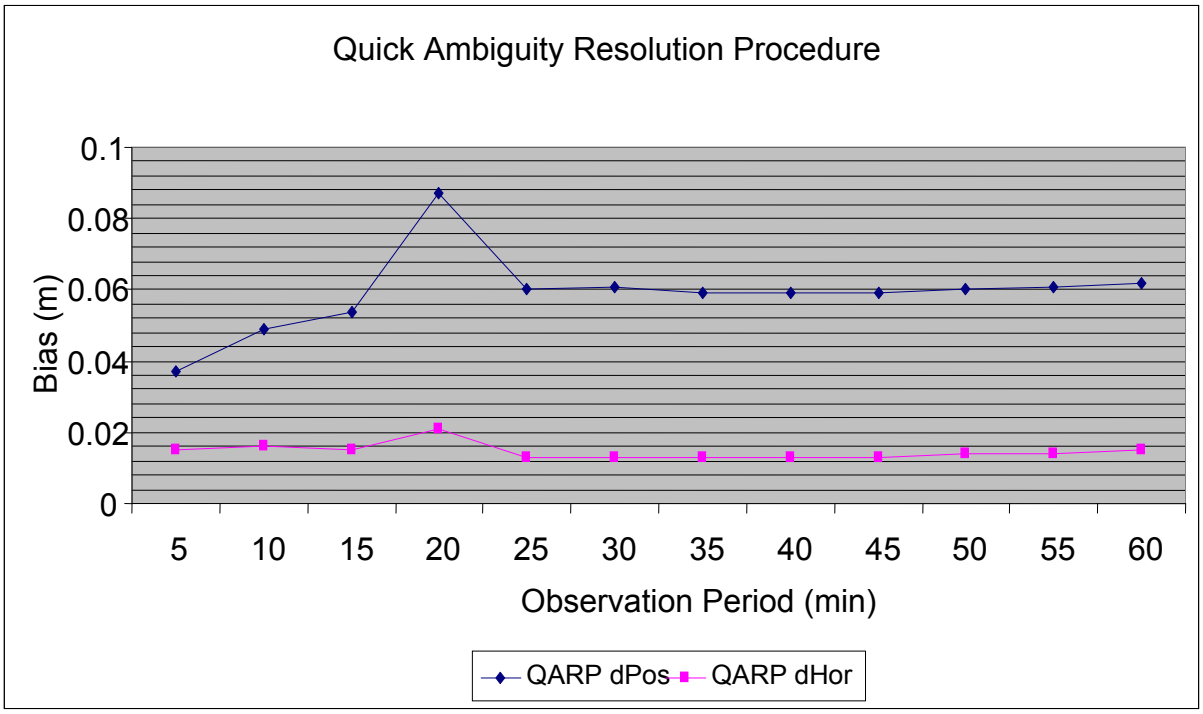

Figure 10-7: Convergence of the Quick Ambiguity Resolution Procedure Method

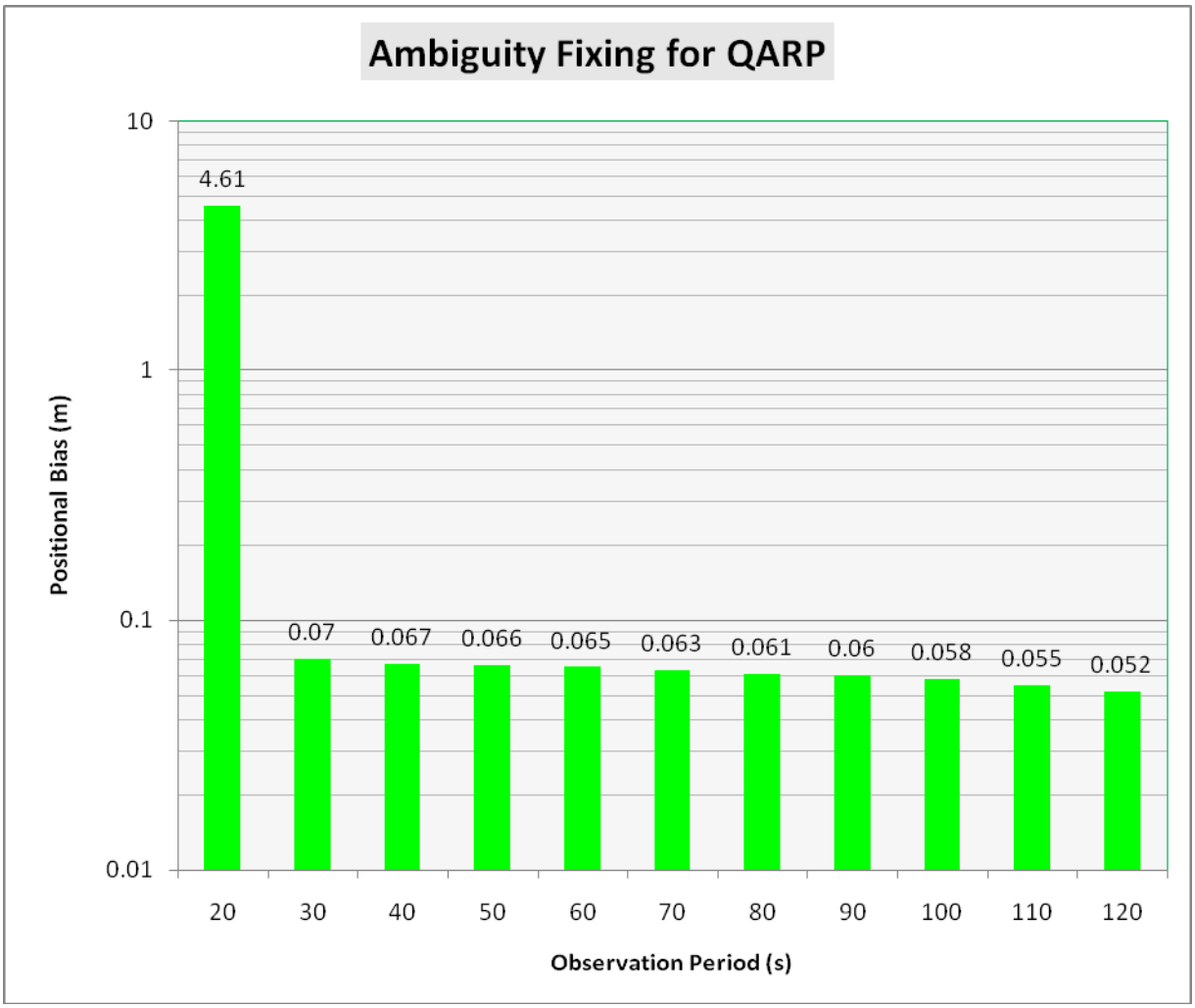

Figure 10-8: Convergence of the Quick Ambiguity Method

10.1.10 Determining Percentage fixes for various Time Windows

In furtherance to the optimum use of GNSS in the Ghanaian environment, the percentage fixes over the 58 km distance between ASFO and AKRO using the Nearest Integer Round Off method which has the lowest success rate was analyzed. This option was used as the intention is to analyze the worse case scenario for the ambiguity fixing, for the estimation of the duration of observation at a station, as a guide to the user in the Ghanaian environment. Various time windows were used to determine the percentage fixes. The Figure 10-9 to Figure 10-14 show the fixes which in this case were considered at 5 cm. or better otherwise was declared as float solution.

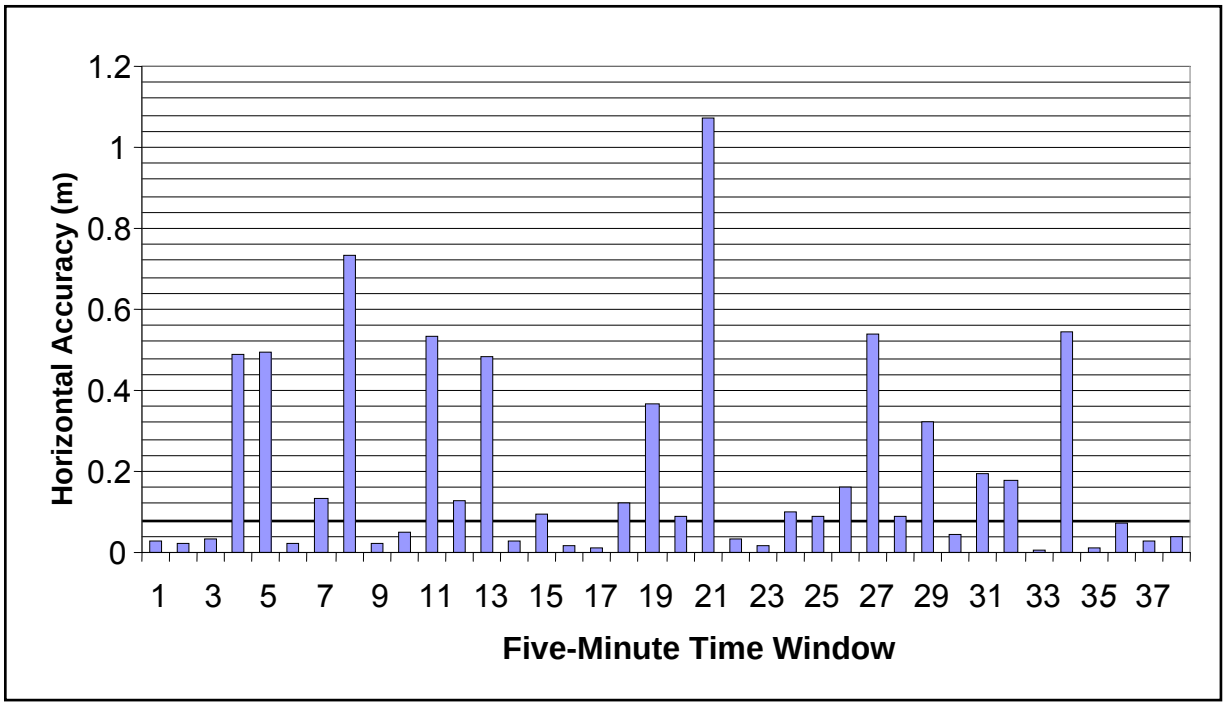

Figure 10-9: The number of fixes for five-minute time windows

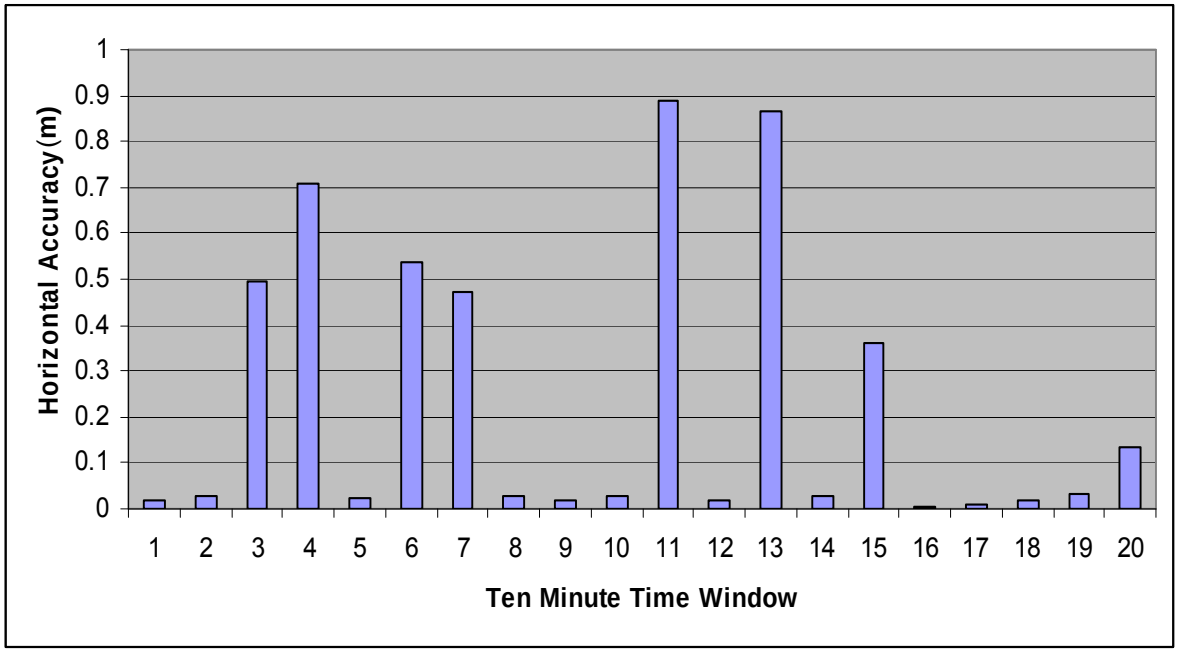

Figure 10-10: The number of fixes for ten-minute time windows

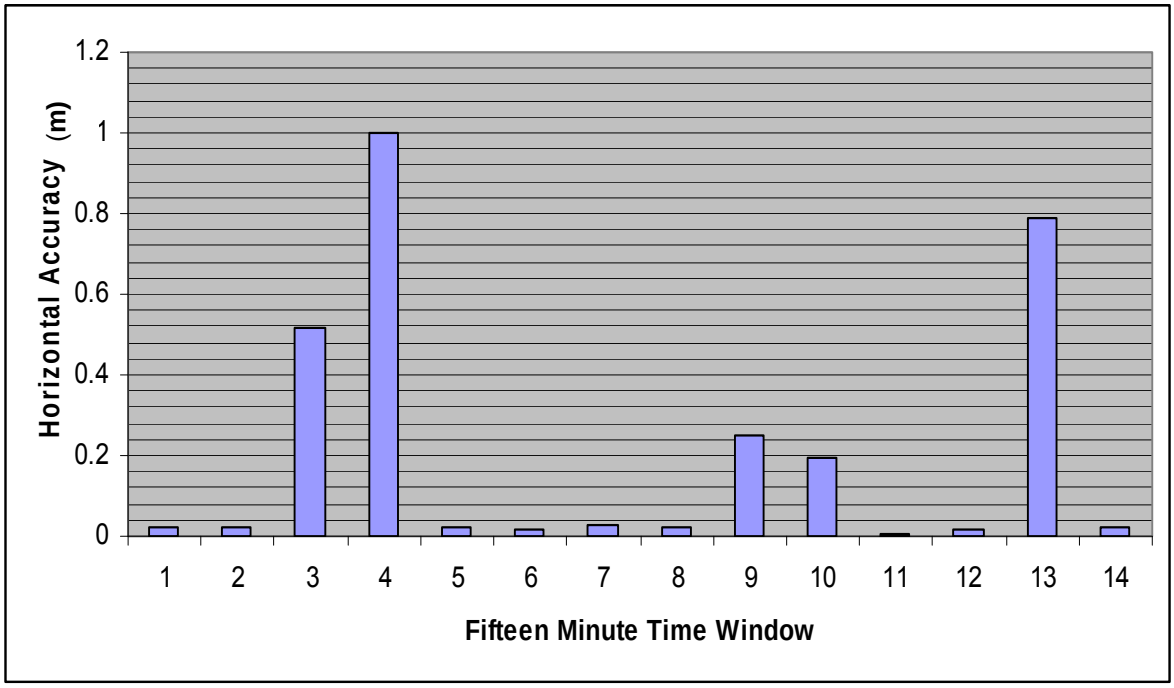

Figure 10-11: The number of fixes for fifteen-minute time windows

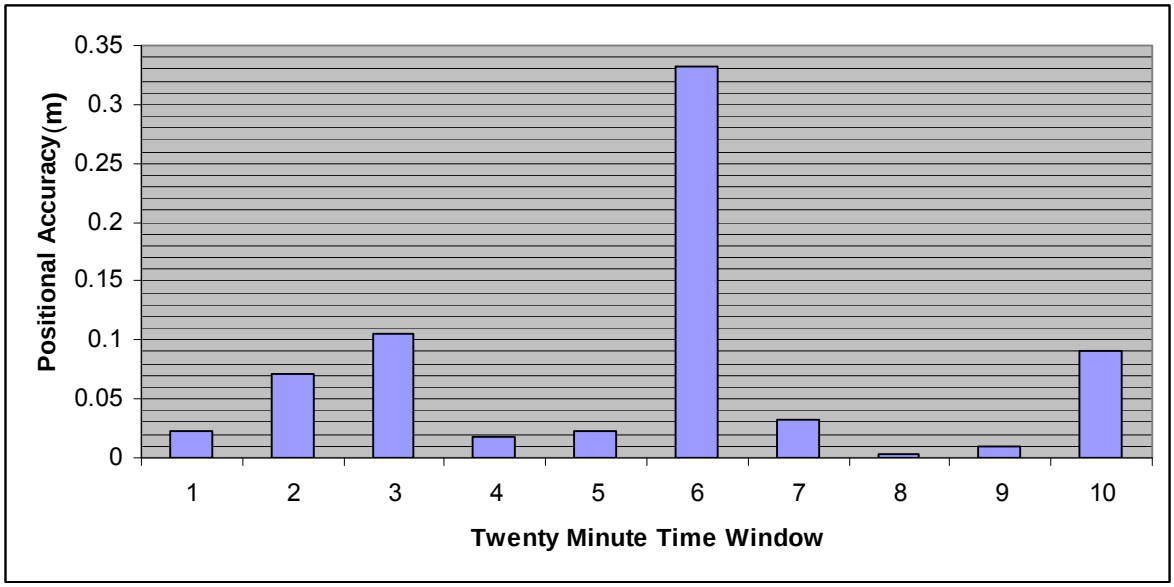

Figure 10-12: The number of fixes for twenty-minute time windows

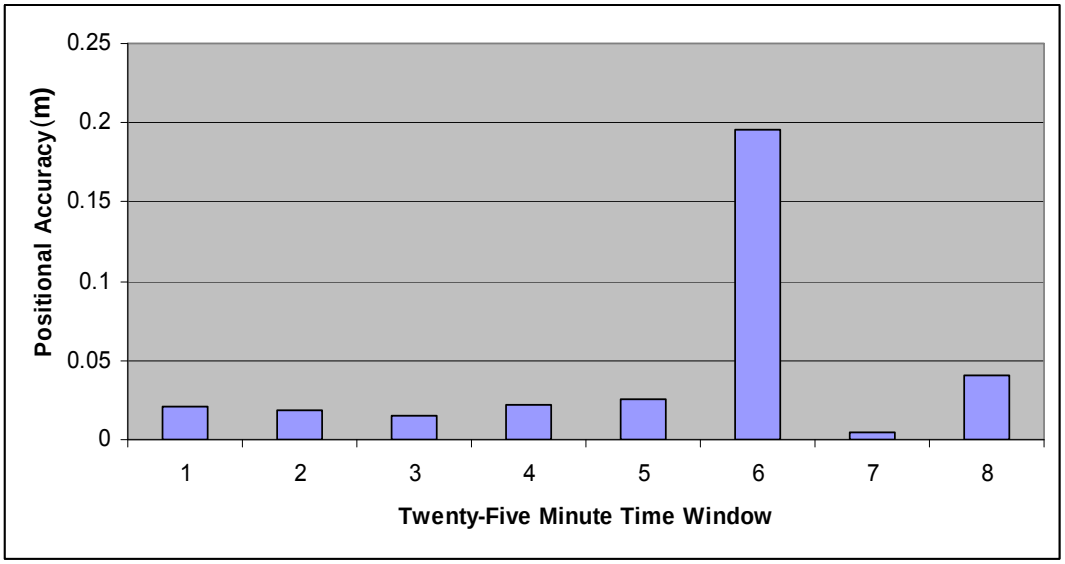

Figure 10-13: The number of fixes for twenty-five-minute time windows

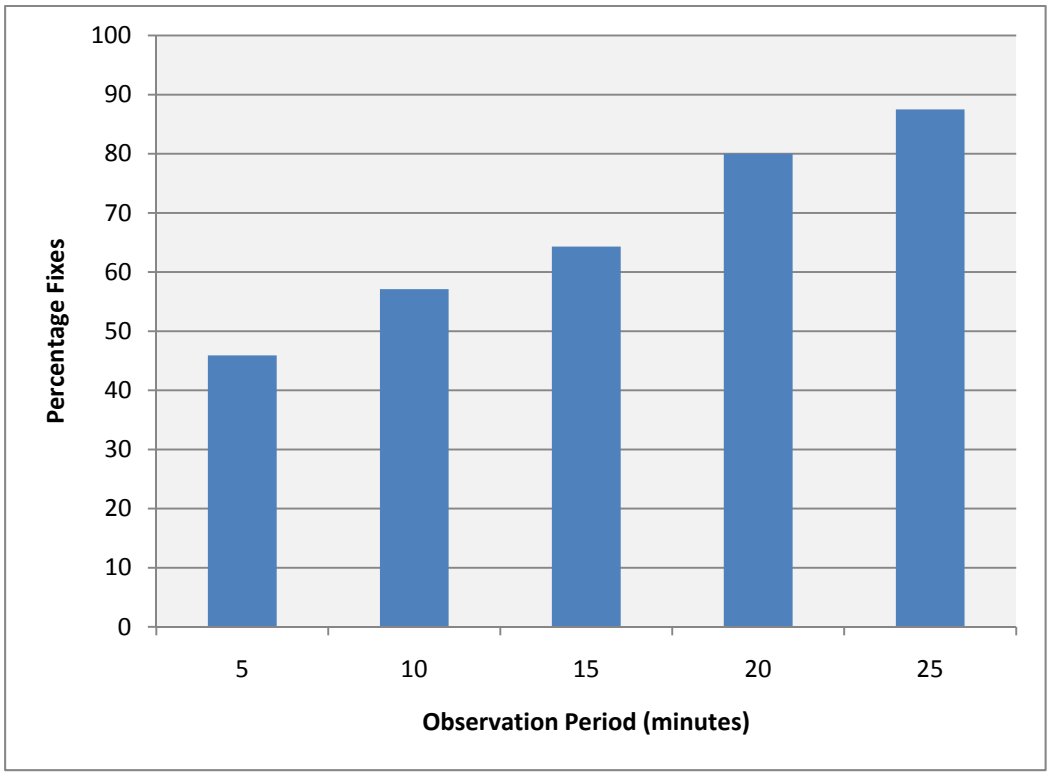

Figure 10-14: A chart showing the trend of percentage fixes with period of observation

The graph shown in Figure 10-14 shows the increasing trend of percentage fixes with the increase in the length of time window. This analysis is important for the determination of the minimum time one has to observe a point for reliable precise results. In this case it is recommended that one spends a minimum of 30 minutes at a station for a baseline of 50 km.

10.2 Code-plus-Carrier Processing

One of the main goals of this study was to be able to use the relatively low cost single frequency receivers to obtain improved accuracies over long baselines. This could be achieved using appropriate processing technique, the Code-plus-Carrier approach. The 194 km Accra (ACRA) – Kumasi (KMSI) and the 1239 km ACRA-NKLG (Libreville, Gabon) baselines have been processed with only L1 float solution. The problem with such long baselines especially in the lower latitude and also near the geomagnetic equator is mainly the severe atmospheric disorders, which is removed using this processing technique.

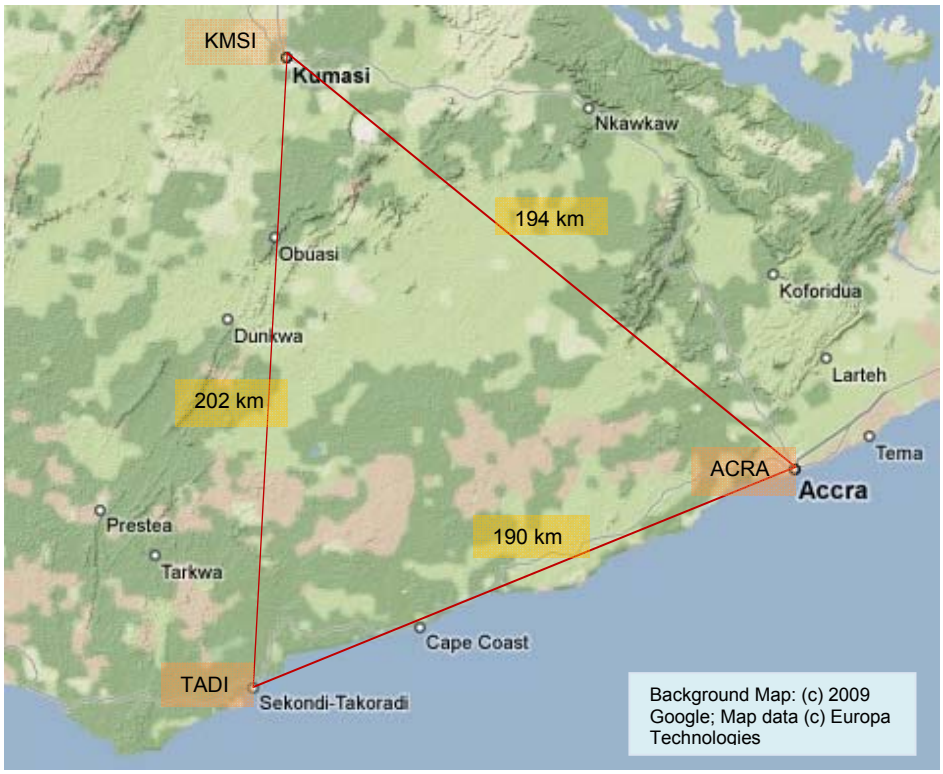

Figure 10-15: Map of the baselines forming the Golden Triangle with the 194 km ACRA-KMSI baseline

10.2.1 Combining Code and Carrier Phase

The additive combination of code and carrier phase measurements results in the elimination of the ionosphere which is a major factor of uncertainty in precise positioning. This is as a result of the dispersive nature of with the group and phase delays with opposite signs, carrier phase advancing while the pseudo-range experiences group delay. What remains is the tropospheric slant delay which is to be modelled and half the ambiguity term which is also estimated. The removal of the ionosphere makes it a great benefit for the numerous single frequency receiver users for long baselines such as between KMSI and ACRA.

Using simplified forms of equation 3-1 and 3-2, the observation equations for pseudorange and carrier phase can be written as

$$PR = \rho + \delta I + \delta T + \varepsilon_{Code} \quad 10\text{-}2$$

$$\varphi = \rho + \lambda N - \delta I + \delta T + \varepsilon_{Phase} \quad 10\text{-}3$$

Adding 10-2 and 10-3 and dividing by two

$$\frac{PR + \varphi}{2} = \rho + \frac{\lambda}{2} N + \delta T + \frac{\varepsilon_{code} + \varepsilon_{Phase}}{2} \quad 10\text{-}4$$

φ	carrier phase observation
PR	pseudorange observation between receiver and satellite
ρ	geometric range between receiver and satellite
δI	Ionospheric delay
δT	Tropospheric delay
N	integer ambiguity
ε_{code}	code noise
ε_{Phase}	phase noise

When the clock bias is as shown in Equation 10-5 is removed after double differencing as pertains to the process. The final expression therefore is as shown in Equation 10-5

$$\frac{PR + \varphi}{2} = \rho + \frac{\lambda}{2} N + \delta T + \varepsilon_{CPC} \quad 10\text{-}5$$

The magnitude of the error due to the tropospheric delay is far larger than the noise therefore the noise component can be neglected.

10.2.2 Analyzing Code-Plus-Carrier Phase for Long Baseline Processing

Single-frequency data for ACRA-KMSI was processed using the Float Ambiguity option in steps of one hour cumulative intervals and both the horizontal and positional biases were analyzed and the results is as shown in Figure 10-16. The result showed a fast convergence within the first hour. This required a further breakdown of the time window to investigate the convergence as shown in Figure 10-17.

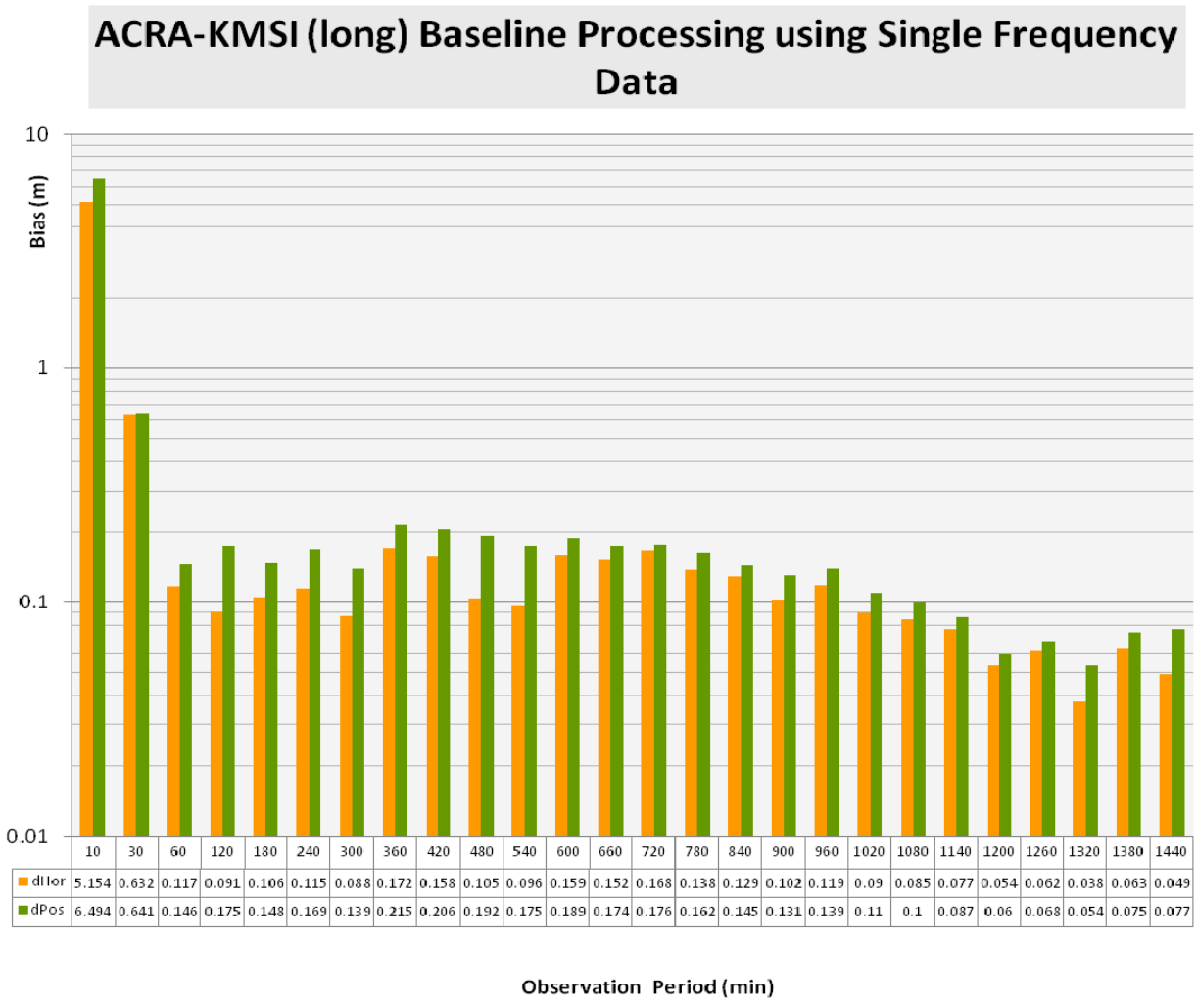

	10	30	60	120	180	240	300	360	420	480	540	600	660	720	780	840	900	960	1020	1080	1140	1200	1260	1320	1380	1440
dHor	5.154	0.632	0.117	0.091	0.106	0.115	0.088	0.172	0.158	0.105	0.096	0.159	0.152	0.168	0.138	0.129	0.102	0.119	0.09	0.085	0.077	0.054	0.062	0.038	0.063	0.049
dPos	6.494	0.641	0.146	0.175	0.148	0.169	0.139	0.215	0.206	0.192	0.175	0.189	0.174	0.176	0.162	0.145	0.131	0.139	0.11	0.1	0.087	0.06	0.068	0.054	0.075	0.077

Figure 10-16: A plot of the biases against time for the 194 km ACRA-KMSI baseline using the code-plus-carrier mode for a single frequency data

The results showed a high positional error of 6.49 m in 10 minutes, and improved rapidly to sub-meter after 30 minutes. Sub-decimetre was attained after 9 hours for the positional accuracy and after 8 hours for the horizontal accuracy. For a 24 hour observation, 5 cm was attainable with the single frequency over this baseline length of 194 km in Ghana using this technique.

To further illustrate the convergence of the solution for this long baseline, cumulative observation periods up to 150 minutes in steps of 10 minutes were analyzed. This showed that sub-decimetre accuracy could be attained within an hour for the 194 km distance using single frequency as shown in Figure 10-17.

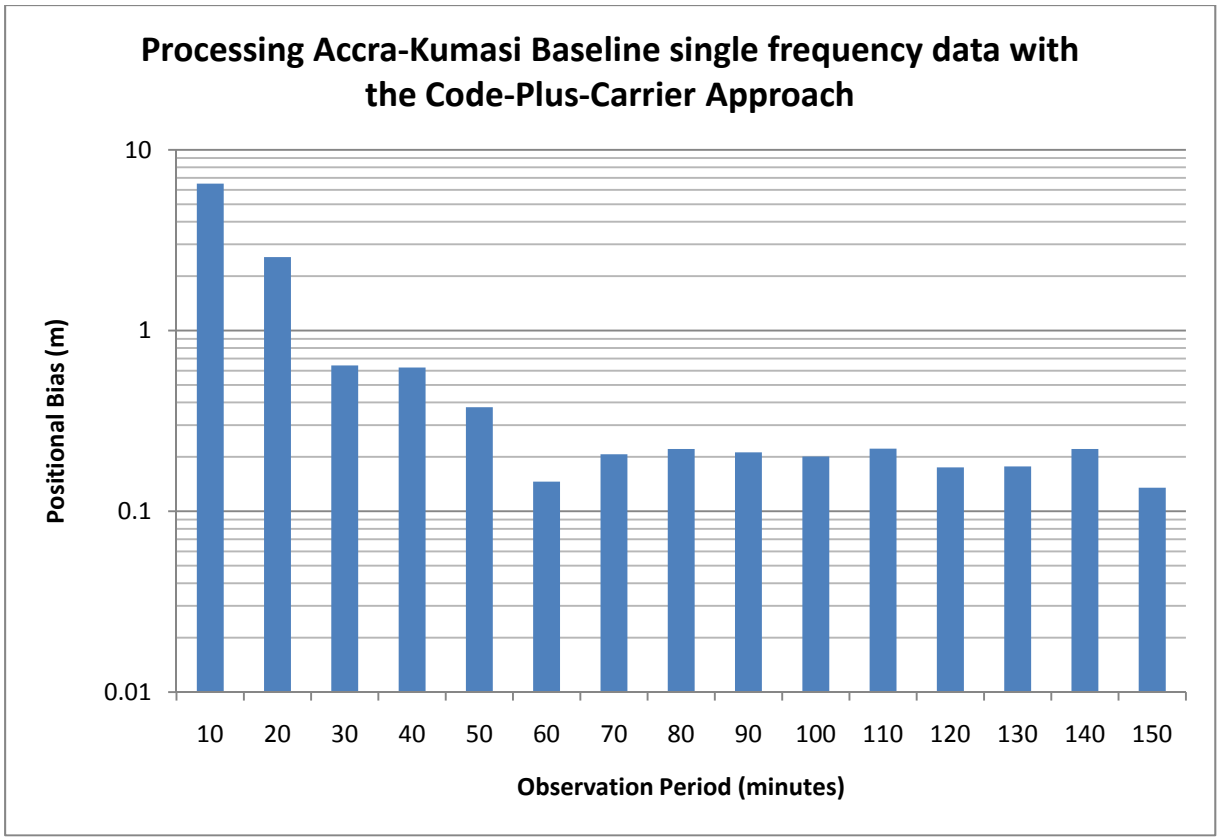

Figure 10-17: A plot of the biases against time in steps of 10 minute for the 194 km ACRA-KMSI baseline using the code-plus-carrier mode for a single frequency data

10.2.3 Analyzing Code-Plus-Carrier Phase for Very Long Baseline Processing

For very long baseline, between the Accra permanent station and the IGS station in Libreville Gabon, which spans over 1239 km, this technique has proved to be effective as sub-decimetre positional accuracy could be achieved after 18 hours of observation. For horizontal accuracy, 3 cm could be achieved as shown in Figure 10-18. This shows that the dominant error which is the distance dependent ionospheric delay, after the mitigation of the troposphere with the GTCE self-estimated ZPD, has also been reduced. The ambiguity in this case is estimated. There is however the effect of site specific errors like multipath which can affect the results.

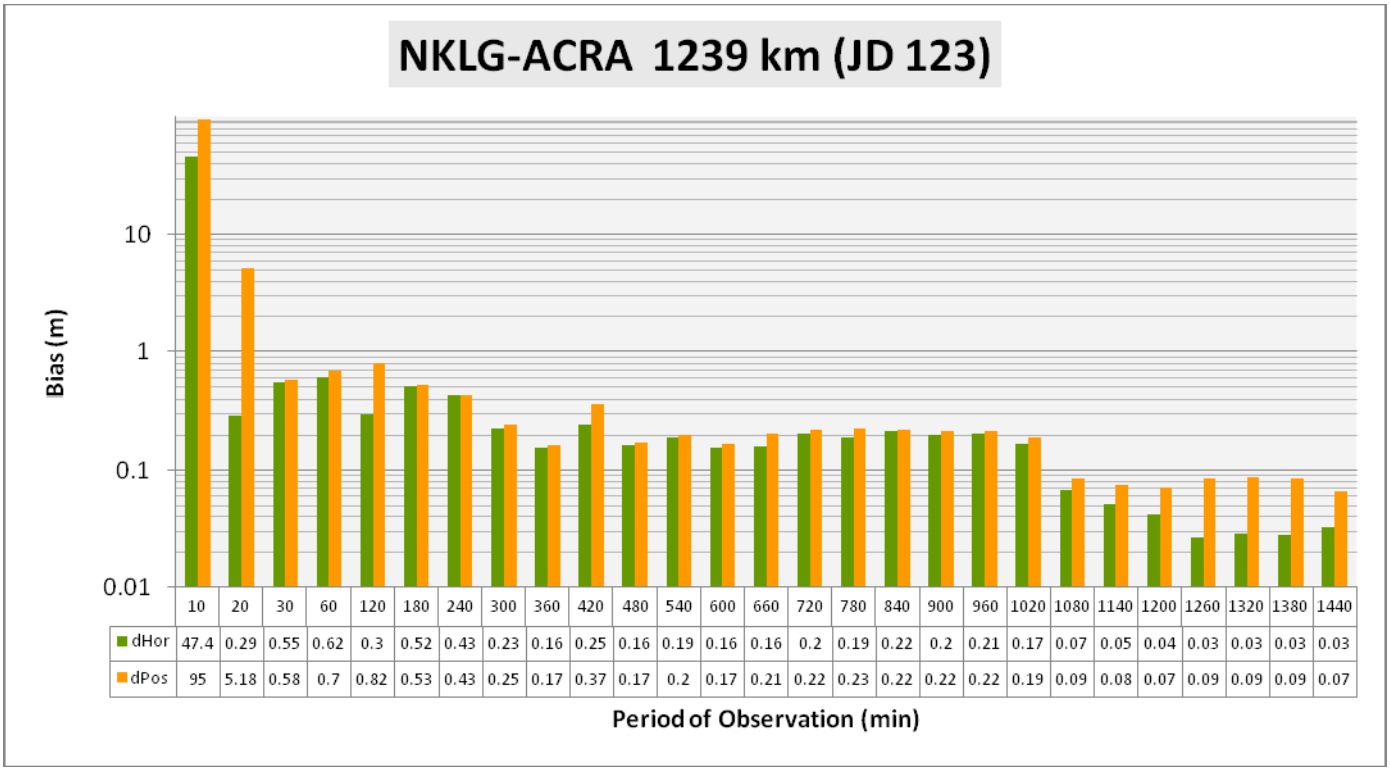

	10	20	30	60	120	180	240	300	360	420	480	540	600	660	720	780	840	900	960	1020	1080	1140	1200	1260	1320	1380	1440
dHor	47.4	0.29	0.55	0.62	0.3	0.52	0.43	0.23	0.16	0.25	0.16	0.19	0.16	0.16	0.2	0.19	0.22	0.2	0.21	0.17	0.07	0.05	0.04	0.03	0.03	0.03	0.03
dPos	95	5.18	0.58	0.7	0.82	0.53	0.43	0.25	0.17	0.37	0.17	0.2	0.17	0.21	0.22	0.23	0.22	0.22	0.22	0.19	0.09	0.08	0.07	0.09	0.09	0.09	0.07

Figure 10-18: A plot of the biases against time for a very long baseline 1239 km between ACRA and NKLG (Gabon) using the code-plus-carrier mode for a single frequency data

For shorter baselines, this method will be beneficial, especially where the ambiguities can be fixed.

11 Corridor Correction Concept

11.1 The newly developed Corridor Correction Concept

As a contribution to the solving of the logistical problems in most developing countries including Ghana, this newly introduced concept aims at using fewer base stations to achieve comparable accuracies as the area correction parameters. Whereas area correction requires three reference stations to model corrections at the rover position within the triangle enclosed, corridor correction models the error along the baseline between two reference stations with the baseline at the centre of the corridor. Off corridor corrections can be derived for up to above ten or even twenty kilometres, depending on the atmospheric condition, making it quite beneficial as the service area can be reasonably large for several applications. This concept like the area correction method models the atmospheric delay along the corridor between two base stations. The troposphere and the ionosphere delay along the corridor are modelled and the interpolated results computed for the rover for either on-corridor or out-of-corridor correction.

The real path of the atmospheric delay is non uniform and depends on the atmospheric condition during the time of observation which varies both spatially and temporally. The accuracy of the correction is dependent on factors like the length of the baseline, the time of the day, situation of the weather front. The longer the corridor, the greater the probability for the rover to encounter disturbed atmospheric conditions. Generally the ionospheric activities are high during afternoon and calm in the night. For a single base station differential corrections PDGPS, a larger error (extrapolation error) is expected as shown in Figure 11-1. This is due to the fact that the only constraint is the base station and therefore the (extrapolation) error in the atmospheric delay is usually relatively large (Figure 11-2). With the introduction of the second base station at B, there is a constrained path for the atmospheric delay modelled between A and B. With a rover positioned on the corridor at a point D, the modelled path gives the delay as R_d, which is usually different from the observed. There is a residual atmospheric delay which is the difference between the real and the modelled (interpolation error).

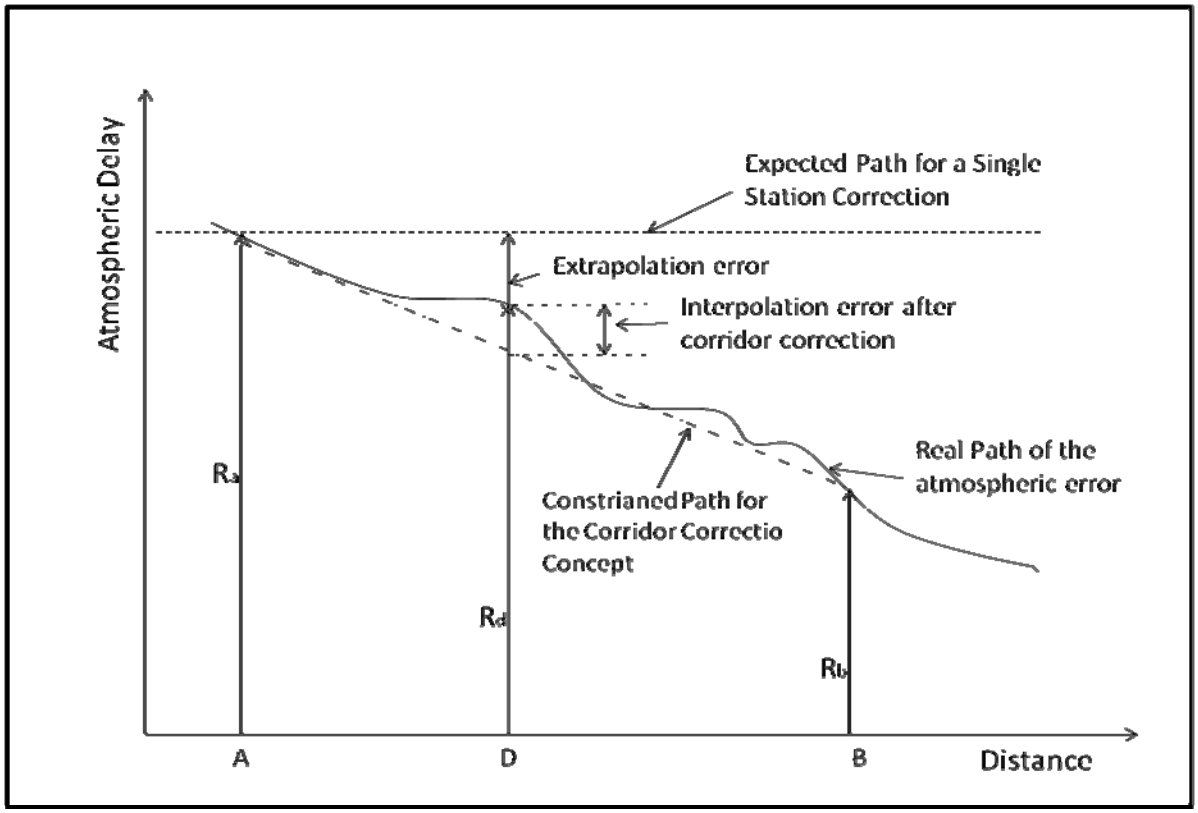

Figure 11-1: Diagram showing the impact of modelling atmospheric delay using Corridor Correction

The atmospheric delay at the rover position Rd can be computed using a simple linear interpolation as shown in the equation below

$$R_d = R_a + (R_a - R_b).\frac{AD}{AB} \qquad 11\text{-}1$$

For a rover located off corridor as shown at C in Figure 11-2 there is an increase in the atmospheric delay as the distance off-corridor increases, for both ionospheric delay and tropospheric delay see the graphs in Figure 11-3 and Figure 11-4. To compute the delay at the point C, the vector AC is projected onto AB to obtain D which is then treated as an imaginary base station as the correction for this point is interpolated from those of the two base stations. The distance CD will now be the distance off corridor and is used as an indicator as to the limit one has to observe off-corridor. The corrections for the rover at C are computed using triangle ACD, see Equation 11-2.

Corridor Correction Concept

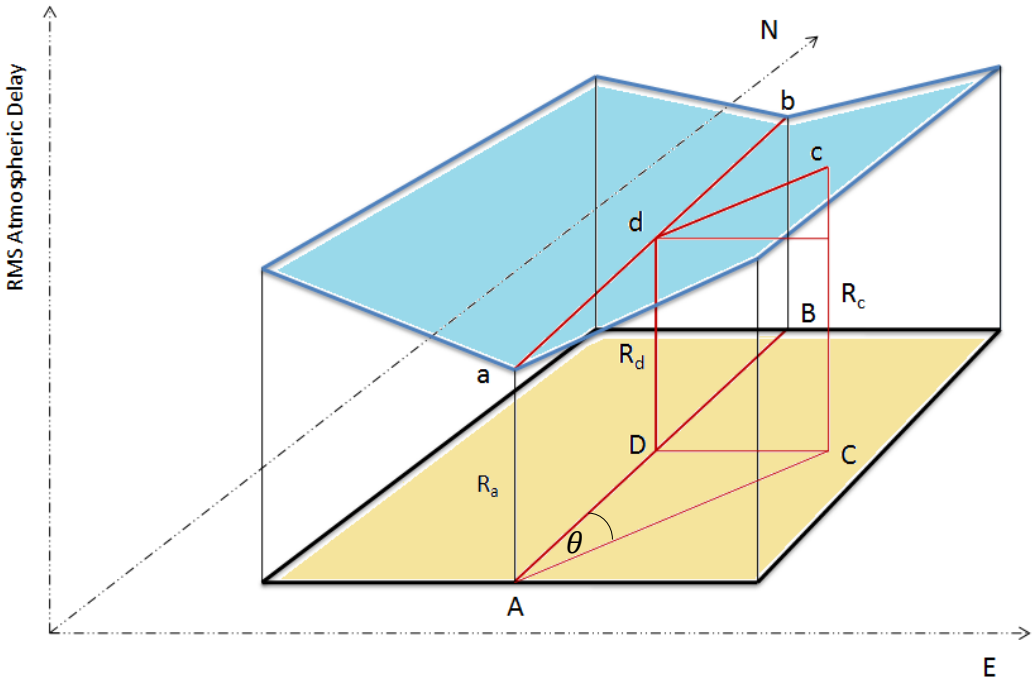

Figure 11-2: Three dimensional scheme for the derivation of Corridor Correction

Unlike the computation using the area correction parameters, the corridor corrections require the use of all the two base stations and the rover in order to compute the distance off corridor that is

$$CD = AC \sin \theta \qquad 11\text{-}2$$

The above equation is the planar approximation which is accurate for lengths applicable in this concept. For the FKP of PrePos however the distance from the nearest base station is used as the reference

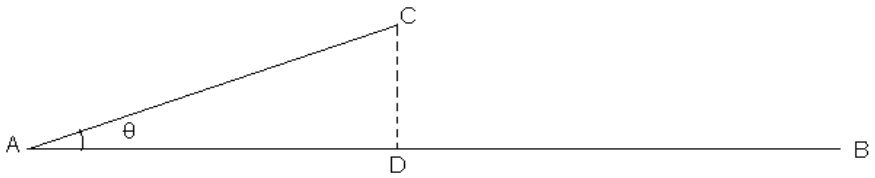

A and B are the base stations, and C, the rover. CD which represents the off-corridor distance is the perpendicular distance from the corridor through the rover position.

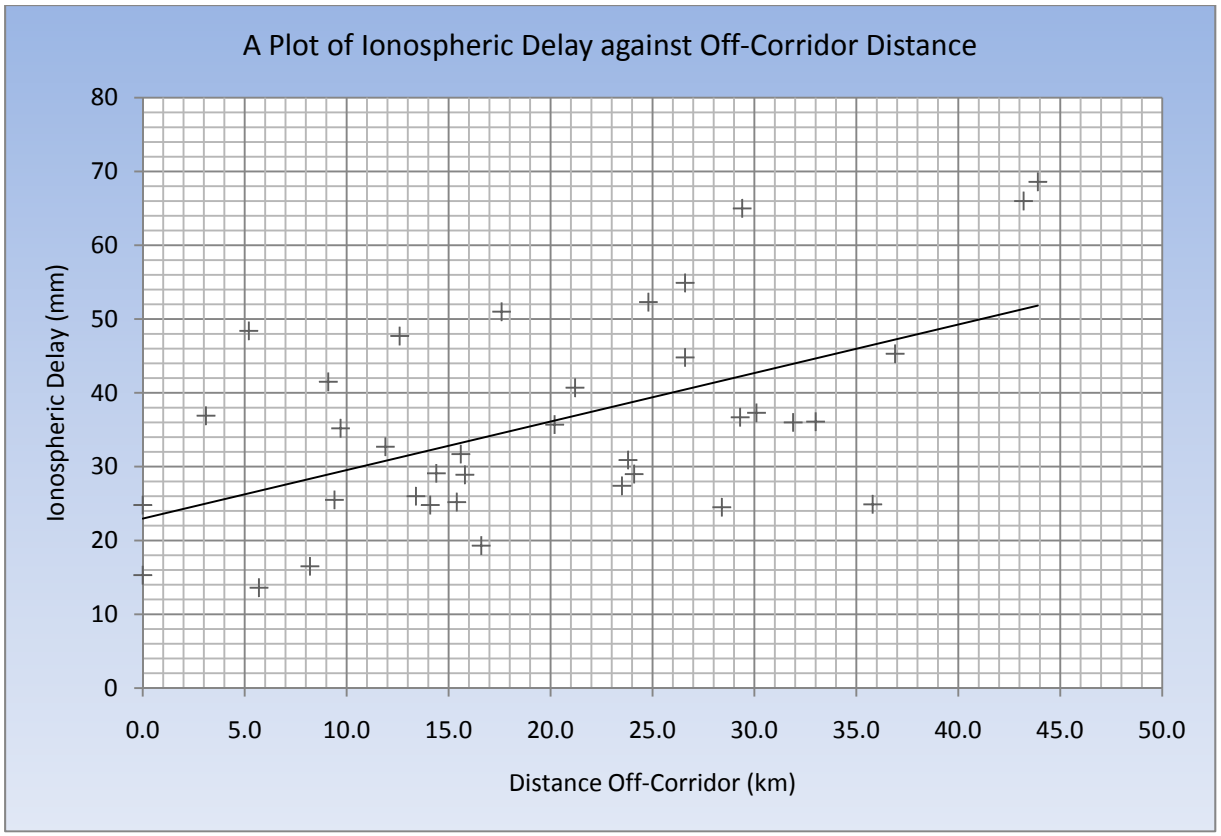

Figure 11-3: Variation of ionospheric delay with off-corridor distance for stations within the Golden Triangle between 18th and 24th May, 2007

A plot of the root-mean-square value of the ionospheric delay computed using NEREUS, against the distance off-corridor shows a positive gradient of 0.66 ppm for the study area as one moved from the corridor during the campaign period. A residual delay (RMS) of 23 mm was obtained on the corridor which is the difference between the actual delay and the modelled. This is a function of the ionospheric activities during the observation period and will be high during a high ionospheric storm.

A plot of tropospheric delay against distance off-corridor indicates an increase in the RMS of the tropospheric delay with distance as shown in the case of the Ionospheric Delay. This however has a smaller gradient of 0.13 ppm, with the residual at the corridor baseline of 19 mm.

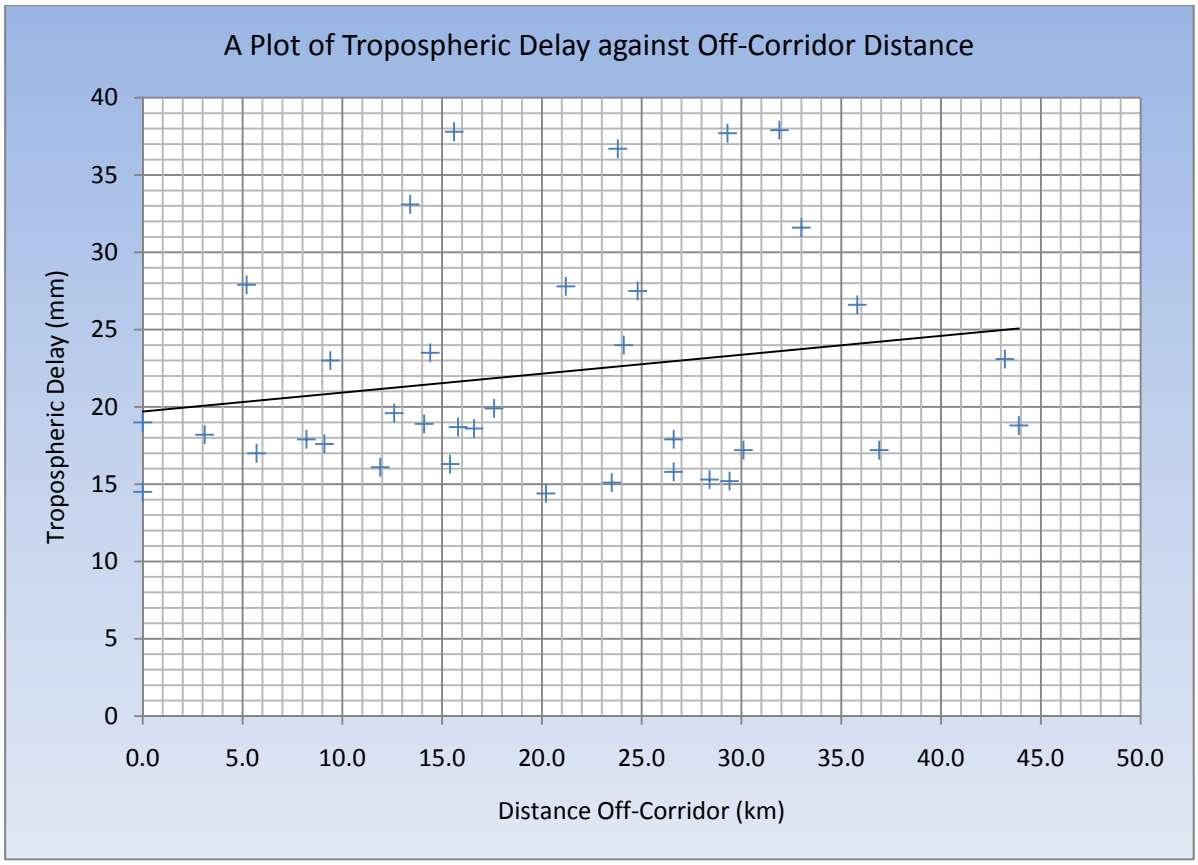

Figure 11-4: Variation of tropospheric delay with off-corridor distance within the Golden Triangle between 18th to 24th May, 2007

11.1.1 Modeling the Atmospheric Error

Both the ionosphere and troposphere were modeled in the satellite-specific mode and in addition station-specific mode for the troposphere was modeled. These have been implemented and can be processed using NEREUS.

11.1.1.1 Ionosphere Satellite-Specific Mode

For carrier phase double difference measurement observed from satellites i and j at receiver stations A and B according to (Schueler E. , 2008), the double difference expression is given as

$$\nabla\Delta\varphi_{ab}^{ij} = \left(\varphi_B^j - \varphi_A^j\right) - \left(\varphi_B^i - \varphi_A^i\right) = \frac{\nabla\Delta\rho_{AB}^{ij}}{\lambda} - \frac{\nabla\Delta ION_{AB}^{ij}}{\lambda} + \frac{\nabla\Delta TROP_{AB}^{ij}}{\lambda} - \nabla\Delta N_{AB}^{ij} \qquad 11\text{-}3$$

And the troposphere residual only contains effect of ionosphere, rest of the geometry and the troposphere

$$\nabla\Delta RES_{IONO} = 60\nabla\Delta\varphi_1 - 77\nabla\Delta\varphi_2 = a_2\nabla\Delta\varphi_1 - a_1\nabla\Delta\varphi_2 \qquad 11\text{-}4$$

Combining Eqn. 11-3 and Eqn. 11-4 the expression below is obtained

$$\nabla\Delta\varphi_{a_1a_2} = a_2\left[\frac{\nabla\Delta\rho}{\lambda_1} + \frac{\nabla\Delta\mathrm{Trop}}{\lambda_1} - \frac{\nabla\Delta\mathrm{ION}_{L_1}}{\lambda_1} - \nabla\Delta N_1\right] - a_1\left[\frac{\nabla\Delta\rho}{\lambda_2} + \frac{\nabla\Delta\mathrm{Trop}}{\lambda_2} - \frac{\nabla\Delta\mathrm{ION}_{L_1}}{\lambda_2}\frac{f_1^2}{f_2^2} - \nabla\Delta N_2\right] \quad 11\text{-}5$$

For double difference ionospheric delay on the L1 frequency

$$\nabla\Delta\mathrm{ION}_{L1} = \frac{a_2\nabla\Delta\varphi_1 - a_1\nabla\Delta\varphi_2 + a_2\nabla\Delta N_1 - a_1\nabla\Delta N_2}{\left(-\frac{a_2}{\lambda_1} + \frac{a_1}{\lambda_2}\frac{f_1^2}{f_2^2}\right)} \quad 11\text{-}6$$

Units in metres

The variance of the double difference ionospheric delay, which follows the law of error propagation, is given as

$$\sigma^2_{\nabla\Delta\mathrm{ION}_{L_1}} = \left(\frac{\partial\nabla\Delta\mathrm{ION}_{L_1}}{\partial\varphi_1}\right)^2\sigma^2_{\Phi_1} + \left(\frac{\partial\nabla\Delta\mathrm{ION}_{L_1}}{\partial\varphi_2}\right)^2\sigma^2_{\Phi_2} \quad 11\text{-}7$$

With

$\sigma_{\Phi_1} = \sigma_{\varphi_1}\lambda_1$ and $\sigma_{\Phi_2} = \sigma_{\varphi_2}\lambda_2$ and $\sigma_{\Phi_1\Phi_2} = 0$

$$\sigma^2_{\nabla\Delta\mathrm{ION}_{L_1}} = \frac{\sigma^2_{\Phi_1} + \sigma^2_{\Phi_2}}{\left(1 - \frac{f_1^2}{f_2^2}\right)^2} \quad 11\text{-}8$$

11.1.1.2 Troposphere (Satellite-Specific mode)

The double difference for tropospheric residual for GPS L1/L2 is as shown below

$\nabla\Delta RES_{TROPO} = 77\nabla\Delta\varphi_1 - 60\nabla\Delta\varphi_2 = a_1\nabla\Delta\varphi_1 - a_2\nabla\Delta\varphi_2$

Similar to the derivation of ionospheric delay in the satellite specific mode, that of the troposphere also employs the equation 11-5

$$\nabla\Delta\varphi_{a_1a_2} = \nabla\Delta\mathrm{Trop}\left[\frac{a_1}{\lambda_1} - \frac{a_2}{\lambda_2}\right] + \frac{a_1\nabla\Delta\rho}{\lambda_1} - \frac{a_2\nabla\Delta\rho}{\lambda_2} - a_1\nabla\Delta N_1 + a_2\nabla\Delta N_2 \quad 11\text{-}9$$

$$\nabla\Delta\mathrm{Trop(m)} = \frac{a_1\nabla\Delta\varphi_1 - a_2\nabla\Delta\varphi_2 - \frac{a_1\,\nabla\Delta\rho}{\lambda_1} + \frac{a_2\,\nabla\Delta\rho}{\lambda_2} + a_1\nabla\Delta N_1 + a_2\nabla\Delta N_2}{\left[\frac{a_1}{\lambda_1} - \frac{a_2}{\lambda_2}\right]}$$

$$= \frac{\nabla\Delta\varphi_1 - \frac{a_2}{a_1}\nabla\Delta\varphi_2 - \frac{\nabla\Delta\rho}{\lambda_1} + \frac{\frac{a_2}{a_1}\,\nabla\Delta\rho}{\lambda_2} + \nabla\Delta N_1 + \frac{a_2}{a_1}\nabla\Delta N_2}{\left[\frac{1}{\lambda_1} - \frac{a_2/a_1}{\lambda_2}\right]} \qquad 11\text{-}10$$

For the variance for $\nabla\Delta\mathrm{Trop}$

$$\sigma^2_{\nabla\Delta\mathrm{Trop}} = \left[\frac{\partial\nabla\Delta\mathrm{Trop}}{\partial\varphi_1}\right]^2 \sigma^2_{\varphi_1} + \left[\frac{\partial\nabla\Delta\mathrm{Trop}}{\partial\varphi_1}\right]^2 \sigma^2_{\varphi_2} \text{ with } \sigma_{\varphi_i} \text{ in (cyc)} \qquad 11\text{-}11$$

With

$\sigma_{\Phi_1} = \sigma_{\varphi_1}\lambda_1$, $\sigma_{\Phi_2} = \sigma_{\varphi_2}\lambda_2$ and $\sigma_{\Phi_1\Phi_2} = 0$

$$\sigma^2_{\nabla\Delta\mathrm{Trop}} = \frac{\sigma^2_{\varphi_1}}{\left(1 - \frac{f_2^2}{f_1^2}\right)^2} + \frac{\sigma^2_{\varphi_2}}{\left(1 - \frac{f_1^2}{f_2^2}\right)^2} \qquad 11\text{-}12$$

11.1.1.3 Troposphere (Station-Specific Mode)

This is carried out using double differencing for the computation of absolute tropospheric delay. Depending on the baseline length, 99% of the true value can be achieved after one hour as in (Schueler E. , 2008). There is however a limitation to this approach as it requires longer observation period or larger network as well as stable weather. NEREUS averages the tropospheric delay of all the stations and computes the standard deviation out of which the mean tropospheric correction parameter can be derived.
The double differential tropospheric residual for stations A and B from the satellites I and is given by

$$\nabla\Delta\mathrm{Trop}^{ij}_{AB} = (m^j_B ZPD^j_B - m^j_A ZPD^j_A) - (m^i_B ZPD^i_B - m^i_A ZPD^i_A) \qquad 11\text{-}13$$

The true value for the ZPD can be obtained from the modeled value, for example from Tropgrid, Numerical Weather Model, GTCE self estimated ZPD, etc. and the residual.

$$\left.\begin{aligned} ZPD_A^j &= ZPD_A + \delta ZPD_A^j \\ ZPD_A^i &= ZPD_A + \delta ZPD_A^i \\ ZPD_B^j &= ZPD_B + \delta ZPD_B^j \\ ZPD_B^j &= ZPD_B + \delta ZPD_B^j \end{aligned}\right\} \qquad 11\text{-}14$$

residual ≙ offsets/model biases

Substituting Eqn. 11-14 into Eqn.11-13

$$\nabla\Delta Trop_{AB}^{ij} = \left(m_B^j \cdot ZPD_B - m_A^j \cdot ZPD_A\right) - \left(m_B^i \cdot ZPD_B - m_A^i \cdot ZPD_A\right) + \left(m_B^j \cdot \delta ZPD_B^j - m_A^j \cdot \delta ZPD_A^j\right) - \left(m_B^i \cdot \delta ZPD_B^i - m_A^i \cdot \delta ZPD_A^i\right). \qquad 11\text{-}15$$

The first two terms on the right–hand-side of equation is the modeled troposphere and the last two terms the residuals.

Hence

$$\nabla\Delta Trop_{ABmodel}^{ij} = (m_B^j \cdot ZPD_B - m_A^j \cdot ZPD_A) - (m_B^i \cdot ZPD_B - m_A^i \cdot ZPD_A) \qquad 11\text{-}16$$

On the assumption that the residuals at a station from different satellites are approximately equal for all stations

That is

$$\delta ZPD_B^j \cong \delta ZPD_B^i$$

Subtracting Eqn. 11-16from 11-15

$$\nabla\Delta Trop_{AB}^{ij} - \nabla\Delta Trop_{ABmodel}^{ij} = \left(m_B^j - m_B^i\right)\delta ZPD_B - \left(m_A^j - m_A^i\right)\delta ZPD_A \qquad 11\text{-}17$$

The correction parameters $(\delta ZPD_A\ \delta ZPD_B\ \delta ZPD_C)$ are obtained using least square adjustment.

11.1.1.4 Deriving Corridor Correction using NEREUS and SEMIKA

GNSS Network Analyzer for SEMIKA Users, NEREUS, which is an add-on to SEMIKA which has been introduced in section 7-1 and further explained in sections 11.1.1.1-3 is used to determine corridor corrections for both the ionospheric and tropospheric propagation delay. Results for the baselines and satellite combinations from the start to the end of epoch for a particular combination of observation,

including the bias, which is the difference between the measured delays and those, computed corridor corrections, standard deviation of the residuals, root-mean-square of the differences, the maximum and the minimum differences are computed. The averages for these values are as well computed as shown in Appendix 4. The computed delays are stored and used by SEMIKA for the atmospheric correction when 'ACTIVE NET' mode is selected as the delay model. Corridor correction has been analyzed using SEMIKA in Chapter 10 alongside other existing modes of atmospheric correction for Ghana and Germany.

In this chapter analysis is made on the newly introduced Corridor Correction using data from both Ghana and Germany, to determine among others its effectiveness as compared with the existing correction methods. The fixing of integer ambiguity which is dependent on factors including observation period, distance between base and rover and atmospheric conditions has been analyzed in the Golden Triangle area of Ghana. To solve the problem of ionosphere for single-frequency receiver users in Ghana, the code-plus-carrier method has been analyzed over long baselines in the Ghanaian environment.

11.2 The Corridor Correction

Corridor correction has been used to generate atmospheric corrections for reference stations located in Thueringia, in the central part of Germany as well as in the Golden Triangle of Ghana. These locations are respectively in the middle and low latitude regions with different atmospheric conditions. While the troposphere is calm in the Middle latitudes, it is quite turbulent in the low latitude regions especially the equatorial region where Ghana is located. Similarly the ionosphere is comparatively stable in Thueringia, located in the middle latitudes while Ghana, which is very close to the geomagnetic equator, suffers from disturbing ionospheric scintillations as well as fluctuations in the ionospheric delay which is more experienced as compared with the situation in Germany. This study demonstrates the effectiveness of CC in the two regions; compares it with other correction methods and its effect under various processing techniques. For this newly developed concept to be accepted for various applications there is the need to compare it with the time tested methods like the Area Correction Parameters and the Standard Correction to let the user know what to expect when using this concept.

11.2.1 Analyzing the effectiveness of Corridor Correction Concept

SEMIKA is used to process data observed from two baselines with both the Standard Correction (SC) technique which employs Tropgrid and Klobuchar for tropospheric and ionospheric corrections respectively, and also with Corridor Correction (CC) modelled using NEREUS. These baselines were analyzed, with a common rover location at Gotha. The graphs in Figure 11-7 and Figure 11-8 show the results of

processing with CC and SC for both the WORB-SONN long baseline and MUEN-ILME short baseline. Refer to Figure 10-1 and Figure 10-2.

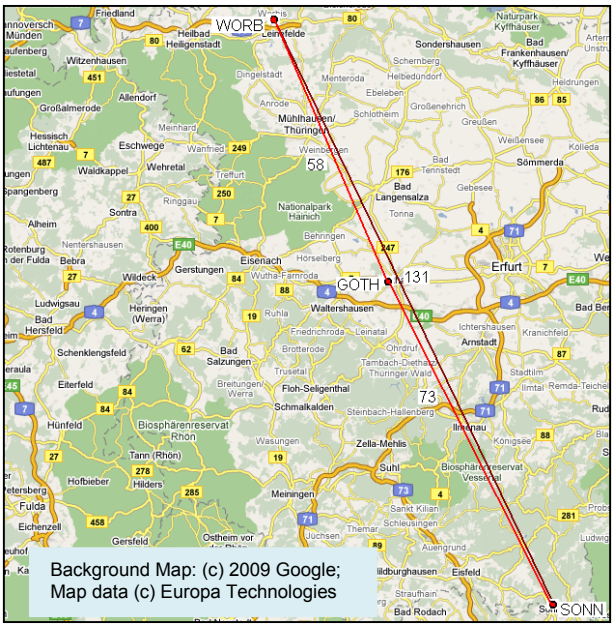

Figure 11-5: The GOTH-WORB-SONN (GWS) arrangement for on-crridor correction for long baseline

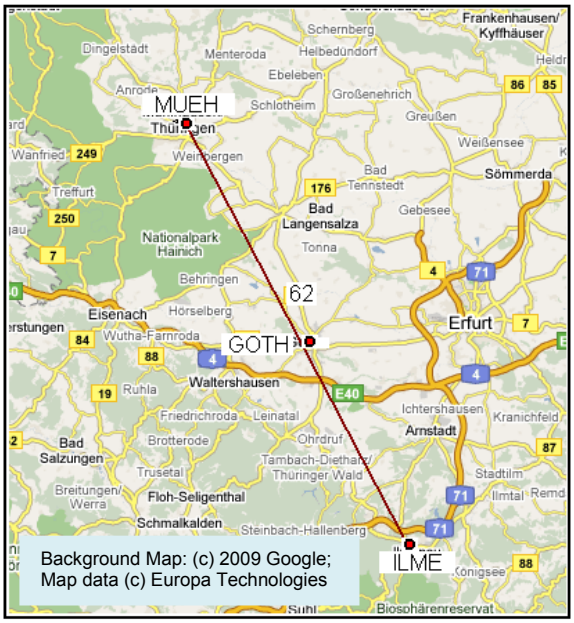

Figure 11-6: The GOTH-MUEH-ILME (GMI) arrangement for on-corridor correction for short baseline

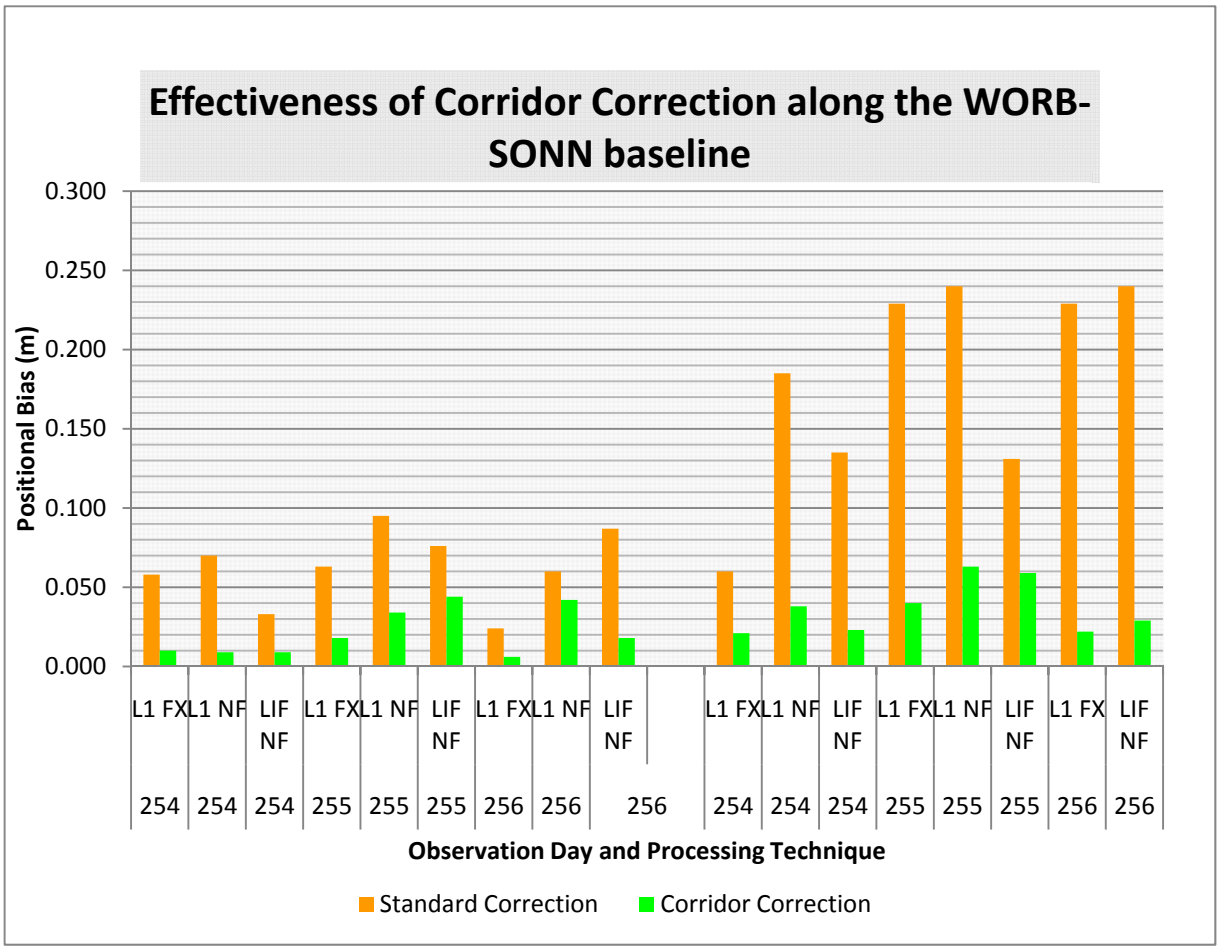

Figure 11-7: A plot showing the impact of Corridor Correction in comparison to Standard Correction at GOTH on the WORB-SONN (long) corridor at two different times of the day

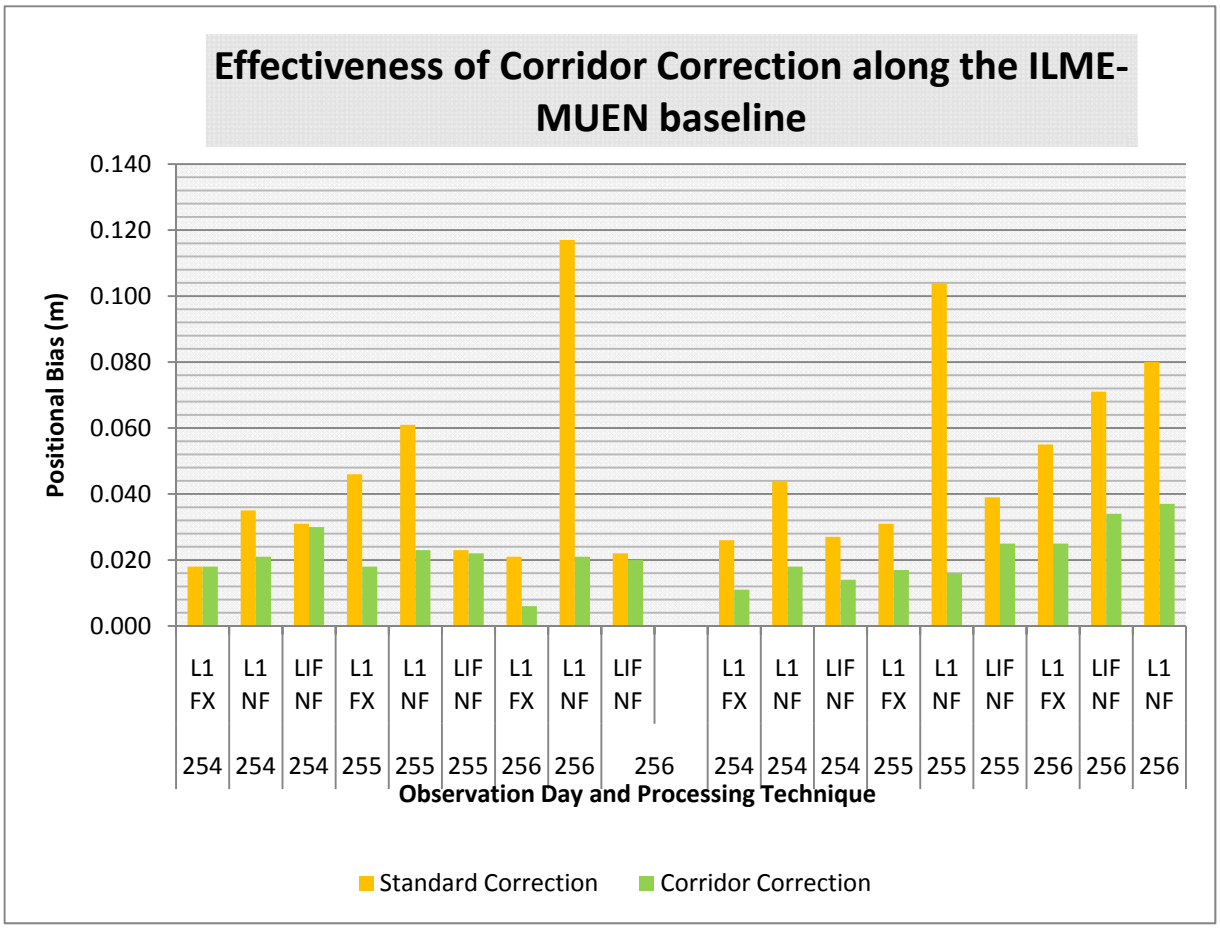

Figure 11-8: A plot showing the impact of Corridor Correction in comparison to Standard Correction at GOTH on the ILME-MUEN (long) corridor at two different times of the day

The Figure 11-7 and Figure 11-8 which demonstrate the effect of Corridor Correction on data observed on three different days, Julian Day (JD) 254, 255 and 256, with different processing approaches, L1 fixed (L1 FX), L1 float (L1 NF) and Ionosphere-free linear combination (LIF NF), clearly show the improvement of the positional biases as compared with the Standard Correction. The first half of each set of data in the figures represents the first 3600 seconds of the day, while the second set represents the period between 12000 and 15600 seconds of the day. Both have equal duration of time, which is one hour.

11.2.2 Effect of Length of Baseline on Corridor Correction

A medium baseline between Ilmenau (ILME) and Muenlhausen, 62 km long and a longer baseline between Worbis (WORB) and Sonnenberg (SONN), which is 131 km, as shown in Figure 11-7 and Figure 11-6, run approximately through Gotha (GOTH), the selected rover station. These were appropriate for an on-line Corridor Correction.

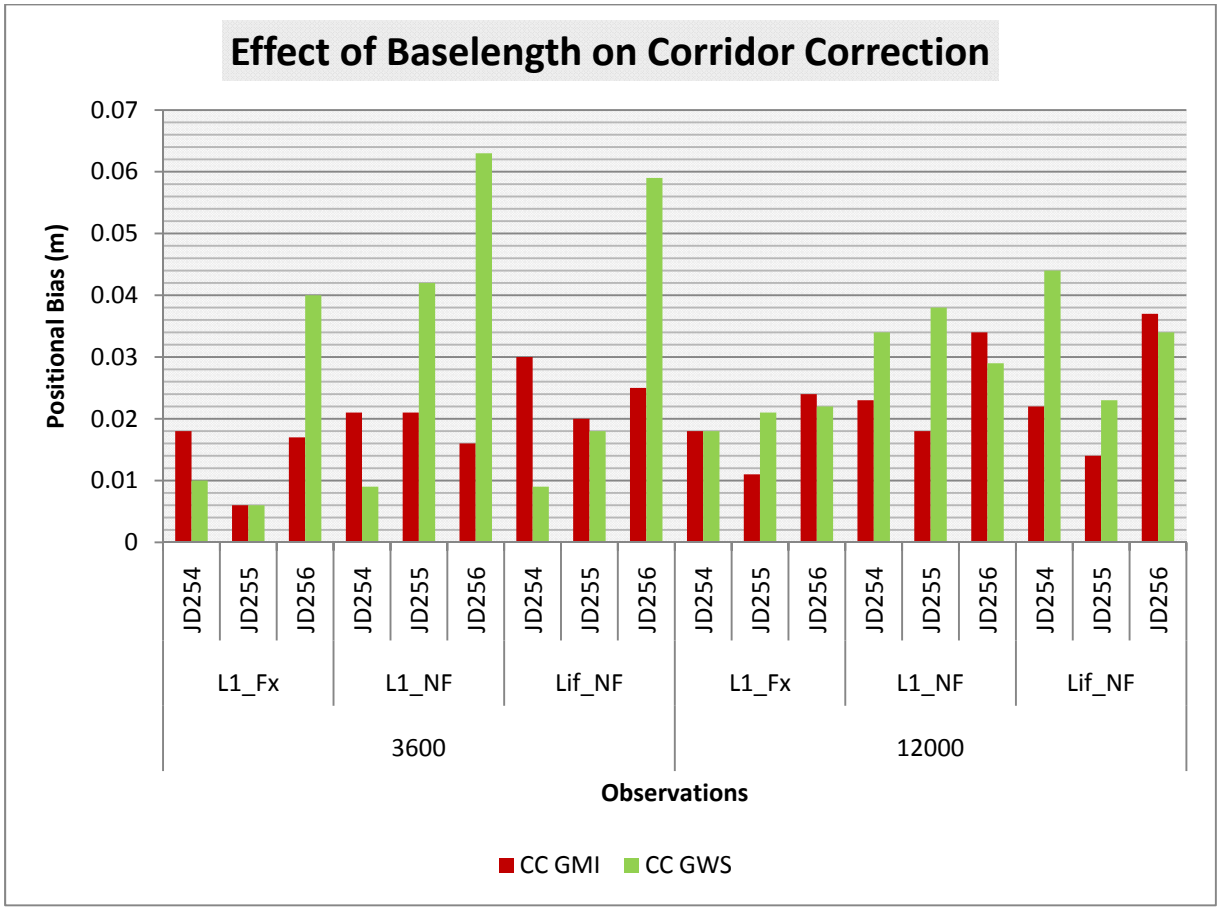

Figure 11-9: A plot of the positional bias at GOTH with the application of Corridor Correction using the MUEH-ILME (CC GMI) short baseline and WORB-SONN (CC GWS) long baseline

The results generally demonstrate that under both long and medium baselines CC effectively improves the accuracy better than the standard correction SC. There were a few marginal cases in the application on the short baseline which is explained in the subsequent sections.

11.2.3 Analysis of Corridor Corrections for Different Satellite Geometry

Analysis has been made on the effect at two different times of observation within a day. With the first time window ending at 3600 seconds of the day for a one hour of data, the second one hour window started at 12000 seconds, a little over two hours

after the first window. Generally the difference of 2 hours was not too long to affect the atmospheric conditions especially the ionosphere, but greatly affects the satellite geometry. Other time dependent factor that can influence the observation is multipath, but this is most likely to have been mitigated at all SAPOS stations as much as possible, though there are occasional compromises resulting from a trade-off between available infrastructure and visibility.

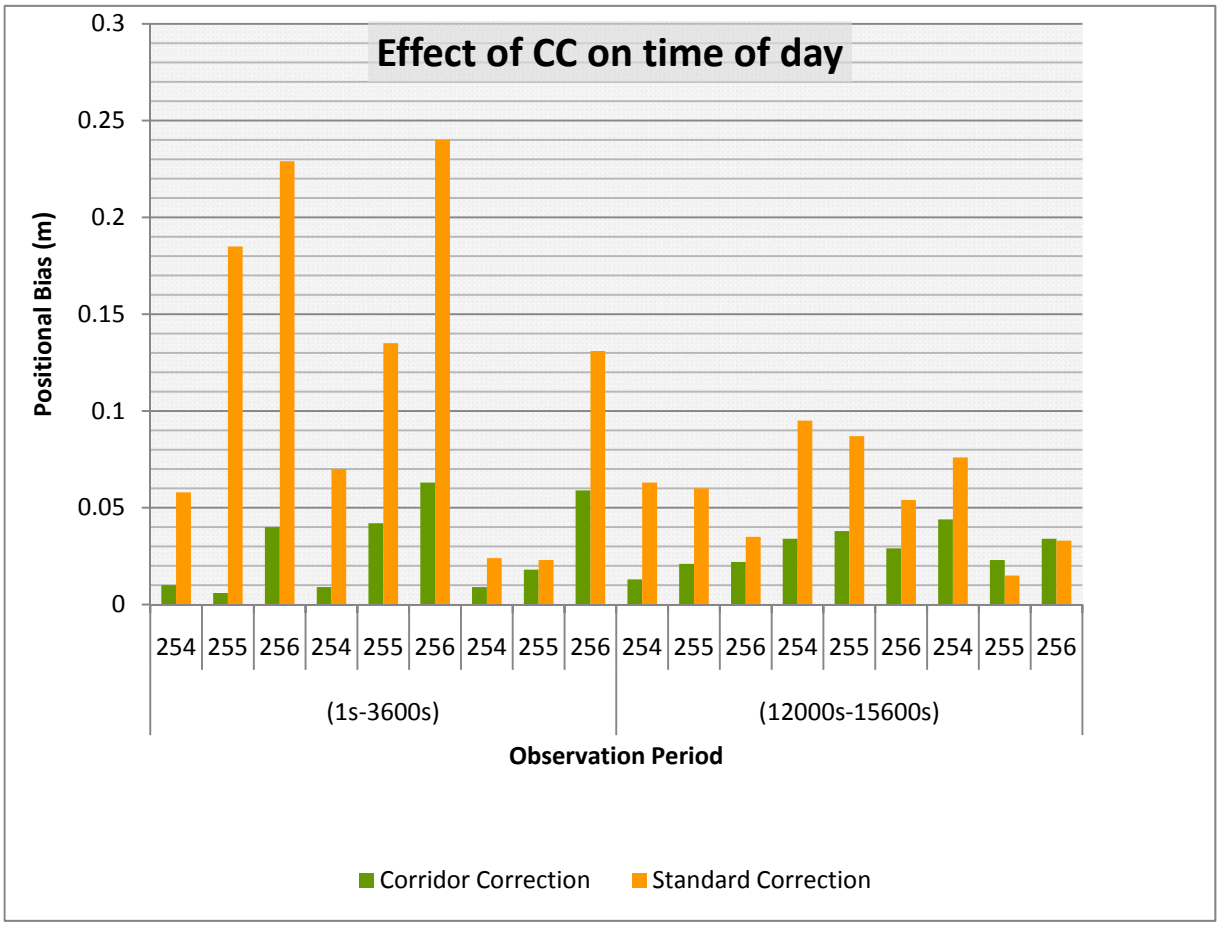

Figure 11-10: A plot of periodic Positional Bias for two one-hour observations beginning at 1-3600 s and 12000-15600 s for three days (Julian days 254, 255, 256) using various processing methods with Standard Correction and Corridor correction

The results shown in Figure 11-10 shows a significant change in the positional biases for the two different time windows which can be attributed to the satellite geometry, The first set of data showing poor positional accuracy implying poor geometry as compared with the second set, which started two hours later. In both cases corridor correction showed better accuracies as compared with the standard correction. The relatively small impact of CC on the second set of data can be alluded to the fact that the cause of dilution of the precision may not be strongly due to the ionosphere and troposphere, implying that the DOP could be due to the clustering of satellites farther away from the horizon.

On the assumption that there is no turbulent atmospheric effect, another possible source of error could be the influence of multipath which cannot be ruled out despite the fact that the SAPOS stations are established with the maximum effort to eliminate multipath.

11.2.4 Effect of the Change in Atmospheric Conditions

One hour time windows at the same time of day for three different days were analyzed. These have almost the same satellite geometry despite the 4 minutes difference between a solar day and the sidereal day used by GPS. There is a greater likelihood of having different atmospheric conditions especially the troposphere which changes more rapidly as compared with the ionosphere. Multipath caused by permanent structures is likely to cancel out due to the repetition.

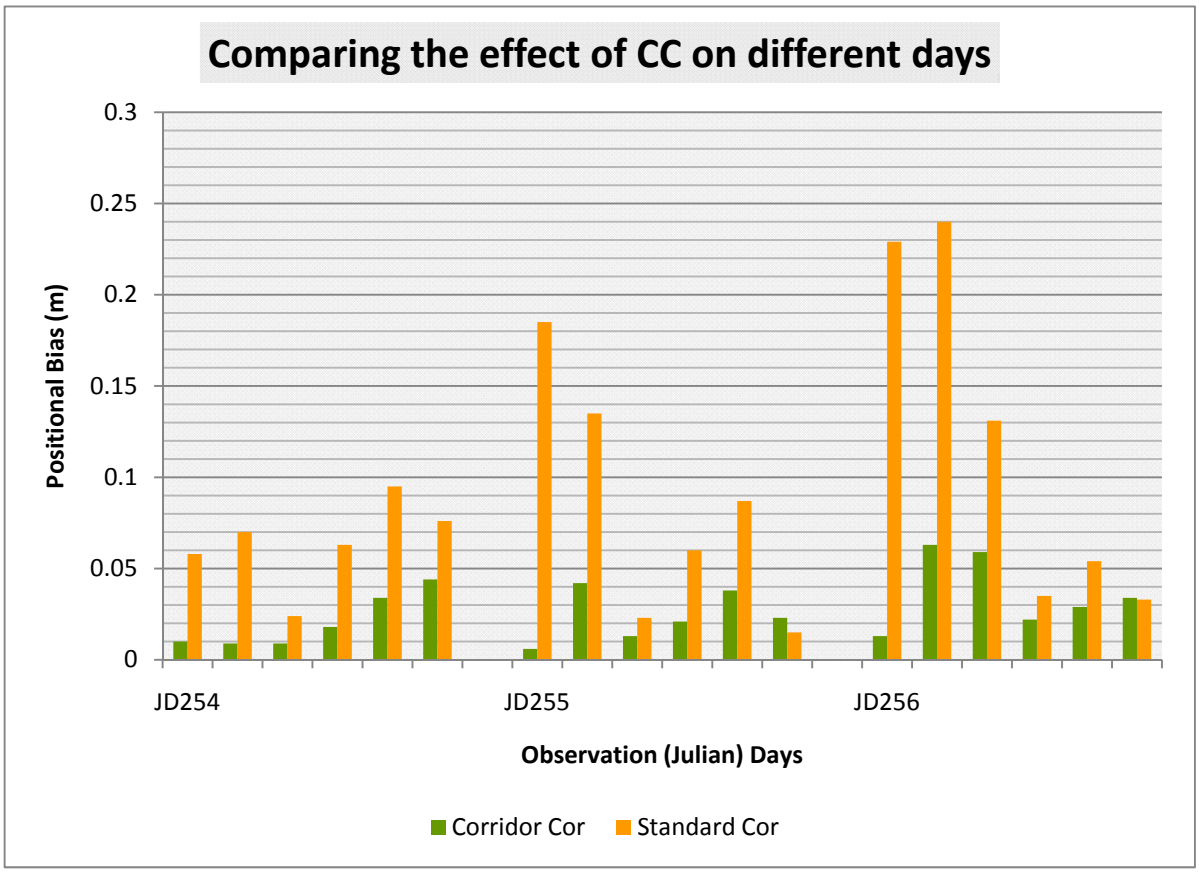

Figure 11-11: Plot showing the variation of Positional Bias for the same time of three consecutive days for Standard Correction and Corridor Correction

The graphs in Figure 11-11 show a general increase in positional bias form the first day JD254 to the third day JD256. There is however improvements in the biases in each day with the use of corridor corrections. There are a few instances where there is an increase in error with the application of corridor correction. This is attributed to the processing technique.

11.2.5 The Effect of CC on various Processing Techniques

Three different processing techniques were used for the processing, the float solution on L1, the fixed solution on L1 and the Ionosphere-Free Linear Combination. The effect of CC on both the float and fixed solutions on L1 is significant but shows a relatively small improvement on the ionosphere-free linear combination. This can be attributed to the fact that the ionosphere is practically removed using the ionosphere-free linear combination technique and CC has to remove only the troposphere.

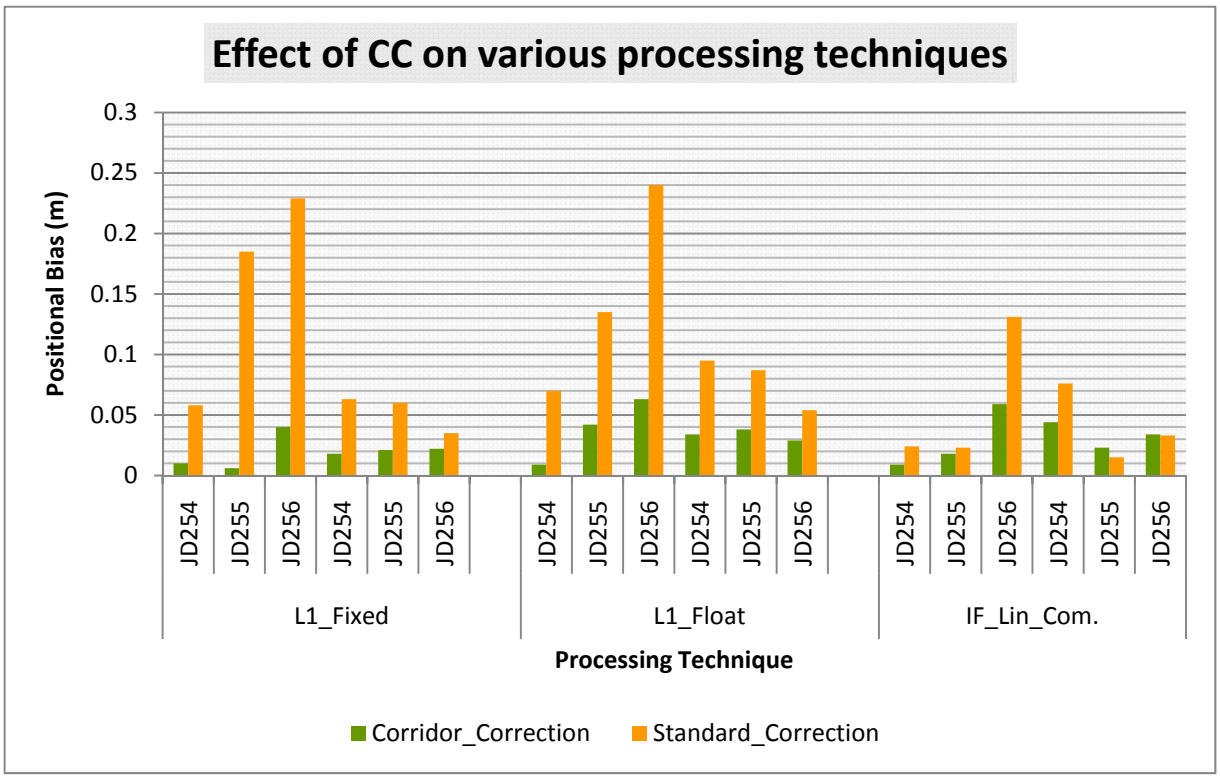

Figure 11-12: A plot showing the effectiveness of Corridor Correction with respect to processing techniques

One significant observation as shown in Figure 11-12 is the worse positional accuracy for the corridor correction shown for IF_LC 255 and 256, as compared the corresponding standard correction. This can be attributed to the higher noise associated with the employment of ionosphere-free linear combination.

11.2.6 Effect of Corridor Correction on Off-Corridor Application

As explained in Chapter Three, the effectiveness the CC reduces as one move away from the centre of the corridor due to spatial de-correlation. To demonstrate this CC was used to process data from Erfurt (ERFU) which is 22 km away from the corridor along the baseline between Worbis (WORB) and Sonnenberg (SONN) and the

results were compared with that processed for Gotha (GOTH) which is 1.3 km from that same baseline. See Figure 11-6

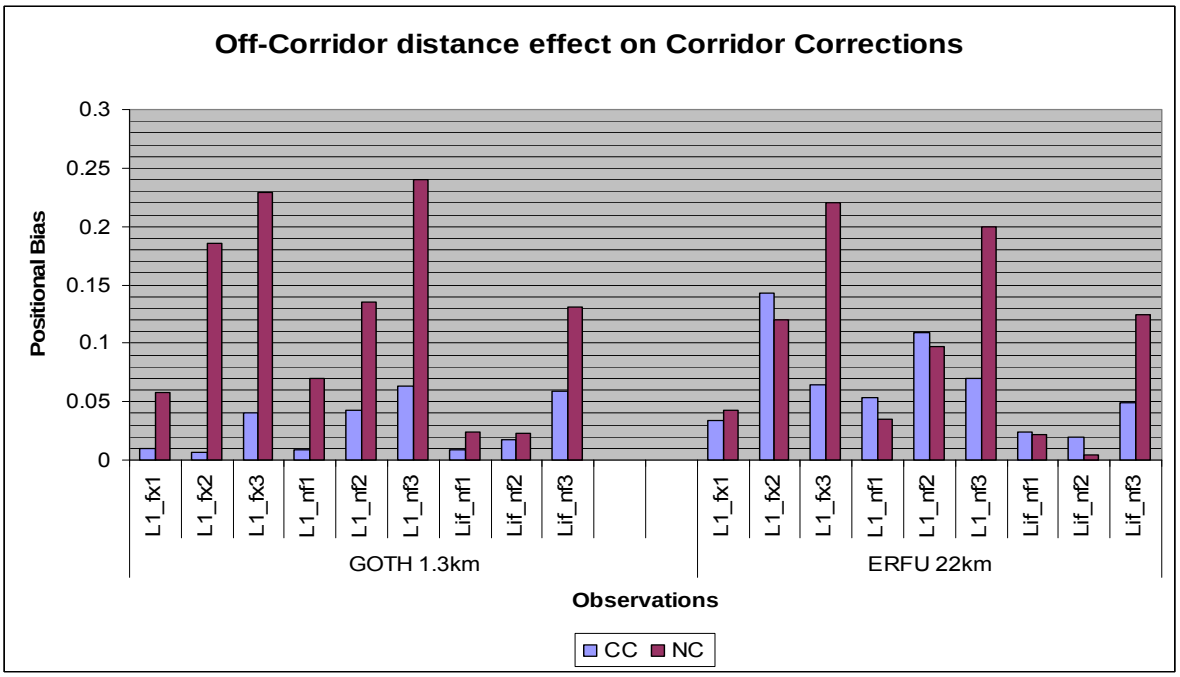

Figure 11-13: Comparison of the impact of Off-Corridor distance on Corridor Correction at GOTH (1.3 km) and ERFU (22 km)

The Figure 11-13 shows an effective improvement on the positional accuracy at GOTH which shows an improvement of 4.3 times that of ERFU, with under virtually the same atmospheric conditions and satellite geometry. There is just a marginal improvement in accuracy at ERFU when corridor correction is compared with standard correction.

11.2.7 The Effect of length of baseline on Corridor Correction

Length of baseline has got a negative impact on the effectiveness of CC, the longer the baseline the less effective the CC becomes. This has been demonstrated with the selected baselines Muenhausen-Ilmenau through-Gotha (GMI) and Worbis-Sonnenberg-through-Gotha (GWS). The shorter the baseline the GMI has a smaller standard deviation for the biases and shows a greater stability as compared with the longer baseline GWS. This is shown in the Figure 11-14. This is as a result of the greater uncertainty and de-correlation in the atmospheric conditions as one move away from a selected point location

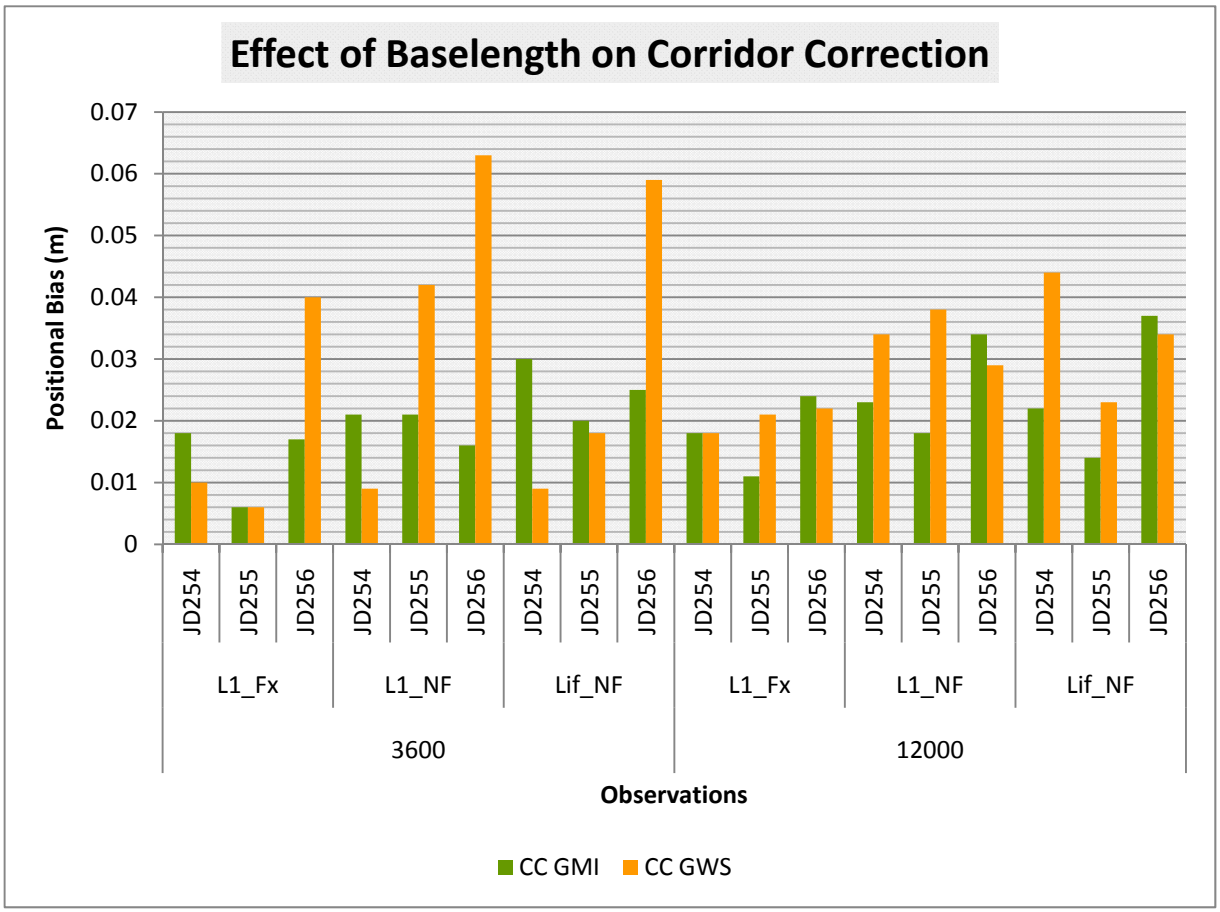

Figure 11-14: Comparison of the stability of Positional Bias for Corridor Correction between short GOTH-MUEH-ILME (CC GMI) and long GOTH-WORB-SONN (CC GWS) baselines

11.2.8 Comparing Corridor Correction (CC) with Area Correction Parameters (ACP) and Standard Correction (SC)

Area Correction was derived for Gotha, using SAPOS stations located at Erfurt (ERFU), Meiningen (Mein) and Muenlhausen (Muen) which form a triangle of sides 47 km, 63 km and 69 km with Gotha almost at the centre. See Figure 11-15. This is compared with Corridor corrections at the same location GOTH using both the long baseline of MUEN-ILME and the shorter baseline WORB-SONN. These were compared with the corresponding Standard Correction (Klobuchar and TROPGRID).

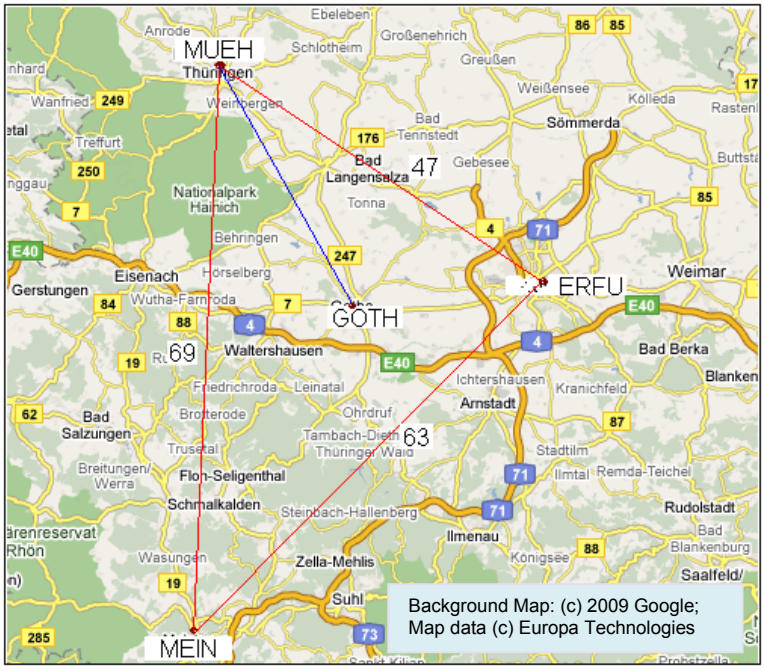

Figure 11-15: A network of stations (GOTH-MUEH-MEIN-ERFU) in Thuringia used to demonstrate Area Correction

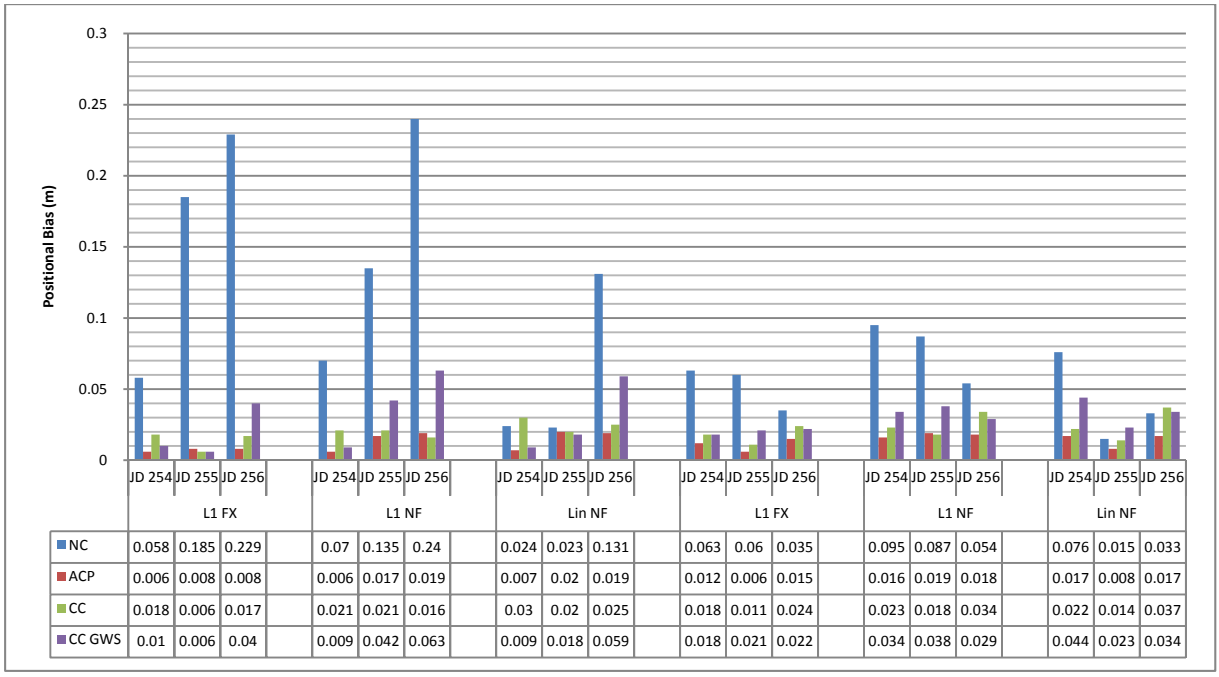

	L1 FX			L1 NF			Lin NF			L1 FX			L1 NF			Lin NF		
	JD 254	JD 255	JD 256	JD 254	JD 255	JD 256	JD 254	JD 255	JD 256	JD 254	JD 255	JD 256	JD 254	JD 255	JD 256	JD 254	JD 255	JD 256
NC	0.058	0.185	0.229	0.07	0.135	0.24	0.024	0.023	0.131	0.063	0.06	0.035	0.095	0.087	0.054	0.076	0.015	0.033
ACP	0.006	0.008	0.008	0.006	0.017	0.019	0.007	0.02	0.019	0.012	0.006	0.015	0.016	0.019	0.018	0.017	0.008	0.017
CC	0.018	0.006	0.017	0.021	0.021	0.016	0.03	0.02	0.025	0.018	0.011	0.024	0.023	0.018	0.034	0.022	0.014	0.037
CC GWS	0.01	0.006	0.04	0.009	0.042	0.063	0.009	0.018	0.059	0.018	0.021	0.022	0.034	0.038	0.029	0.044	0.023	0.034

Figure 11-16: Comparing three correction concepts SC, ACP and CC

It can be observed that the difference in accuracy between CC and ACP is marginal as compared with SC (Tropgrid/Klobuchar) in most cases. The performance of the ionosphere-free linear combination is generally better than the single frequency solutions, both float and fixed. This is so despite the noisy nature resulting from the linear combination as the contribution of ionospheric delay outweighs the noise. The averages for their biases have been shown in Figure 11-17.

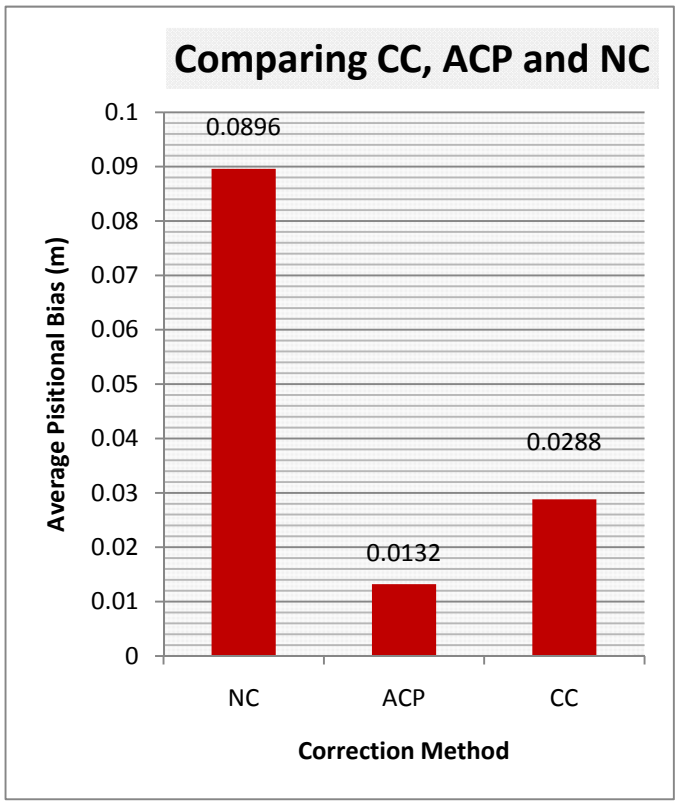

Figure 11-17: Comparing the average positional bias of the three correction methods

11.2.9 Analyzing Numerical Weather Model, GTCE Self Estimated Zenith Path Delay, Corridor Correction, Area Correction Parameters and Standard Correction

In addition to the modelled atmospheric delays using ACP and CC, other models can also be used to provide corrections and among these are the Numerical Weather Model (NWM) and the Self Estimated Zenith Path Delay (EST_ZPD) by GTCE which can be utilized by SEMIKA. These have been analyzed along with ACP, CC and NC as shown in Figure 11-18.

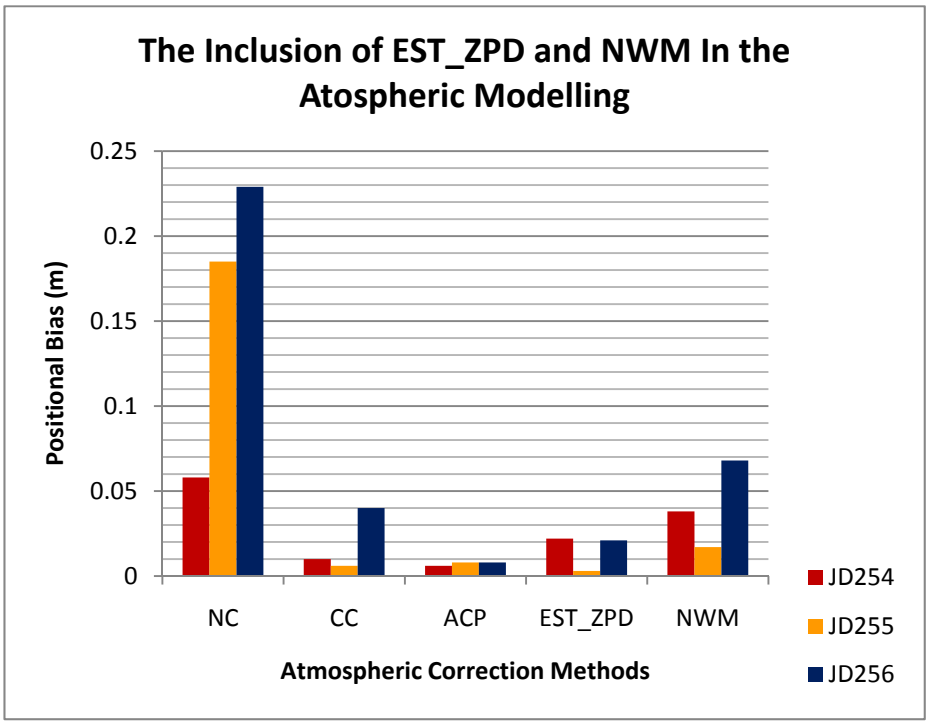

Figure 11-18: Comparing the effectiveness of SC, CC, ACP, EST_ZPD and NWM

The results at GOTH showed a good performance of the EST_ZPD which incidentally had the best overall result on the Julian Day 225 (JD255). The averages of the biases are as shown in Figure 11-19. ACP has a better stability and is generally better on average.

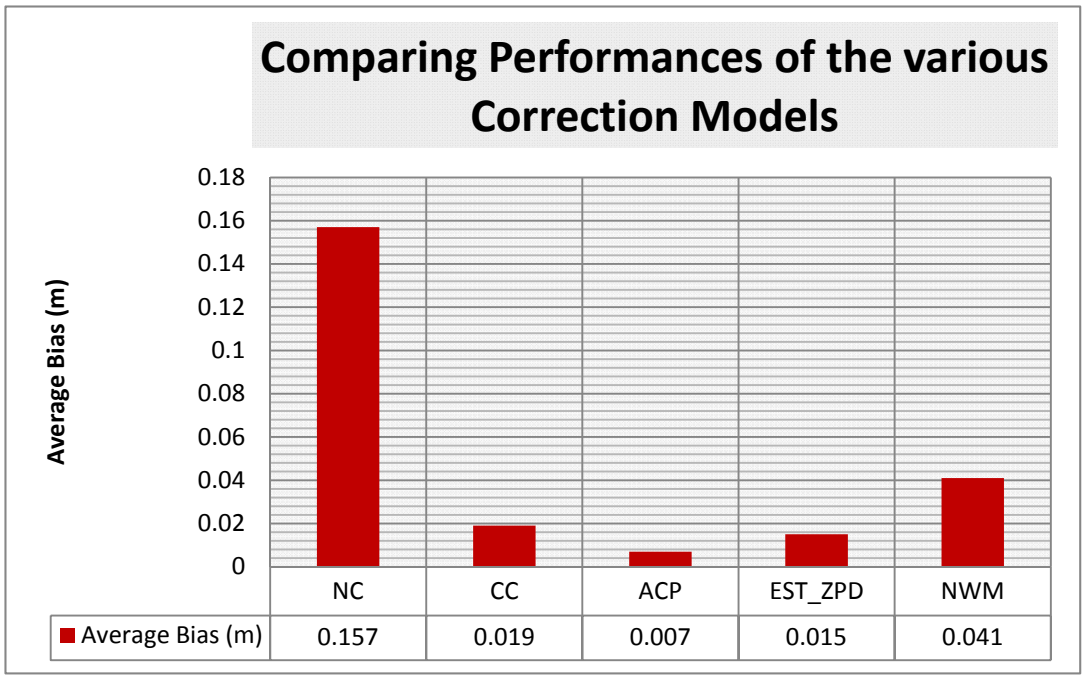

Figure 11-19: Comparison of the performances of various correction models

11.2.10 Corridor Correction in the Golden Triangle of Ghana

Following the various analyses performed with the data from the SAPOS network in Thueringia, the study was extended to the Golden Triangle of Ghana where conditions are quite different in terms of accuracies in the a-priori coordinates of the newly established network as compared with the time tested SAPOS coordinates, and also the turbulent atmospheric conditions in this tropical country.

Two baselines used for the CC analysis included Accra-Assin Fosu, (ACRA-ASFO) baseline which is 122 km long and Akroso, AKRO the rover is 23.6 km off the corridor.

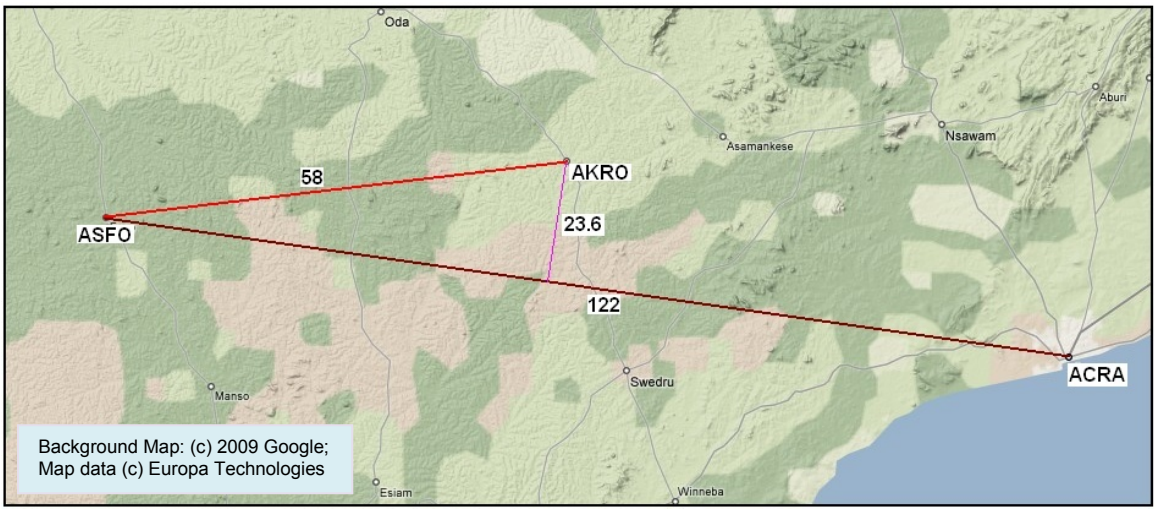

Figure 11-20: Baseline (ACRA-ASFO) for corridor correction with AKRO as rover

A second baseline is the Accra-Kade ACRA-KADE baseline which is 92 km with the rover position Awaham Nkwanta AWAN 6.9 km off the corridor.

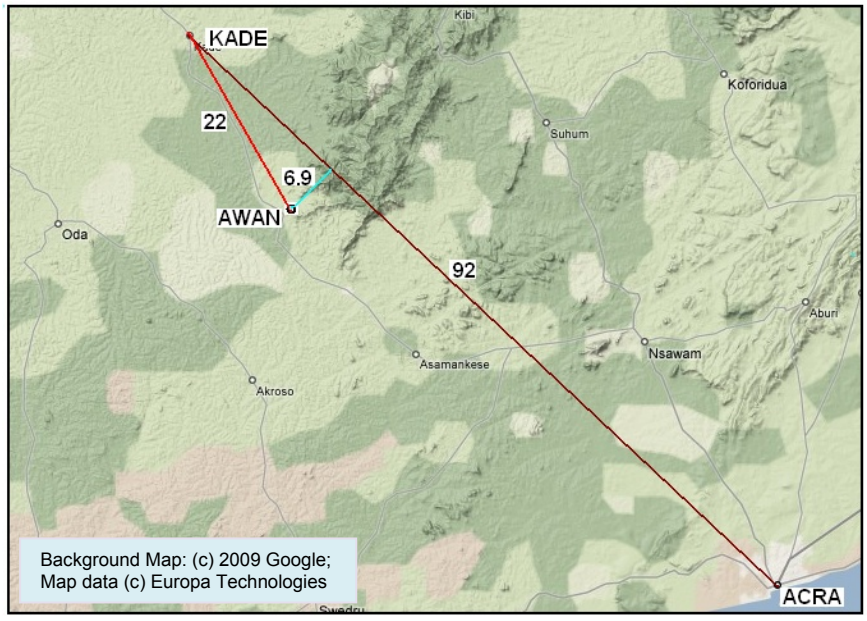

Figure 11-21: The ACRA-KADE baseline for corridor correction with AWAN as the rover

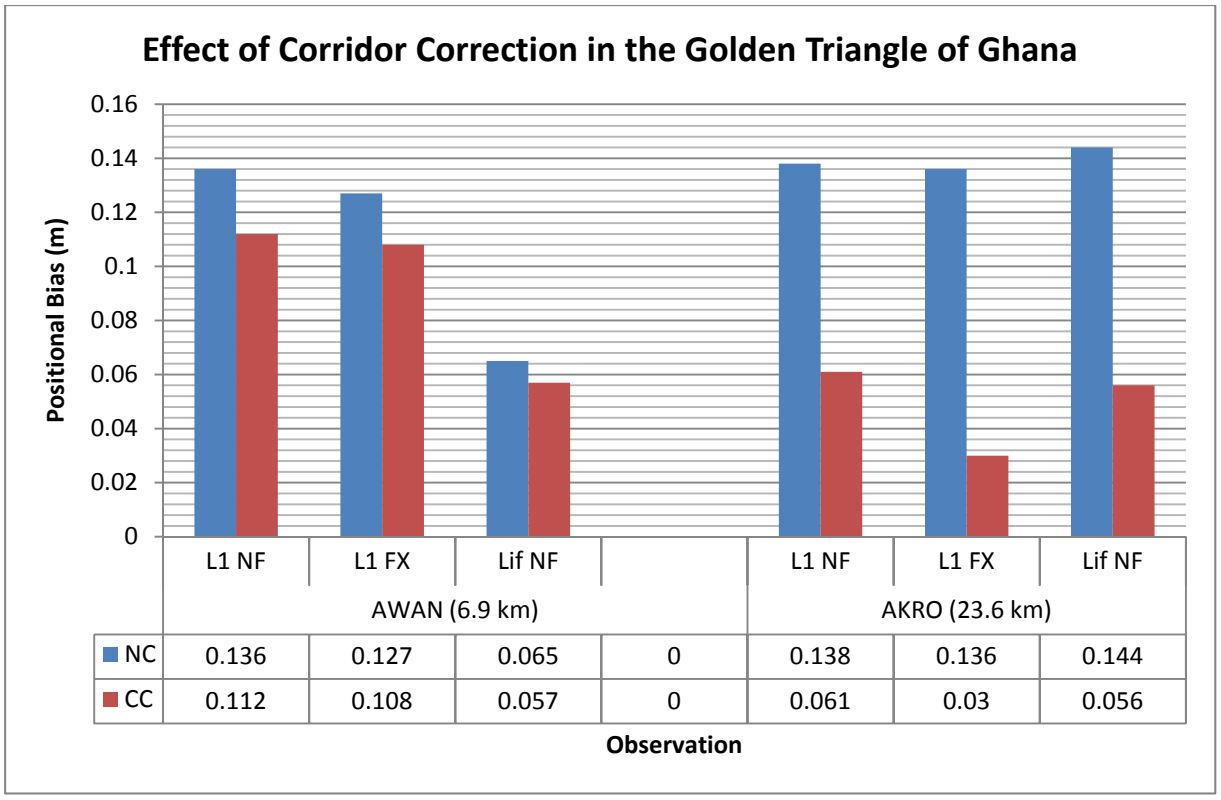

Figure 11-22: A plot showing the performance of Corridor Correction at AKRO and AWAN in the Golden Triangle of Ghana

Just like the results in Thueringia, the results of the performance of CC is very much dependent on the distance off-corridor in the GT of Ghana, shows the dependence of CC on the nearness of the rover to the corridor. AKRO which is almost 24 km off-corridor, Figure 11-20, shows a very poor results and almost equal to the Standard Correction, which has no correction for the troposphere and Klobuchar model for ionosphere correction. AWAN which is 6.9 km off-corridor, Figure 11-21, however shows a remarkable improvement for the CC from the Standard Correction as shown in Figure 11-22. The ionosphere-free linear combination shows a significant bias which is an indication that troposphere is quite active as compared with that in Thueringia as shown in Figure 10-7

11.2.11 The effect of Area Correction Parameters in the Golden Triangle of Ghana

The use of ACP in the Golden Triangle of Ghana was analyzed with the formation of a network made up of the Accra permanent station and the ASFO and KADE hub stations enclosing the two selected rovers AKRO and AWAN. The results as displayed in Figure 11-25 and Figure 11-26 show the performance of ACP at AWAN to be better as compared with that of AKRO. This may be attributed to the fact that AWAN is closer to one the reference stations KADE and also the baseline ACRA-KADE, while AKRO is quite far from any of them. See Figure 11-23 and Figure 11-24.

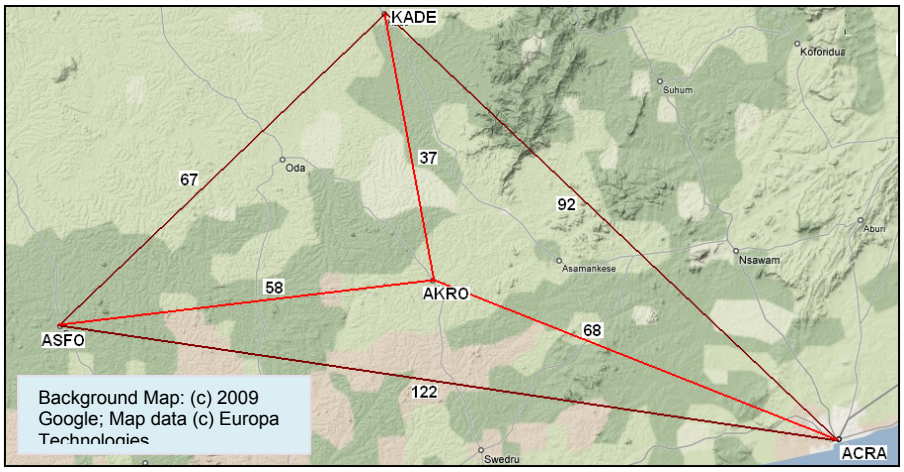

Figure 11-23: A network of stations AKRO (rover), KADE-ASFO-ACRA (reference stations) in the Golden Triangle for Area Correction Parameter determination

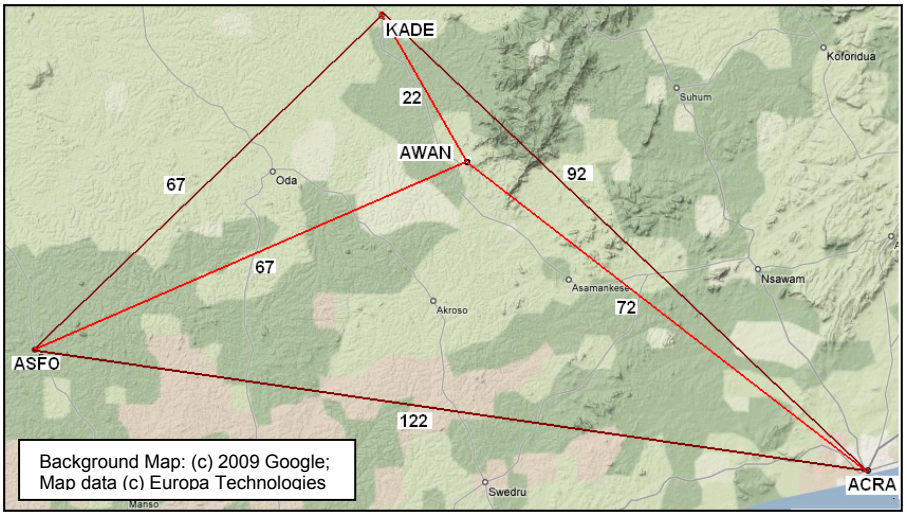

Figure 11-24: A network of stations AWAN (rover), KADE-ASFO-ACRA (reference stations) in the Golden Triangle for Area Correction Parameter determination

11.2.12 Comparison of Various Correction Models in Ghana

Various correction models including Corridor Correction (CC), Area Correction Parameters (ACP), Standard Correction NC (TK) which uses the blind model, TROPGRID for the tropospheric corrections and Klobuchar model for the ionospheric correction, No Correction NC (NK), which is not corrected for troposphere but uses Klobuchar for ionosphere correction, have been compared. In addition NWM (ZK) which uses ZPD estimated from GTCE for troposphere correction and Klobuchar model for the ionosphere correction, and NWM (ZA) which uses the GTCE self-estimated ZPD files for troposphere correction but uses ionosphere correction derived from CC (active net), have also been compared. The results have been summarized for both positional and horizontal biases for AKRO in Figure 11-25 and Figure 11-26.

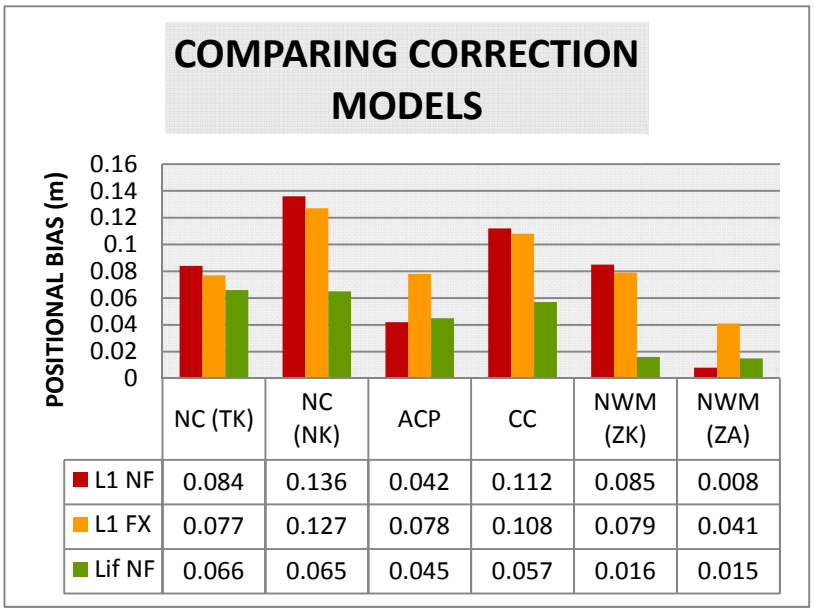

	NC (TK)	NC (NK)	ACP	CC	NWM (ZK)	NWM (ZA)
L1 NF	0.084	0.136	0.042	0.112	0.085	0.008
L1 FX	0.077	0.127	0.078	0.108	0.079	0.041
Lif NF	0.066	0.065	0.045	0.057	0.016	0.015

Figure 11-25: Comparison of various correction models and the processing methods at AKRO (23.6 km off-corridor)

Comparing the accuracies for the NWM (ZK) and NWM (ZA), the improved accuracy in the latter can be attributed to the introduction of the NEREUS derived ionospheric correction of the corridor correction. This is confirmed by the fact that there is only a marginal change where the iono-free linear combination was used in both cases.

Comparing NC (NK), and NC (TK) correction models, the latter which differs from the other by the introduction of TROPGRID shows a significant difference in the accuracies. This confirms the effectiveness of the blind model in mitigating tropospheric effect.

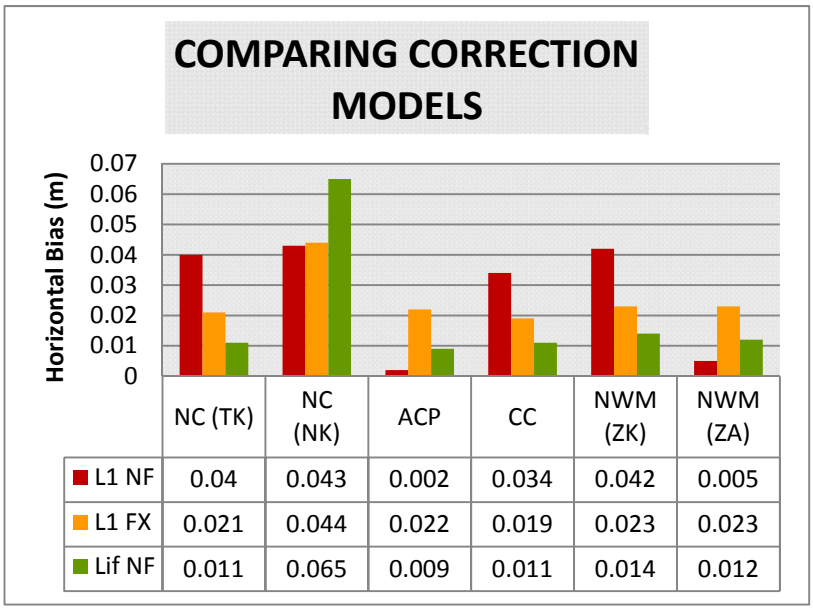

	NC (TK)	NC (NK)	ACP	CC	NWM (ZK)	NWM (ZA)
L1 NF	0.04	0.043	0.002	0.034	0.042	0.005
L1 FX	0.021	0.044	0.022	0.019	0.023	0.023
Lif NF	0.011	0.065	0.009	0.011	0.014	0.012

Figure 11-26: Comparison of various correction models and the processing methods at AKRO (23.6 km off-corridor) in the horizontal plane

The poor performance of CC shown in Figure 11-25 can be attributed to the distance off-corridor at AKRO which is 23.6 km off-corridor, this improved in the case of AWAN, 6.9 km off corridor, as shown in Figure 11-27. This is further illustrated by the Table 11-1. The inclusion of ACP in the analysis at this juncture is to have an idea as to the performance on this newly introduced system to the already existing and well tested and accepted ACP.

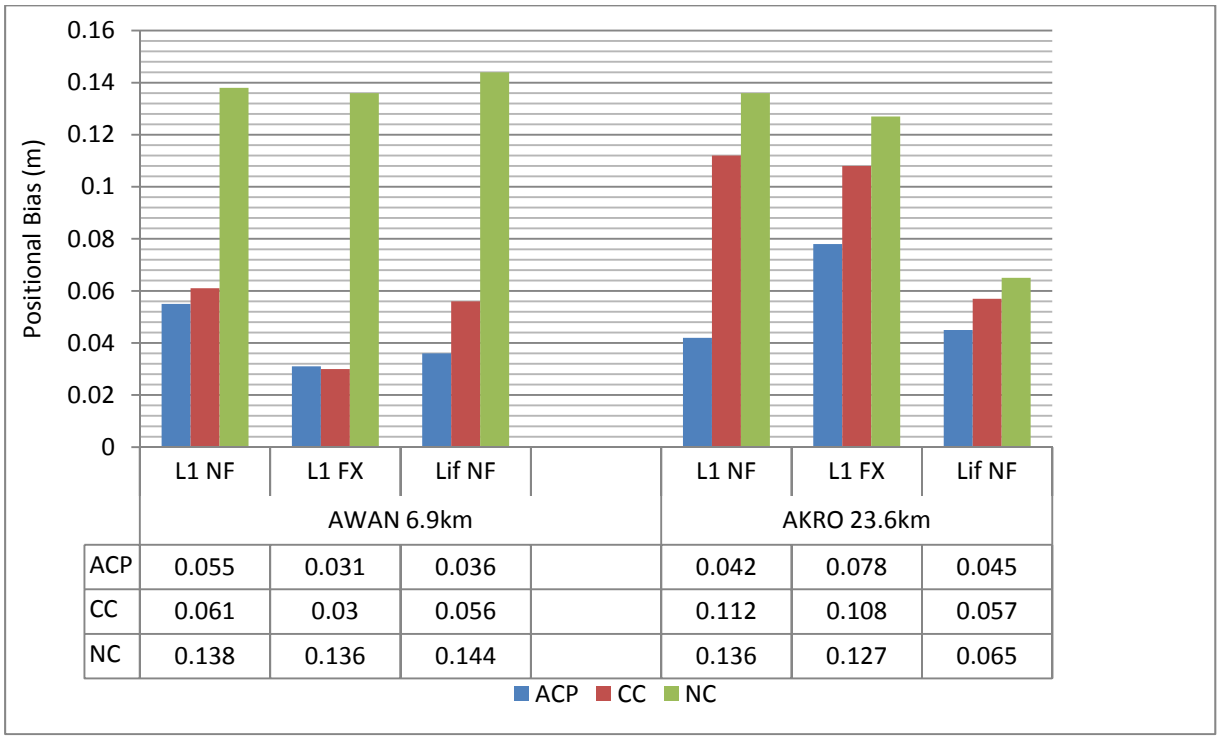

Figure 11-27: The effect of distance on the positional biases for ACP and CC

	NC (NK)	ACP	CC
AKRO (23.6 km)	100%	50.3%	81.4%
AWAM (6.9 km)	100%	29.2%	35.2%
Ratio	1.0	1.72	2.31

Table 11-1: Analyzing the EFFECT OF proximity of a rover to the baselines.

This analysis is made by comparing the biases of the two models with the “No Correction” model which only employs Klobuchar model for the ionospheric correction and no correction of troposphere for both AWAN and AKRO which are located at 6.9 km and 23.6 km respectively. Corridor Correction performed very poorly at AKRO which was 23.6 km away from the corridor, as compared with the Area Correction model. This however improved at AWAM where the off-corridor distance was reduced. This shows the limitation of corridor correction, which deteriorates as the distance from the corridor increases from the baseline. Although the same trend has been demonstrated by the Area Correction, it is to a lesser extent as seen in Table 11-1. This can be explained by the fact that in the case of ACP, one approaches another baseline while moving away from one baseline, which is not the case for CC.

12 Conclusion and Recommendations

12.1 Conclusion

The Geodetic Reference Network (GRN) for Ghana covering the Golden Triangle has been established. This comprises of 3 permanently operating reference stations which serve as primary control points and 17 second order network located in and around the Golden Triangle of Ghana. This reference network which is based on the ITRF05 at the epoch 2007.39 was realised using mainly the PrePos GNSS Suite software. The standard deviations in the X-, Y- and Z-coordinates for these twenty established points comprising the primary and secondary points were 1.72 cm, 1.09 cm and 0.45cm respectively in the Cartesian coordinate system. These translate to an average of 1.71 cm and 1.20 cm in the vertical and horizontal components respectively. This has since been accepted by the Survey Department of Ghana and is currently in use as the approved geocentric coordinates within the Golden Triangle of Ghana

To be able to make use of the wealth of old data based on the classical old War Office 1926 Reference Ellipsoid a set of seven transformation parameters has been determined based on the Helmert's formula. Although Helmert's approach was preferred due to its ability to provide reasonably acceptable results beyond the area where the common points are located, the Polynomial Function Approach was used as well for the same purpose and was found to provide comparable or even slightly better residuals. The Helmert's approach provided a mean residual of 0.674 m in the easting, 0.755 m in the northing and 1.502 m in the radial directions, whereas the Polynomial Function approach provided 0.477 m in the easting and 0.778 m in the northing.

To address the vertical reference datum for the country which is based on the mean-sea-level established over eight decades ago, the GRN has been linked to the mean-sea-level by co-locating the Takoradi Harbour Tide Gauge with a GNSS reference station to determine the geoid separation so as to obtain the orthometric height from the ellipsoidal height. This separation is expected to be similar to that at the TADI permanent station which is located about 2 km away. The initial results show a difference of 2.2 cm, which is within acceptable limits. This geoid at TADI which is 25,586 m has a difference of 2.456 m from the EGM96 which is 23.13 m. This lays foundation for the investigation of geoid correction which is needed to obtain orthometric height with GNSS before the determination of a national geoid model. There is however the need to observe on these stations for a longer period to analyze the time-series in order to ensure the removal of variations associated with tidal and short-period effects. Similar investigations must be made at various locations to increase the confidence in its use.

For optimum use of precise GNSS positioning, the time to fix ambiguity fixing plays an important role. This has been investigated in the Ghanaian environment using various ambiguity fixing techniques. The Nearest Integer Round-Off method, which had the poorest overall performance as compared with the other approaches, has been applied over a baseline of 58 km to estimate the optimum time of observation under the Ghanaian environment. The result showed that one has to spend a minimum of 30 minutes at a station to have over 90% success rate in fixing for a baseline of 50 km. This should be one of the pillars of standards and recommended practices for the use of GNSS in Ghana.

The most disturbing obstacles to the provision of reliable and precise positioning in the project area are the turbulent tropospheric and ionospheric delays. These have been addressed using various approaches which include the use of appropriate processing techniques including the code-plus-carrier technique which removes the ionospheric delay. The use of the GTCE ZPD files also reduces the tropospheric delay thereby making it possible to attain sub decimetre positional accuracy with a single frequency signal over 194 km baseline after 18 hours and 16 hours for horizontal accuracy. It was possible to obtain 4 cm and 5 cm in the horizontal and 3-dimensional positional accuracies respectively within 24 hours. With the use of NKLG (IGS) and ACRA (GRN) stations, which are separated by a distance of 1239 km, sub-decimetre positional accuracy was attained after 18 hours, and accuracy of 3 cm within 24 hours with single frequency over this very long baseline.

The use of the GTCE self-estimated zenith path delay (ZPD) files proved to be very effective in the reduction of the tropospheric error, when combined with the ionosphere correction component of the Active Net of NEREUS e.g. CC as shown in 10.1.11, one gets a very improved accuracy. There was a significant difference between the use of the ZPD file and the Klobuchar model.

TROPGRID, which is a blind model, composed of a gridded database showed a significant impact in the mitigation of the troposphere as observed in this study. This showed an improvement of about 60% in positional bias and 50% horizontal bias by comparing the ‘NC (TK), which uses TROPGRID for the tropospheric correction, with NC (NK) which does not correct for the troposphere.

The NEREUS derived Area Correction Parameters applied in this study showed improved accuracy by removing the effects of both ionospheric and tropospheric delays. This has been found to be very effective in Thuringia (Figure 11-19) and in the Golden Triangle of Ghana (Figure 11-26).

The newly introduced Corridor Correction concept has been analyzed with data from both the Golden Triangle (GRN, Ghana) and Thuringia (SAPOS, Germany) and has been found to be reliable for atmospheric corrections both in Ghana and Germany. Factors that were found to affect the effectiveness of this correction were

- Length of the baseline between the reference stations
- Satellite geometry
- Atmospheric Conditions
- The off-corridor distance of the rover

Generally the shorter the baseline, the better the accuracy derived as demonstrated using the Ilmenau-Muenlhausen baseline of 62 km as against Worbis-Sonnenberg baseline of 131 km, all in Thuringia. This has been demonstrated by Figure 11-9 in section 10.1.2

The two-hour separation between the observation times for the three days of observation was enough to greatly affect the satellite geometry than factors like the atmospheric conditions for the corridor corrections. The difference in positional bias shown graphically Figure 11-10 shows the impact of satellite geometry on the effectiveness of corridor correction

Analysis of the same time on different days was made to find the impact of the atmospheric conditions on corridor corrections as the satellite geometry is practically the same for time of day. The result showed better results on the first day that is Julian Day 254, but worsened on the Julian Day 255 with only a marginal change on the and Julian day 256. The conclusion that can be drawn from this is that, the atmospheric condition was favourable for corridor corrections on the first day, but worsened on the second and did not improve on the third day.

Analyzing data for Gotha and Erfurt which are 1.3 km and 22 km respectively from the Worbis-Sonnenberg baseline, there was a demonstration of the deterioration of the effectiveness of corridor correction at Erfurt, while there was an improvement of 4.3 time at Gotha, the was barely any effect at Erfurt as explained in section 10.1.5 and Figure 11-13. The 6.9 km off-corridor distance of AWAN and 23.6 km of AKRO from the 92 km Accra-Kade baseline and the 122 km Accra-Assin Fosu baseline respectively, showed similar trend. While there was a 2.8 times improvement of corridor correction as against the standard correction at AWAN, AKRO was improved only 1.2 times. Therefore there is the need to define the width of the corridor which depends on the severity of the ionosphere in the area as well as the nature of the troposphere at the moment of observation. Observation between 18th and 24th May 2007 showed an increase of 0.66 ppm as a user moves away from the corridor and a residual delay of 23 mm at the corridor for the ionospheric delay. Similarly, analysis of the tropospheric delay showed a residual of 19 mm at the corridor and an increase of 0.13 ppm as a user moves away from the corridor. It is recommended to limit its use to within 10 km off-corridor if the user requires accuracy comparable to that derived from the Area Correction Parameter.

12.2 Recommendations

For the established National GNSS Reference Network to be functional and beneficial to the user community, the following recommendations are made:

- Provision of Standards and Recommended Practices to serve as a guide to the user community especially as most users are not familiar with this technology
- The implementation of proposed nationwide network designed in this study should be flexible to incorporate stations that may be established by other organizations to avoid duplication
- A national set of Transformation Parameters should be determined, to replace the one determined for the Golden Triangle in this project
- Grid-Look-Up approach covering the whole country should be employed to ensure a better accuracy for the use of transformation parameters in the country, as it has been demonstrated in this study that a more localized set of common points provides a more accurate set of transformation parameters
- Time-series analysis of the TKTG and TADI stations should be made periodically to investigate the vertical reference datum for the country
- A national geoid model should be derived from gravity and GNSS/leveling benchmarks so as to add to the potential of GNSS in terms of applications that require height determination
- Research should be encouraged within the West Africa sub-region especially the ones that will be focused on finding solutions to problems associated with the geographical location

A. Symbols and Notations

ρ	true range (distance between satellite and receiver antenna)
τ^S	true time at the satellite
φ	carrier phase
ε_{code}	carrier phase noise
ε_{cpc}	code-plus-carrier noise
ε_{phase}	pseudorange noise
dt_r	receiver clock correction
dt^s	satellite clock correction
N_{iono}	refractive index in the ionosphere
ρ_{iono}	upper limit of the ionosphere
ρ_{trop}	upper limit of the troposphere
g_m	weighted mean gravity acceleration
k_3	refraction coefficient
$m_H(\varepsilon)$	mapping function for the hydrostatic delay
$m_W(\varepsilon)$	mapping function for the wet delay
R_d	gas constant of dry air
T_M	mean temperature]
δr_1	distance dependent error for L1
δr_2	distance dependent error for L2
Φ_1, λ_1	latitude and longitude in system 1
Φ_m, λ_m	approximate geographic coordinates
M_d	molar weight of dry air
N_{hyd}	hydrostatic refractive index
N_{trop}	refractive index in the troposphere
N_{wet}	surface wet refractive index
R_d	specific gas constant
R_0	universal gas constant
$\bar{V}(t_{ref})$	velocity vector of station at reference epoch t_{ref} in meters
$\bar{X}(t_{ref})$	ECEF position vector at observation epoch t_{ref} in meters
$\bar{X}(t)$	ECEF position vector at observation epoch t in meters

Z_w^{-1}	inverse compressibility of water
$\Delta \mathrm{E}_{\mathrm{AE}}$	correction in the easting
$\Delta \mathrm{N}_{\mathrm{AE}}$	correction in the northing,
ΔR_{AE}	correction in the vertical
a	semi-major axis
b	semi-minor axis
C	obliquity factor
c	speed of light in vacuum
c_0	speed of propagating signals in vacuum
C_{ij}	coefficient of polynomial
dS_j	coordinate component differences
e	partial water vapor
E	angle of elevation of satellite in radians
E_0	FKP in east-west direction for geometric (ionosphere-free) signal in ppm
E_1	FKP in east-west direction for the ionosphere signal (influence on narrow-lane) in ppm
f	carrier frequency
f	flattening
GM	gravitational parameters of the earth
GM_2	gravitational parameters of the moon
GM_3	gravitational parameters of the sun
h	ellipsoidal height
H	orthometric height
h_2	nominal second degree Love dimensionless number (0.609)
$\delta \mathrm{I}$	ionospheric delay
I_t	zenith ionospheric delay at the local time
$k_{0,1}$	constant
K_1,K_2,K_3	are the refraction constants
l_2	nominal second degree Shida dimensionless number (0.085)
L_o	length of monument
n	Prime vertical radius
N	geoidal undulation
N	Integer ambiguity

n	order of polynomial
N_0	FKP in north-south direction for geometric (ionosphere-free) signal in ppm
N_1	FKP in north-south direction for the ionospheric signal (influence on narrow-lane) in ppm
PR	pseudorange between receiver R and satellite S.
t	observation epoch in decimal years
dt_r	Receiver clock time
t_{ref}	reference epoch in years as given in the network solution file
δT	tropospheric delay
α_e	Coefficient of linear expansion
ΔL	linear expansion
Δt	Change in temperature
$\Delta\lambda$	change in Longitude
$\Delta\varphi$	change in Latitude
θ_g	Greenwich mean Siderial time
λ	longitude
λ	water vapour lapse rate
λ_{min}	Minimum Value of Longitude
λ_R	reference geographic longitude in WGS84
φ	latitude
φ_{min}	Minimum Value of Latitude
φ_R	reference geographic latitude in WGS84
T	temperature

B. List of Acronyms

AAI	Airport Authority of India
ACP	Area Correction Parameters
AFREF	African Reference Frame
AGP	African Geoid Project
AOR	Atlantic Ocean Region
AOR-W	Atlantic Ocean Region - West
ASQF	Application Specific Qualification Facilities
BRRI	Building and Road Research Institute
CA (C/A)	Coarse Acquisition
CC	Corridor Correction
CERSGIS	Centre for Remote Sensing and Geographic Information Services
CNS/ ATM	Communication, Navigation. Surveillance Air Transport Management
CSIR	Council for Scientific and Industrial Research
DCC	Data Coordination Centre
DGNSS	Differential Global Navigation Satellite System
DORIS	Doppler Orbitography Radiopositioning Integrated by Satellite
DVP	Development Verification Platform
EC	European Commission
EGM	Earth Gravitational Model
EGNOS	European Geostationary Network Overlay Service
ENT	EGNOS Network Time
EOP	Earth Orientation Parameters
EPA	Environmental Protection Agency
ESA	European Space Agency
ETG	European Tripartite Group
FAS	Floating Ambiguity Solution
FKP	Flaechen Korrektur Parametern (Area Correction Parameters)
GAGAN	GPS/GLONASS and Geo Augmentation
GEO	Geostationary Orbit
GEONET	GPS Earth Observation Network
GES	Ground Earth Station

GERMP	Ghana Environmental Resources Management Project
GIC	Galileo Integrity Channel
GIS	Geographic Information System
GLONASS	Global Navigation Satellite System
GNSS	Global Navigation Satellite System
GPS	Global Positioning System
GRN	GNSS (Geodetic) Reference Network
GSD	Geological Survey Department
GSM	Global System for Mobile Communication
GTRF	Galileo Terrestrial Reference Frame
GUS	Ground Uplink Station
IAG	International Association Geodesy
ICAO	International Civil Aviation Organization
ICT	Information and Communication Technology
IERS	International Earth Rotation and Reference Systems Service
INLUS	Indian Navigation Land Uplink Station
INMCC	Indian Master Control Centre
INRES	Indian Reference Station
IONEX	Ionosphere Map Exchange
IOR	Indian Ocean Region
IPP	Ionosphere Piercing Point
IRNR	Institute of Renewable Natural Resources
ISRO	Indian Space Research Organization
ITRF	International Terrestrial Reference Frame
IUGG	International Union of Geodesy and Geophysics
JCAB	Japanese Civil Aviation Bureau
KNUST	Kwame Nkrumah University of Science and Technology
LAMBDA	Least Squares Ambiguity Decorrelation Adjustment
LAP	Land Administration Project
LTR	Land Title Registration
MAC	Master Auxiliary Concept
MCA	Millennium Challenge Account
MCC	Master Control Centre
MEO	Medium Earth Orbiting (satellites)

MSAS	MTSAT-Satellite-based Augmentation System
MSL	Mean Sea Level
MTSAT	Multi-functional Transport Satellite
NAFGIM	National Framework for Geospatial Information Management
NARSDA	National Space Research and Development Agency
NEPAD	New Partnership for Africa's Development
NGA	National Geospatial-Intelligence Agency
NGS	National Geodetic Agency
NIMA	National Imagery and Mapping Agency
NIROM	Nearest Integer Round-off Method
NLES	Navigation Land Earth Station
NMO	National Mapping Organization
NPF	Network Processing Facility
NTRIP	Network Transport of RTCM via Internet Protocol
NWM	Numerical Weather Model
OSASM	Observation Space Ambiguity Search Method
PACF	Performance Assessment System
PDGPS	Phase Differential Global Positioning System
PGS	PrePos GNSS Suite
PNDCL	Provisional National Defense Council Law
POR	Pacific Ocean Region
PZ-90	Parametry Zemli 1990 Goda–Parameters of the earth Year 1990
QARP	Quick Ambiguity Resolution Procedure
QZSS	Quasi-Zenith Satellite System
RECTAS	Regional Centre for Training in Aerospace Survey
R-GEO	GEO Ranging
RIMS	Ranging and Integrity Monitoring Stations
RINEX	Receiver Independent Exchange
RTCM	Radio Technical Commission for Maritime Services
RTK	Real Time Kinematics
SAPOS	Satellitenpositionierungsdienst (Satellite Positioning Service)
SBAS	Satellite Based Augmentation System
SC	Standard Correction
SCIGN	Southern California Integrated GPS Network

SD	Survey Department
SDI	Spatial Data Infrastructure
SINEX	Solution Independent Exchange
SLR	Satellite Laser Ranging
SNAS	Satellite Navigation Augmentation System
SPD	Slant Path Delay
SRI	Soil Research Institute
TCPD	Town and Country Planning Department
TEQC	Translation, Editing and Quality Checks
TTC	Trimble Total Control
TT&C	Tracking Telemetry and Command
UDRE	User Differential Range Error
UHF	Ultra High Frequency
UNECA	United Nations Economic Commission for Africa
UNOOSA	United Nations Office for Outer Space Affairs
UTC	Universal Coordinated Time
VHF	Very High Frequency
VLBI	Very Long Baseline Interferometry
VRA	Volta River Authority
VRS	Virtual Reference Station
VTEC	Vertical Total Electron Content
WAAS	Wide Area Augmentation System
WAD	Wide Area Differential
WAFREF	West Africa Reference Frame
WGS84	World Geodetic System 1984
WMS	Wide-Area Master Station
WRS	Wide-Area Reference Station
ZHD	Zenith Hydrostatic Delay
ZPD	Zenith Path Delay
ZWD	Zenith Wet Delay

C. References

ABB-Group. (1999). *The VRA Integrated Network Project-A Unique Broadband Communication Network for VRA and VoltaCom in Ghana.* Retrieved from http://library.abb.com/global/scot/scot221.nsf/veritydisplay/5f94c96958db8cbdc1256cf50058ea33/$File/710_Ghana_REN.pdf

Abousalem, M., Mogallul, S., Lucin, S., Tubalin, O. (2001). The New Thales DG 16 GPS Receiver. *ION International Technical Meeting,, September 11-14, ION GPS 2001.* Salt Lake City, Utah.

Altamimi Z., D. Gambis, C Bizouard. (2007). Rigourous Combination to ensure ITRF and EOP consistency. *Journees Systems de reference-spatio-temporal 20-21 September, BIPM.* Sevres, France.

Alves P., G. Lachapelle, M.E. Cannon. (2004). In-Receiver Multiple Reference Station RTK Solution. *Institute of Navigation Satellite Division Technical Meeting, GPS04.* Long Beach, California, USA.

Amponsah, P. E. (2004). Seismic Activity in Ghana, Past, Present and Future. *Annals of Geophysica* , 539-543.

Amponsah, P. (2002). Seismic Activity in Relation to Faults Systems in Southern Ghana. *Journal of African Science* , 227-234.

Andam, K. (2004). Bricks, Blocks and the Future of Administrative Capital of Ghana. *Ghana Academy of Arts and Sciences Inaugural Lecture.*

Anza, P. (2008). The N40b NigComSat Mess. *Newswatch Magazine* .

Aragon-Angel A., Orus R., Hernandez-Pajares, M., J. Sanz. (2003). Preliminary NeQuick assessment for future single frequency users of Galileo. *5th Geomatic Week.* Barcelona, Spain.

Arias E. F.; W. Lewandowaki. (2008). Use of international reference for GNSS operations. *Third Meeting of ICG, 8-12, December, 2008.* Pasadena, California, USA.

Askne J., H Nordius. (1987). Estmation of Tropospheric Delay for Microwaves from Surface Weather Data. *Radio Science Volume 22, No.3* , May/June 379-386.

Bacon, B., A.O. Quaah. (1981). Earthquake Activity in South-Eastern Ghana 1977-1980. *Bulletin of the Seismological Soceity of America, Vol. 71, No 3* , pp. 771-785.

Baki Iz, H. (2006). How do Unmodelled Systematic Mean Eea Level Variation affect long term Sea Level Trend Estimates from Tide Gauge Data. *Journal of Geodesy, Vol. 80 DOI 10.1007/s00190-006-0028x* , pp. 40-46.

Bisnath, S., D. Wells, D. Dodd. (2003). Evaluation of commercial phase-based WADGPS services for marine applications. *Institute of Navigation GPS/GNSS, 9-12, September.* Portland, Oregon, USA.

References

Brocard, D., T. Maier, C. Busquet. (2000). *EGNOS Rangong and Monitoring Stations (RIMS).* Retrieved January 2008, from http://www.egnos-pro.esa.int/publications/GNSS%202000/GNSS2000_rims.pdf

Brown H., R. Keenan, B. Richter, L. Troyer. (2005). Advances in Ambiguity Resolution for RTK applications using the New RTCM V3.0 Master Auxiliary Messenger. *ION GNSS 18th International Technical Meeting of the Satellite Division, 13-16 September, 2005.* Long Beach, California, USA.

Chen, W., C. Hill. (2005). Evaluation Procedure for Coordinate Transformation. *Journal of Surveying Engineering* , 43-49.

Cosentino, R. J., D. W Diggles. (1996). Differential GPS. In E. Kaplan, *Understanding GPS Principles and Applications* (pp. 321-383). Mobile Communication Series, ISBN 0-89006-793-7.

Donghyun, K., Langley, R.B. (2000). A reliable approach for ambiguity resolution of long-baseline kinematic GPS applications;. *13th International Technical Meeting of the Satellite Division of the ION, 19-22 September, 2000*, (pp. 1081-1091). Salt Lake City, Utah.

Douglas, B. (1991). Global Sea Level Rise. *Journal of Geophysical Research Vol 96* , 6981-6992.

Euler, H.-J. (2005). *Reference Network Information Distribution - IAG Working Group 4.5.1 Network RTK.* Retrieved February 2008, from http://www.network-rtk.info/

Euler, H-J., B. E. Zebhauser, B.R. Townsend, G. Wuebbena. (2002). Comparison of Different Proposals for Reference Station Network Information Distribution Formats. *15th International Technical Meeting of the Satellite Division of the ION, September 2002.* Portland, Oregon, USA.

Ezigbalike, D., D Berhanu. (2006). Role of ECA in the Implementation 0f AFREF. *AFREF Technical Workshop, 9-13 July 2006.* University of Cape Town, South Africa.

Faalong, J.Y., M.Agbeko, E. Amammoo-Otchere, B. Akuetteh. (2006). Capacity Building in Digital Mapping and GIS for boosting the Agricultural Sector Development of GIS driven Horticulture Produce Implementation System Managing Export Sector. *5th FIG Regional Conference, Accra, 8-11 March,.* Accra, Ghana.

Fernandes R.M.S., Y. Poku-Gyamfi, F. Yeboah, J.P.F Ferreira, S. Djaba, E Nkebi. (2008). Computing Mean-Sea-Levil changes in Ghana. *FIG Working Week 2008, 14-19 June 2008.* Stockholmm Sweden

Fliegel, H. F., T.E. Gallini, E.R. Swift. (1992). Global Positioning System Radiation Force Model for Geodetic Applications. *Journal of Geophysical Research, Vol. 97, No 81* , pp. 559-568.

Gauthier, L., P. Michel, J. Ventura-Traveset, J. Benedicto . (2001, February). The First Step in Europe's contribution to the Global Navigation Satellite System. *European Space Agency Bulletin 105* .

References

Gold-Coast-Survey. (1936). *Gold Coast Survey Records.* Accra Ghana: Survey Department of Ghana.

Gordon, R. G. (1998). The Plate Tectonic Approximation Non-Rigidity, Diffuse Plate Boundaries and Global Plate Reconstruction. *Annual Review, Earth Planet Science* .

Graham T., A.D. Christophe, J. Sannier, J.C.Taylor. (2000). Mapping Systems and GIS: A Case Study of Ghana using Ghana National Grid. *The Geographical Journal, Vol 166 No 4* , pp. 306-311.

Grove-Rasmissen, J. (2002). *Atmospheric Water Vapour Detection using Satellite GPS Profilling,.* Copenhagen: PhD Thesis Copenhagen University, Faculty of Science, Neils Bohr Institute of Astronomy, Physics and Astronomy.

Hein G.W., B. Eissfeller. (1986). *The Basic Observation Equations of Carrier Phase Measurements to the Global Positioning System Including General Orbit Modeling.* Munich: GPS Research 1985, Institute of Astronomical and Physical Geodesy, Federal Armed Forces University.

Hein, G. W. (2000). From GPS and GLONASS via EGNOS to Galileo – Positioning and Navigation in the Third Millennium. *GPS Solutions Vol 3, No 4* , 39-47.

Henaku, B. (1999). Implementation of GNSS in Africa. *Technical Forum on GNSS, 26 July 1999* . UNISPACE III.

Herring, T. (2003). *Principle of Global Positioning System, Lecture 08.* Retrieved 2008, from http://www.core.org.cn/NR/rdonlyres/Earth--Atmospheric--and-Planetary-Sciences/12-540Principles-of-the-Global-Positioning-SystemSpring2003/BD01DAE4-A216-454A-A1FD-471AF564A2F8/0/12540lec08.pdf

Higgins, M. (2002). Australia's Changing Surveying Infrastructure from Marks in the Ground to Virtual Reference Station . *FIG XXII International Congress, 19-26, April .* Washington DC USA.

Hiroshi, H., M.Saito, T. Iwahashi, S. Usui. (2004). Network based high accuracy real time GPS positioning for GCP correction of high resolution satellite imagery. *IEEE International Conference on Multimedia*, (pp. 1587-1590).

Hofmann-Wallenhof B., H. Lichtenegger, J Collins . (1994). *Global Positioning System; Theory and Practice, Third Revised Edition .* New York: Springler-Verlag Wien, ISBN 3-211-82591-6.

Hudnut, K.W., Y. Bock, J.E. Geletzka, F.H. Webb, W.H. Young . (2001). The Southern California Integrated GPS Network. *The 10th International Symposium on Deformation Measurement, 19-22 March, 2001.* Orange, California, USA.
IERS. (1996). Retrieved 2007, from http://hpiers.obspm.fr/eop-pc

Imakire, T., Y. Nakahori. (2001). GPS Earth Observation Network (GEONET) of Japan. *FIG Working Week 2-11, May 2001. .* Seoul, Korea.

Jain, P. (2008). Indian Satellite Navigation Programme: An update . *45th Session of S&T Subcommittee of UN-COPOUS, 11-22, February, 2008 .* Viena, Austria.

JCAB-Japan. (2003). MSAS (MTSAT Satellite-Based Augmentation System) Status. *11th Air Navigation Conference 22 September - 3 October, 2003.* Montreal, Canada.

Karikari, I. (2006). Ghana's Millennium Challenge Account and the Land Component: A Holistic Approach? . *XXII FIG Congress 8-13 October, 2006.* Munich, Germany.

KASC. (2007). *Signal Transmission by MSAS*. Retrieved January 2009, from http://www.kasc.go.jp_english/msas_01.htm

Kenyon, S. (2006). Gravity Field and the Geoid. *AFREF Technical Workshop 9-13 July, 2006.* University of Cape Town, South Africa.

Kenyon, S., Factor. (2007). *Towards the next Earth Gravity Model.* Retrieved November 4, 2008, from http://earth-info.nima.mil/GandG/wgs84/gravitymod/new_egm/EGM08_papers/EGM-2007-final.pdf

Kibe, S. (2003). Indian Plan for Satellite-based navigation system for civil aviation. *Current Science Vol. 84 No. 11, June 2003* , 1405-1411.

Klobuchar, J. (1996). Ionospheric Effect on GPS. In J. J. Spilker, & B. W. Parkinson, *GPS Theory and Practice, Vol. 1* (pp. 1215-1238).

Kouba, J. P. (2000). *GPS Precise Point Positioning using IGS Orbit Products.* Retrieved October 2007, from http://www.geod.nrcan.gc.ca/publications/papers/pdf/final.pdf

Kouba, J. (2002). Sub-daily Earth rotation parameters and the international GPS service orbit/clock solution products. *Studia Geophysica et Geodaetica 46* , 9-25.

Krueger, E., T. Schueler, G. W. Hein, A. Martellucci, G. Blarzino. (2004). *Galileo Tropospheric Correction Approaches developed within GSTB-V1.* Retrieved August 2007, from http://forchung.unibw-muenchen.de/ainfo.php?&id=518

Kuntu-Mensah, P. (1997). *Land Tenure and Title Registration.* Retrieved March 2006, from http://www.spatial.maine.edu/~onsrud/Landtenure/countryreport/Mensah-ghana.htm

Kuntu-Mensah, P. (2006). On the Implementation of Land Title Registration in Ghana. *5th FIG Regional Conference 8-11 March, 2006.* Accra, Ghana.

Lahaye, F., J. Kouba. (1994). *IGSREPORT-0832 IGS Final Clock Orbit Comb (730).* Retrieved June 2007, from http://www.igs.org/mail/igsreport/1994/msg00146.html

Lambeck, K. (1988). Geophysical Geodesy: The slow Deformation of the Earth. *Oxford Science Pub. Oxford UK* .

References

Landau, H. (1988). *On the use of the Global Positioning System in Geodesy and Geodynamics, Model Formulation, Software Development and Analysis.* Munich, Germany: PhD Dissertation, Federal Armed Forces University.

Landau, H., U. Vollath, X. Chen . (2002). Virtual Reference Station Systems. *Journal of Global Positioning Systems, Vol. 1, No. 2* , 137-143.

Leick, A. (1995). *GPS Satellite Surveying, 2nd Edition, ISBN 0-471-30626-6.* John Wiley and Sons.

Lemmens, M. (2007). Beidou. *GIM International, October 2007* , p. Vol 21 Issue 10.
LINZ. (n.d.). *Earth Geoid Model 1996 (EGM96).* Retrieved May 2007, from Land Information, New Zealand: http://www.linz.govt.nz/geodetic/datums-projections-heights/vertical-datums/earth-gravity-model-1996/index.aspx

Mader, G. (1999). GPS Antenna Calibration at the National Geodetic Survey. *GPS Solutions Vol. 3 No. 1* .

Mannucci, A. J, B. T. Tsurutani, B. A. Iijima, A. Komjathy, A. Saito, W. D. Gonzales, F. L. Guarnieri, J. U. Kozyra and R. Skoug. (2005). *Daytime Global Ionospheric Response to the interplanetary events of 29-30 October, 2003 'Halloween Storms'.* Geophy. Res. Lett., 32, L12S02 doi 10.1029/2004GL021467 .

Marsh, D. (2004). *Numerical Modeling of the stratosphere, Mesosphere and Thermosphere .* Boulder, USA: National Center for Atmospheric Research.

McCarthy, D. D. (1992). *IERS Standards. IERS Technical Note 13.* Paris: Observatoire de Paris.

Mendes, V.B., R.B. Langley. (1995). Zenith Wet Tropospheric Delay Determination Using Prediction Models: Accuracy Analysis. *Cartografia e Cadasto No. 2* , pp. 41-47.

Merry, C. (2003). The African Geoid Project and Its Relevance to the Unification of African Vertical Reference Frames. *2nd FIG Regional Conference, 2-5, December. 2003 .* Marrakech, Morocco.

Minmin, L. (2005). RTCM 3.0 Implementation in South Alberta Network. *18th International Technocal Meeting of the Satellite Division, Institute of Navigation, September 2005.* Long Beach, California, USA.

Misra, P., P. Enge. (2001). *Global Positioning System – Signals, Measurements and Performance.* Lincoln, MA, USA: Gangap-Jamuna Press ISBN 0-9709544-0-9.

Mugnier, C. (2000). Grids and Datum, Republic of Ghana. *Photogrammetric Engineering and Remote Sensing, June* .

Musa, T. A., Samsung, L., & Rizos, C. (2005). Low Latitude troposphere: A preliminary study using GPS CORS data in South East Asia. *National Technical Meeting of the Institute of Navigation.* San Deigo, California USA.

Neilan, R. (2008). *Expert Advice: Reference Frame for Africa*. (Questext US Technology Group) Retrieved December 2008, from www.gpsworld.com: http://www.nxtbook.com/nxtbooks/questex/gps0908/#/10

Neilan, R., Wonnacott, R. (2002). *"Establishing A Continental Reference System in Africa: AFREF" Proposal to International Council for Science on behalf of IUGG/IAG, IGS/IERS and ISPRS.*

NEPAD. (2004). *Infrastructure Short-Term Action Plan (STRAP), Second Review of Implementation Progress and the Way Forward; Continental Synthesis Report.* Retrieved June 2008, from http://www.afdb.org/fileadmin/uploads/afdb/Documents/Project-and-Operations/26006464-EN-STAP-REVIEW-REPORT-FINAL-2004.PDF

Odame-Larbi, W. (2008). *Land Administration in Ghana.* Retrieved December 2008, from http://www.fig.net/commission7/verona_am_2008/ppt/13_sept/10_1_larbi.pdf

Odjik, D. (2002). *Fast Precise GPS Positioning in the Presence of Ionospheric Delays.* Delft, Netherlands: Dissertation, Department of Mathematical Geodesy and Positioning, Delft University ISBN 90-80147-2-7.

O'Keefe, K. (2001). Comparison of Troposphere Mapping Functions. *ENGO Presentation, April 2001.* Calgary, Canada.

ONSALA, S. O. (2007 (Last Update), November 23). *Ocean Tide Loading (OTL)*. (Chalmers University of Technology) Retrieved 2008, from http://www.oso.chalmers.se/~loading/

Pavlis, N. K., Holmes, S. A., Kenyon, S. C., & Factor, J. K. (2008). The EGM2008 Global Gravitation Model. *American Geographic Union, 2008AGUFM.GAO1P.*

Petrovski, I., S. Kawaguchi, H. Torimoto, K. Fuji, M. E. Cannon and G. Lachapelle. (2001). The Issue of Practical Implementation of Commercial RTK Service. *14th International Technical Meeting of the Satellite Division of the Institute of Navigation, September 11-14, 2001.* Salt Lake City, Utah.

Phillips H.A, J.R. Ridgeway, J-B. Minster, D. Yi, C. Bentley. (1999). *Tidal Corrections.* Retrieved April 2007, from Geoscience Laser Altimetry System (GLAS): http://www/csr.utexas.edu/glas/atbd.html

PNDCL152. (1986). *The Land Title Registration Law.* Republic of Ghana.

Poku-Gyamfi, Y. (2000). *Kumasi City Roads Traffic and Transportation Information System .* Kumasi: MPhil Thesis, School of Engineering, Kwame Nkrumah University of Science and Technology.

Poku-Gyamfi, Y; Hein, G.W. (2006). Framework for the Establishment of a Nationwide Network of Global Navigation Satellite System (GNSS) – A Cost-effective Tool for Land Development in Ghana. Accra Ghana: 5th FIG Regional Conference, 8-11, March.

Prah, B. (2004). *The Cadastral LIS as a Tool for Land Conflict Resolution in Rural Communities of Ghana.* Jakarta. Indonesia: 3rd FIG Regional Conference 3-7, October, 2004.

Prasad, N., A. D. Sarma. (2007). Preliminary analysis of grid ionospheric vertical error for GAGAN. *GPS Solution , Vol 11 No. 4*.

Pudder, L. (2006). GNSS in Ghana. *GEO-Connexion International Magazine* .

Ray, J., D. Dong, Z. Altamimi. (2004). IGS Reference Frames: Status and Future Improvements. *Vol. 8 No. 4, pg 251-266.* Springler Berlin/Heidelberg.

Rossbach, U. (2001). *Positioning and Navigation Using the Russian Satellite System GLONASS.* Munich Germany: PhD Thesis,(Studiengang Geodaesie und Geoinformation), Federal Armed Forces University .

SAPOS. (2004). *Satellite Positioning of the German State Survey.* Hannover, Germany: Central Bureau, SAPOS.

Schaer S., W. Gurtner, J Feltens. (1998). IONEX: IONosphere Map EXchange Format Version 1. *Proceedings of the IGS AC Workshop. Febraury 1-11.* Darmstadt, Germany.

Schmid R., P. Steinberger, M. Rothacher. (2005). Benefit from Absolute GPS Antenna Phase Centre Modelling. *COMET-Advances in GPS Data Modelling 9-10, November.* London: Departmant of Geomatic Engineering, University College of London.

Schueler, E. (2008). *Schnelle präzise Positionierung mit GPS und GALILEO unter Nutzung aktiver Referenznetwerke.* München, Germany: Dissertation, Studiengang, Luft und Raumfahrtechnik, Universität der Bundeswehr, November, 2008.

Schueler, T. (2001). *On Ground-based Tropospheric Delay Estimation.* Retrieved 2005, from http://forschung.unibw-muenchen.de/ainfo.php?&id=520

Schueler, T., G.W. Hein, B. Eisfeller. (2001). *Tropospheric Delay Prediction in Wide Area Augmentation Systems Using Numerical Weather Fields:.* Retrieved April 2007

Schueler, T., G.W. Hein, B. Eissfeller. (2000). *Improved Tropospheric Delay Modeling using an Integrated Approach of Numerical Weather Models and GPS.* Retrieved 2007, from http://forschung.unibw-muenchen.de/papers/hcdx94nm3lit3jbxdntetjeswfohsr.pdf

Seebany, D. B., T. Walter, J. Blanch, P. Enge. (2007). *Bounding Higher Order Ionosphere Errors for the Dual Frequency GPS User.* Retrieved 2008, from http://waas.stanford.edu/~wwu/papers/gps/PDF/DattaBaruaIONGNSS06.pdf

Seeber, G. (1993). *Satellite Geodesy. Foundations , Methods and Applications.* Berlin: Walter de Gruyter.

Silayo, E. (2005). Searching for an Affordable and Acceptable Cadastral Survey Method. *From Pharoahs to Geoinformatics - FIG Working Week and GSDI-8, 16-21, Apri,l 2005.* Cairo, Egypt.

Singh, A. (2004). Communication Navigation Surveillance / Air Traffic Management (CNS/ATM) Beyond 2012 . *Map Asia Conference 2004.* Beijing China.

SinoDefence. (2008). *Beidou 1 Satellite Navigation Experimental Systems.* Retrieved January 2009, from http://www.sinodefence.com/space/spacecraft/beidou1.asp

Snow, J. (2007). GPS, WAAS and LAAS UPDATE. *Texas Aviation Conference 19 April 2007.* Corpus Christi, USA.

Somieski, A. C. (2007). Evaluation and Comparison of Different Methods of Ionospheric Delay Mitigation for Future Galileo Mass Market Receivers. *ION GNSS 29th International Technical Meeting of the Satellite Division, 25-28, September 2007.* Fort Worth, Texas, USA.

Spilker, J. J. (1996). Tropospheric Effects on GPS Vol 1. In B. W. Parkinson, J. J. Spilker, & P. P. Axelrad, *Global Positioning System: Theory and Applications* (pp. 517-546). Washington D. C. USA: American Institute of Aeronautics and Astronautics.

Suleiman, N. (2006). The Activities of the National Space Research & Development Agency, Nigeria, in the area of Global Navigation Satellite System (GNSS). *UN/Zambia/ESA GNSS Technologies in SSA Workshop, 26-30 June 2006.* Lusaka Zambia.

Sumio U., Hiroshi H., Junshiro K., Koji W., Satoshi T. (2004). *Nation-Wide RTK-GPS based on FKP method and Applications for Human navigation and Location Based Services.* Retrieved October 26, 2009, from Mitsubishi Electric Company: http://www.mitsubishielectric.co.jp/pas/thesis/ICME1127B.pdf

Takac, F. W. (2008). Smart RTK: A Novel Method of Processing Standardized RTCM Network RTK Information for High Precision Positioning. *ENC GNSS 2008, 22-25 April 2008.* Toulouse, France.

Takeshi, S. (2004). A Decade of GEONET: 1994-2003: The Continuous GPS Observation in Japan and its Impact on Earthquake Studies. *Research News - Earth Planets Space , Vol 56 pg 29-41*.

Teunissen, P. J. G; Odjik, D. (2003). Rank-defect integer eatimation, and phase-only modernized GPS ambiguity solution. *Journal of Geodesy* , pp. 523-536.

Teunissen, P. (1995). The least squares ambiguity decorrelation adjustment: a method for fast GPS integer ambiguity estimation. *Journal of Geodesy. Vol 70 pages 65-82.* Springer Verlag.

Ventura-Traverset, J. (2003). European Geostationary Navigation Overlay Service, EGNOS. *National Technical Meeting of the Institute of Navigation, 22-24 January, 2003.* Anaheim, California, USA.

Ventura-Traverset, J. P. (2001). *Architecture, mission and signal processing aspect of the EGNOS System: the first European implementation of GNSS.* Retrieved 2006, from http://www.egnos-pro.esa.mt/Publications/DSP%202000/EGNOS_DSP2001.pdf

Vermille, H. (2002). Direct transformation from geocentric coordinates to geodetic coordinates. *Journal of Geodesy* , 76: 451-454.

Vollath, U. (2004). The Factorized Multi-Carrier Ambiguity Resolution (FAMCAR) Approach for Efficient Carrier-Phase Ambiguity Estimation. *ION Meeting of the Satellite Division, 21-24 September, 2004.* Long Beach California USA.

Vollath, U., H. Landau, X. Chen;. (n.d.). *Network RTK - Concept and Performance.* Retrieved 2005, from http://www.gpsnet.dk/showimg.php?ID=371

Watson, C., P. Tregoning, R,Coleman. (2006). The Impact of Solid Earth Tide Model on GPS Coordinate and Tropospheric Time Series. *Geophysical Research Letters, AGU , 33(L08306) 1-4*.

Weber, G., H. Gebhard, D. Dettmeing. (2003). Network Transport of RTCM via Internet Protocol (NTRIP);. *IAG Conference*, *2003-7-03, RTCM Paper 167-203/CS104-314.* Sapporro, Japan.

Wegener, V; Wanninger, L. (2005). Communication Options for Network RTK / SAPOS® Realization. *2nd WORKSHOP ON POSITIONING, NAVIGATION AND COMMUNICATION (WPNC'05) & 1st ULTRA-WIDEBAND EXPERT TALK (UET'05)*, (pp. 115-118).

Wonnacott, R. (2007). GNSS as a Multi-Disciplinary Tool for Africa's Development . *ALC2007 on Space Science and Technology 2-4 October , 2007.* Pretoria South Africa.

Wonnacott, R. (2006). The AFREF Project. *International GNSS Service Workshop, 8 May, 2006.* Darmstadt Germany.

Wuebbena, G., & Bagge, A. (2002). *RTCM Message Type 59−FKP for transmission of FKP.* Garbsen Germany: Geo++® White Paper, Nr. 2002.01.

D. APPENDIX

12.3 ACCURACY ANALYSIS OF AREA CORRECTIONS

IONOSPHERE (SATELLITE-SPECIFIC MODE):

Baseline Names	Identifiers and Indices	Satellites Sys PRN	Start [s]	End [s]	Bias [mm]	Std. Dev. [mm]	RMS [mm]	Min [mm]	Max [mm]
KADE (01)	AWAN (04)	G16 G18	11710	13060	90.9	18.7	92.8	25.4	139.2
KADE (01)	AWAN (04)	G16 G22	11710	19680	-0.3	14.3	14.2	102.4	22.1
KADE (01)	AWAN (04)	G16 G03	11710	20060	-1.7	9.8	9.9	-38.8	24.2
ACRA (02)	AWAN (04)	G16 G22	11710	19680	-0.3	14.3	14.2	-102.4	22.1
ACRA (02)	AWAN (04)	G16 G03	11710	20060	-1.7	9.8	9.9	-38.8	24.2
ASFO (03)	AWAN (04)	G16 G18	11710	13060	90.9	18.7	92.8	25.4	139.2
ASFO (03)	AWAN (04)	G16 G22	11710	19680	-0.3	14.3	14.2	-102.4	22.1
ASFO (03)	AWAN (04)	G16 G31	11710	14210	2.3	13.7	13.9	-27.9	40.0
ASFO (03)	AWAN (04)	G16 G03	11710	20060	-1.7	9.8	9.9	-38.8	24.2
KADE (01)	AWAN (04)	G16 G19	14680	20060	-7.7	15.5	17.3	-69.8	46.7
ACRA (02)	AWAN (04)	G16 G19	14680	20060	-7.7	15.5	17.3	-69.8	46.7
ASFO (03)	AWAN (04)	G16 G19	14680	20060	-7.7	15.5	17.3	-69.8	46.7
KADE (01)	AWAN (04)	G16 G11	16700	20060	-13.3	16.6	21.3	-75.0	26.2
ACRA (02)	AWAN (04)	G16 G11	16700	20060	-13.3	16.6	21.3	-75.0	26.2
ASFO (03)	AWAN (04)	G16 G11	16700	20060	-13.3	16.6	21.3	-75.0	26.2
KADE (01)	AWAN (04)	G16 G20	17480	20060	1.5	12.6	12.7	-26.3	31.1
ACRA (02)	AWAN (04)	G16 G20	17480	20060	1.5	12.6	12.7	-26.3	31.1
ASFO (03)	AWAN (04)	G16 G20	17480	20060	1.5	12.6	12.7	-26.3	31.1
ACRA (02)	AWAN (04)	G16 G14	18730	20060	703.0	22.2	703.4	653.8	759.8
KADE (01)	AWAN (04)	G03 G20	20070	25480	-3.3	7.4	8.1	-25.0	16.0
KADE (01)	AWAN (04)	G03 G01	20070	25480	2.0	9.8	10.0	-20.1	25.2
KADE (01)	AWAN (04)	G03 G19	20070	25480	-2.3	8.5	8.8	-23.4	21.8
KADE (01)	AWAN (04)	G03 G11	20070	25480	-5.0	12.9	13.8	-39.6	35.0
KADE (01)	AWAN (04)	G03 G16	20070	22980	3.2	11.4	11.8	-36.3	34.0
ACRA (02)	AWAN (04)	G03 G20	20070	25480	-3.3	7.4	8.1	-25.0	16.0
ACRA (02)	AWAN (04)	G03 G01	20070	25480	2.0	9.8	10.0	-20.1	25.2
ACRA (02)	AWAN (04)	G03 G19	20070	25480	-2.3	8.5	8.8	-23.4	21.8
ACRA (02)	AWAN (04)	G03 G11	20070	25480	-5.0	12.9	13.8	-39.6	35.0
ACRA (02)	AWAN (04)	G03 G16	20070	22980	3.2	11.4	11.8	-36.3	34.0
ASFO (03)	AWAN (04)	G03 G20	20070	25480	-3.3	7.4	8.1	-25.0	16.0
ASFO (03)	AWAN (04)	G03 G01	20070	25480	2.0	9.8	10.0	-20.1	25.2
ASFO (03)	AWAN (04)	G03 G19	20070	25480	-2.3	8.5	8.8	-23.4	21.8
ASFO (03)	AWAN (04)	G03 G11	20070	25480	-5.8	13.1	14.3	-39.6	35.0
ASFO (03)	AWAN (04)	G03 G16	20070	22980	3.2	11.4	11.8	-36.3	34.0
KADE (01)	AWAN (04)	G03 G23	24530	25480	-4.2	12.7	13.3	-42.8	20.1
ACRA (02)	AWAN (04)	G03 G23	24530	25480	-4.2	12.7	13.3	-42.8	20.1
ASFO (03)	AWAN (04)	G03 G23	24530	25480	-4.2	12.7	13.3	-42.8	20.1
KADE (01)	AWAN (04)	G19 G20	25490	29840	-0.7	9.8	9.9	-22.7	21.7
KADE (01)	AWAN (04)	G19 G01	25490	29840	5.3	12.2	13.3	-69.0	37.2
KADE (01)	AWAN (04)	G19 G23	25490	29840	3.6	9.6	10.3	-18.1	22.7
KADE (01)	AWAN (04)	G19 G11	25490	29840	-0.6	15.3	15.3	-36.2	42.7
KADE (01)	AWAN (04)	G19 G03	25490	29840	5.3	11.3	12.5	-15.4	47.3
ACRA (02)	AWAN (04)	G19 G20	25490	29840	-0.7	9.8	9.9	-22.7	21.7
ACRA (02)	AWAN (04)	G19 G01	25490	29620	5.4	11.7	12.9	-31.1	37.2
ACRA (02)	AWAN (04)	G19 G23	25490	29840	3.6	9.6	10.3	-18.1	22.7
ACRA (02)	AWAN (04)	G19 G11	25490	29840	-0.6	15.3	15.3	-36.2	42.7
ACRA (02)	AWAN (04)	G19 G03	25490	29840	5.3	11.3	12.5	-15.4	47.3
ASFO (03)	AWAN (04)	G19 G20	25490	29840	-0.7	9.8	9.9	-22.7	21.7
ASFO (03)	AWAN (04)	G19 G01	25490	29840	5.3	12.2	13.3	-69.0	37.2
ASFO (03)	AWAN (04)	G19 G23	25490	29840	3.6	9.6	10.3	-18.1	22.7
ASFO (03)	AWAN (04)	G19 G11	25490	29840	-0.6	15.3	15.3	-36.2	42.7

ASFO (03)	AWAN (04)	G19	G03	25490	29840	5.3	11.3	12.5	-15.4	47.3
KADE (01)	AWAN (04)	G19	G13	28490	29840	8.2	9.1	12.2	-24.4	23.8
ACRA (02)	AWAN (04)	G19	G13	28490	29840	8.2	9.1	12.2	-24.4	23.8
ASFO (03)	AWAN (04)	G19	G13	28490	29840	8.2	9.1	12.2	-24.4	23.8
KADE (01)	AWAN (04)	G23	G20	29850	32830	0.5	8.6	8.6	-18.9	28.5
KADE (01)	AWAN (04)	G23	G13	29850	32830	4.0	8.7	9.5	-15.1	32.8
KADE (01)	AWAN (04)	G23	G19	29850	32830	11.3	9.6	14.8	-13.7	33.0
KADE (01)	AWAN (04)	G23	G11	29850	32830	4.9	8.4	9.7	-15.6	27.1
KADE (01)	AWAN (04)	G23	G03	29850	31930	104.7	14.9	105.7	71.5	135.3
ACRA (02)	AWAN (04)	G23	G20	29850	32830	0.5	8.6	8.6	-18.9	28.5
ACRA (02)	AWAN (04)	G23	G13	29850	32830	4.0	8.7	9.5	-15.1	32.8
ACRA (02)	AWAN (04)	G23	G19	29850	32830	11.3	9.6	14.8	-13.7	33.0
ACRA (02)	AWAN (04)	G23	G11	29850	32830	4.9	8.4	9.7	-15.6	27.1
ACRA (02)	AWAN (04)	G23	G03	29850	31930	21.3	14.9	26.0	-11.9	52.0
ASFO (03)	AWAN (04)	G23	G20	29850	32830	0.5	8.6	8.6	-18.9	28.5
ASFO (03)	AWAN (04)	G23	G13	29850	32830	4.0	8.7	9.5	-15.1	32.8
ASFO (03)	AWAN (04)	G23	G19	29850	32830	11.3	9.6	14.8	-13.7	33.0
ASFO (03)	AWAN (04)	G23	G11	29850	32830	4.9	8.4	9.7	-15.6	27.1
ACRA (02)	AWAN (04)	G23	G25	31460	32830	3.2	15.3	15.5	-26.8	38.4
ASFO (03)	AWAN (04)	G23	G25	31460	32830	3.2	15.3	15.5	-26.8	38.4
KADE (01)	AWAN (04)	G02	G10	53310	54900	1.0	9.6	9.6	-15.9	18.0
KADE (01)	AWAN (04)	G02	G04	53310	54900	1.0	25.0	25.0	-39.2	55.6
ACRA (02)	AWAN (04)	G02	G10	53310	54900	1.0	9.6	9.6	-15.9	18.0
ACRA (02)	AWAN (04)	G02	G04	53310	54900	1.0	25.0	25.0	-39.2	55.6
ASFO (03)	AWAN (04)	G02	G10	53310	54900	1.0	9.6	9.6	-15.9	18.0
ASFO (03)	AWAN (04)	G02	G04	53310	54900	1.0	25.0	25.0	-39.2	55.6
KADE (01)	AWAN (04)	G02	G28	53320	54900	1.9	11.7	11.8	-19.2	32.6
ACRA (02)	AWAN (04)	G02	G28	53320	54900	1.9	11.7	11.8	-19.2	32.6
ASFO (03)	AWAN (04)	G02	G28	53320	54900	1.9	11.7	11.8	-19.2	32.6
AVERAGE VALUES						13.3	12.2	24.7	-102.4	759.8

Baseline Ids Names and Indices		Satellites Sys	PRN	Start [s]	End [s]	Bias [mm]	Std.Dev. [mm]	RMS [mm]	Min [mm]	Max [mm]
KADE (01)	AWAN (04)	G16	G18	11710	13060	-13.2	30.5	33.0	-75.9	101.7
KADE (01)	AWAN (04)	G16	G22	11710	19680	29.0	17.9	34.1	-19.0	105.4
KADE (01)	AWAN (04)	G16	G03	11710	20060	19.7	16.1	25.4	-28.9	68.0
ACRA (02)	AWAN (04)	G16	G22	11710	19680	29.0	17.9	34.1	-19.0	105.4
ACRA (02)	AWAN (04)	G16	G03	11710	20060	19.7	16.1	25.4	-28.9	68.0
ASFO (03)	AWAN (04)	G16	G18	11710	13060	-13.2	30.5	33.0	-75.9	101.7
ASFO (03)	AWAN (04)	G16	G22	11710	19680	29.0	17.9	34.1	-19.0	105.4
ASFO (03)	AWAN (04)	G16	G31	11710	14210	44.8	39.2	59.5	-18.2	139.6
ASFO (03)	AWAN (04)	G16	G03	11710	20060	19.7	16.1	25.4	-28.9	68.0
KADE (01)	AWAN (04)	G16	G19	14680	20060	24.7	30.3	39.0	-43.3	135.3
ACRA (02)	AWAN (04)	G16	G19	14680	20060	24.7	30.3	39.0	-43.3	135.3
ASFO (03)	AWAN (04)	G16	G19	14680	20060	24.7	30.3	39.0	-43.3	135.3
KADE (01)	AWAN (04)	G16	G11	16700	20060	9.9	33.9	35.2	-70.1	98.2
ACRA (02)	AWAN (04)	G16	G11	16700	20060	9.9	33.9	35.2	-70.1	98.2
ASFO (03)	AWAN (04)	G16	G11	16700	20060	9.9	33.9	35.2	-70.1	98.2
KADE (01)	AWAN (04)	G16	G20	17480	20060	9.8	26.5	28.2	-37.3	60.8
ACRA (02)	AWAN (04)	G16	G20	17480	20060	9.8	26.5	28.2	-37.3	60.8
ASFO (03)	AWAN (04)	G16	G20	17480	20060	9.8	26.5	28.2	-37.3	60.8
ACRA (02)	AWAN (04)	G16	G14	18730	20060	8.7	54.1	54.5	-77.5	118.4
KADE (01)	AWAN (04)	G03	G20	20070	25480	-17.2	10.7	20.2	-46.7	15.3
KADE (01)	AWAN (04)	G03	G01	20070	25480	16.4	11.3	19.9	-11.8	47.4
KADE (01)	AWAN (04)	G03	G19	20070	25480	-0.3	11.2	11.2	-25.9	33.2
KADE (01)	AWAN (04)	G03	G11	20070	25480	10.4	16.5	19.5	-30.2	76.9
KADE (01)	AWAN (04)	G03	G16	20070	22980	27.5	29.7	40.4	-28.1	103.0
ACRA (02)	AWAN (04)	G03	G20	20070	25480	-17.2	10.7	20.2	-46.7	15.3
ACRA (02)	AWAN (04)	G03	G01	20070	25480	16.4	11.3	19.9	-11.8	47.4

ACRA (02)	AWAN (04)	G03 G19	20070	25480	-0.3	11.2	11.2	-25.9	33.2
ACRA (02)	AWAN (04)	G03 G11	20070	25480	10.4	16.5	19.5	-30.2	76.9
ACRA (02)	AWAN (04)	G03 G16	20070	22980	27.5	29.7	40.4	-28.1	103.0
ASFO (03)	AWAN (04)	G03 G20	20070	25480	-17.2	10.7	20.2	-46.7	15.3
ASFO (03)	AWAN (04)	G03 G01	20070	25480	16.4	11.3	19.9	-11.8	47.4
ASFO (03)	AWAN (04)	G03 G19	20070	25480	-0.3	11.2	11.2	-25.9	33.2
ASFO (03)	AWAN (04)	G03 G11	20070	25480	8.6	17.4	19.4	-30.2	76.9
ASFO (03)	AWAN (04)	G03 G16	20070	22980	27.5	29.7	40.4	-28.1	103.0
KADE (01)	AWAN (04)	G03 G23	24530	25480	13.0	16.0	20.6	-33.3	41.7
ACRA (02)	AWAN (04)	G03 G23	24530	25480	13.0	16.0	20.6	-33.3	41.7
ASFO (03)	AWAN (04)	G03 G23	24530	25480	13.0	16.0	20.6	-33.3	41.7
KADE (01)	AWAN (04)	G19 G20	25490	29840	-6.3	10.0	11.8	-31.3	16.9
KADE (01)	AWAN (04)	G19 G01	25490	29840	31.1	15.8	34.8	-27.1	92.0
KADE (01)	AWAN (04	G19 G23	25490	29840	-0.9	13.5	13.5	-25.7	42.5
KADE (01)	AWAN (04)	G19 G11	25490	29840	10.4	13.2	16.8	-22.2	44.5
KADE (01)	AWAN (04)	G19 G03	25490	29840	17.3	11.5	20.8	-5.0	61.5
ACRA (02)	AWAN (04)	G19 G20	25490	29840	-6.3	10.0	11.8	-31.3	16.9
ACRA (02)	AWAN (04)	G19 G01	25490	29620	31.2	15.5	34.8	-8.4	92.0
ACRA (02)	AWAN (04)	G19 G23	25490	29840	-0.9	13.5	13.5	-25.7	42.5
ACRA (02)	AWAN (04)	G19 G11	25490	29840	10.4	13.2	16.8	-22.2	44.5
ACRA (02)	AWAN (04)	G19 G03	25490	29840	17.3	11.5	20.8	-5.0	61.5
ASFO (03)	AWAN (04)	G19 G20	25490	29840	-6.3	10.0	11.8	-31.3	16.9
ASFO (03)	AWAN (04)	G19 G01	25490	29840	31.1	15.8	34.8	-27.1	92.0
ASFO (03)	AWAN (04)	G19 G23	25490	29840	-0.9	13.5	13.5	-25.7	42.5
ASFO (03)	AWAN (04)	G19 G11	25490	29840	10.4	13.2	16.8	-22.2	44.5
ASFO (03)	AWAN (04)	G19 G03	25490	29840	17.3	11.5	20.8	-5.0	61.5
KADE (01)	AWAN (04)	G19 G13	28490	29840	30.1	13.6	33.0	-4.7	56.9
ACRA (02)	AWAN (04)	G19 G13	28490	29840	30.1	13.6	33.0	-4.7	56.9
ASFO (03)	AWAN (04)	G19 G13	28490	29840	30.1	13.6	33.0	-4.7	56.9
KADE (01)	AWAN (04)	G23 G20	29850	32830	19.8	10.1	22.2	-1.6	40.8
KADE (01)	AWAN (04)	G23 G13	29850	32830	8.4	7.9	11.5	-13.2	31.5
KADE (01)	AWAN (04)	G23 G19	29850	32830	26.4	11.2	28.7	4.9	66.0
KADE (01)	AWAN (04)	G23 G11	29850	32830	24.9	8.8	26.5	5.2	47.0
KADE (01)	AWAN (04)	G23 G03	29850	31930	-44.2	32.0	54.5	-102.5	44.0
ACRA (02)	AWAN (04)	G23 G20	29850	32830	19.8	10.1	22.2	-1.6	40.8
ACRA (02)	AWAN (04)	G23 G13	29850	32830	8.4	7.9	11.5	-13.2	31.5
ACRA (02)	AWAN (04)	G23 G19	29850	32830	26.4	11.2	28.7	4.9	66.0
ACRA (02)	AWAN (04)	G23 G11	29850	32830	24.9	8.8	26.5	5.2	47.0
ACRA (02)	AWAN (04)	G23 G03	29850	31930	62.7	32.0	70.4	4.4	151.0
ASFO (03)	AWAN (04)	G23 G20	29850	32830	19.8	10.1	22.2	-1.6	40.8
ASFO (03)	AWAN (04)	G23 G13	29850	32830	8.4	7.9	11.5	-13.2	31.5
ASFO (03)	AWAN (04)	G23 G19	29850	32830	26.4	11.2	28.7	4.9	66.0
ASFO (03)	AWAN (04)	G23 G11	29850	32830	24.9	8.8	26.5	5.2	47.0
ACRA (02)	AWAN (04)	G23 G25	31460	32830	44.5	21.6	49.4	5.7	91.7
ASFO (03)	AWAN (04)	G23 G25	31460	32830	44.5	21.6	49.4	5.7	91.7
KADE (01)	AWAN (04)	G02 G10	53310	54900	17.5	11.4	20.8	-12.5	43.0
KADE (01)	AWAN (04)	G02 G04	53310	54900	14.7	13.7	20.1	-21.4	41.7
ACRA (02)	AWAN (04)	G02 G10	53310	54900	17.5	11.4	20.8	-12.5	43.0
ACRA (02)	AWAN (04)	G02 G04	53310	54900	14.7	13.7	20.1	-21.4	41.7
ASFO (03)	AWAN (04)	G02 G10	53310	54900	17.5	11.4	20.8	-12.5	43.0
ASFO (03)	AWAN (04)	G02 G04	53310	54900	14.7	13.7	20.1	-21.4	41.7
KADE (01)	AWAN (04)	G02 G28	53320	54900	22.4	11.5	25.2	-7.1	45.5
ACRA (02)	AWAN (04)	G02 G28	53320	54900	22.4	11.5	25.2	-7.1	45.5
ASFO (03)	AWAN (04)	G02 G28	53320	54900	22.4	11.5	25.2	-7.1	45.5
AVERAGE VALUES					15.1	17.2	26.8	-102.5	151.0

TROPOSPHERE (STATION-SPECIFIC MODE):

Baseline Ids Names and Indices		Satellites Sys PRN		Start [s]	End [s]	Bias [mm]	Std.Dev. [mm]	RMS [mm]	Min [mm]	Max [mm]
KADE (01)	AWAN (04)	G16	G18	11710	13060	-14.0	32.9	35.6	-83.7	108.9
KADE (01)	AWAN (04)	G16	G22	11710	19680	29.7	19.3	35.4	-19.1	115.2
KADE (01)	AWAN (04)	G16	G03	11710	20060	19.5	17.0	25.9	-32.0	72.4
ACRA (02)	AWAN (04)	G16	G22	11710	19680	27.2	17.8	32.5	-29.2	96.2
ACRA (02)	AWAN (04)	G16	G03	11710	20060	16.7	16.4	23.4	-29.8	69.2
ASFO (03)	AWAN (04)	G16	G18	11710	13060	-15.7	24.7	29.2	-62.7	94.4
ASFO (03)	AWAN (04)	G16	G22	11710	19680	26.7	16.1	31.2	-15.6	87.3
ASFO (03)	AWAN (04)	G16	G31	11710	14210	39.9	38.0	55.0	-25.9	136.0
ASFO (03)	AWAN (04)	G16	G03	11710	20060	23.2	18.5	29.7	-23.3	69.4
KADE (01)	AWAN (04)	G16	G19	14680	20060	23.6	31.6	39.4	-45.1	131.1
ACRA (02)	AWAN (04)	G16	G19	14680	20060	22.2	29.4	36.8	-49.0	152.8
ASFO (03)	AWAN (04)	G16	G19	14680	20060	30.9	35.9	47.4	-47.7	159.2
KADE (01)	AWAN (04)	G16	G11	16700	20060	7.6	35.2	35.9	-75.3	105.2
ACRA (02)	AWAN (04)	G16	G11	16700	20060	11.7	31.0	33.1	-62.2	98.9
ASFO (03)	AWAN (04)	G16	G11	16700	20060	14.2	33.8	36.6	-69.5	98.6
KADE (01)	AWAN (04)	G16	G20	17480	20060	9.1	28.0	29.4	-44.4	62.7
ACRA (02)	AWAN (04)	G16	G20	17480	20060	10.9	24.4	26.7	-36.5	69.4
ASFO (03)	AWAN (04)	G16	G20	17480	20060	9.8	24.4	26.2	-35.6	58.0
ACRA (02)	AWAN (04)	G16	G14	18730	20060	5.1	51.1	51.1	-86.6	103.4
KADE (01)	AWAN (04)	G03	G20	20070	25480	-18.8	11.8	22.2	-51.9	17.2
KADE (01)	AWAN (04)	G03	G01	20070	25480	15.8	11.9	19.7	-15.7	50.7
KADE (01)	AWAN (04)	G03	G19	20070	25480	-0.4	12.1	12.1	-30.3	36.8
KADE (01)	AWAN (04)	G03	G11	20070	25480	8.7	18.1	20.1	-33.8	80.5
KADE (01)	AWAN (04)	G03	G16	20070	22980	26.2	30.2	39.9	-34.3	103.9
ACRA (02)	AWAN (04)	G03	G20	20070	25480	-13.0	10.0	16.4	-35.0	17.5
ACRA (02)	AWAN (04)	G03	G01	20070	25480	15.8	12.0	19.9	-19.1	46.3
ACRA (02)	AWAN (04)	G03	G19	20070	25480	0.2	11.2	11.2	-26.3	33.2
ACRA (02)	AWAN (04)	G03	G11	20070	25480	12.1	20.0	23.3	-42.0	86.7
ACRA (02)	AWAN (04)	G03	G16	20070	22980	26.2	27.5	38.0	-20.0	103.7
ASFO (03)	AWAN (04)	G03	G20	20070	25480	-17.8	10.9	20.9	-45.8	18.1
ASFO (03)	AWAN (04)	G03	G01	20070	25480	19.3	12.3	22.9	-17.4	51.3
ASFO (03)	AWAN (04)	G03	G19	20070	25480	-1.3	10.5	10.6	-21.9	34.2
ASFO (03)	AWAN (04)	G03	G11	20070	25480	3.7	16.5	16.9	-49.9	59.8
ASFO (03)	AWAN (04)	G03	G16	20070	22980	31.3	30.5	43.7	-24.0	99.3
KADE (01)	AWAN (04)	G03	G23	24530	25480	12.1	16.7	20.6	-38.6	40.4
ACRA (02)	AWAN (04)	G03	G23	24530	25480	9.4	15.2	17.8	-33.5	44.8
ASFO (03)	AWAN (04)	G03	G23	24530	25480	13.4	16.1	20.9	-24.3	41.9
KADE (01)	AWAN (04)	G19	G20	25490	29840	-6.8	10.8	12.7	-34.6	18.2
KADE (01)	AWAN (04)	G19	G01	25490	29840	32.4	16.4	36.3	-27.5	94.3
KADE (01)	AWAN (04)	G19	G23	25490	29840	-1.5	13.9	14.0	-29.2	44.5
KADE (01)	AWAN (04)	G19	G11	25490	29840	11.2	14.3	18.1	-22.4	45.9
KADE (01)	AWAN (04)	G19	G03	25490	29840	17.0	12.2	21.0	-7.5	66.0
ACRA (02)	AWAN (04)	G19	G20	25490	29840	-3.2	10.5	10.9	-29.2	21.4
ACRA (02)	AWAN (04)	G19	G01	25490	29620	30.1	16.0	34.0	-9.5	86.7
ACRA (02)	AWAN (04)	G19	G23	25490	29840	1.7	13.3	13.4	-25.7	43.1
ACRA (02)	AWAN (04)	G19	G11	25490	29840	10.5	14.3	17.7	-29.8	48.6
ACRA (02)	AWAN (04)	G1	G03	25490	29840	18.7	11.0	21.7	-6.5	51.9
ASFO (03)	AWAN (04)	G19	G20	25490	29840	-7.9	10.8	13.4	-35.0	22.5
ASFO (03)	AWAN (04)	G19	G01	25490	29840	29.7	15.9	33.7	-19.6	95.6
ASFO (03)	AWAN (04)	G19	G23	25490	29840	-1.2	13.9	14.0	-37.5	41.0
ASFO (03)	AWAN (04)	G19	G11	25490	29840	11.7	14.3	18.4	-25.2	48.3
ASFO (03)	AWAN (04)	G19	G03	25490	29840	18.8	12.5	22.6	-7.0	69.9
KADE (01)	AWAN (04)	G19	G13	28490	29840	29.1	14.1	32.3	-6.7	58.5
ACRA (02)	AWAN (04)	G19	G13	28490	29840	33.1	13.7	35.8	9.2	64.2
ASFO (03)	AWAN (04)	G19	G13	28490	29840	33.7	15.9	37.2	-5.2	67.9
KADE (01)	AWAN (04)	G23	G20	29850	32830	20.5	10.7	23.1	-3.0	42.7
KADE (01)	AWAN (04)	G23	G13	29850	32830	8.4	8.8	12.2	-16.6	33.7
KADE (01)	AWAN (04)	G23	G19	29850	32830	27.7	11.9	30.1	2.8	67.0

KADE (01)	AWAN (04)	G23	G11	29850	32830	26.6	9.5	28.3	1.3	52.9
KADE (01)	AWAN (04)	G23	G03	29850	31930	-43.0	32.3	53.7	-100.6	53.0
ACRA (02)	AWAN (04)	G23	G20	29850	32830	23.1	12.0	26.0	-7.9	47.5
ACRA (02)	AWAN (04)	G23	G13	29850	32830	10.1	9.0	13.5	-14.9	36.4
ACRA (02)	AWAN (04)	G23	G19	29850	32830	23.7	12.8	26.9	-0.5	71.9
ACRA (02)	AWAN (04)	G23	G11	29850	32830	22.9	9.7	24.9	-4.2	46.8
ACRA (02)	AWAN (04)	G23	G03	29850	31930	61.7	37.0	71.9	-4.4	173.0
ASFO (03)	AWAN (04)	G23	G20	29850	32830	18.5	12.3	22.3	-9.0	52.8
ASFO (03)	AWAN (04)	G23	G13	29850	32830	7.3	8.4	11.2	-11.3	28.2
ASFO (03)	AWAN (04)	G23	G19	29850	32830	27.9	10.8	29.9	6.3	65.2
ASFO (03)	AWAN (04)	G23	G11	29850	32830	22.7	10.2	24.9	-6.0	48.4
ACRA (02)	AWAN (04)	G23	G25	31460	32830	48.2	21.1	52.6	9.7	97.7
ASFO (03)	AWAN (04)	G23	G25	31460	32830	41.4	21.8	46.7	-0.9	91.2
KADE (01)	AWAN (04)	G02	G10	53310	54900	19.3	13.5	23.5	-13.4	51.8
KADE (01)	AWAN (04)	G02	G04	53310	54900	16.1	15.3	22.2	-23.6	45.4
ACRA (02)	AWAN (04)	G02	G10	53310	54900	14.7	10.2	17.9	-11.9	40.6
ACRA (02)	AWAN (04)	G02	G04	53310	54900	11.4	11.7	16.3	-19.2	44.3
ASFO (03)	AWAN (04)	G02	G10	53310	54900	15.3	11.2	19.0	-12.7	41.8
ASFO (03)	AWAN (04)	G02	G04	53310	54900	15.6	15.9	22.3	-19.6	56.6
KADE (01)	AWAN (04)	G02	G28	53320	54900	21.6	13.1	25.3	-14.1	47.7
ACRA (02)	AWAN (04)	G02	G28	53320	54900	23.6	10.5	25.8	-0.6	44.6
ASFO (03)	AWAN (04)	G02	G28	53320	54900	24.4	10.2	26.4	1.0	54.8
AVERAGE VALUES						15.1	17.7	27.0	-100.6	173.0

Field Data Sheet

GEODETIC REFERENCE NETWORK (GRN) FIELD SHEET			
Date		Location	
Day of year		Weather Desdription	
Receiver type		Serial number of receiver	
Observation Station		Station identity	
Observer		Logging interval	
Pillar type		Pillar Condition	
Observation start time		Observation end time	
Instrument Height Height 1…… Height 2…… Height 3…… Height (mean)…….		Comments:	

Site Sketch:

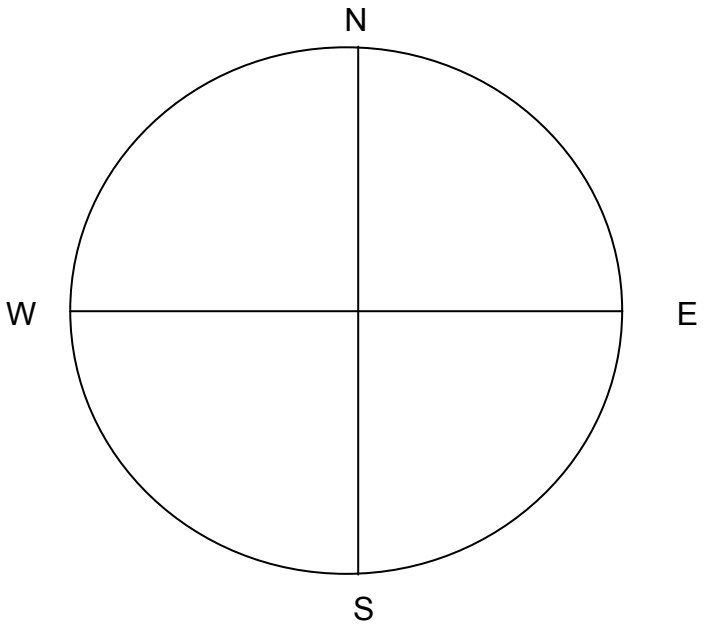

12.4 PREPOS SINEX File (Combined Network Results)

```
*SOLUTION INDEPENDENT EXCHANGE FORMAT (SINEX) FOR SPACE GEODESY
* - SINEX VERSION 1.00
* - TECHNIQUE IS GPS (P)
*-------------------------------------------------------------------
+FILE/REFERENCE
 DESCRIPTION        GRN SURVEY DEPT GHANA
 OUTPUT             COMBINED NETWORK RESULTS
 CONTACT            YAW POKU-GYAMFI
 SOFTWARE           PREPOS GNSS SUITE - MODULE GTCE/DITON
 HARDWARE           NOT SPECIFIED
 INPUT              SINEX FILE (COORDINATE SOLUTION/X)
-FILE/REFERENCE
*-------------------------------------------------------------------
+INPUT/ACKNOWLEDGMENTS
*AGY
DESCRIPTION_____________________________________________________________
 CCC GRN SURVEY DEPT GHANA
-INPUT/ACKNOWLEDGMENTS
*-------------------------------------------------------------------
SITE/ID
*CODE  PT DOMES_     T  STN  Description    APP_LON      APP_LAT        APP_H
 ACRA  A    ACRA     P  ACRA       ACRA      5 35 26.8    - 0 10 56.8     84.2
 NKLG  A  32809M002  P  NKLG    32809M002    0 21 14.1      9 40 19.7     31.5
 MAS1  A  31303M002  P  MAS1    31303M002   27 45 49.5    - 15 37 59.8    197.2
 KMSI  A  KMSI       P  KMSI       KMSI      6 42 37.4    - 1 31 41.2     311.0
 TADI  A  TADI       P  TADI       TADI      4 53 55.4    - 1 45  9.4     62.0
 KADE  A  KADE       P  KADE       KADE      6  6 25.4    - 0 50 12.7     182.8
 ASFO  A  ASFO       P  ASFO       ASFO      5 42  1.7    - 1 16 46.3     189.2
-SITE/ID
*-------------------------------------------------------------------
+SITE/RECEIVER
*
SITE   PT SOLN T DATA_START      DATA_END        DESCRIPTION    S/N      FIRMWARE
 ACRA    A   P   07:141:00000    07:141:86390        RT2                   2.111
 NKLG    A   P   07:141:00030    07:141:82800   TRIM 4000SSI    3919   Nav 7.29 Si
 MAS1    A   P   07:141:00000    07:141:86390     ASH Z-XII3     0    NAV CD00, 1
 KMSI    A   P   07:141:00000    07:141:86390        RT2         0         2.111
 TADI    A   P   07:141:00000    07:141:86390        RT2         0         2.111
 KADE    A   P   07:141:00000    07:141:86390        RT2         0         2.111
 ASFO    A   P   07:144:00000    07:144:86390        RT2         0         2.111

-SITE/RECEIVER
*-------------------------------------------------------------------
+SITE/ANTENNA
*SITE   PT SOLN T  DATA_START      DATA_END     DESCRIPTION   S/N
 ACRA   A   P     07:141:00000    07:141:86390    SOK702        0
 NKLG   A   P     07:141:00030    07:141:82800   TRM29659.00   2201
 MAS1   A   P     07:141:00000    07:141:86390    AOAD/M_T     271
 KMSI   A   P     07:141:00000    07:141:86390    SOK702        0
 TADI   A   P     07:141:00000    07:141:86390    SOK702        0
 KADE   A   P     07:141:00000    07:141:86390    SOK702        0
 ASFO   A   P     07:144:00000    07:144:86390    SOK702        0
-SITE/ANTENNA
*-------------------------------------------------------------------


+SITE/GPS_PHASE_CENTER
```

```
*                    UP_    NORTH_ EAST       UP_  NORTH_ EAST__
*DESCRIPTION S/N     L1->ARP(M)             L2->ARP(M)     AZ_EL
   SOK702          0 0.0684 0.0030-0.0010  0.0709-0.0006-0.0014    ABSO_NGS
 TRM29659.00  2201   0.0910 0.0018 0.0000  0.1201 0.0011 0.0000    ABSO_NGS
 AOAD/M_T      271   0.0912 0.0006-0.0005  0.1201-0.0001-0.0006    ABSO_NGS
  SOK702           0 0.0684 0.0030-0.0010  0.0709-0.0006-0.0014    ABSO_NGS
  SOK702           0 0.0684 0.0030-0.0010  0.0709-0.0006-0.0014    ABSO_NGS
  SOK702           0 0.0684 0.0030-0.0010  0.0709-0.0006-0.0014    ABSO_NGS
  SOK702           0 0.0684 0.0030-0.0010  0.0709-0.0006-0.0014    ABSO_NGS
-SITE/GPS_PHASE_CENTER
*------------------------------------------------------------------------
+SITE/ECCENTRICITY
*                                                    UP     NORTH    EAST
*SITE  PT SOLN T DATA_START__   DATA_END_    AXE ARP->BENCHMARK(M)
 ACRA   A   P   07:141:00000   07:141:86390  UNE 0.1000  0.0000  0.0000
 NKLG   A   P   07:141:00030   07:141:82800  UNE 3.1090  0.0000  0.0000
 MAS1   A   P   07:141:00000   07:141:86390  UNE 0.0330  0.0000  0.0000
 KMSI   A   P   07:141:00000   07:141:86390  UNE 0.1000  0.0000  0.0000
 TADI   A   P   07:141:00000   07:141:86390  UNE 0.1000  0.0000  0.0000
 KADE   A   P   07:141:00000   07:141:86390  UNE 1.4620  0.0000  0.0000
 ASFO   A   P   07:144:00000   07:144:86390  UNE 1.5250  0.0000  0.0000
-SITE/ECCENTRICITY
*------------------------------------------------------------------------

+SOLUTION/EPOCHS
*CODE PT SOLN T _  DATA_START_ __ DATA_END__ _       MEAN_EPOCH_
 ACRA   A 1  P    07:142:86395   07:142:86395       07:142:86395
 NKLG   A 1  P    07:142:86395   07:42:86395        07:142:86395
 MAS1   A 1  P    07:142:86395   07:142:86395       07:142:86395
 KMSI   A 1  P    07:142:86395   07:142:86395       07:142:86395
 TADI   A 1  P    07:142:86395   07:142:86395       07:142:86395
 KADE   A 1  P    07:142:86395   07:142:86395       07:142:86395
 ASFO   A 1  P    07:142:86395   07:144:43195       07:143:64795
-SOLUTION/EPOCHS
*------------------------------------------------------------------------
+SOLUTION/ESTIMATE
 IND  TYPE   CODE  PT SOLN   REF_EPOCH_    UNITS     ESTIMATED VALUE      STD_DEV
1    STAX   ACRA  A     1 07:142:86395 m    1    6348052.68133245   0.004959
2    STAY   ACRA  A     1 07:142:86395 m    1     -20212.88223989   0.004092
3    STAZ   ACRA  A     1 07:142:86395 m    1     617243.59690209   0.002139
4    STAX   NKLG  A     1 07:142:86395 m    1    6287385.76130324   0.000058
5    STAY   NKLG  A     1 07:142:86395 m    1    1071574.57717845   0.000058
6    STAZ   NKLG  A     1 07:142:86395 m    1      39132.94659181   0.000058
7    STAX   MAS1  A     1 07:142:86395 m    1    5439192.21929807   0.000058
8    STAY   MAS1  A     1 07:142:86395 m    1   -1522055.44475204   0.000058
9    STAZ   MAS1  A     1 07:142:86395 m    1    2953454.89145883   0.000058
10   STAX   KMSI  A     1 07:142:86395 m    1    6332788.12828255   0.006506
11   STAY   KMSI  A     1 07:142:86395 m    1    -168938.56046497   0.005489
12   STAZ   KMSI  A     1 07:142:86395 m    1     740370.54025989   0.002809
13   STAX   TADI  A     1 07:142:86395 m    1    6352080.52195052   0.006505
14   STAY   TADI  A     1 07:142:86395 m    1    -194364.54585395   0.005440
15   STAZ   TADI  A     1 07:142:86395 m    1     541029.36096353   0.002770
16   STAX   KADE  A     1 07:142:86395 m    1    6341683.08159441   0.006455
17   STAY   KADE  A     1 07:142:86395 m    1     -92631.92018500   0.005420
18   STAZ   KADE  A     1 07:142:86395 m    1     674048.03345628   0.002786
19   STAX   ASFO  A     1 07:143:64795 m    1    6345407.17522182   0.007192
20   STAY   ASFO  A     1 07:143:64795 m    1    -141728.75074639   0.006108
21   STAZ   ASFO  A     1 07:143:64795 m    1     629324.06742072   0.003166
-SOLUTION/ESTIMATE
```

```
+SOLUTION/APRIORI
*
IND TYPE_CODE PT   SOLN _REF_EPOCH_ UNIT S         APRIORI VALUE      STD_DEV_
 1   STAX    ACRA    A   1 07:142:86395 m   1       6348052.68826858   0.006631
 2   STAY    ACRA    A   1 07:142:86395 m   1        -20212.88312388   0.005510
 3   STAZ    ACRA    A   1 07:142:86395 m   1        617243.59846069   0.002816
 4   STAX    NKLG    A   1 07:142:86395 m   1       6287385.76130298   0.000075
 5   STAY    NKLG    A   1 07:142:86395 m   1       1071574.57720195   0.000075
 6   STAZ    NKLG    A   1 07:142:86395 m   1         39132.94659220   0.000075
 7   STAX    MAS1    A   1 07:142:86395 m   1       5439192.21929825   0.000075
 8   STAY    MAS1    A   1 07:142:86395 m   1      -1522055.44475217   0.000075
 9   STAZ    MAS1    A   1 07:142:86395 m   1       2953454.89145836   0.000075
10   STAX    KMSI    A   1 07:142:86395 m   1       6332788.13086263   0.008564
11   STAY    KMSI    A   1 07:142:86395 m   1       -168938.56008286   0.007252
12   STAZ    KMSI    A   1 07:142:86395 m   1        740370.54222100   0.003666
13   STAX    TADI    A   1 07:142:86395 m   1       6352080.52276967   0.008572
14   STAY    TADI    A   1 07:142:86395 m   1       -194364.54853310   0.007197
15   STAZ    TADI    A   1 07:142:86395 m   1        541029.36221834   0.003621
16   STAX    KADE    A   1 07:142:86395 m   1       6341683.09808751   0.008496
17   STAY    KADE    A   1 07:142:86395 m   1        -92631.91680859   0.007166
18   STAZ    KADE    A   1 07:142:86395 m   1        674048.03485997   0.003638
19   STAX    ASFO    A   1 07:143:64795 m   1       6345407.20287974   0.010990
20   STAY    ASFO    A   1 07:143:64795 m   1       -141728.74166167   0.009471
21   STAZ    ASFO    A   1 07:143:64795 m   1        629324.07407533   0.004920
```

12.5 PREPOS NEADS Network Adjustment File

3D NETWORK ADJUSTMENT RESULTS - PREPOS GNSS SUITE (MODULE NEADS)
NUMBER OF POINTS TO BE ADJUSTED : 42
NUMBER OF FIDUCIAL POINTS ......: 0 (DATUM DEFECTS: 0)
NUMBER OF POINTS IN SINEX FILE .: 5 (TOTAL: 7, ELIMINATED: 2)
NUMBER OF POINTS FROM SEMIKA ...: 50
TOTAL NUMBER OF OBSERVATIONS ...: 171
TOTAL NUMBER OF PARAMETERS .....: 126
STATISTICAL DEGREES OF FREEDOM .: 39
STD.DEV. OF UNIT WEIGHT A PRIORI: 0.3 mm
STD.DEV. OF UNIT WEIGHT A POST. : 0.4 mm
DOMINANT EIGENVALUE OF NETWORK .: 14.0 mm (196.3 mm²)

FINAL COORDINATES AT REFERENCE EPOCH 2007.390:

ID	X [m]	Y [m]	Z [m]
ACRA	6348052.681 ± 0.007	-20212.882 ± 0.005	617243.597 ± 0.003
KMSI	6332788.128 ± 0.009	-168938.560 ± 0.007	740370.540 ± 0.004
TADI	6352080.522 ± 0.009	-194364.546 ± 0.007	541029.361 ± 0.004
KADE	6341683.082 ± 0.008	-92631.920 ± 0.007	674048.034 ± 0.004
ASFO	6345407.175 ± 0.009	-141728.751 ± 0.008	629324.067 ± 0.004
AKOS	6340187.138 ± 0.013	5916.015 ± 0.012	693630.689 ± 0.003
AKRO	6345564.337 ± 0.031	-84885.370 ± 0.022	638056.369 ± 0.007
ANSU	6325647.707 ± 0.034	-180057.465 ± 0.024	798084.883 ± 0.009
APAM	6350787.213 ± 0.022	-81407.555 ± 0.017	583332.576 ± 0.005
ASUB	6343991.999 ± 0.023	-45870.599 ± 0.012	656450.268 ± 0.005
BARE	6330440.752 ± 0.027	-192684.758 ± 0.021	755315.113 ± 0.007
DEDS	6336420.263 ± 0.018	-30479.966 ± 0.013	726610.838 ± 0.004
EJSU	6332800.818 ± 0.014	-162440.859 ± 0.010	741693.374 ± 0.003
ELMI	6351356.921 ± 0.019	-148750.377 ± 0.015	563220.582 ± 0.004
JAMA	6329617.012 ± 0.033	-159704.179 ± 0.025	771354.582 ± 0.009
JUSO	6335813.855 ± 0.043	-128807.116 ± 0.037	725133.427 ± 0.009
KATA	6346169.830 ± 0.024	-7215.792 ± 0.013	636569.206 ± 0.005
KNGO	6334684.452 ± 0.015	-134496.181 ± 0.012	730769.046 ± 0.004
MAMF	6344637.416 ± 0.025	-13509.064 ± 0.020	655606.800 ± 0.007
NANI	6335269.925 ± 0.031	-156146.906 ± 0.023	723533.841 ± 0.007
NKWN	6336366.794 ± 0.018	-86269.289 ± 0.018	723494.733 ± 0.004
NKWT	6336666.372 ± 0.048	-84673.839 ± 0.051	725640.186 ± 0.011
NSUO	6341808.320 ± 0.059	-217709.798 ± 0.048	645757.441 ± 0.012
NYAN	6349294.509 ± 0.017	-46938.168 ± 0.012	602857.884 ± 0.004
OBRA	6347620.924 ± 0.102	-61967.047 ± 0.067	621119.348 ± 0.018
OBUA	6338570.535 ± 0.017	-185719.357 ± 0.012	684512.241 ± 0.004
OFSE	6340469.394 ± 0.018	-126360.212 ± 0.012	679783.246 ± 0.005
OSNO	6339340.602 ± 0.038	-53389.526 ± 0.018	700079.988 ± 0.007
POAN	6335460.896 ± 0.042	-187460.010 ± 0.022	714150.813 ± 0.007
PPRM	6346696.648 ± 0.025	11749.825 ± 0.013	630892.299 ± 0.005
PRAM	6341714.762 ± 0.021	-82896.345 ± 0.020	676390.452 ± 0.004
PRAS	6338453.732 ± 0.036	-114324.021 ± 0.037	703224.437 ± 0.009
PUMP	6352233.252 ± 0.013	-203885.517 ± 0.009	535639.549 ± 0.003
SALT	6350984.849 ± 0.014	-117105.975 ± 0.016	574738.720 ± 0.004
SBSO	6341641.164 ± 0.071	-142384.569 ± 0.136	668219.748 ± 0.027
SNCH	6340650.685 ± 0.041	10876.357 ± 0.045	688698.440 ± 0.009
TPRA	6345578.401 ± 0.028	-171389.924 ± 0.016	619288.503 ± 0.006
WISO	6328716.633 ± 0.038	-222856.919 ± 0.020	762594.119 ± 0.008
WNBA	6349968.225 ± 0.011	-70722.530 ± 0.007	593005.924 ± 0.002
ASAS	6347537.393 ± 0.047	-166338.255 ± 0.029	602325.783 ± 0.009
KROB	6342846.265 ± 0.026	5561.643 ± 0.020	671150.091 ± 0.007
AWAN	6343878.253 ± 0.036	-80798.416 ± 0.027	656032.723 ± 0.007

APPENDIX